University of Southampton

Faculty of Engineering and Applied Science
School of Engineering Sciences
Ship Science

Design Aspects of Catamarans Operating at High Speed in Shallow Water

by *M.P Abdul Ghani*

Thesis submitted for the degree of
Doctor of Philosophy
June 2003

SUPERVISOR: Professor P.A Wilson

This report is dedicated to,
my beloved mother and family

UNIVERSITY OF SOUTHAMPTON

ABSTRACT

FACULTY OF ENGINEERING AND APPLIED SCIENCE
SCHOOL OF ENGINEERING SCIENCES
SHIP SCIENCE

Doctor of Philosophy

DESIGN ASPECTS OF CATAMARANS OPERATING AT HIGH SPEED IN SHALLOW WATER

by Mohamad Pauzi Abdul Ghani

The thesis describes the investigation into the design aspects of the high-speed displacement catamaran. This work is an extension of the existing database on the high-speed displacement hull form series namely the NPL series. The experimental test programme has been extended in the current research to investigate the influence of bulbous bows on the high-speed displacement catamaran performance in deep and shallow water conditions. Four bulbous bows have been developed by ranging bulbous bow's projecting length, between 1.25% to 6.25% of the length of waterline. These bulbous bows have been designed and faired to the parent hull, NPL5b or known as a Model 5b of the NPL Series, whilst the after body and the fore body from amidships to $0.3L_{pp}$ are kept unchanged. However, the cross section parameter has been fixed at value 0.303 i.e. the ratio of the bulbous bow cross section area at forward perpendicular to the midship section area. Measurements of total resistance, wash, trim and sinkage have been made up to a Froude number of unity in deep and shallow water. In addition to the calm water tests, these models were also tested in regular waves covering a wavelength to ship length ratio λ/L between 0.5 and 2.0 whilst the wave height was maintained at 0.030 m. Measurements of added resistance in waves, pitch, heave and wash cuts were made. Thin ship theory computer codes namely *wavel3d.for* and *wave3d3ss.for* have been used to validate the measured wash cuts.

It was found that the experimental and numerical investigations provide a better understanding of the basic physics of wash, resistance and seakeeping of high speed displacement catamarans fitted with bulbous bows operating in deep and shallow water.

The results of the systematic experimental investigation with respect to the influence of bulbous bows on wash, resistance and seakeeping provide invaluable information with a view to developing design guidance at the preliminary design phase and for validation purposes.

Acknowledgements

I wish to express my sincere thanks to my supervisor, Professor Philip Wilson for his guidance and advice without which the completion of this work would not be possible.

I am also grateful to Professor Molland for his help and advice.

My thanks also is due to Dr Dominic Taunton, Dr Sattaya Chandraprabha, Omer and my Malaysian colleagues (Abu, Ober, Chop, Nawal, Taqi, PakAli) for the assistance during the experimental part of the work.

I also like to thank Universiti Teknologi Malaysia(UTM) and Public Services Department of Malaysia for their financial support for me to undertake this study.

Contents

List of Figures

List of Tables

Nomenclature

Symbols and abbreviations used

GKN	Towing Tank No. 3, GKN Westland Aerospace Ltd., Isle of Wight
Lamont	Lamont Tank, University of Southampton
NPL	National Physical Laboratory
$SIHE$	Towing Tank, Southampton Institute for Higher Education
Demihull	One of the hulls which make up the catamaran
AP	After Perpendicular
FP	Forward Perpendicular
L	Ship Length, m
B	Ship Breadth, m
T	Draught, m
D	Depth, m
h	Water depth, m
∇	Volume of displacement, m^3
$\triangle$	Mass displacement, kg
$S_\circ$	Static wetted surface area, m^2
s	Separation between catamaran demihull centrelines, m
C_B	Block Coefficient
C_P	Prismatic Coefficient
g	Gravity acceleration, $9.81 m/s^2$
ρ	Density of water, $1000 kg/m^3$ for FW and $1025 kg/m^3$ for SW
u, v	Speed or velocity, m/s
F_n, F_{nl}	Length Froude Number $[v/\sqrt{gL}]$
F_{nh}	Depth Froude Number $[v/\sqrt{gh}]$
H_{max}	Maximum wash height, m
H_{nd}	Non-dimensional wash height
C_T	Coefficient of total resistance
C_W	Coefficient of wave-making resistance
C_F	Coefficient of frictional resistance
C_R	Coefficient of residuary resistance

C_V	Coefficient of viscous resistance, $C_T = C_T - (1+k)C_F$
$(1+k)$	Form factor
R_{AW}	Added resistance in waves, N
σ_{AW}	Non-dimensional added resistance in waves
λ	Wavelength, m
ζ_a	Wave amplitude, m
Z_a	Heave amplitude, m
θ_a	Wave slope
$\omega_e\sqrt{L/g}$	Non-dimensional frequency
$\frac{R}{\Delta}$	Specific Resistance

Chapter 1

Introduction

1.1 Background

The maritime industry is continuing to develop in response to new technology and customer demands. In 1998 the world's fast ferry market has been valued at approximately US \$4.5billion of which there are approximately 700 of such vessels around the world. Stena, for example, recently paid around £65M for their latest new vessel [37].

In recent years fast ferries which are capable of speeds in excess of 40 knots in water depth less than 10m have been operational. As high-speed operations near sensitive shorelines increase, complaints from the public on extensive wave wake or wake wash from these fast vessels increase also. Although the leading waves in the wash are very small in terms of wave amplitude compared to storm waves, they have a very long period and build in height rapidly in shallow water at the shoreline thereby causing substantial surges on beaches as well as breaching sea walls at high tide. This wake wash is likely to have environmental effects such as shoreline erosion as well as endangering swimmers and small boats. During 1997, as a consequence of public concern, the Danish Maritime Authority (1997) issued a governmental order which requires that the high-speed craft operator/owner has to show evidence that the ship-generated waves do not exceed a prescribed wave height criterion in shallow water along the entire route. Similar criteria exist for other regions, such as the Puget Sound, Seattle, some navigable inland waterways in the Netherlands and the River Thames, UK [59]. There are other areas which are equally sensitive to damage such as the Paramatta River in Australia, the Solent (i.e. particularly the route between Southampton and Isle of Wight), Nantucket, the Mare Island Channel and the East Bay Estuary in San Francisco Bay.

Wake wash or normally known as wash results from ship-generated waves. There is a general awareness of the importance of ship-generated waves in design. However, until re-

1.3 Scope of the Present Work

The research area of high speed displacement craft is wide. Therefore the present study will mainly concentrate on the wash, resistance and seakeeping produced by the proven hull form, one of the NPL series. This hull form also has been slightly modified by incorporating cylindrical bulbous bows into it.

The main objectives of this research are,

- Model experiments to provide a better understanding of the basic physics of wash, resistance and seakeeping of high speed displacement catamaran fitted with bulbous bows operating in deep and shallow water.
- Further model experiments in regular waves to study the influence of bulbous bows and wave lengths on the added resistance, pitch, heave and wash.
- To compare the experimental results of wash cuts with thin ship theory.
- To provide potential ship designers with a useful data base of wash, resistance and seakeeping of high speed displacement catamaran fitted with bulbous bows.

1.4 Outline of the Thesis

Chapter 2 presents an overview of the previous reported research on wake wash for design. In particular it draws our attention to the limited availability of literature covering wake wash generated by high speed displacement craft. A description of the current wake wash research methodologies used, together with their important elements and characteristics are also given.

In Chapter 3, a description of the bulbous bow design for high speed displacement craft together with their important parameters and characteristics are presented. This chapter also describes the tank testing for monohull and catamaran configurations at the Lamont and SIHE tanks. The experimental results i.e. the effect of bulbous bows on the resistance components, sinkage and trim are presented. The effect of bulbous bows on waves wash are also given.

Chapter 4 describes the experimental work in regular waves at SIHE tank. In addition to total model resistance, heave and pitch, the wave cuts in waves are also recorded. The wash deduced from these wave cuts were compared to the wash obtained in calm water previously in Chapter 3. The effect of bulbous bows on resistance, heave, pitch and as well as wash are also described.

Considering the variation in water depth and ship speed, it is prudent to continue the experimental work mentioned in Chapters 3 and 4 into a shallow water condition as reported in Chapter 5.

Having recognised the need to supplement the experimental work with theoretical investigation, a computer program using thin ship theory has been used to compare the measured and calculated wave cuts as described in Chapter 6. This covers the experiments in three different establishments namely Lamont, SIHE and GKN towing tanks. The computer program also gives a theoretical values of wave pattern resistance coefficients. It should be noted that this wave pattern resistance coefficient, C_{wp} is only part of the wave-making resistance coefficient, C_w.

Finally, in Chapter 7, the research results are discussed, recommendation for future research are made and conclusions drawn. This presentation includes the bulbous bows ranking and design trade-off of Wash, Resistance and Seakeeping on high-speed displacement craft performance.

Chapter 2

The Wash of High-Speed Craft: State of the Art

2.1 Background

In order to develop an appropriate measure it is necessary to review the principal characteristics of the well-established wave pattern which is generated by a ship in deep water. As a ship moves through the surface of a body of water, a wave pattern consisting of divergent and transverse waves is generated. Diverging waves are created at the bow and stern and will generally remain separated throughout their travel. Transverse waves also created at the bow and stern will, however, combine to form a single series of waves. Kelvin (1887) found that, for any deep water speed, the diverging and transverse waves form a constant pattern and meet to form a locus of cusps whose angle with the sailing line is 19°28" . This cusps locus angle varies for real ships. For example for thin ships the cusps locus angle is lower at higher speeds. The cusps locus line also often intersects with the sailing line at a point ahead of the ship's bow [90]. A typical Kelvin wave pattern is shown in Figure 2.1. Kelvin's theory also predicts that the transverse and diverging waves meet at a common tangent that forms an angle of 54°44" with the sailing line of the disturbance. Lord Kelvin analytically investigated the wave pattern generated by a single point disturbance moving across the surface of deep water and generating groups of waves that move forward with directions of travel that vary continuously between $\pm 90°$ of the direction of travel of the disturbance (i.e. sailing line).

Havelock extended the work of Kelvin to show that the wave height at the cusp points decrease at a rate inversely proportional to the cube root of the distance from the disturbance, while the transverse wave heights along the sailing line decrease at a rate inversely proportional to the square root of the distance from the distance. Clearly any wash generated will gradually die out as it travels into the distance. Thus, at greater distances from the ship, the diverging waves become more prominent than the transverse waves.

The transverse waves celerity is equal to the ship speed. Thus, using linear wave theory, their length and period can be calculated for a given ship speed and water depth. The divergent waves have a celerity less than the ship speed and equal to $V \cos\theta$ where V is the ship speed and θ is equal to $54°44"$(maximum) given by Kelvin as described in previous paragraph. Consequently all the wash components radiate out in lines from the ship in a delta like formation. The longer faster waves are on the outside of the wash and have larger values of θ compared to the slower shorter waves with crests swept further back.

In general, a significant number of papers on the study of wake wash from high-speed craft were published during the 1990's.

Gadd (1994)[34] presented an approximate theoretical prediction method to predict the characteristics of high-speed boat wash by calculating the waves resulting from a distribution of surface pressure. It was treated as varying only in the longitudinal direction x axis over a rectangle whose length is the boat length L and whose width B is such that the area BL is equal to the water plane area of the boat. This prediction method is limited to high-speed hull forms with transom sterns whose immersed areas when at rest are a significant proportion of the maximum cross section. Gadd (1999)[35] proposed an Egger type analysis to deduce far field waves from model tests in a limited width of towing tank where the measurement of waves sufficiently far from the track is not possible.

Whittaker et al (1999)[109] carried out an investigation of the wash of high-speed ferries operating in Belfast Lough. The objective was to gain a better understanding of the physical processes of the wash, which aimed at producing a standardised methodology for assessing the environmental impact of high-speed ferry operating in coastal region. Several approaches and steps were employed to investigate wash effect in order to compliment or to cross check between them.

- An ultra-sonic measuring system mounted on fixed structure was used to monitor the elevation of the water surface. 150 wash time traces were recorded for the two fast ferries.
- A series of physical model testing.
- Computer modelling by using CFD which modelling of the ship water interaction using Shipflow.
- The wave transformation program, MIKE 21 developed by DHI was used to model how the wash waves are transformed by the seabed topography as they travel from the line of generation along the track of the vessel to the shoreline.

The wash produced by high speed displacement craft is classified in terms of depth Froude number as suggested by Havelock(1908)[42] such as,

- Sub-Critical Wash. $F_{nh} < 1$
- Critical Wash. $F_{nh} = 1$.
- Super-Critical. $F_{nh} > 1$.

Similar work was also reported by Henrik Konfed-Hansen(1999)[59] on investigation of wave pattern or wake wash from high-speed craft in Danish waters by field measurements, model experiments and numerical wave modelling. A description is also given of the phenomena and application of an efficient numerical model to describe wave propagation and transformation from the ferry route to the nearby coast. The model also includes the effects of refraction and shoaling due to varying depth. The DHI's MIKE 21NSW (Near-shore Spectra Wave model) is used for that purpose. The basic equations in MIKE 21 NSW were derived from the conservation equation for the spectral wave action density based on an approach proposed by Holthuijsen et al (1989)[47]. The model includes the effects of refraction and shoaling due to varying depth, wave generation due to wind, and energy dissipation due to bottom friction, wave breaking and also the effects of ambient current. The output of this model basically consists of wave height, wave period and wave directions. For a ship moving steadily in water of uniform finite depth, the nature of the wash which it creates will closely depend upon two non-dimensionless parameters; the length-based Froude number $F_{nl} = \frac{V_s}{\sqrt{gL_w}}$ and the depth-based Froude number $F_{nh} = \frac{V_s}{\sqrt{gh}}$.

In Henrik Konfed-Hansen's work (1998)[58], the results and analysis of full-scale wake wash measurements from a few Danish ferry routes were presented. These measurements have been supplemented by wave propagation modelling to develop methods which predict the areas of particular concern. These prediction methods are required in the planning of new ferry routes. A wake wash criterion, $H_h \leq 0.5\sqrt{\frac{4.5}{T_h}}$ where H_h is the maximum wave height of the long-periodic waves having mean wave period of T_h seconds was introduced. These criteria are applicable at a still water depth of 3 m.

In the sub-critical speed range ($F_{nh} < 0.6 - 0.7$) the wave system consists of diverging and transverse waves in a restricted wedge-shaped Kelvin wake, where the cusps are about $19°28''$ and almost independent of the ship speed [60] [77]. In this speed range, the wave period of the diverging waves is proportional to the ship speed $T \approx 0.27V_s$, where V_s in knots. For depth-Froude numbers beyond one (supercritical speed range), the transverse waves disappear and the wave system is characterised by a Havelock-like wave pattern i.e taken a convex form. This is typical for high-speed craft operating in coastal waters. The divergent waves are now contained within an angle which depends on the speed of the ship. In the transcritical speed range ($F_{nh} \approx 0.9 - 1.1$), transverse and divergent waves merge together into wave fronts which are almost nearly straight and perpendicular to the ship's track. High amplitude waves are typically generated at these speeds. Wake wash generated by high-speed craft is markedly different to waves from conventional ships. Wave measuring programs have demonstrated that the high-speed craft generates diverging wave pattern consisting of groups of long period waves and short periodic waves. The long waves from large carrying fast ferries normally have more than 9 seconds wave period. These waves have a relatively larger wave height growth during shoaling and wave refraction which is caused by seabed irregularities in deeper waters. The result is that the waves when reaching the shore consist of higher breaking waves and have a larger run-up than traditional ship waves and the breakers have more of a plunging effect. The waves will arrive faster than ordinary Kelvin waves and particularly during calm weather conditions, people on the beach will not be prepared for a breaking wave appearing without any warning. This is a main reason for the public concern over wake wash from high-speed craft [58]. The work of Taatø et al (1998)[98] concluded that the propulsion system on large high-speed craft (water jets) may cause increased wave heights of 20-40% compared to the bare hull.

The correlation between hull characteristics such as length of waterline L_{LWL} and length to beam ratio $\frac{L}{B}$ to the wash characteristics has been carried out by Stumbo [95] and Dand [17]. This was achieved by measuring the wake wash characteristics of numerous aluminum catamarans of various displacements, lengths and hull forms. A submerged pressure sensor was used to record wave height and wave period and with these two components, wash height and wash energy density can be determined for various ship speeds. An assumption is made that in deep water, after a wave travels a certain distance from the point of generation, gravity will cause the wave to assume a sinusoidal wave profile and then linear wave theory can be applied. Based on this assumption, the author had used classic wave theory to quantify and characterize the wash produced by various hull forms. It is suggested that a design goal of low wake wash could be achieved by designing a vessel which achieves hump speed as early as possible with the lowest possible hump wash height and energy density. From the graph produced it was shown that the hump speed varied proportionally with the length L_{LWL} and the wash height and energy density at hump speed were inversely proportional to the length to beam ratio, $\frac{L_{LWL}}{B}$. It was concluded that water line length and length-to-beam ratio were very important parameters in the design of low wash ships. In a successive paper [97], he presented the wash prediction by computational fluid dynamics using a nonlinear free surface module, FSWAVE coupled to a three-dimensional panel method, VSAERO. VSAERO/FSWAVE can be thought of as combined Green's Theorem/Velocity Method approach to a panel method, where Green's Theorem is applied to solid bodies and Velocity Method is used on the free surface. He also introduced criteria of acceptable wake wash for Washington

State Ferries. The no harm level was established at

- Wash height of 28 cm, measured 300 m from sailing line.
- Wash energy density of 2450 joules/m in the highest significant wave of the wave train as measured 300 m from sailing line.

as shown in Figure 2.2 and Figure 2.3 respectively.

Bertram (1999)[3] discussed the utilization of nonlinear wave resistance codes to predict wash generated by high-speed craft. The codes involved were VSAERO, FSWAVE and SHALLO which are very similar and representative for a widely used class of boundary element codes (commonly known as panel codes). From his computer prediction and full-scale measurement results analysis, he concluded that wash depends on the size and shape of the ship, speed, water depth and a distance to shore. The main design parameters are the hull slenderness and the displacement. Long slender lightweight hulls with fine entrance, rounded bottoms, and smooth transition to the stern profile are likely to produce low wash characteristics. However, the characteristics that produce low wash might not be those that produce favourable seakeeping characteristics, good space utilization, or high transport efficiency. It was concluded that the numerical wash prediction could predict with sufficient accuracy the wash near the ship and in rectangular channels with rigid walls for the subcritical and supercritical speed.

The full-scale measurement or a field study approach to the wake wash generated by by high speed ferries problem has been carried out by Hannon, et al (1999)[41]. This field study was carried out on site at Loch Ryan where Stena Line operates their HSS1500, Lynx wave-piercing catamaran and Ro-Ro ferries, SeaCat Scotland utilizes a wave-piercing catamaran while P&O operates a Jetliner planing monohull and two Ro-Ro ferries. This was solely a field measurement works and the result very much depended on the recorded wave elevation time history.

It is accepted practice to obtain a time history for the longitudinal cut of wave elevation as a ship passes a wave measurement devices as described by Sorensen, [90][91]. These time histories can be obtained, from either model or full-scale experiments, through the use of common measurement tools such as capacitance or resistance wave probes, submerged pressure transducers and wave rider buoys. Measurements such as significant wave height and a wave energy may well be more representative of the distribution of wave heights and periods within any given ship-generated wave pattern than maximum wave height as proposed by Sorensen, et al[92][94]. Sorensen(1973)[93] recorded a height of ship-generated waves produced by different types of ship at 100 feet, 500 feet and 1000 feet from sailing line as shown in Table 2.1. This data has also been plotted in Figure 2.4 and Figure 2.5.

These figures show the influence of depth Froude number, length Froude number and distance from sailing line on the wash height and their decay rate.

Vessel Type	L m	B m	T	DISPL tonnes	d m	V knots	H100 m	H500 m	H1000 m
Cabin Cruiser	7	2.5	0.5	2.722	12.2	6	0.2	0.1	
						10	0.4	0.2	
Coast Guard	12.2	3	1.1	9.072	11.6	6	0.2	0.3	
Cutter						10	0.5		
						14	0.7		
Tugboat	13.7	4	1.8	26.3	11.3	6	0.2	0.1	
						10	0.5	0.3	
Rescued Craft	19.5	3.9	3	31.8	12.2	6	0.1		
						10	0.4	0.2	
						14	0.6	0.3	
Fireboat	30.5	8.5	3.4	311.2	11.9	6	0.1	0.06	
						10	0.5	0.3	
						14	0.9	0.8	
Barge	80.2	16.8	4.3	4917	12.8	10	0.4	0.2	0.1
Tanker	153.6	20.1	8.5	17100	17.1	14		0.5	0.3
						18		1.6	1.4

Table 2.1: Data of ship-generated waves[92]

Based on the model tests results Khattab (1999)[57] found that the wash amplitude was proportional to the cube of boat speed. He also concluded from his various model tests that the generated wash depends on Froude number, slenderness ratio, half-angle of entrance, bow section shape, waterline shape, stern shape, forward prismatic coefficient and position of longitudinal centre of buoyancy.

Macfarlane and Renilson (1999)[69] listed the parameters which should be considered when dealing with ship-generated waves prior to conducting the experiment and/or reporting wave wake results. They discussed this at length in their paper.

The most accurate way of obtaining wake wash or ship-generated waves is by means of experiment, either on full-scale or with models. However it would sometimes be useful to make approximate theoretical predictions of the waves in the preliminary stage to judge the suitability and acceptability of the boat. The use of CFD codes to model these phenomena has its own limitations. They do not permit calculations of the far field wave pattern and more often the calculation is limited to an area within three to five ship lengths.

2.2 Flow Field Generated by a Travelling Ship

The wave system generated by a travelling ship consists of divergent and transverse waves travelling at the same ship speed. Transverse waves travel along the ship length where the divergent waves travel away from the ship. The transverse wave system consists of a set of waves generated by the bow, shoulders and stern [83].

The generated wave system is the result of the pressure field around the ship. The ship wave is due to the high pressure and starts with a crest but at the shoulder the pressure is negative and the wave starts with a trough. At the stern of the ship the pressure is low and the stern wave starts with a trough.

The generated wave system travels at the same ship speed. For a sinusoidal wave travelling in water depth, d, the amplitude of constant pressure contours of the wave profile at a depth Z_p from the surface is expressed by

$$\zeta_p = \zeta_o \frac{\cosh[k(d - Z_p)]}{\cosh(kd)} \sin(kx - \omega t) \tag{2.1}$$

where k is the wave number, λ is the wave length and ω is the wave frequency. wave speed as a function of wave length and water depth is given by,

$$V_w = \sqrt{\frac{g\lambda}{2\pi} \tanh[\frac{2\pi h}{\lambda}]} \tag{2.2}$$

The total kinetic and potential energy of the wave is proportional to the square of the wave amplitude and it is defined by,

$$E = \frac{1}{2}\rho g \zeta^2 \tag{2.3}$$

Divergent waves propagate at a speed normal to the wave crest equal to $V_w \cos\theta$ where θ is the angle between the normal to wave crest and ship speed. This means that the propagation of the divergent waves is slower than the transverse wave.

2.3 Investigation of Ship Waves and Wake Wash

There are many rules of thumb that can be followed to minimize wake wash and these are fairly well understood. Long thin lightweight hulls with fine entrance, rounded bottoms and smooth transition to stern profile are more likely to produce low wash characteristics when compared to heavy, blunt, beamy and fiat-bottom vessels. However in the design process, the hull characteristics that produce low wash may not be those that produce good seakeeping, good space utilization or high-transport efficiency. Almost none of the High-Speed Craft(HSC) designs have a small wash amplitude as a primary design parameter in their design spiral. Therefore there is no comparable knowledge of different HSC concepts ability, to generate small wash amplitude.

Therefore, an accurate means of predicting wash characteristics is required. Generally, this could be carried out in four different ways:

a) Analytically, that is based on a theoretical basis.

b) Experimentally, by means of model test.

c) Empirically, through statistical observations.

d) Directly, with trials of ships after they are built but too late.

Both theoretical and experimental studies help the designers to determine the influences of various ship parameters and features on wake wash. The wake wash or wave system for a given hull form could be determined by analytical means or measured physically in towing tank. Traditionally, model tests have provided a reasonably accurate relative profile of wash characteristics compared to full scale or field measurement. However model basin and model scaling introduce certain uncertainties to the process predicting absolute characteristics. The wall and bottom effect of model basin of finite and depth, for example cannot be easily or accurately taken care of.

2.3.1 Experimental Approaches

Tests would be conducted in a towing tank at appropriate scaled model and water depth for a proposed route. Normally, because of the limited width of such a tank, it would not permit the direct measurement of waves sufficiently far from the track or sailing line of the craft to be relevant to the practical condition.

2.3.2 Analytical Approaches

Inui (1962)[55] classifies ship waves calculation methods into two groups, direct and indirect.

In the direct method, the wave pattern is calculated directly from hull geometry. This method is best represented by Guilloton (1951,1960)[39] in which the hull form is represented by the summation of a series of *wedges* defined in terms of the second differences of hull offsets. Velocity potentials and wave profiles are calculated for each wedge section.

From a set of tabulated functions representing the wave profile generated by each wedge, the wave system profile can be obtained by addition of the contribution from each wedge.

For the indirect approach (e.g. Havelock, 1932,1943-44)[45][42][44] either a continuous distribution of infinitesimal sources located on the hull centreline plane or a small number of finite sources distributed in some fashion over the centreline plane or some other suitable location is used to generate a wave system equivalent to that generated by the given hull form. This approach also known as *thin-ship theory.*

In addition to above methods for the prediction of wash, a boundary element method (BEM) or more commonly known as panel codes was used by Brizzolara, et al [9] and Betram, et al [3]. Boussinesq type model was used by Jiang [56] to model ship waves and wave propagation over large distances.

Raven [81] developed a coupled wave-making and wave propagation model, which is based on coupling a steady free surface potential flow code, RAPID, used for the prediction of waves generation with a non-linear Boussinesq type model used for the prediction of wave propagation.

Leer-Andersen, et al [65] used a CFD code, SHIPFLOW, for the prediction of wash in order to optimise hull forms for wash reduction.

Hughes [50] used CFD methods to examine the unsteady effects on the wake wash as a ship moves from deep water into shallow water.

Both the Navier-Stokes and the full potential flow options require huge amounts of computational time whilst for the purpose of initial design, thin-ship theory is more cost effective.

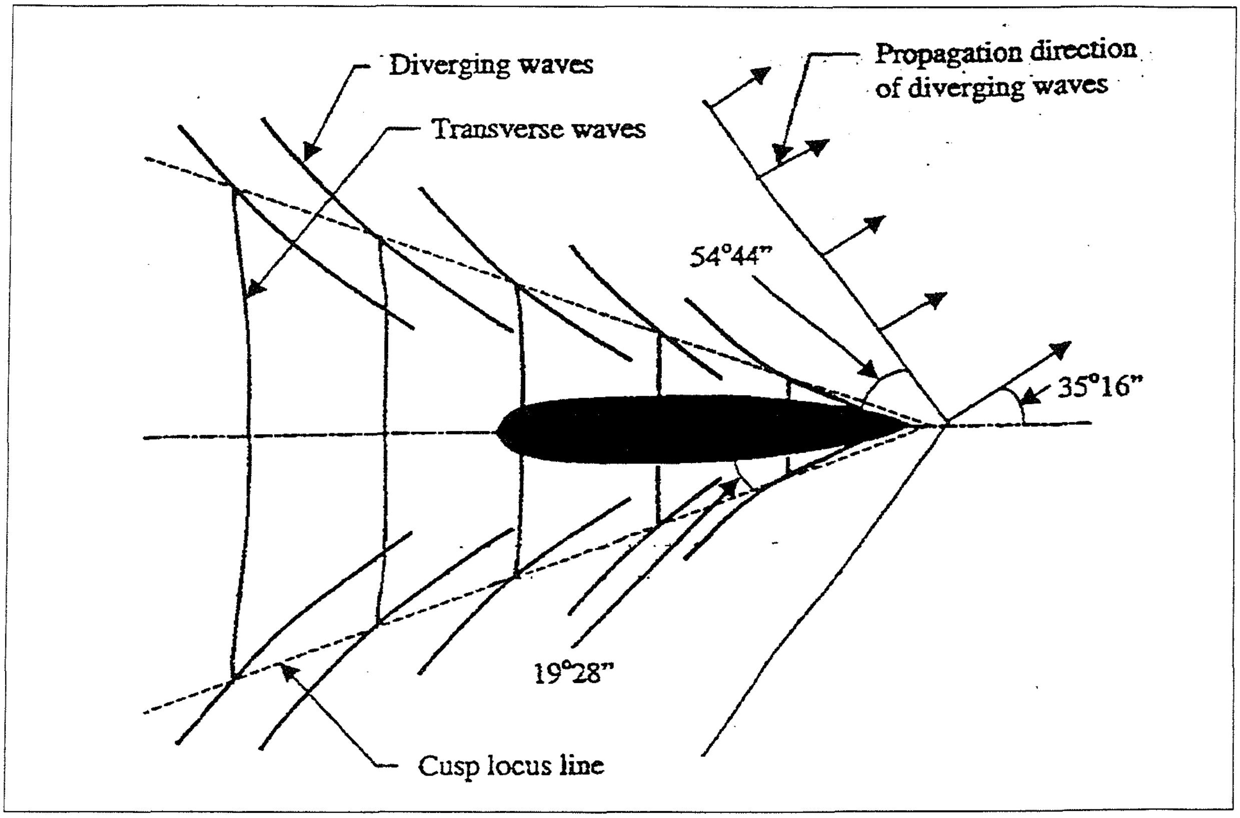

Figure 2.1: Ship-Generated Waves

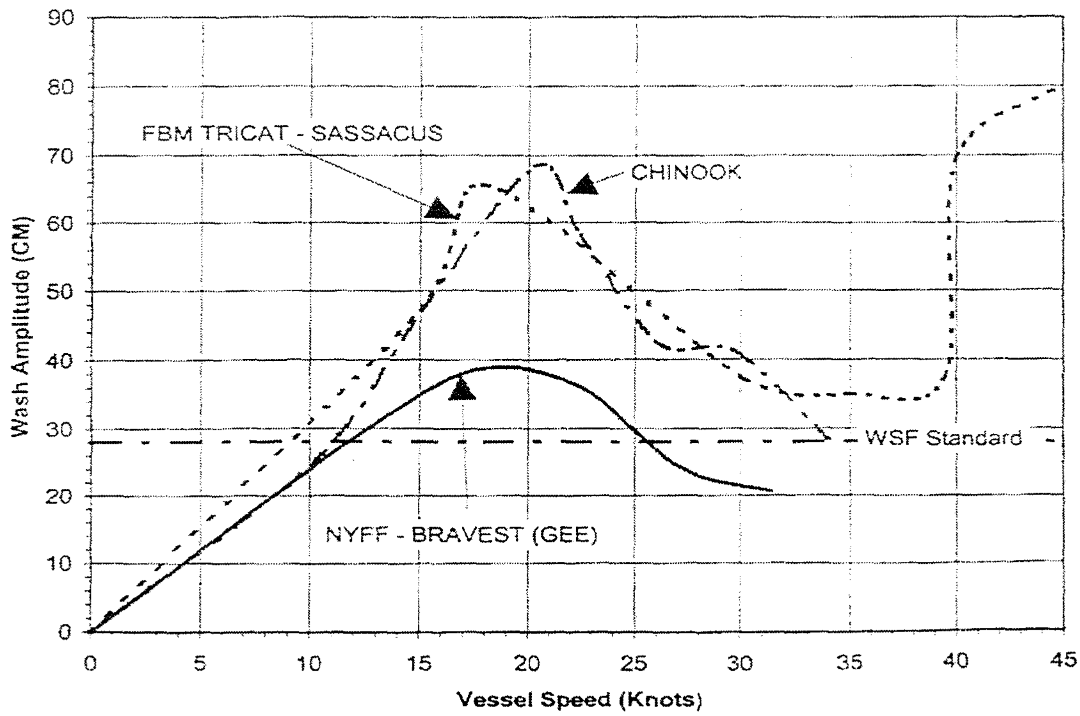

Figure 2.2: Wash amplitude against speed for three vessels[95]

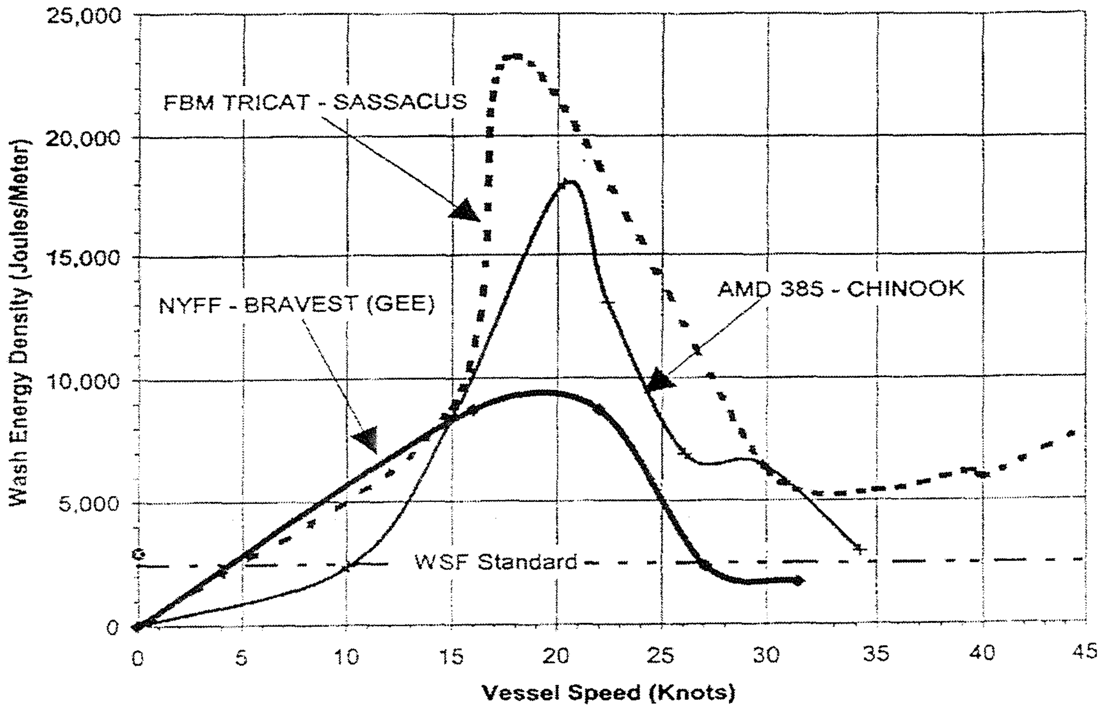

Figure 2.3: Wash energy against speed for three vessels[95]

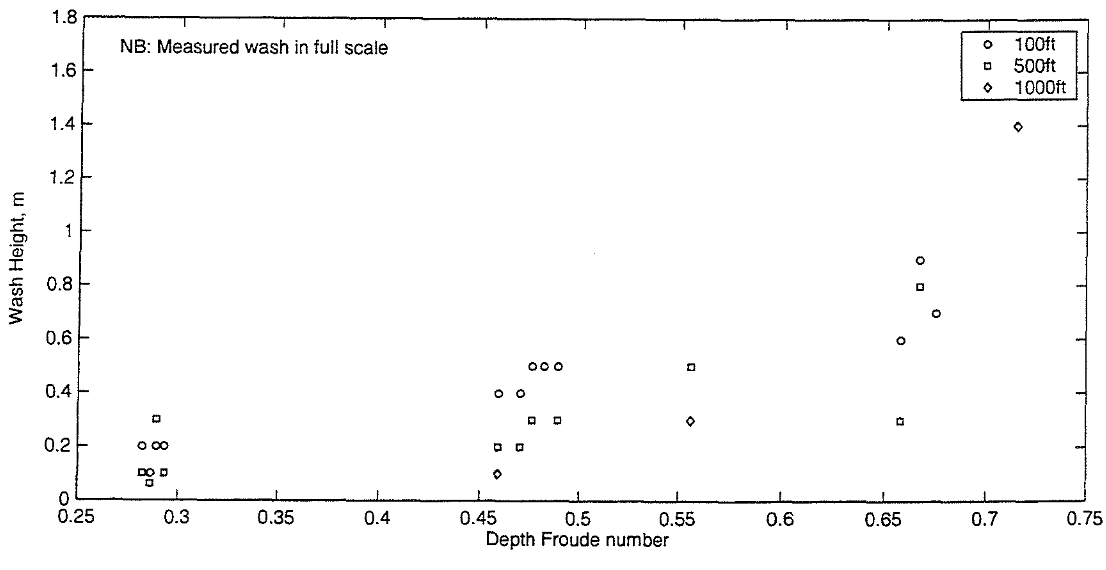

Figure 2.4: Wash height against depth Froude number

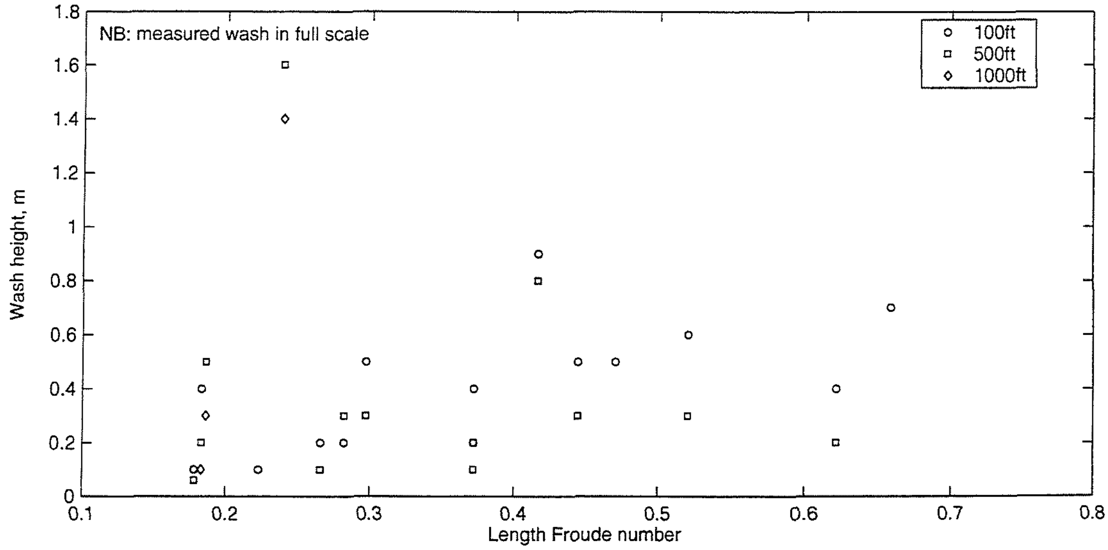

Figure 2.5: Wash height against length Froude number

Chapter 3

The Effect of Bulbous Bows on Wake Wash and Ship Resistance

3.1 General

Although the study of ship-generated waves has been carried out since the middle of the nineteenth century, emphasis has been placed on the determination of a ship's resistance resulting from the energy expended in generating a wave pattern. It has been accepted and recognized that the use of a bulbous bow can reduce a ship's wave-making resistance. A quantitative relationship between the character of the waves generated by a ship, as a function of the ship type, size, draught, speed, water depth etc is often desirable in the investigation of wake wash. In this study, the effects of bulbous bow on the wash are explored.

This study will focus on the effect of bulbs on wake wash attributes such its height and period generated by high-speed displacement craft. When low wash is of prime concern, catamaran hulls might be an attractive alternative to monohulls, because of their inherent wave-cancelling potential. In the present study the NPL5b series catamaran has been chosen as an object for further investigation.

The aim of this work is to find the best combination of the existing hullform of the high-speed displacement catamaran (NPL5b) and bulbous bow/bulb type that have considerably less wake wash without compromising other attributes such as seakeeping ability and resistance & propulsion of the vessel.

The approach of the study is to incorporate different bulbous bows into the existing NPL5b series catamaran hull form. The framework of the approach for undertaking the research outlined can be explained by addressing the following three phases of development:

- First Phase - Bulbous Bow Design.
- Second Phase - Model Preparation.
- Third Phase - Tank Testing.

3.2 Bulbous Bow Design

3.2.1 Background

Bulbous bows are used on almost all modern ocean-going ships. They actually create their own wave system, which cancels the hull's bow wave. A properly designed bulbous bow can certainly improve the running efficiency of a hull and reduce vertical accelerations as well. A number of new designs incorporate a bulbous bow and some yachts utilize a retrofitted bulbous bow to improve their performance at sea.

A bulbous bow was discovered rather than invented. Model testing studies in the United State with warships established that the ram stem projecting below the water had a resistance decreasing effect. A torpedo boat model showed that an underwater torpedo discharge tube ending in the forward stem also reduced the resistance. D.W Taylor was the pioneer when it was recognized that the bulbous bow reduces the wave making resistance.[84]

Havelock(1928)[43] calculated the surface wave pattern around the sphere immersed in a uniform stream. He found out a wave trough just aft the sphere, which suggested the possibility of partly cancelling the bow wave of the hull by locating the sphere below the surface in vicinity to the stem.[43]

Wigley (1935-36)[112] carried out calculation of wave profiles and wave making resistance based on Havelock's work and published the basic theory for the bulbous bow. At low speed he found the total resistance to be increased due to additional frictional resistance and hence viscous resistance. At higher speeds, the reduction in wave resistance due to the interference between the wave systems of the hull and bulbous bow, which if properly positioned, is more than sufficient to overcome the frictional and form resistance of the bulbous bow and the total resistance is reduced accordingly.

General rules concerning the position and size of bulbous bows and the speeds at which it will be useful have been drawn by Wigley(1936)[112] i.e.

1. The useful speed range is generally from F_n=0.24 to 0.57.
2. The top of the bulb should not approach too near to the water surface; and as a working rule it is suggested that the immersion of the highest part of the bulb should be equal or greater than its own total diameter.

Inui(1962)[55] showed mathematically and by model tests that a bulbous bow could largely cancel the wave system produced by the bow of the ship. The resulting effect would be a substantial reduction of the energy loss due to waves and thus a decrease in hull resistance.

Since Inui's work, a great interest in the large protruding bulbs has developed throughout the world.

3.2.2 Theory of Bulbous Bow

The addition of a bulbous bow to a hull will reduce the total resistance by lowering of the wave-making resistance through attenuation of ship's bow wave system. Furthermore, Kracht(1978)[61] stated that a bulb acts to reduce viscous resistance by smoothing the flow around the forebody of the ship. Therefore, the beneficial and effectiveness of a bulbous bow depends on the waves it generates and the flow around it. So it is quite obvious that parameters of the bulbous bow such as the size, the position and the form of the bulb body will affect the wave generation and hence the resistance of the ship. Kracht further describes bulbous bow form as *an additive* or *implicit* bulb, where an additive bulb increase the displacement of the ship but is not the case for implicit bulb which the sectional area curve of the original ship is changed. In practical terms for ships already built, an additive bulb will be the best solution, while for new designs an implicit bulb might be advantageous.

For slender hull forms such as a NPL5b catamaran, the primary reduction in resistance is due to the reduction of the free wave system of the ship. This reduction of the free wave system is accomplished by cancellation, which depends on the phase and amplitudes of the waves created by the bulb and the ship, the two may cancel totally. The phase difference of the two wave systems is determined by the location of the bulb, and the amplitude of the bulb's wave is determined by bulb volume.

Generally the type of bulb or bulbous bow can be broadly classified into three main types as shown in figure 3.1.

- Delta Type

  This delta type indicates a concentration of the bulb volume toward the baseline with the drop-shaped cross sectional area, A_{BT}. The Taylor bulb and pear-shape bulb belong to this group. However this type of bulbous bow are no longer built today due to their unfavourable properties.

- Nabla Type

  This group of bulbous bow also has a drop-shaped cross sectional area A_{BT} but with center of area in the upper-half near to the free surface. All modern bulbous bows belong to this group because of its favourable seakeeping properties.

- O Type

  This O-Type has an oval sectional area A_{BT} and central volumetric concentration. All circular, elliptical and cylindrical shaped bulbs belong to this group.

They also could be defined by the following form characteristics:

1. Shape of section
2. Length of projection beyond perpendicular
3. Area ratio

Kracht(1978)[61] introduced six non-dimensional quantities bulb parameters for classification of bulb form as follows:

- Breadth Parameter

$$C_{BB} = \frac{B_B}{B_{MS}}$$

  where

  B_B is the maximum breadth of the bulb area A_{BT} at the FP.

  B_{MS} is the breadth of midships.

- Length Parameter

$$C_{LPR} = \frac{L_{PR}}{L_{PP}}$$

  where

  L_{PR} is the protruding length of the bulb

  L_{PP} is length between perpendicular of ship

- Depth Parameter

$$C_{ZB} = \frac{Z_B}{T_{FP}}$$

  where

  Z_B height of the foremost point of bulb over the base.

  T_{FP} ship draught at FP

- Cross section Parameter

$$C_{ABT} = \frac{A_{BT}}{A_{MS}}$$

where

A_{BT} is the cross sectional area of bulbous bow at FP.

A_{MS} is the midships sectional area of the ship

- Lateral Parameter

$$C_{ABL} = \frac{A_{BL}}{A_{MS}}$$

where

A_{BL} is the area of ram bow in the longitudinal plane

- Volumetric Parameter

$$C_{\nabla PR} = \frac{\nabla_{PR}}{\nabla_{WL}}$$

where

∇_{PR} is the nominal volume of the protruding part of bulbous bow

∇_{WL} is ship's volume displacement.

Bulb No.	C_{LPR}	C_{BB}	C_{ZB}	C_{ABL}	C_{ABT}	$C_{\nabla PR}$
0	0.011	0.194	0.293	0.064	0.125	0.0014
1	0.034	0.165	0.46	0.174	0.086	0.0028
2	0.030	0.165	0.46	0.165	0.088	0.0030
3	0.040	0.165	0.46	0.219	0.088	0.0039
4	0.034	0.200	0.46	0.174	0.106	0.0035
5	0.030	0.200	0.46	0.165	0.106	0.0036
6	0.040	0.200	0.46	0.219	0.106	0.0047
7	0.020	0.165	0.46	0.110	0.088	0.0020
8	0.010	0.165	0.46	0.056	0.088	0.0010

Table 3.1: Kracht bulb parameters

Bulbous bow cross section A_{BT} influences the size of the wave generated, while its length L_{PR} determines the phase of the bulbous bow generated waves and also its volume is related to the amplitude. One important parameter is depth below the surface. If the bulbous bow submergence is too deep it will not be of much benefit in reducing wave resistance, but if it is too shallow it may breach the surface at higher speeds.

The forward end of the bulbous bow can be spherical or an elliptical shape.

The cross section can be cylindrical or others as mentioned in previous section or of varying cross section along its length. The shape or cross section is usually determined by seakeeping consideration and other factors such as resistance as well as production kindliness.

Due to the complexities of the hydrodynamics interactions between bulbous bow and main hull it is difficult to present a completely analytical approach to bulbous bow design. Therefore, the development of the bulbous bow for a ship is an empirical and iterative process or sometimes prone toward trial and error process.

3.2.3 Bulbous Bow for NPL5b series Hull Form

The bulb design was focused on phase differences by changing the length of bulbous bow. Bulbous bows with circular cross section are preferred for further investigation in relation to wave wash because of their simple building procedure as well as other advantages. Schneekluth(1987)[84],in his studies on this type of bulbous bow that the potential danger of slamming effects can be avoided. This type of bulbous bow was also recommended by Kracht(1978)[61] for the slender hull form. It fits well with U and V types of forebody sections and offers space for sonar equipment if required.

The diameter of the bulbous bow was chosen based on several design parameters as suggested by Tuck(1965)[107], Kracht(1978)[61] and Roddan(1999)[82]. The summary of those results are shown in Table 3.2. Consideration of those parameters, the 48mm diameter has been chosen for this particular model for further investigation.

Although, the projecting length L_{PR} is varied but it is not allowed to project longitudinally beyond the upper end of the stem for safety reasons, in consideration of anchor handling, docking and manoeuvring.

Four different bulbous bows have been developed by varying the bulbous bow's projecting length L_{PR} between 20mm and 100mm. These bulbous bows have been designed and faired to the parent hull, whilst the afterbody and the forebody from amidship to $0.3L_{pp}$ is kept unchanged.

The cross section parameter,C_{ABT} has been fixed at value 0.131 i.e the ratio of bulbous bow cross section area at FP to the midships section area. Other bulbous bow details are shown in Table 3.3.

Design Parameter	Approx. D_{bulb}	Remarks
Roddan[82]	58mm to 63mm	based on draught and clearance to MSL
Tuck(1965)[103]	48 mm	based on draught and clearance to MSL
Kracht's C_{ZB}[61]	42mm	depth parameter
Kracht's C_{LPR} & $C_{\nabla PR}$	26mm	length parameter, too small
Kracht's C_{ABT}	31mm	cross-section parameter

Table 3.2: Summary of bulb diameter

Bulb No.	C_{LPR}	C_{BB}	C_{ZB}	C_{ABL}	C_{ABT}	$C_{\nabla PR}$
Bulb01	0.013	0.331	0.329	0.119	0.303	0.0032
Bulb02	0.028	0.331	0.329	0.320	0.303	0.0098
Bulb03	0.044	0.331	0.329	0.521	0.303	0.0163
Bulb04	0.063	0.331	0.329	0.763	0.303	0.0241

Table 3.3: Bulbous Bow Parameters for NPL5b Hull

3.3 Model Tests

The wash measurement experiments were conducted in three different establishments namely the University of Southampton Lamont Tank and the Southampton Institute's tank for deep water condition whereas the GKN Westland Aerospace Ltd.'s tank, Isle of Wight was used for the shallow water condition. The details of these tanks are given in Table 3.4.

Length	30.0 m
Breadth	2.40 m
Depth	1.20 m
Max. Carriage Speed	3.0 m/s

A. Lamont Tank Details

Length	60.0 m
Breadth	3.70 m
Depth	1.80 m
Max. Carriage Speed	4.2 m/s

B. SIHE Tank Details

Length	200.0 m
Breadth	4.60 m
Depth	0.40 m
Max. Carriage Speed	14.0 m/s

C. GKN Westland Tank Details

Table 3.4: Towing Tanks Details

3.3.1 Description of Models

The hulls of the models were made of Glass Reinforced Plastics(GRP) with epoxy resin. They were built in two halves, one half from station 0 (AP) up to station 8 of which their forms were maintained as an original NPL5b hull and another portion from station 8 to stem which underwent slight modification in order to accommodate the bulbous bow. These two portions were joined at a bulkhead at station 8 and are removable.

Figure 3.3 illustrates the removable part of the bulbous bow and other details.

Details of the models used in the investigation are given in Table 3.5. Figures 3.4, 3.5, 3.6 and 3.7 show part of the model fabrication stages.

Item	NPL	NPL_{bulb01}	NPL_{bulb02}	NPL_{bulb03}	NPL_{bulb04}
L, m	1.6	1.6	1.6	1.6	1.6
B, m	0.145	0.145	0.145	0.145	0.145
T, m	0.073	0.073	0.073	0.073	0.073
∇, m^3	0.006461	0.006771	0.006817	0.006862	0.006917
WSA, m^2	0.267	0.315	0.319	0.323	0.327
LCB,m	-0.065	-0.062	-0.056	-0.050	-0.043
L/B	11.0	11.0	11.0	11.0	11.0
B/T	2.0	2.0	2.0	2.0	2.0
$L/\nabla^{\frac{1}{3}}$	8.591	8.457	8.438	8.420	8.397
C_B	0.380	0.400	0.403	0.405	0.408
C_P	0.676	0.709	0.715	0.718	0.723
C_M	0.564	0.564	0.564	0.564	0.564
C_W	0.736	0.736	0.736	0.736	0.736

Table 3.5: Models Particulars

The model was towed horizontally at the longitudinal centre of gravity and at an effective height of one third of the draught above the keel. The models were fitted with turbulence stimulation studs of 3.2mm diameter and 2.5mm height at a spacing of 25mm. Those studs were situated 37.5mm aft of the stem. No underwater appendages were attached to the models.

3.3.2 Instrumentation and measurements

The total model resistance was measured by using the Wolfson Unit dynamometer. The accuracy of the total resistance was found to be within the range of $\pm 0.02N$. Trim was measured with an angular potentiometer incorporated into the towing fitting. The accuracy of this potentiometer was in the range of $\pm 0.05°$.

The wash or wave cuts during the run was measured by three wave probes; details as mentioned in the following section.

3.3.3 Test Conditions and Presentation of Results

During the model tests to measure the wash, resistance and trim were also recorded. The model was tested extensively over the chosen speed range. All wave probes were located at the optimum longitudinal position for the longest possible wave traces. The position of the wave probes from the centreline of the tank are shown in Table 3.6 and Table 3.7. The Time taken to complete the timed run was recorded by the operator from a chronometer. All other data was recorded by the computer. Figure 3.8 and Figure 3.9 show the computerised data acquisition system.

Probe No.	Distance from Tank's Centreline	y/L
Probe 1	1.015 m	0.63
Probe 2	0.865 m	0.54
Probe 3	0.755 m	0.47

Table 3.6: The wave probes position for Lamont tank

Probe No.	Distance from Tank's Centreline	y/L
Probe 1	1.42 m	0.89
Probe 2	1.23 m	0.77
Probe 3	1.11 m	0.69

Table 3.7: The wave probes position for Southampton Institute tank

All tests were carried out in calm water over a wide range of speeds corresponding to the length Froude number 0.3 to 0.6 and 0.26 to 1.02 for Lamont tank and Southampton Institute tank respectively.The corresponding Reynolds number R_n for the models within those speed range was between 1.85×10^6 and 3.54×10^6. Before testing began, all bulbs were appended to a 1.6m NPL5b series catamaran fitted with a removable bow section. Each model configuration was ballasted to a designed waterline, 0.0725m at level trim.

Data reduction and corrections

All resistance data were reduced to coefficient form using fresh water density ($\rho = 1000 kg/m^3$), model speed(V) and wetted surface area at rest S_o;

Resistance Coefficient= $\left(\frac{R}{1/2\rho S_o V^2}\right)$

Corrections were applied as necessary to the measured data.

Temperature correction

Some of the model tests were carried out during summer 2001. During this time the water temperature varied from $18°C$ to $18.5°C$. The total resistance measurements were corrected to the standard temperature of $15°C$ by modifying the frictional resistance component as follows:

$$C_{T_{15}} = C_{T_{test}} - C_{F_{test}} + C_{F_{15}} \tag{3.1}$$

where the subscript $'15'$ represents values at $15°C$ and the subscript $'test'$ represents measurements made at the test temperature.

Blockage effect

As in the previous work by Insel and Molland [54] and Couser [15], viscous blockage effects on the models were neglected.

According to Racliffe, A.T. et al[80] blockage can be taken into account by using the following relationship between the corrected model speed V_m and the speed V of the towing carriage:

$$V_m = \alpha.V \tag{3.2}$$

with:

$$\alpha = \frac{1}{1-(k_m)m}$$

$$k_m = 1 + \exp(-10.m)$$

$$m = \frac{A_M}{A_{TK}}$$

Table 3.8 shows speed correction factors α of the model used at 3 different establishments. It illustrates only small correction factors α involved, so the blockage can be ignored. Shallow water effects were also neglected.

Tank	W_{tank}	H_{tank}	m	k_m	α
Lamont	2.40	1.20	0.0041	1.9594	1.0082
SIHE	3.70	1.80	0.0018	1.9822	1.0036
GKN	4.60	0.40	0.0065	1.9372	1.0127

Table 3.8: Speed Correction Factor,α

3.3.4 Results

Wash or Wave traces

There are several methods which can be used to analyze the measured data. The first approach utilizes the wave energy method, i.e the calculation of the energy of the wave system at the measuring position. The second approach, is based on the maximum and minimum amplitude of the generated wave (or to find the highest wave in the measured data).

The wash elevation for model NPL5b series catamaran fitted with bulb01 with varying speed are shown in Figures 3.10 and 3.11. Figures 3.12 and 3.13 show the wash elevation produced by the model fitted with bulb02 and for model fitted with bulb03 and bulb04 their wash elevation are shown in Figures 3.14 to 3.15 and 3.16 to 3.17 respectively. They show four sets of wave cuts measured at different Froude numbers. In each set contains three sets of wave cuts measured at different distances from the sailing line of the 1.6m catamaran model.

From those figures, generally they show that the principal effect of increasing Froude number is to increase the size of the wash for vessel operating in Froude number range 0.31 to 0.55. In addition to this, it was also found out from those figures that the wave observed often possessed both a trough followed by a crest.

Figures 3.18, 3.19, 3.20, and 3.21, shows a comparison of the experimental results of four different hull configuration at two different probe locations i.e. the nearer and the farthest from the model's sailing line for Froude numbers 0.31, 0.33, 0.36, 0.39, 0.42, 0.48, 0.54 and 0.57.

For the sake of simplicity, it is prudent to present those wave cuts in term of maximum and minimum wash amplitude as shown in Figures 3.22 and 3.23. This is based on the maximum wash height, H_{max} deduced from the wave cuts at each speed.

From these two figures, it is clearly shown that the wash can be reduced by incorporating a bulbous bow into the basic hull form (which is designated as *ori* in the Figures 3.22 and 3.23). Figure 3.22 shows that at Froude number above 0.42 to 0.57 those bulbous bows reduced maximum and minimum wash amplitudes by approximately 28% to 64%

and 20% to 61% respectively. For the farthest wave probe $y/L = 0.63$ the reduction in wash amplitudes is in between 2% to 60%, see Figure 3.23. As shown in these figures, the waves amplitudes given by bulb01, bulb02 and bulb03 are almost coincides each other and they are preferable compared to bulb04 in this condition.

The experimental results from the Southampton Institute's towing tank are shown in Figures 3.24, 3.25, 3.26, for catamaran, $s/L = 0.2$ at Froude number 0.51, 0.71 and 1.02 respectively. For the catamaran $s/L = 0.3$, the results are shown in Figures 3.27, 3.28 and 3.29. Whereas, Figures 3.30, 3.31 and 3.32 shows the wash generated by catamaran, $s/L = 0.4$ at Froude number 0.51, 0.71 and 1.02 respectively. They show the four bulbous bows produce almost similar wash pattern and the same wash height but with different phase shift. This is probably due to these bulbous bows have the same shape with a small different in volume and length.

The effect of demihull separation on wash are given in Figures 3.33 to 3.36. These figures show that as the hull separation is increased, the wash amplitude decreases in a similar manner to resistance in this speed range as shown in Figure 3.46.

Maximum wave height

Figures 3.37 and 3.38 are plots of the maximum wave height for those models as function of length Froude number at two different probe locations.

The ship wave height is closely related to wave-making resistance of the ship which varies with length Froude number, Fn Newman(1977)[77]. The maximum wave height in deep water is inversely proportional to a cubic root of a distance from the sailing line Havelock(1908)[42]. Considering this, the non-dimensional maximum wave height as shown in equation 3.4 was introduced in order to investigate their changes with Fn.

$$H_{nd} = (H_{max}/B)(y/L)^{1/3} \tag{3.4}$$

As shown in Figures 3.39 and 3.40, the non-dimensional wave height for all models with and without bulb increase with Fn until critical value. At $Fn \simeq 0.5$ they attain the peak values. When $Fn > 0.5$, these values decrease with Fn. The changes of non-dimensional maximum wave heights with Fn appear to be similar to those of wave-making resistance coefficients as expected. Although the data has some scatter, it is clear that the non-dimensional wave heights depend mainly upon length Froude number as well as other parameters such as the depth Froude number and water depth to draught ratio.

Specific resistance

Figures 3.41 and 3.42 are plots of the specific resistance against Froude number in monohull and catamaran, $s/L = 0.2$ configurations respectively. Figure 3.41 shows that the resistance decreases with increasing bulbous bow volume. Bulb04 illustrated this point by having the lowest specific resistance over the considered speed range for monohull configuration and vice-versa for catamaran, $s/L = 0.2$.

Residuary resistance

The residuary resistance coefficient C_R has been derived from $C_T - C_F$. The experimental results are presented in terms of residuary resistance coefficient C_R or C_r are shown in Figures 3.43 to 3.45. Figure 3.46 shows the residuary resistance coefficient of Model 5b or NPL5b without bulbous bow which is reproduced from Couser(1996)[15].

Residuary resistance is important as it provides a readily available tool for powering purposes and a means of comparing the relative merits of changes in the hull form parameters. By comparing Figures 3.43, 3.44 and 3.45 with Figure 3.46, they clearly show that the influence of bulbous bow in reducing the residuary resistance coefficient by at least 30%. In detail, for catamaran $s/L = 0.2$, the percentage reduction in residuary resistance coefficient in comparison with the original hull form are 34% for bulb01, 30% for bulb02, 40% for bulb03 and 38% for bulb04. This percentage increases as separation ratio increases.

It should be noted that the residuary resistance coefficient is non-dimensionalized using wetted area and that the wetted area increases by 22.5% in going from the normal(non bulb) bow to the bow with bulb04 (Table 3.5). The volume (hence displacement, $\triangle$) increases by 7.1% in going from the normal bow to bulb04. If the comparison is based on the specific resistance ($R/\triangle$) the percentage reduction in $R/\triangle$ in comparison with the original hull form are 9% for bulb01, 8.5% for bulb02, 11.8% for bulb03 and 11.9% for bulb04.

Wave resistance

The ITTC-1957 line has been used in analysing the tests results. The form factors have also been evaluated by Prohaska's method in order to investigate the effect of bulbous bows on viscous resistance as shown in Table 3.9.

Typical wave resistance results defined in the following equations for monohull and catamaran configurations respectively.

$$C_{w_{15}} = C_{T_{15}} - C_{F_{15}}(1 + k) \tag{3.5}$$

$$C_{w15} = C_{T15} - C_{F15}(1 + \beta k) \tag{3.6}$$

where $(1 + k)$ is a form factor for monohull and $(1 + \beta k)$ represents the form and interference factors for catamaran. These factors can be obtained by Prohaska plot as shown in Figures 3.47 and 3.48.

These wave resistance coefficients could be used to determine the effectiveness of bulbous bow.

Bulb no.	mono	s/L=0.2
Bulb01	1.33	1.57
Bulb02	1.40	1.58
Bulb03	1.64	1.68
Bulb04	1.39	1.83

Table 3.9: Monohull and Catamaran s/L=0.2 Form Factors(Lamont Tank)

The typical wave resistance coefficients, C_w as defined in Equations 3.5 and 3.6 are presented in Figure 3.49 and 3.50.

It has been shown in the literature that the wake wash effects are site-specific and a practical standard methodology for assessing fast ferry wash has not been established.

Since wave resistance is an indicator of the energy contained in the ship generated waves or wash of a vessel, it is prudent to introduce the bulbous bow efficiency K_{BB}, in order to judge the effectiveness of bulbous bow in minimizing wash of a vessel.

$$K_{BB} = \frac{C_{w_{ori}} - C_{w_{bb}}}{C_{w_{ori}}} \times 100\% \tag{3.7}$$

where

$C_{w_{ori}}$ is a wave resistance coefficient without bulbous bow.

$C_{w_{bb}}$ is a wave resistance coefficient with bulbous bow.

In order not to confine the user to the particular values of $(1 + k)$ or $(1 + \beta k)$ derived in this work, this formula also could be written in term of residuary resistance coefficient as shown in the equation below where the designer is able to choose a suitable form factor from this work or other sources.

$$K_{BB} = \frac{C_{R_{ori}} - C_{R_{bb}}}{C_{R_{ori}}} \times 100\% \tag{3.8}$$

$C_{R_{ori}}$ is a residuary resistance coefficient without bulbous bow.

Page 32 is missing from volume

The changes of non-dimensional wash heights with length Froude number F_n seem similar to those of wave-making resistance.

Non-dimensional wash height produced by catamaran, $s/L = 0.2$ is less than monohull in some places. This is probably due to wave cancelling effects of catamaran.

The higher the separation, the lower the critical Froude number becomes. It changes from $F_n = 0.46$ for $s/L = 0.4$ to $F_n = 0.51$ for $s/L = 0.2$ as shown in Figures 3.43 and 3.44.

It is also important to note that those with circular cross section bulbous bows offer significant reduction in wave-making resistance coefficient as well as reduction in wash height together with the practical advantage of a simple construction procedure.

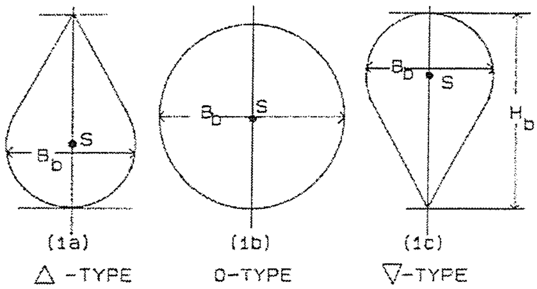

Figure 3.1: Types of bulbous bow

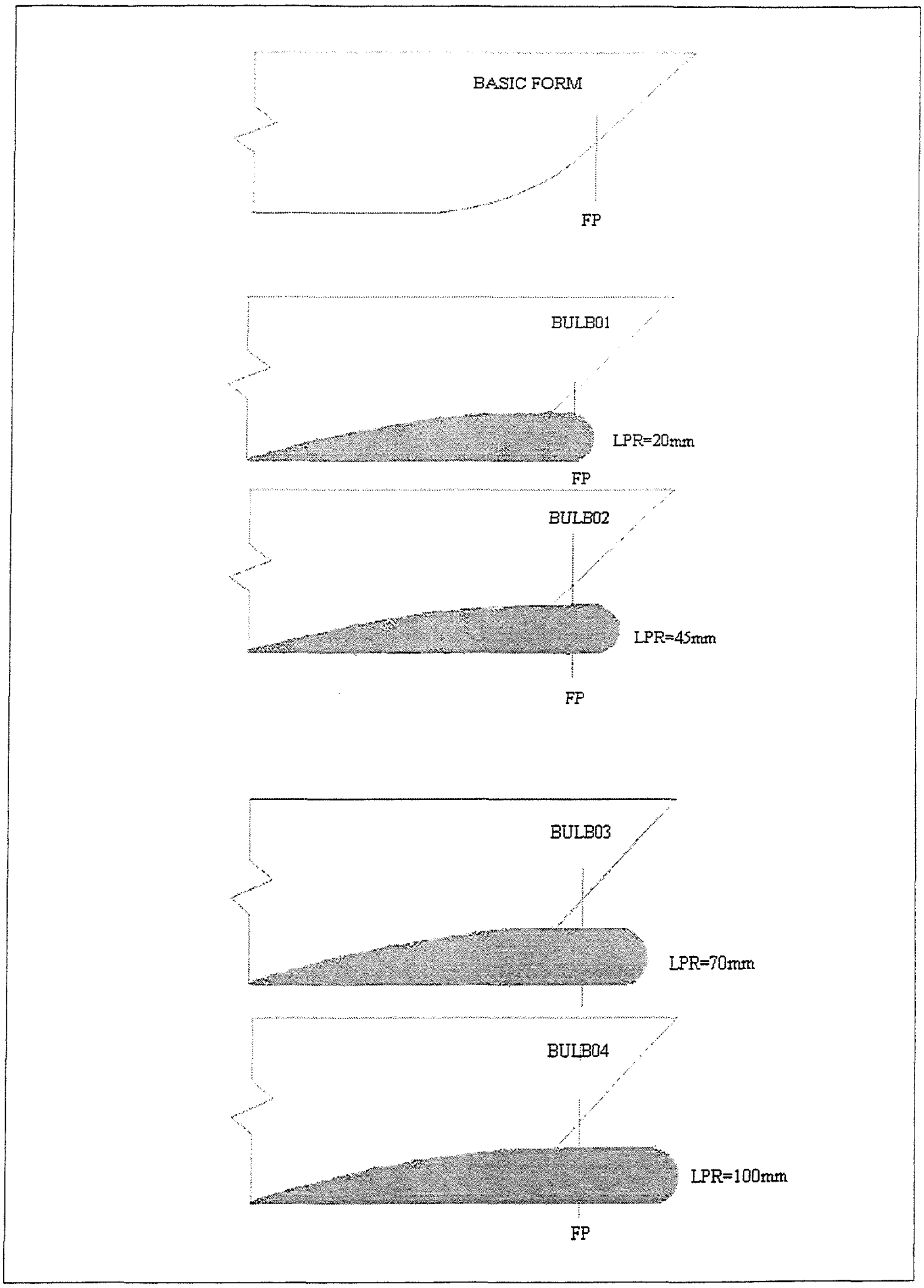

Figure 3.2: Profile of Bulbous Bows

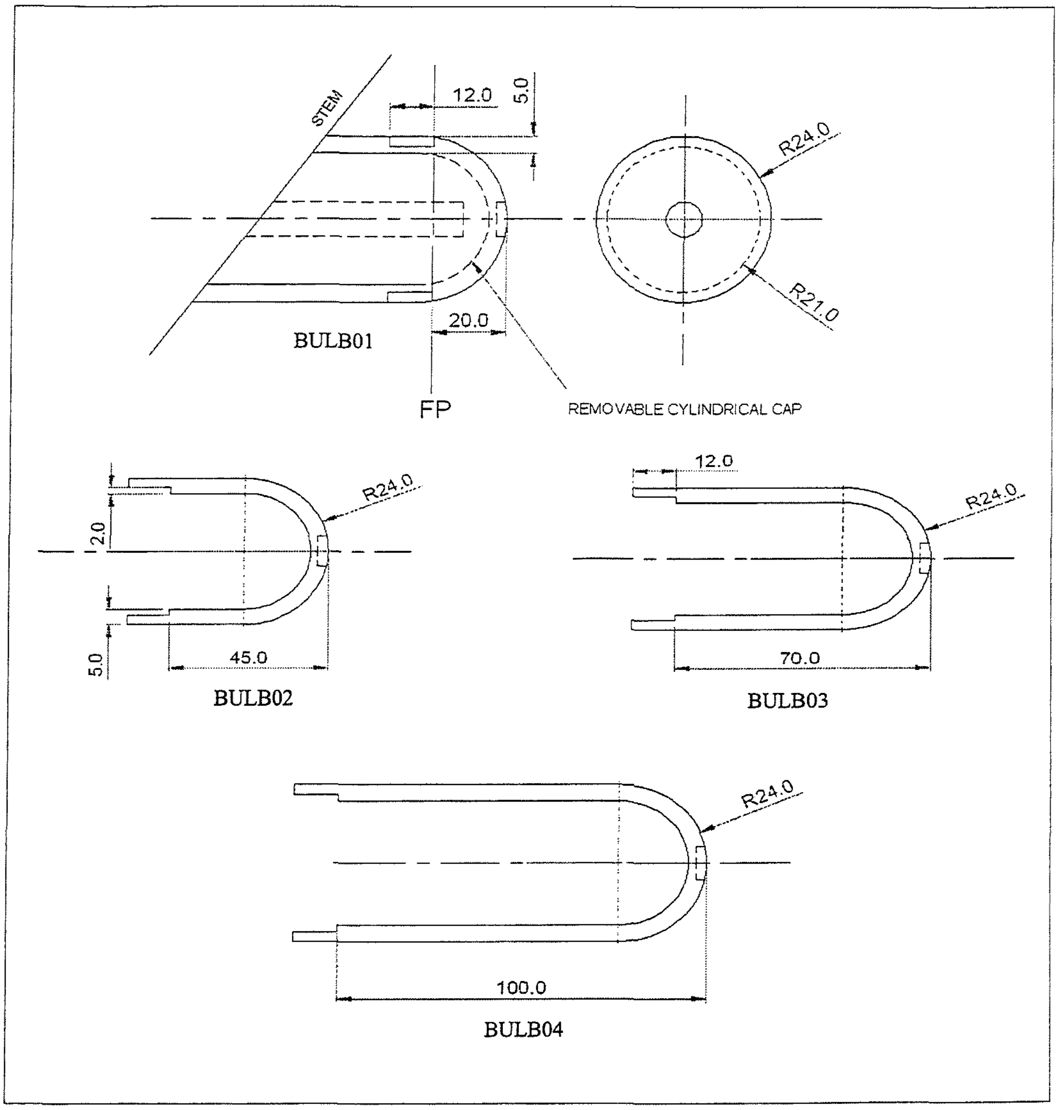

Figure 3.3: Bulbous Bow's Details

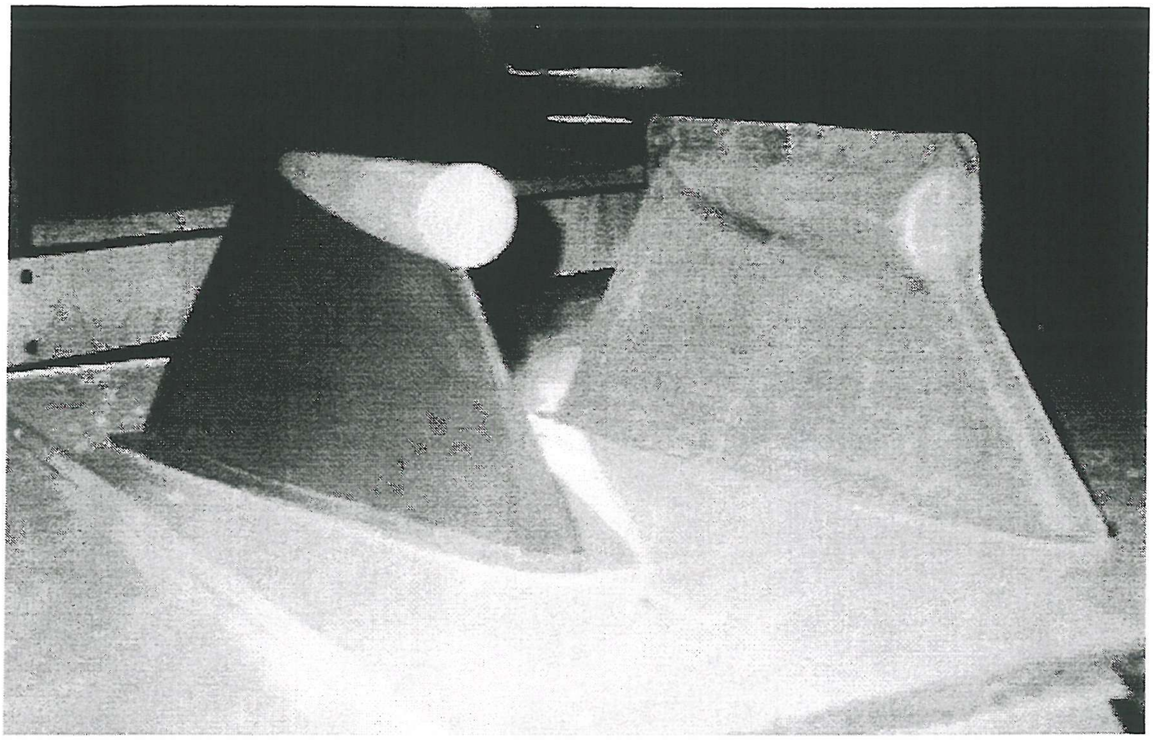

Figure 3.4: Bulbous Bow's plug and mould

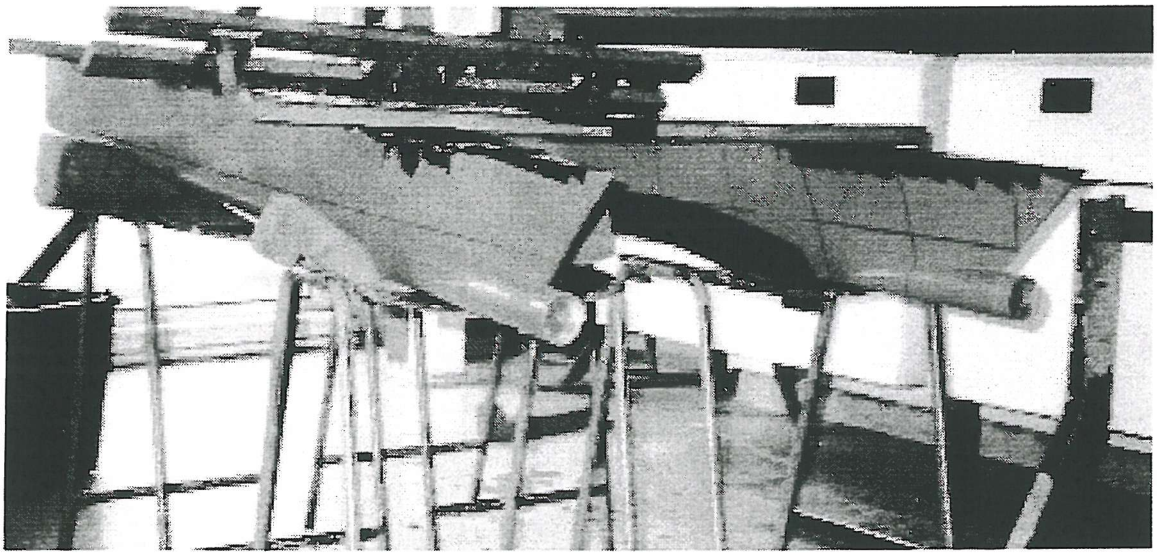

Figure 3.5: Catamaran with Bulbous Bow Adaptor/holder

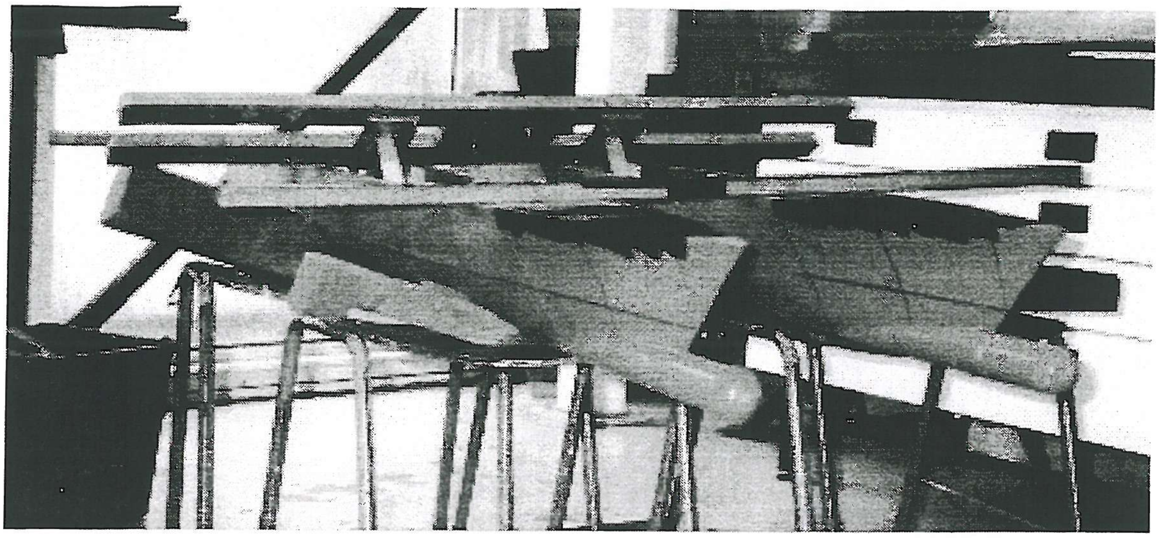

Figure 3.6: Catamaran with one of removable bulbous bow

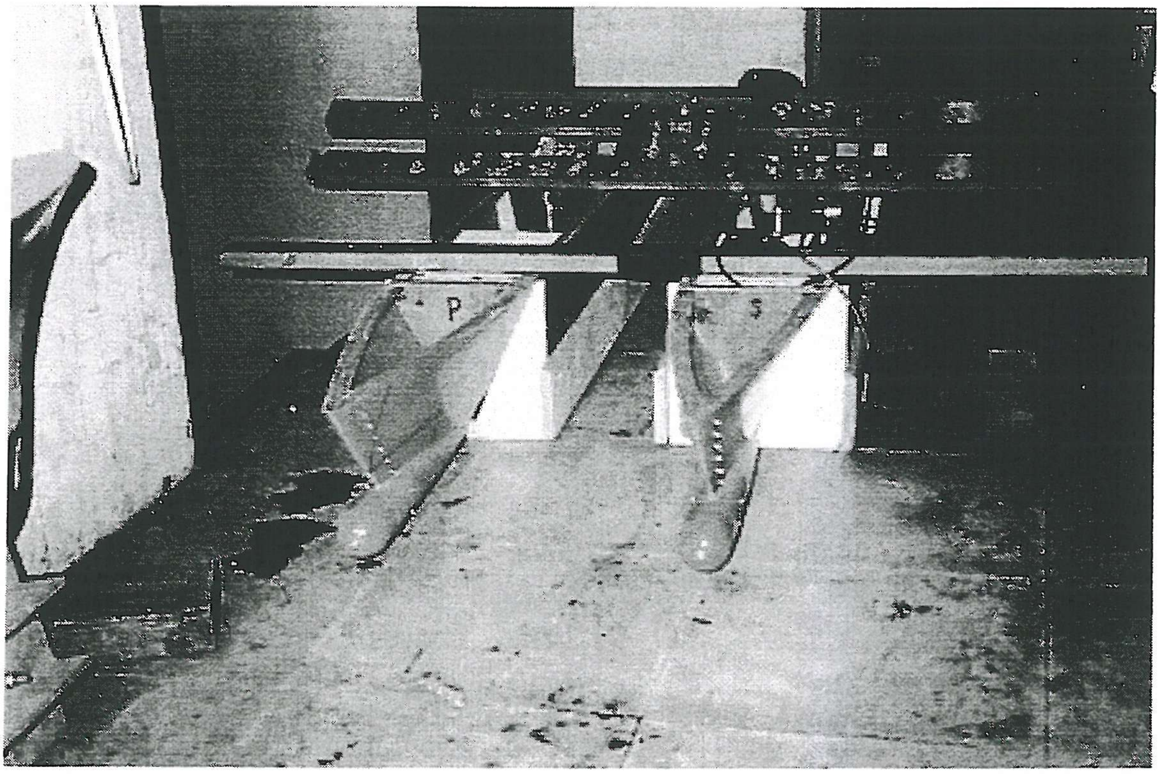

Figure 3.7: Model ready for testing

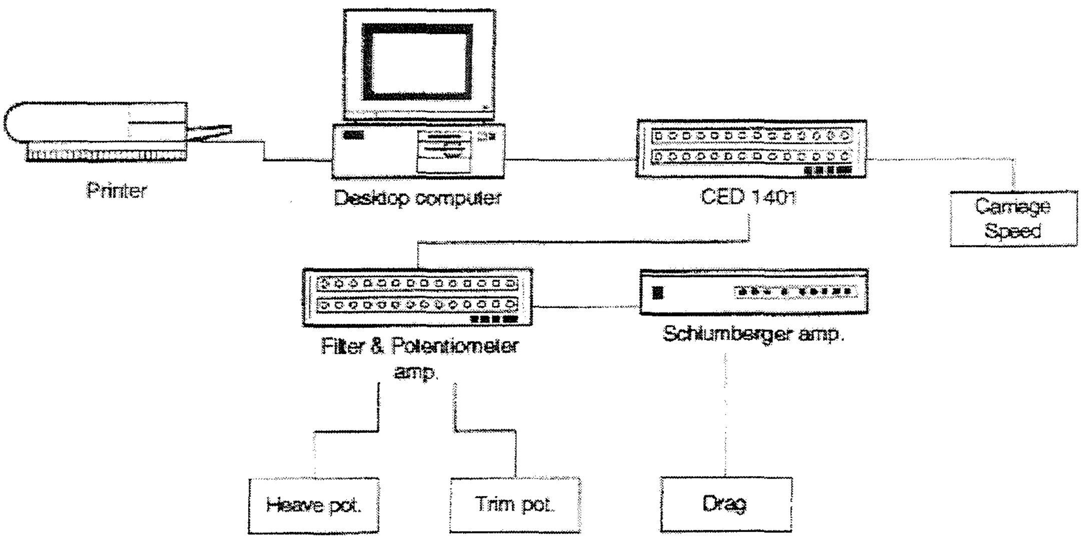

Figure 3.8: Schematic of data acquisition system

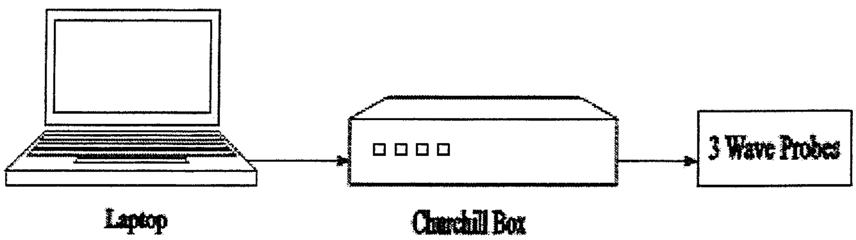

Figure 3.9: Schematic of wash measurement system

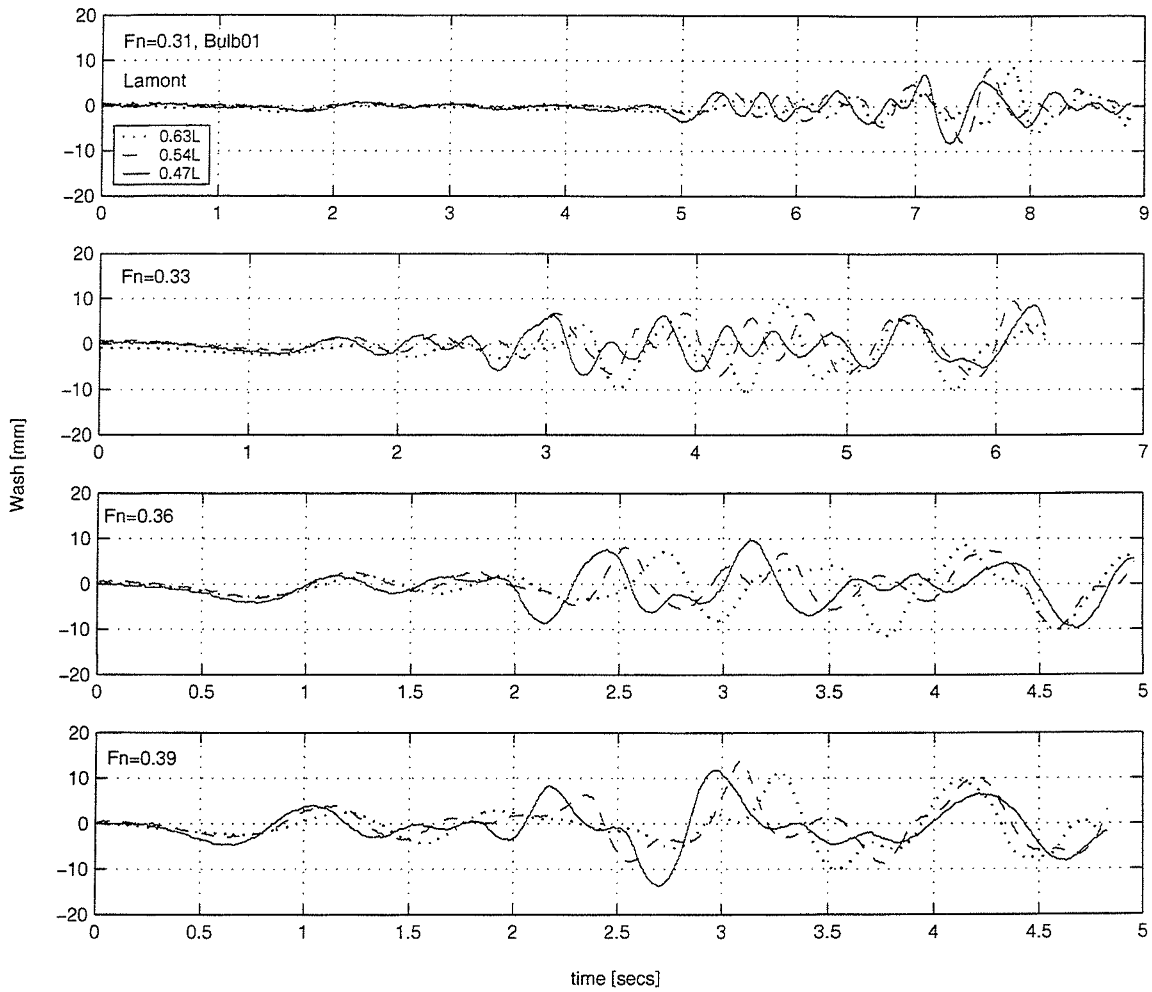

Figure 3.10: Catamaran s/L=0.2 with bulb01: Experimental wash for F_n=0.31-0.39

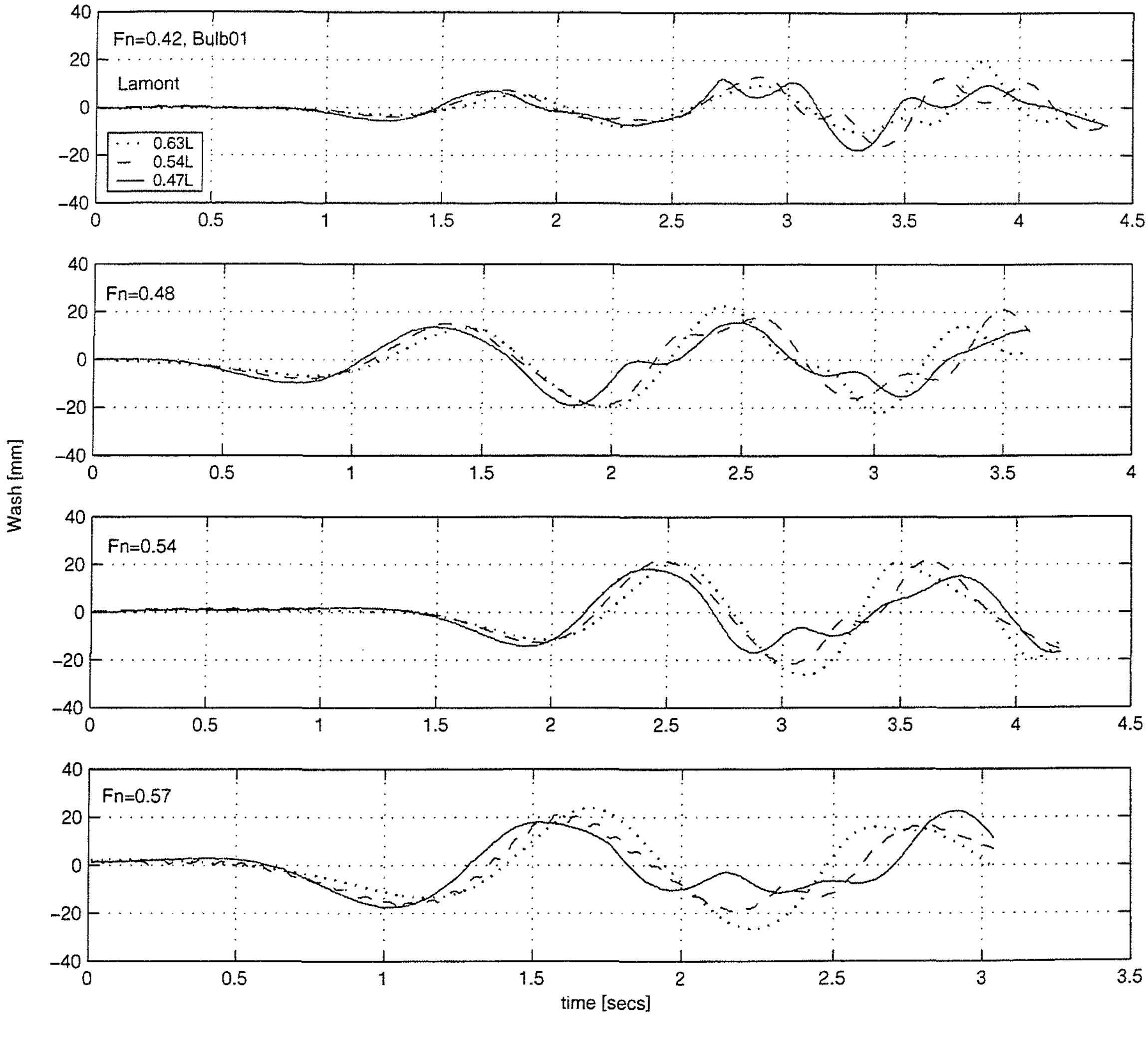

Figure 3.11: Catamaran s/L=0.2 with bulb01: Experimental wash for F_n=0.42-0.57

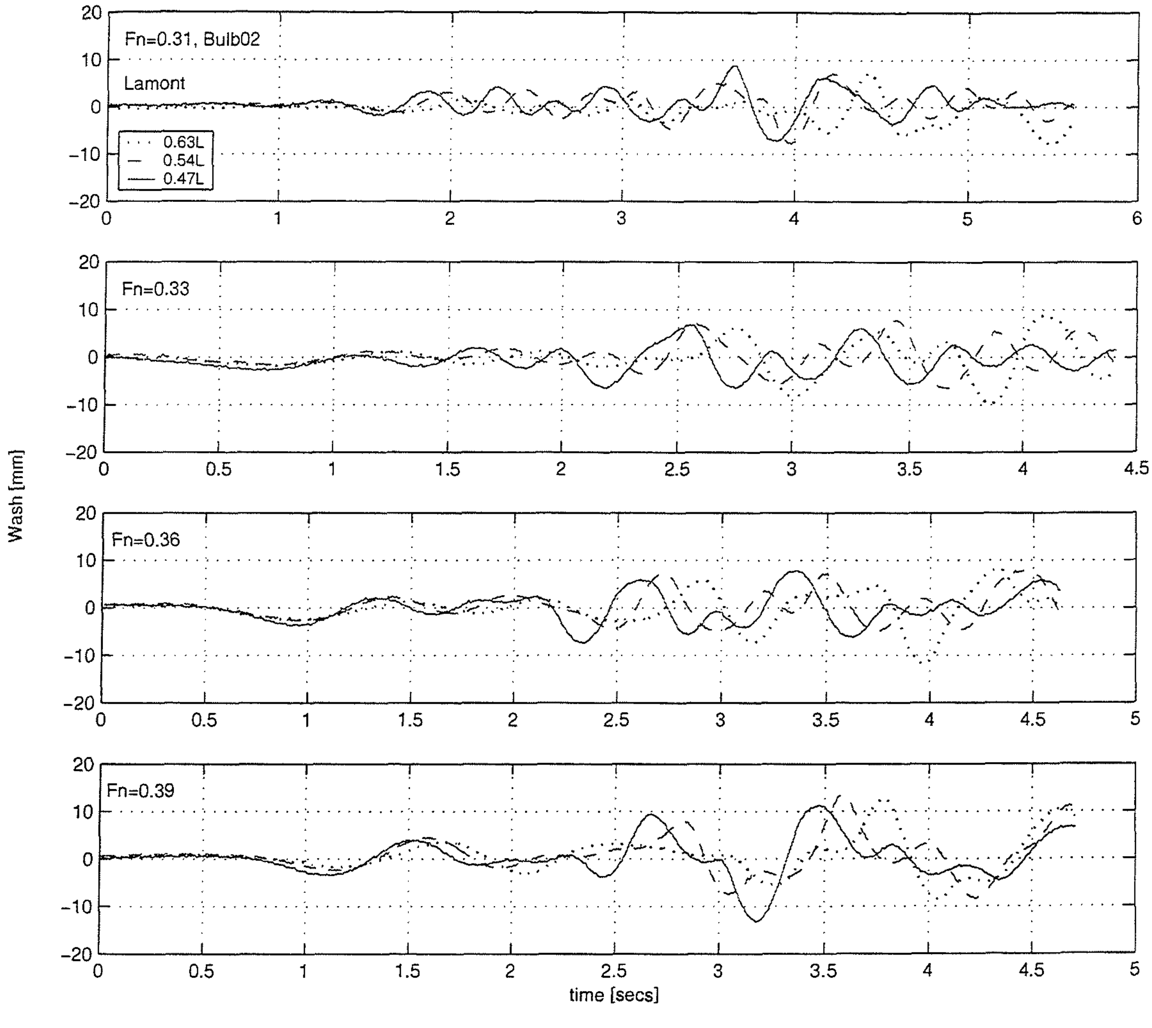

Figure 3.12: Catamaran s/L=0.2 with bulb02: Experimental wash for F_n=0.31-0.39

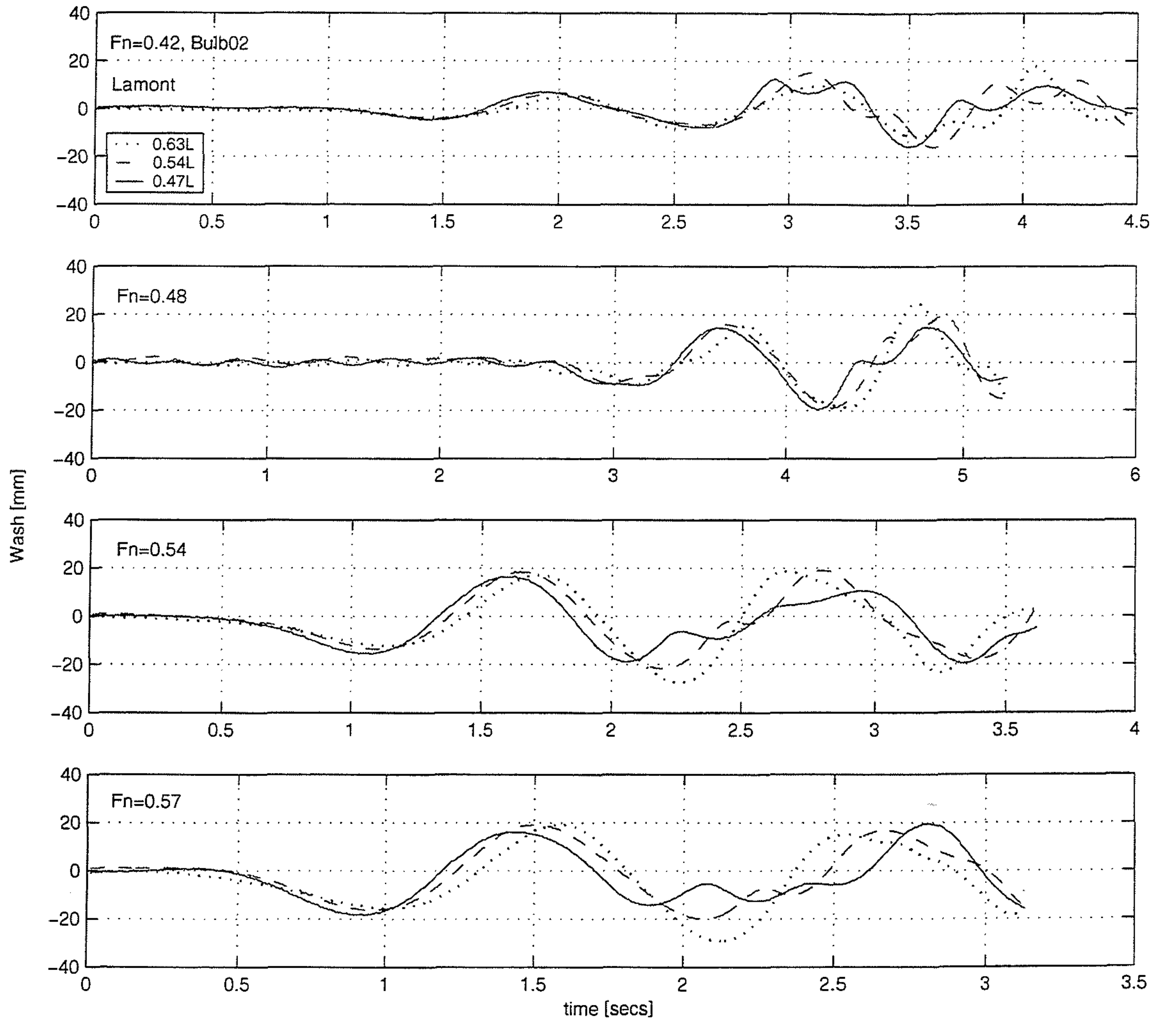

Figure 3.13: Catamaran s/L=0.2 with bulb02: Experimental wash for F_n=0.42-0.57

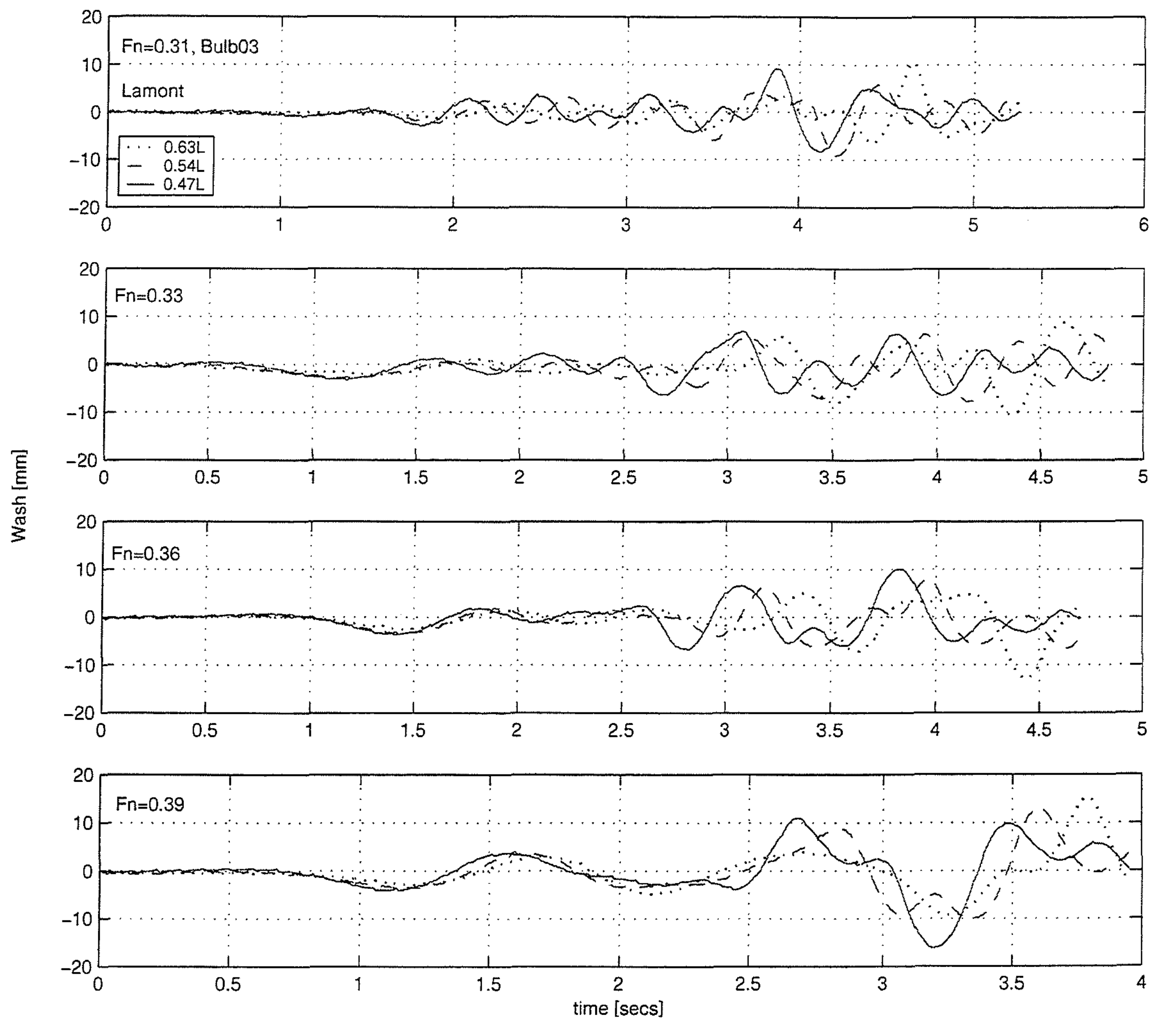

Figure 3.14: Catamaran s/L=0.2 with bulb03: Experimental wash for F_n=0.31-0.39

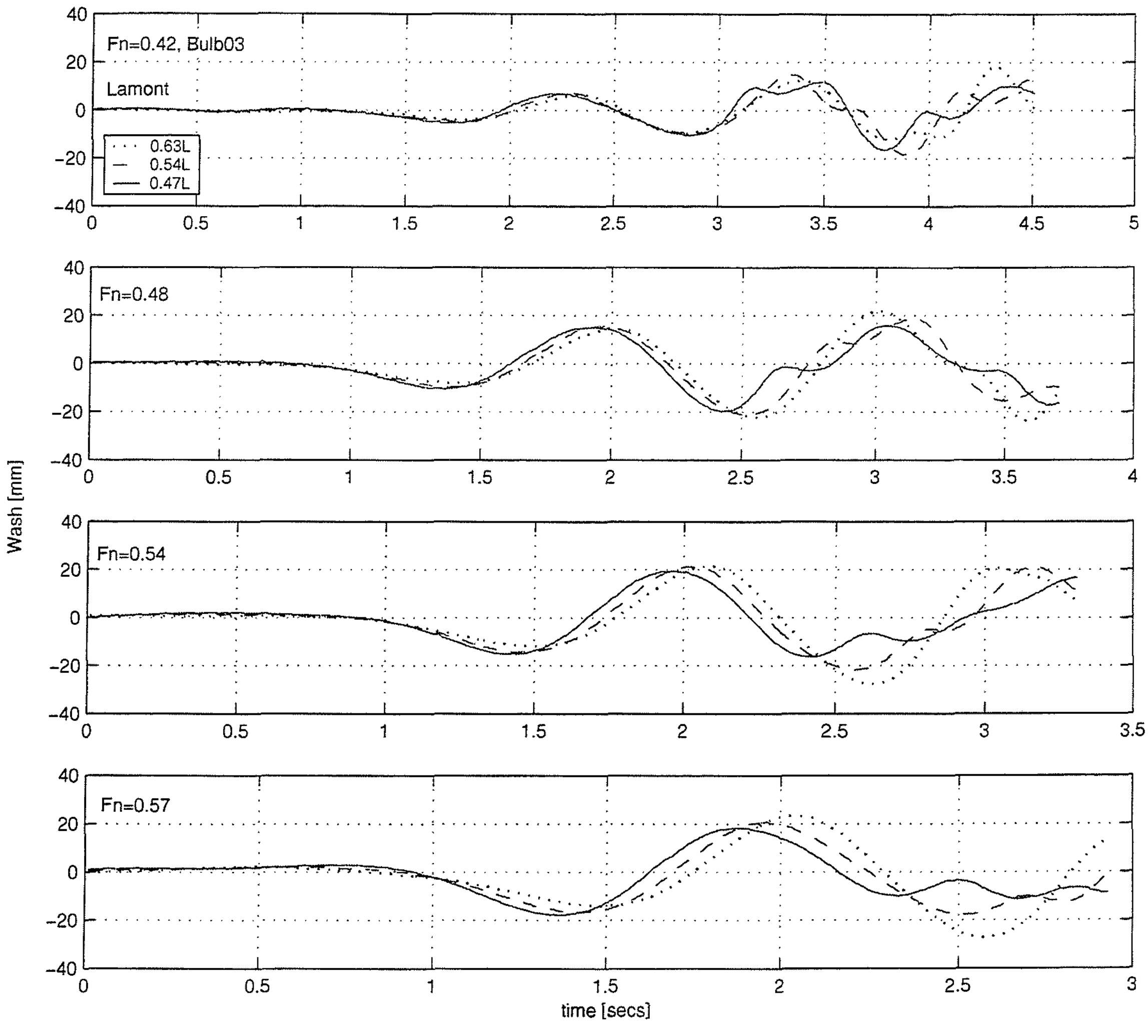

Figure 3.15: Catamaran s/L=0.2 with bulb03: Experimental wash for F_n=0.42-0.57

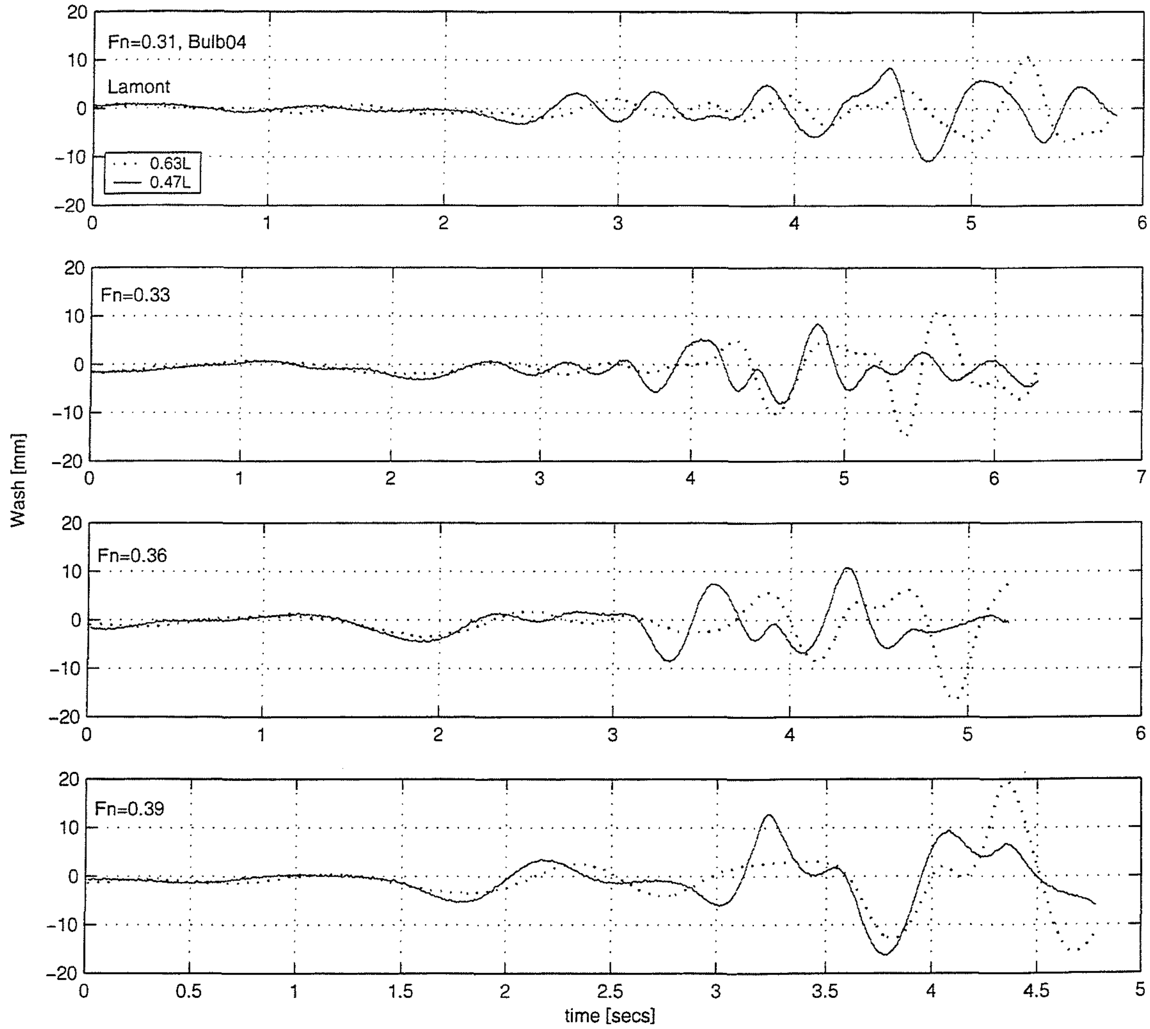

Figure 3.16: Catamaran s/L=0.2 with bulb04: Experimental wash for F_n=0.31-0.39

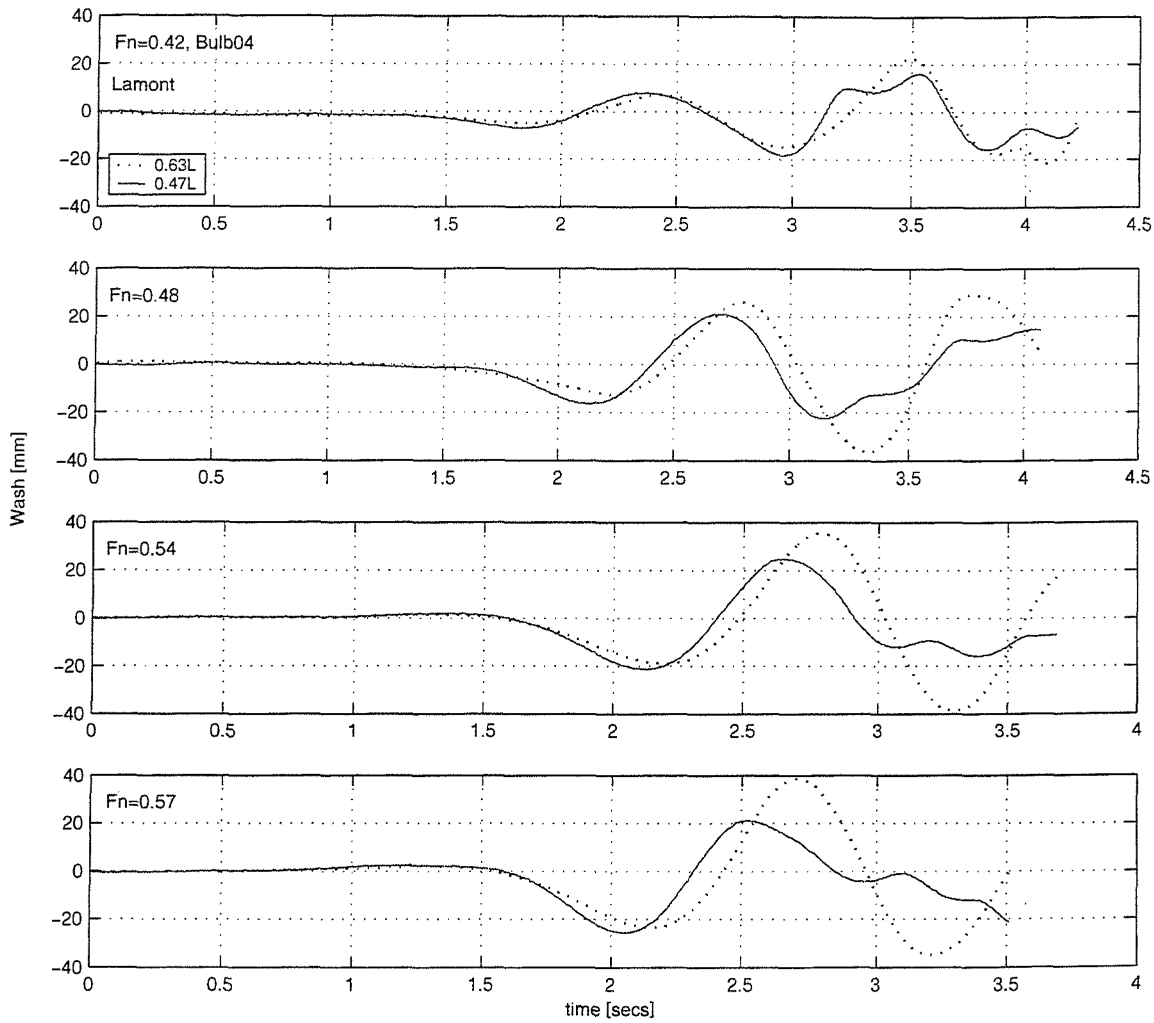

Figure 3.17: Catamaran s/L=0.2 with bulb04: Experimental wash for F_n=0.42-0.57

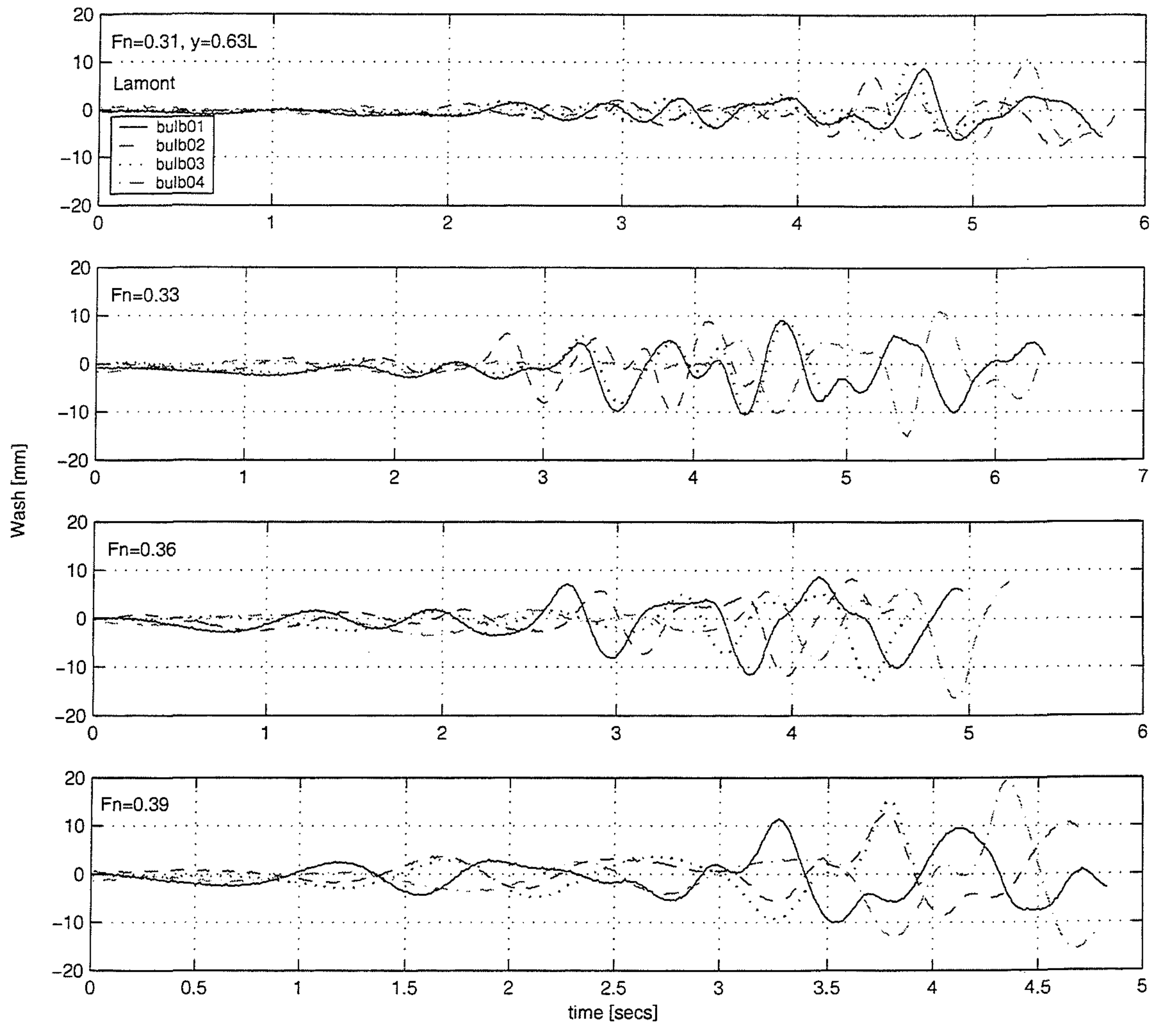

Figure 3.18: Catamaran s/L=0.2:Experimental wash at $y = 0.63L$ for F_n=0.31-0.39

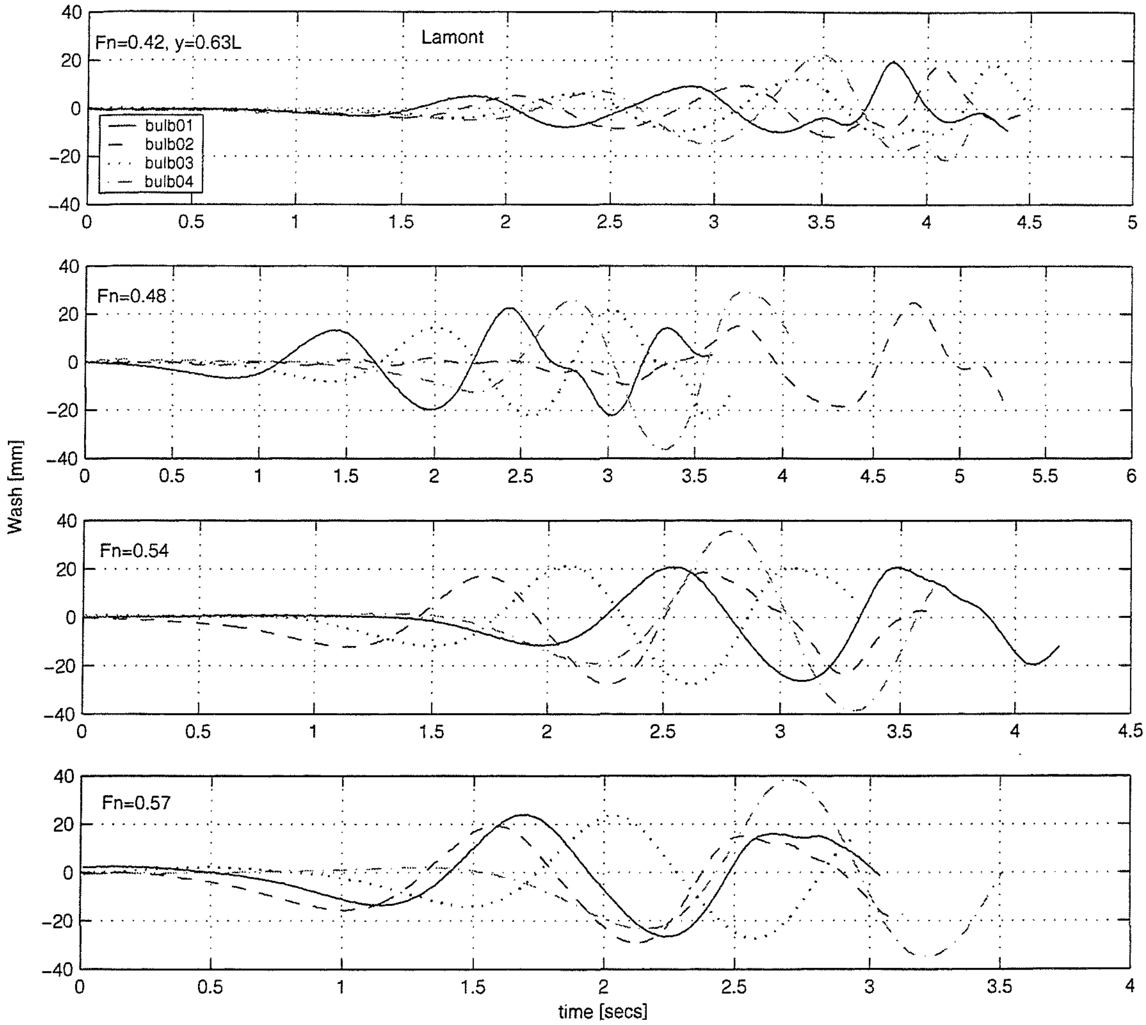

Figure 3.19: Catamaran s/L=0.2: Experimental wash at $y = 0.63L$ for F_n=0.42-0.57

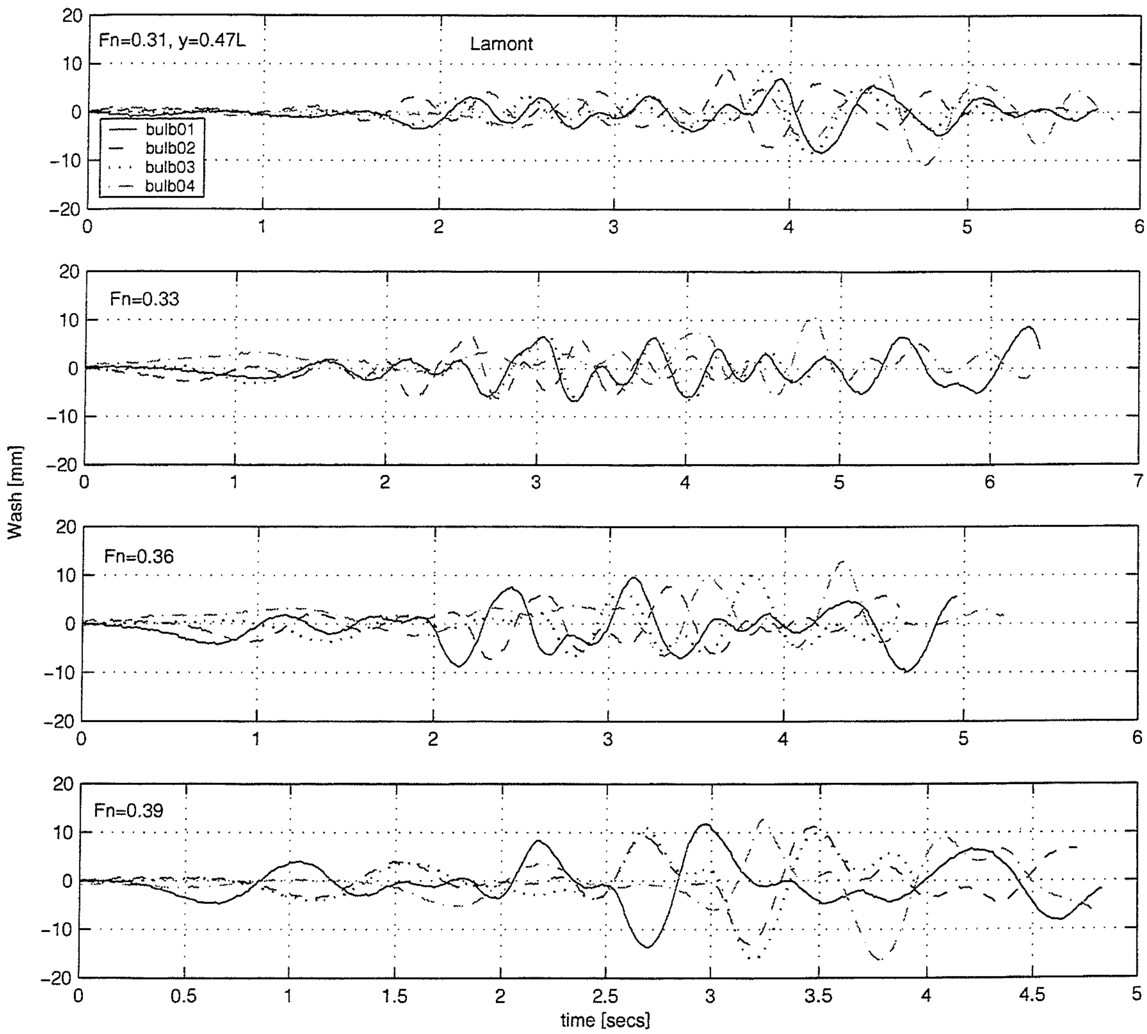

Figure 3.20: Catamaran s/L=0.2: Experimental wash at $y = 0.47L$ for F_n=0.31-0.39

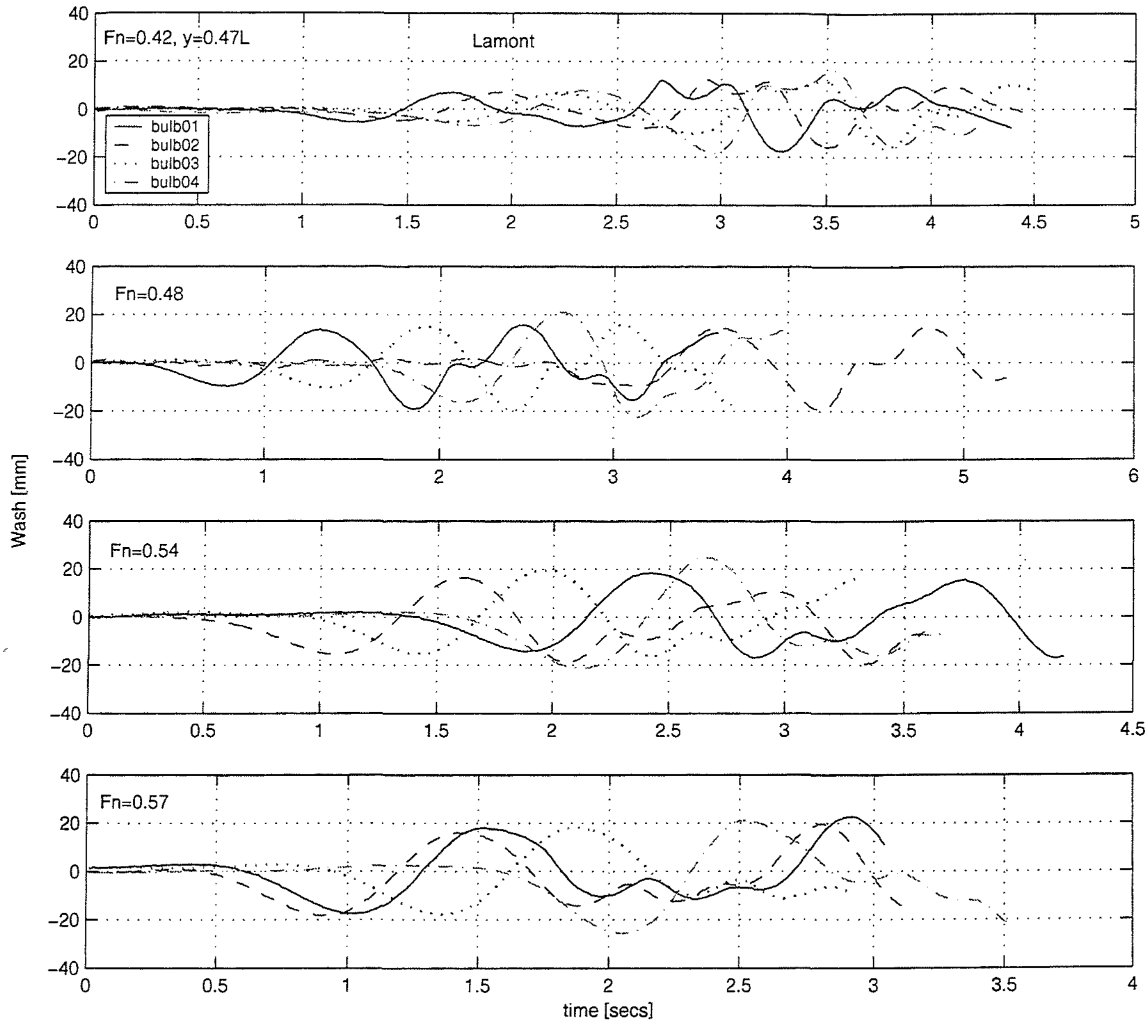

Figure 3.21: Catamaran s/L=0.2: Experimental wash at $y = 0.47L$ for F_n=0.42-0.57

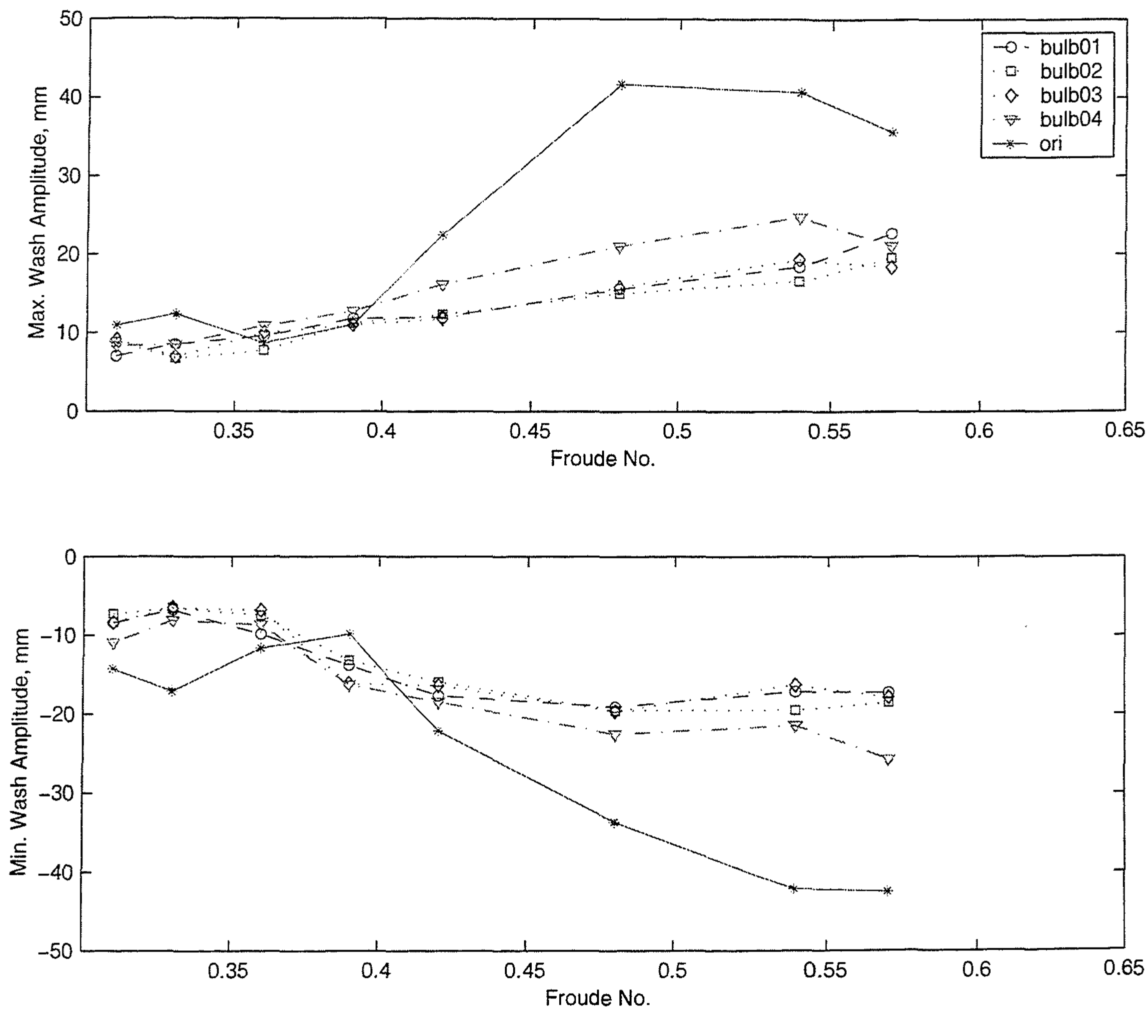

Figure 3.22: Catamaran s/L=0.2: Maximum and Minimum Wash Amplitude at $y = 0.47L$

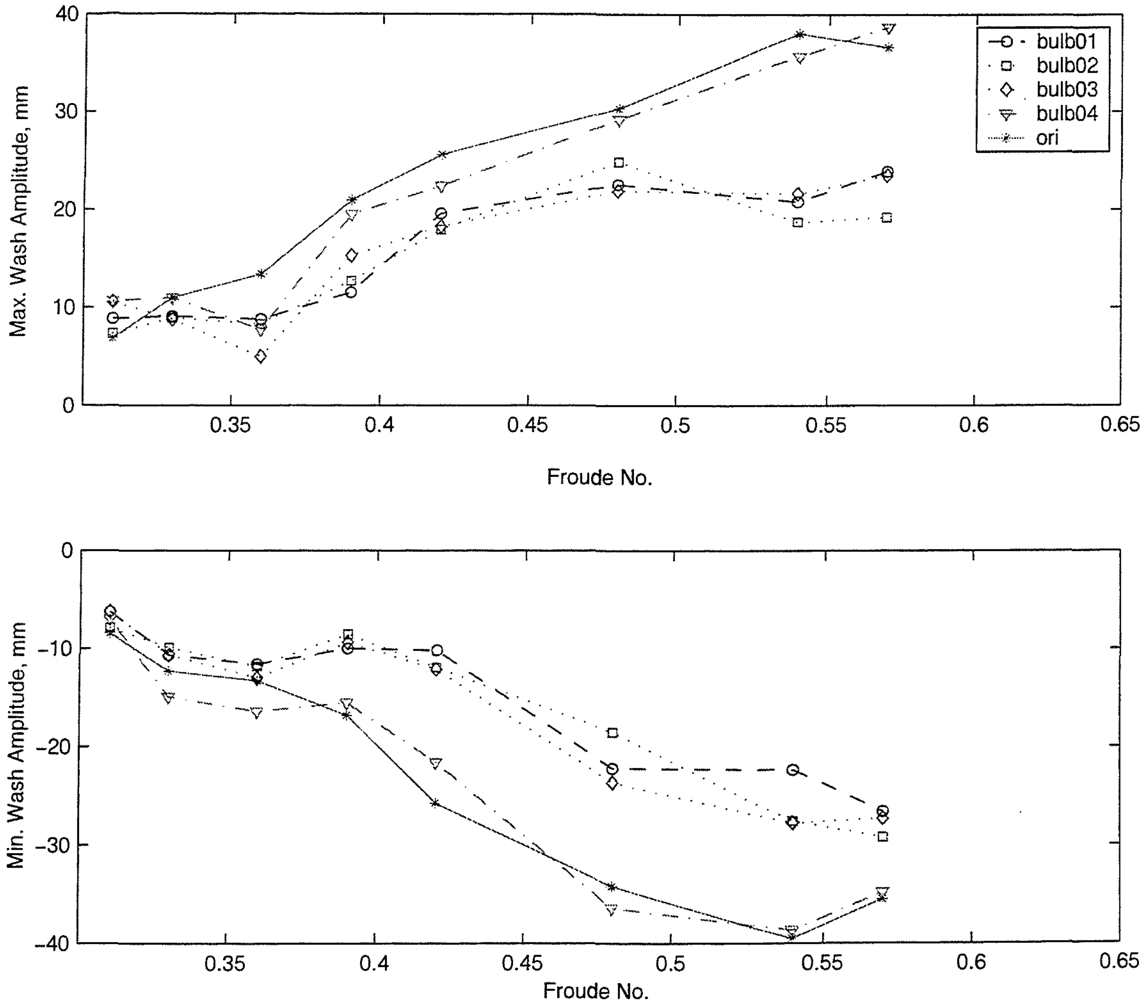

Figure 3.23: Catamaran s/L=0.2: Maximum and Minimum Wash Amplitude at $y = 0.63L$

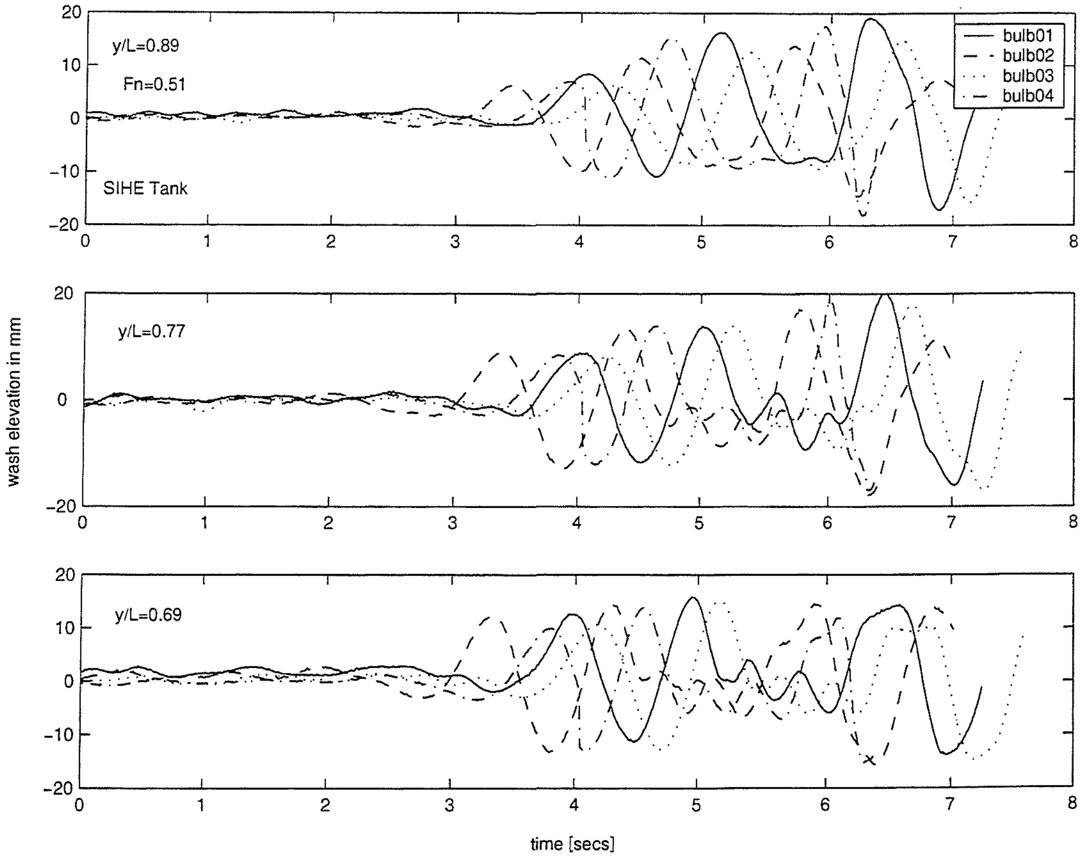

Figure 3.24: Catamaran s/L=0.2: Experimental wash at three different probes locations for F_n=0.51

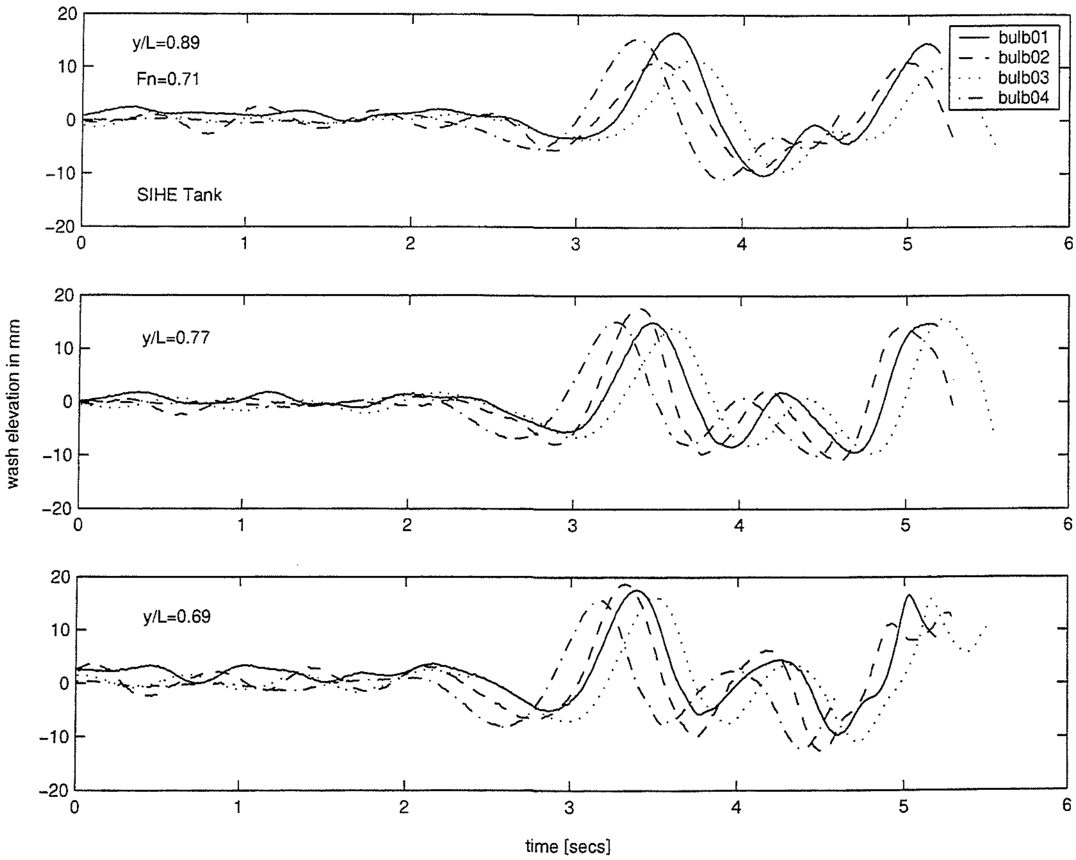

Figure 3.25: Catamaran s/L=0.2: Experimental wash at three different probes locations for F_n=0.71

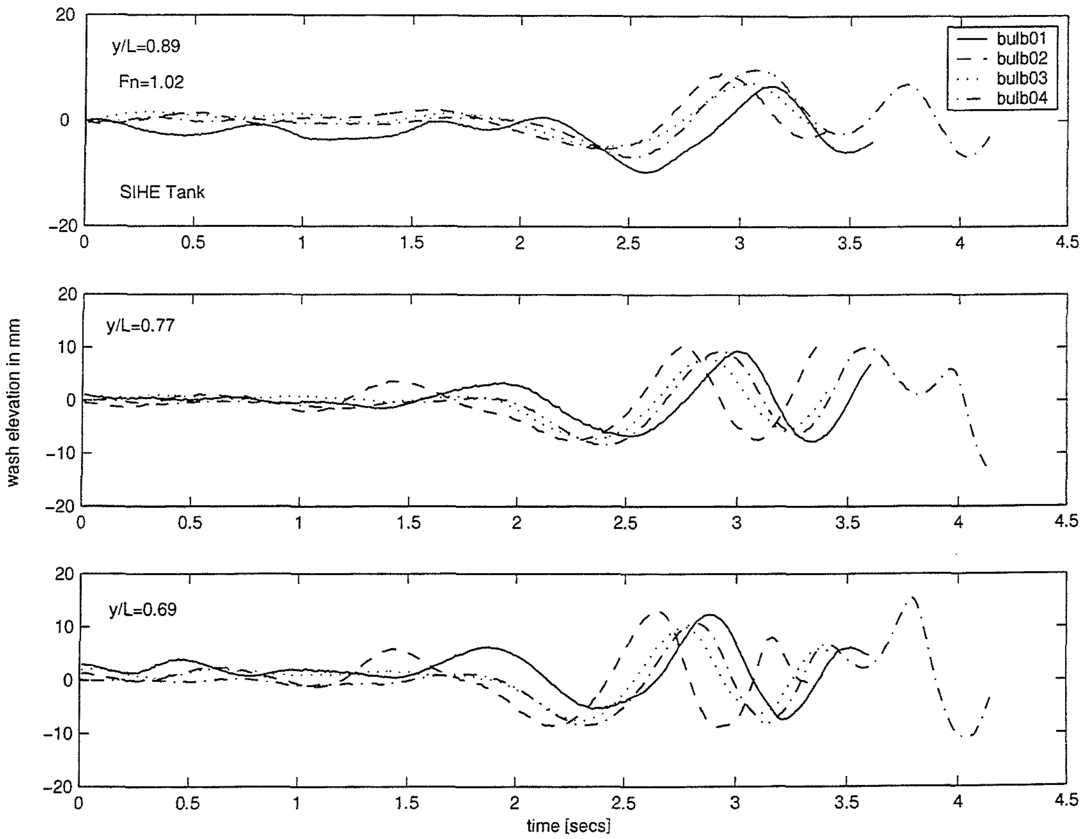

Figure 3.26: Catamaran s/L=0.2: Experimental wash at three different probes locations for F_n=1.02

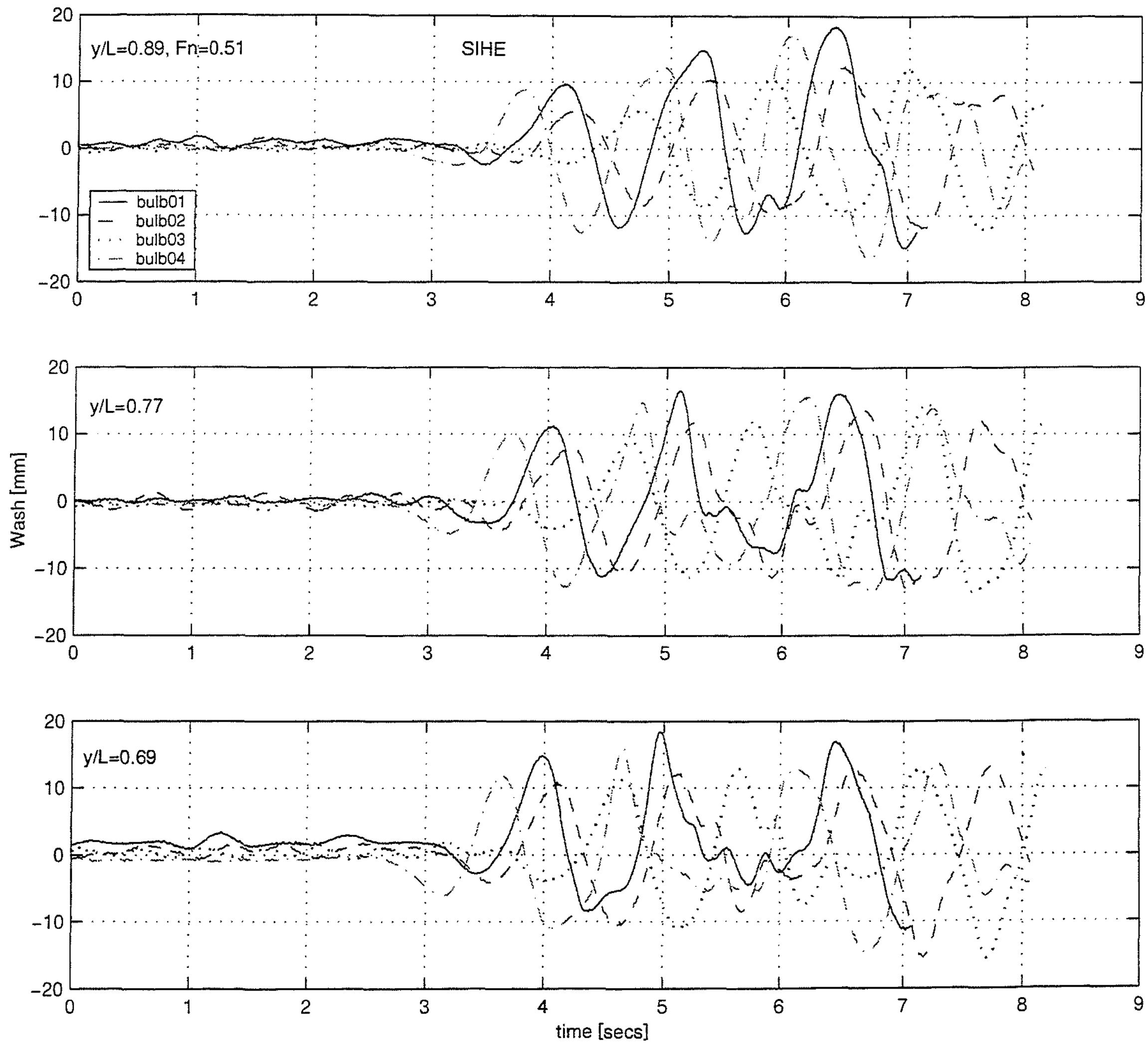

Figure 3.27: Catamaran s/L=0.3: Experimental wash at three different probes locations for F_n=0.51

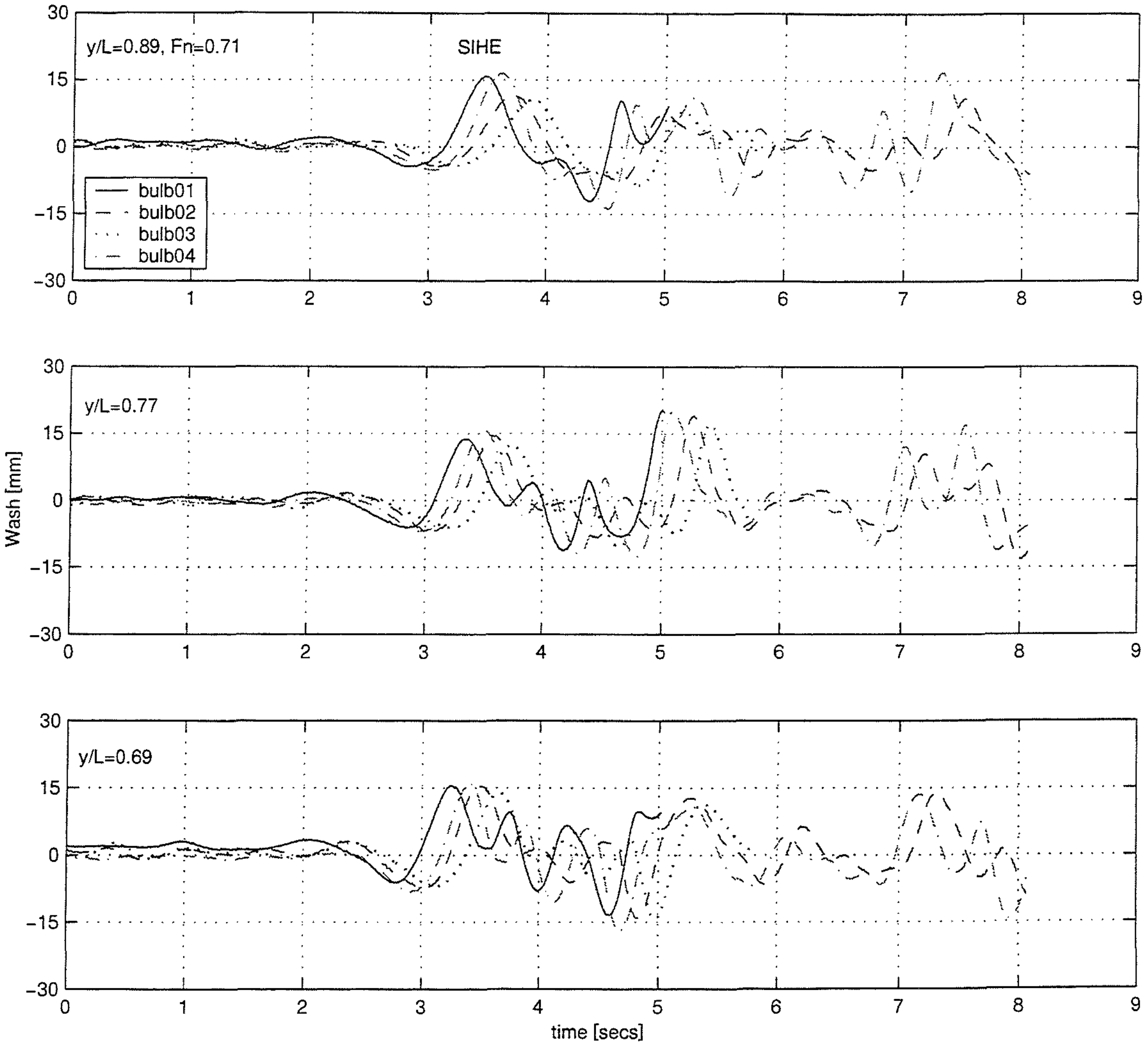

Figure 3.28: Catamaran s/L=0.3: Experimental wash at three different probes locations for F_n=0.71

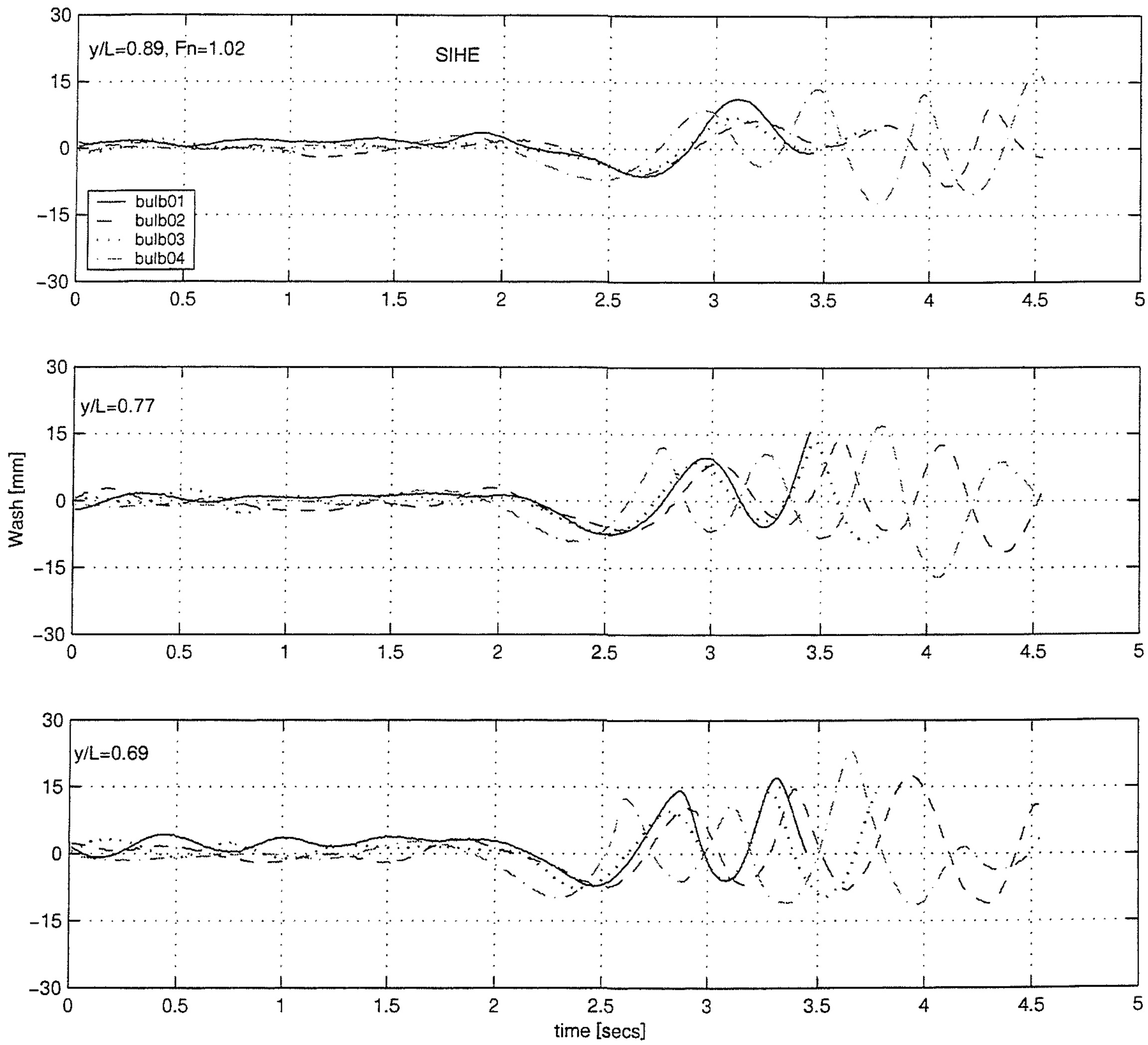

Figure 3.29: Catamaran s/L=0.3: Experimental wash at three different probes locations for F_n=1.02

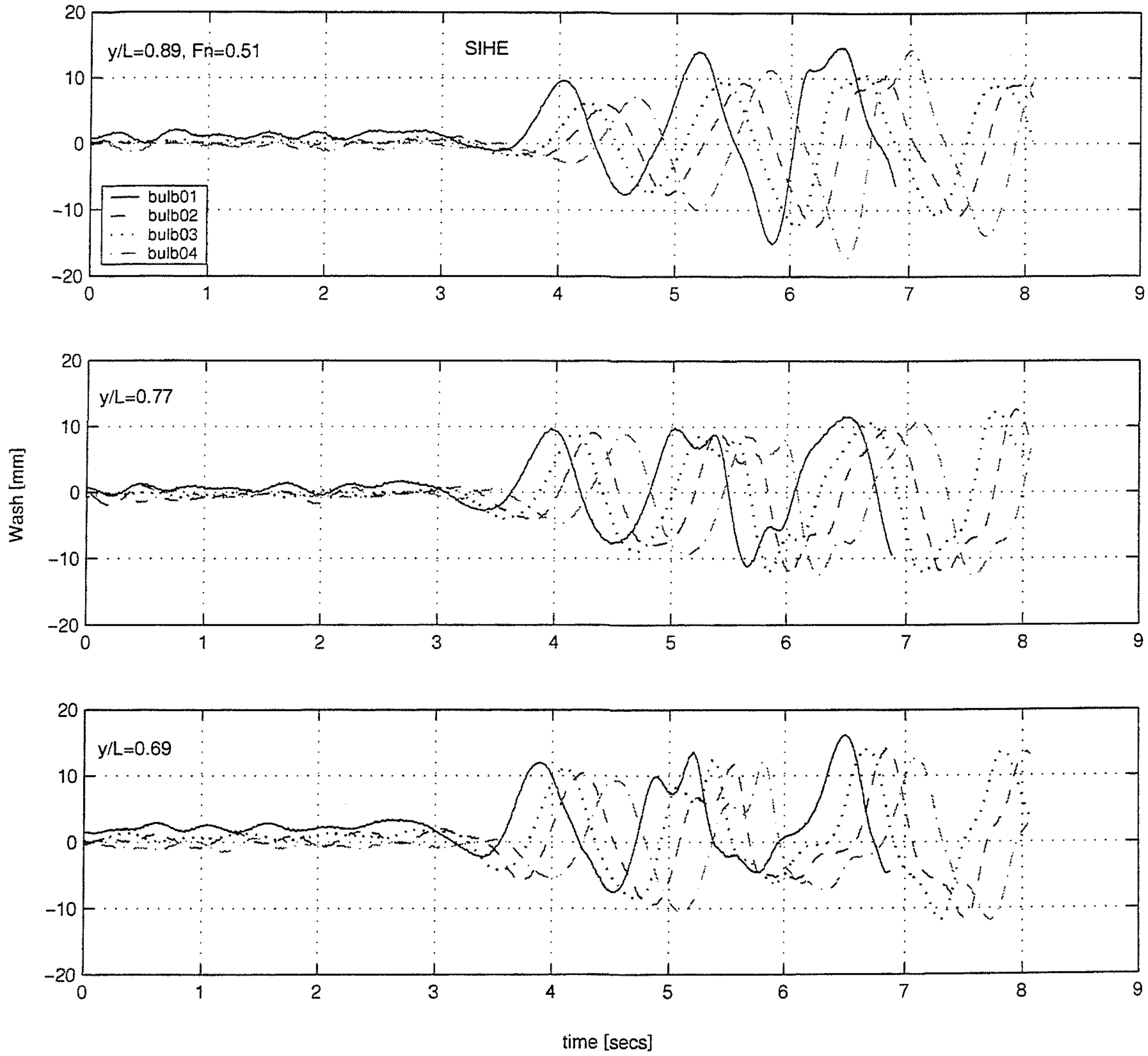

Figure 3.30: Catamaran s/L=0.4: Experimental wash at three different probes locations for F_n=0.51

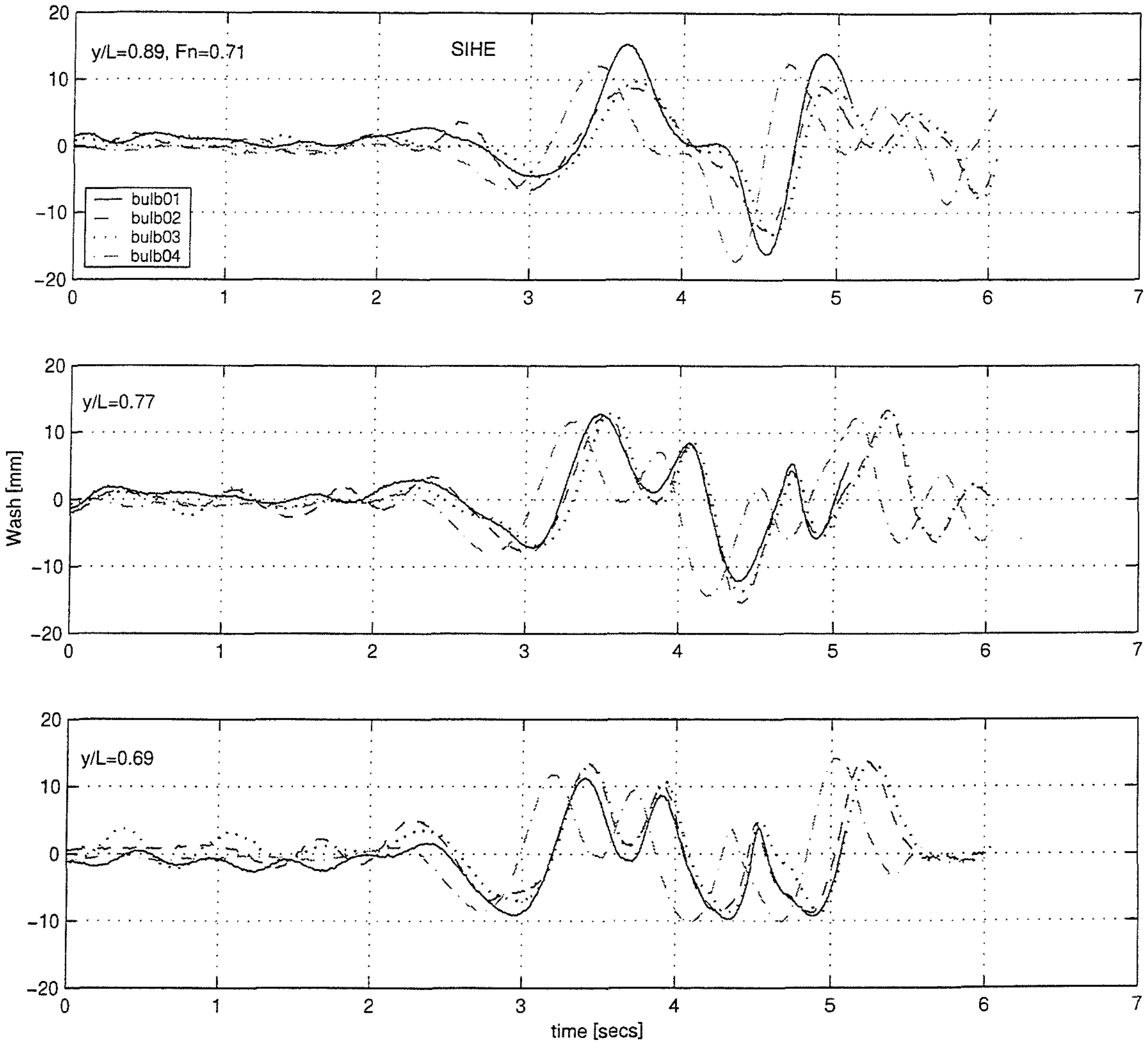

Figure 3.31: Catamaran s/L=0.4: Experimental wash at three different probes locations for F_n=0.71

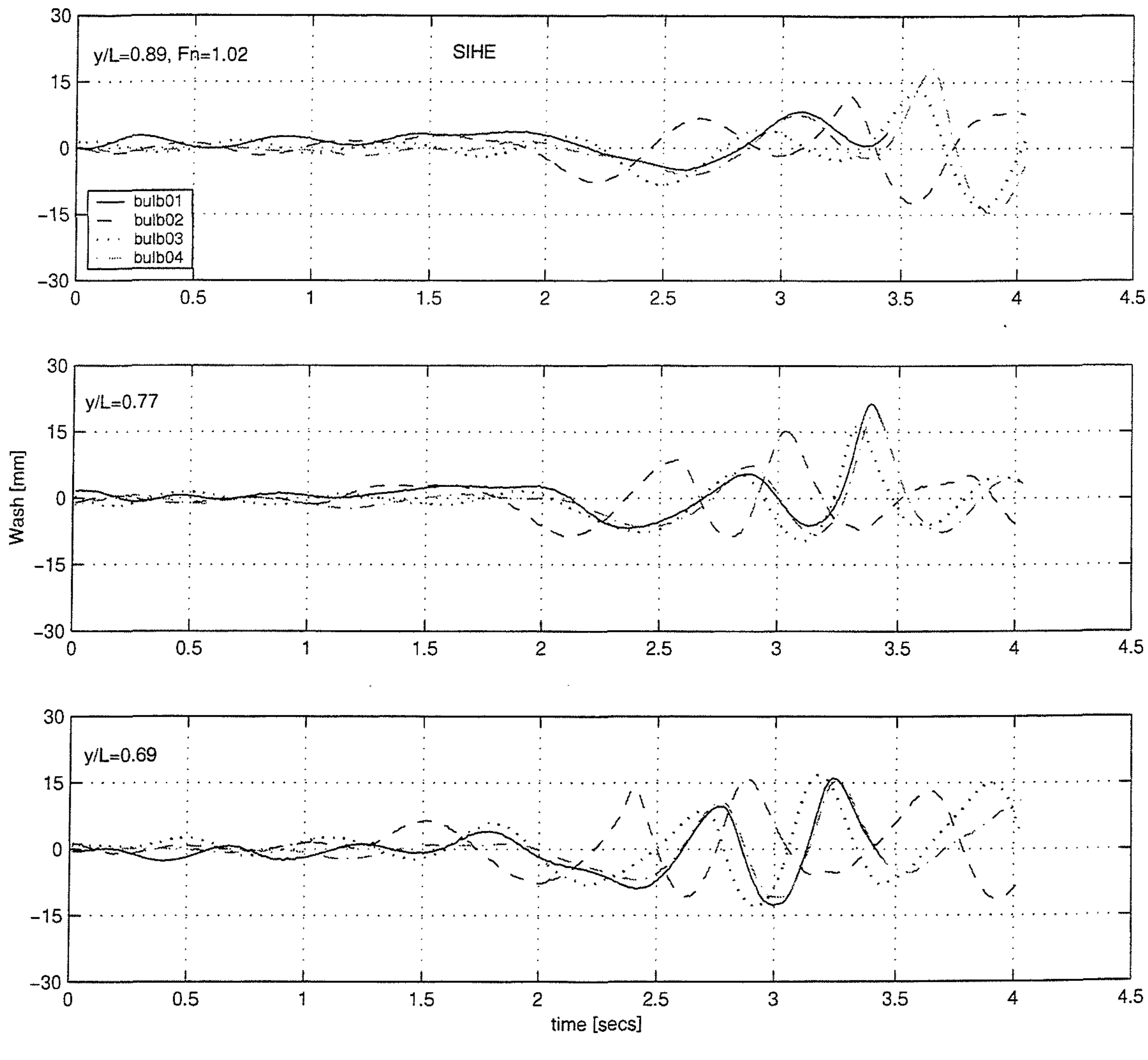

Figure 3.32: Catamaran s/L=0.4: Experimental wash at three different probes locations for F_n=1.02

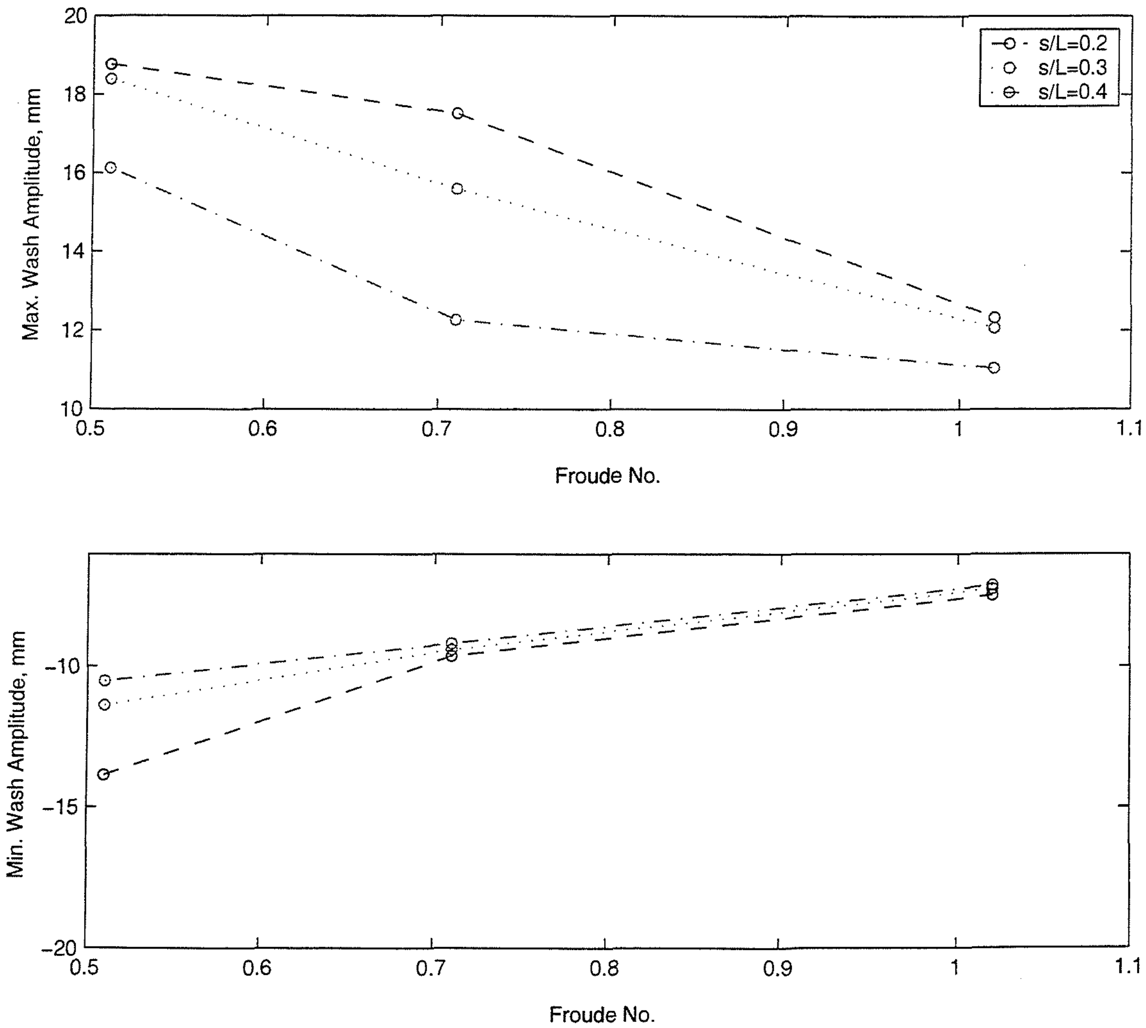

Figure 3.33: Catamaran with bulb01: The Effect of s/L on Wash at $y = 0.69L$

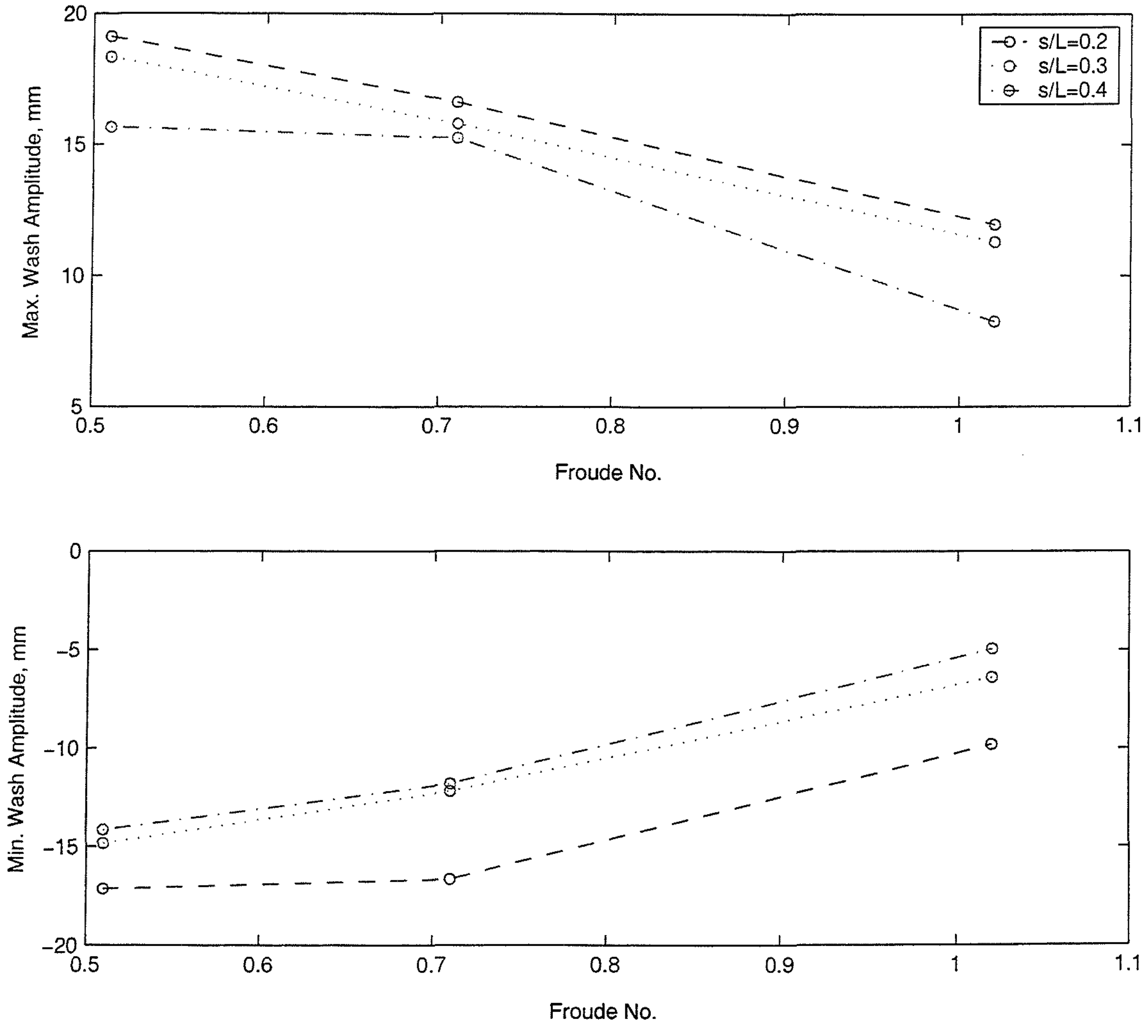

Figure 3.34: Catamaran with bulb01: The Effect of s/L on Wash at $y = 0.89L$

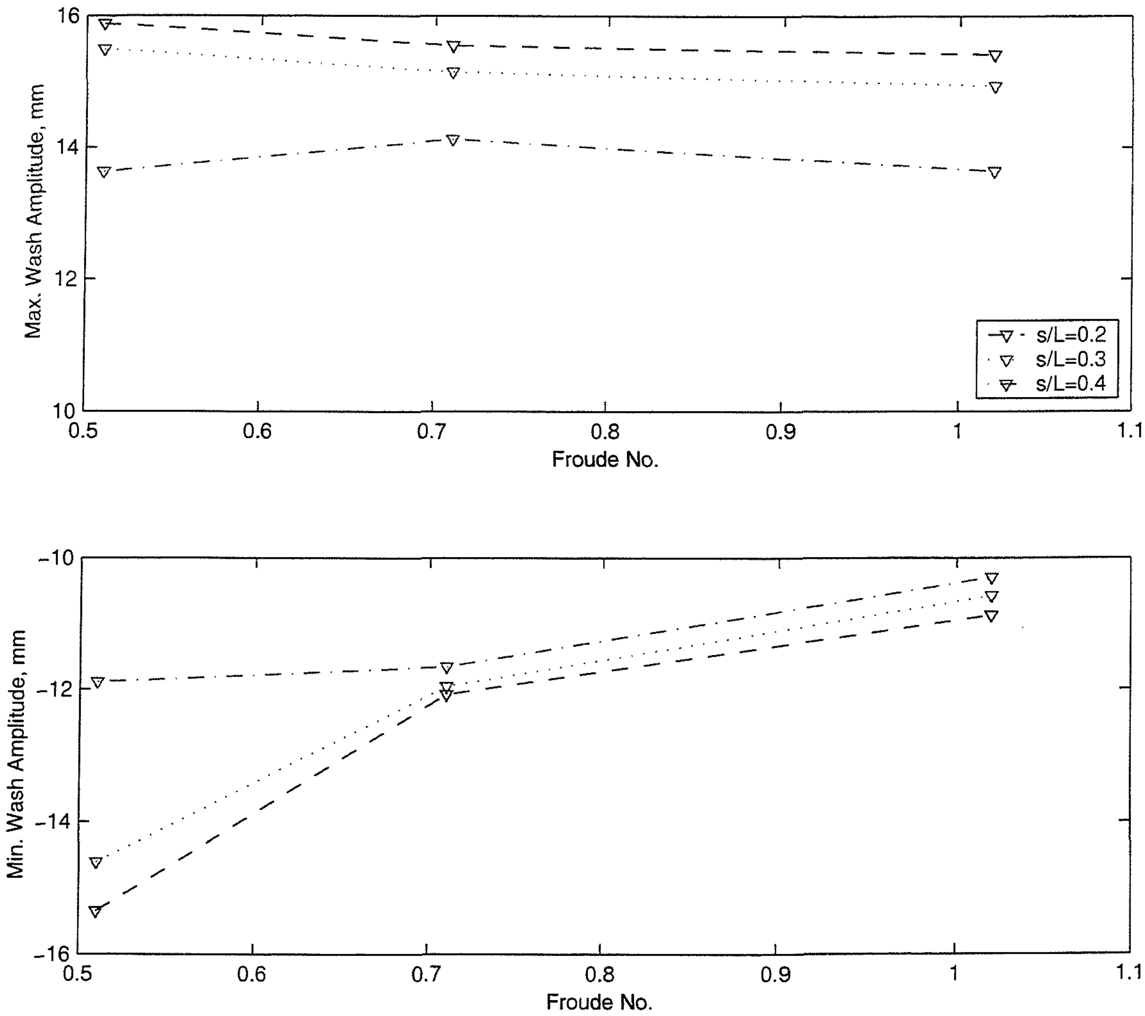

Figure 3.35: Catamaran with bulb04: The Effect of s/L on Wash at $y = 0.69L$

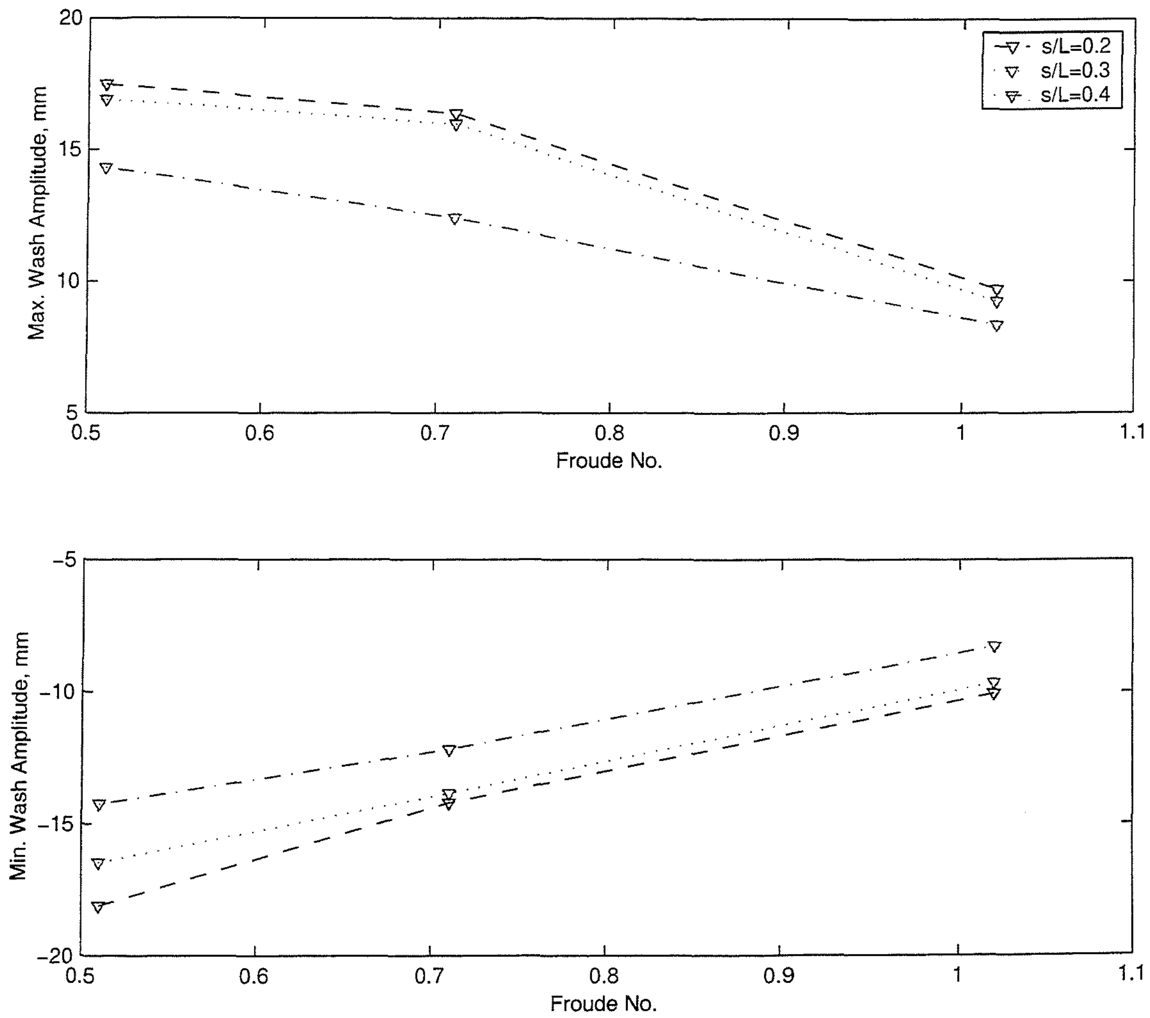

Figure 3.36: Catamaran with bulb04: The Effect of s/L on Wash at $y = 0.89L$

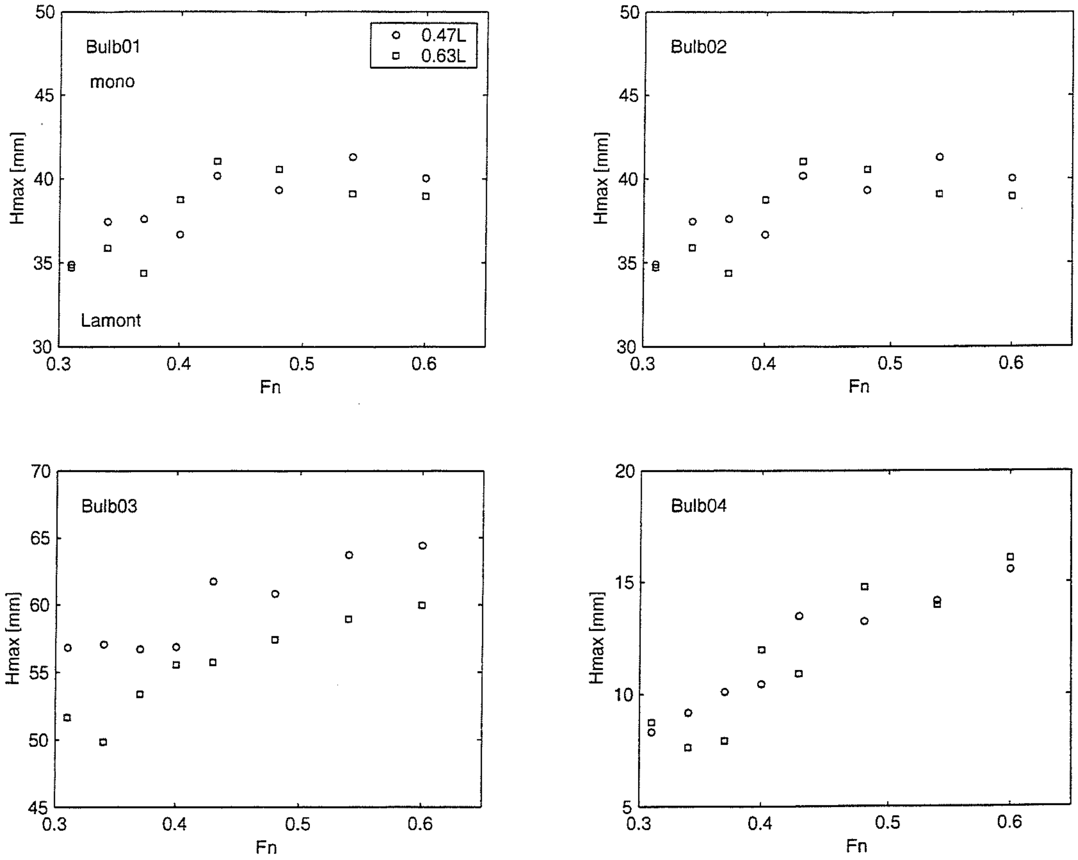

Figure 3.37: Monohull: Maximum wash height by different bulbs

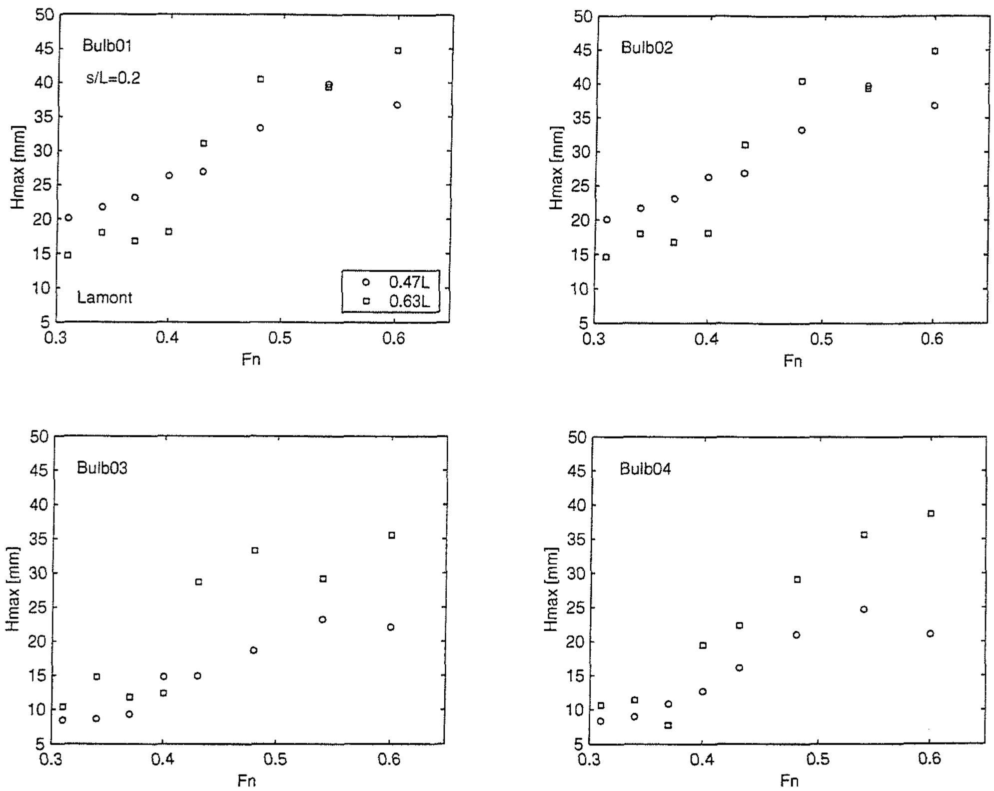

Figure 3.38: Catamaran s/L=0.2: Maximum wash height by different bulbs

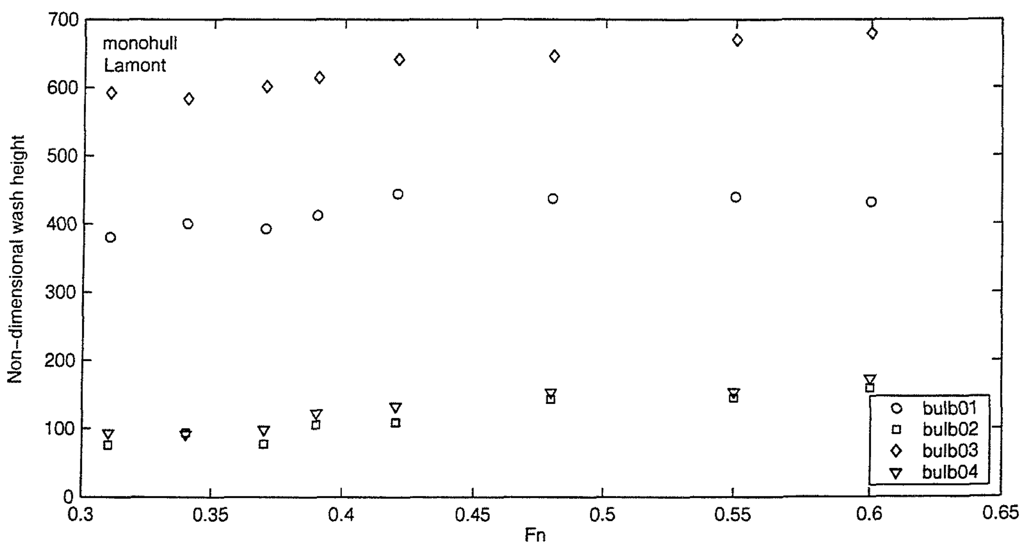

Figure 3.39: Monohull: Non-dimensional maximum wash height

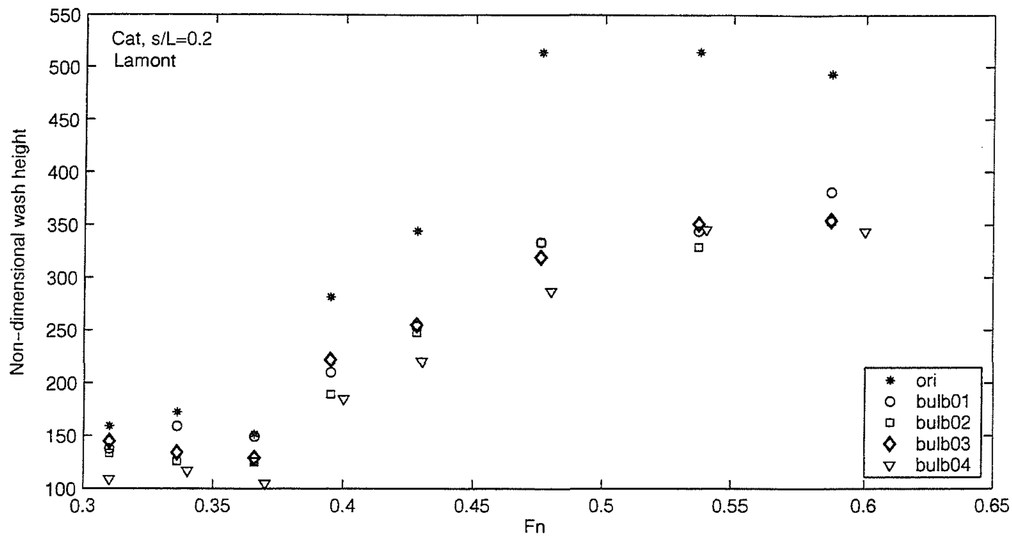

Figure 3.40: Catamaran s/L=0.2: Non-dimensional maximum wash height

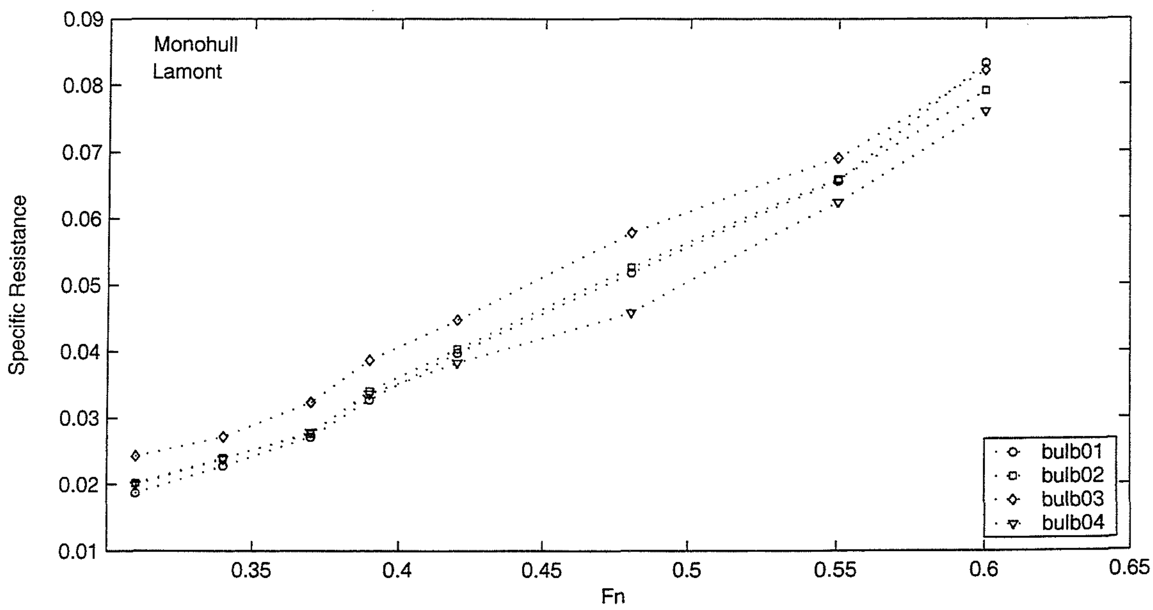

Figure 3.41: Monohull: Specific Resistance

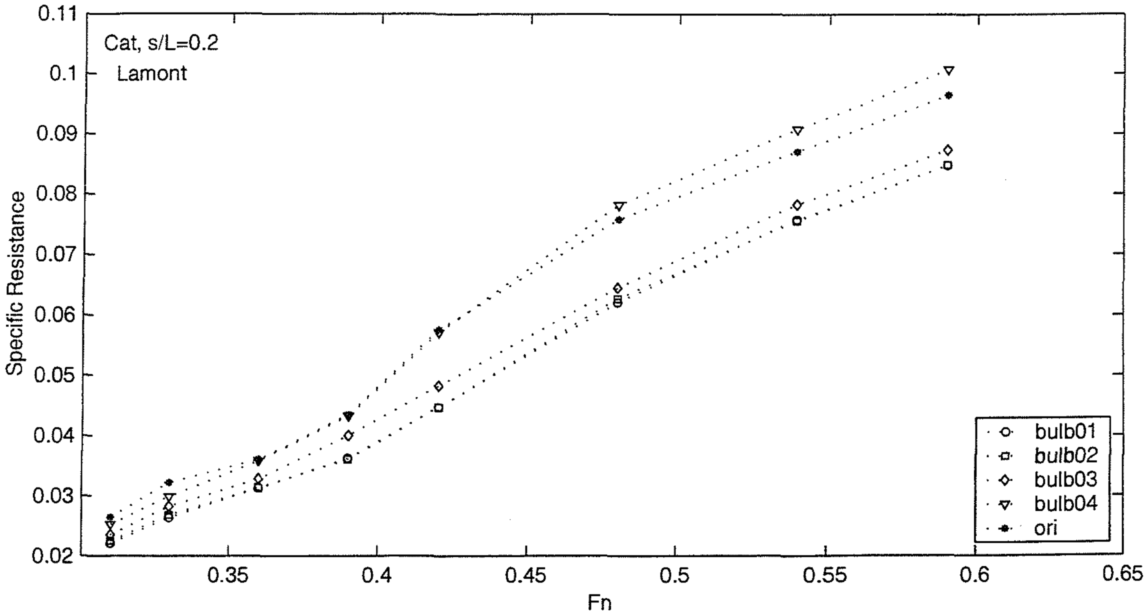

Figure 3.42: Catamaran s/L=0.2: Specific Resistance

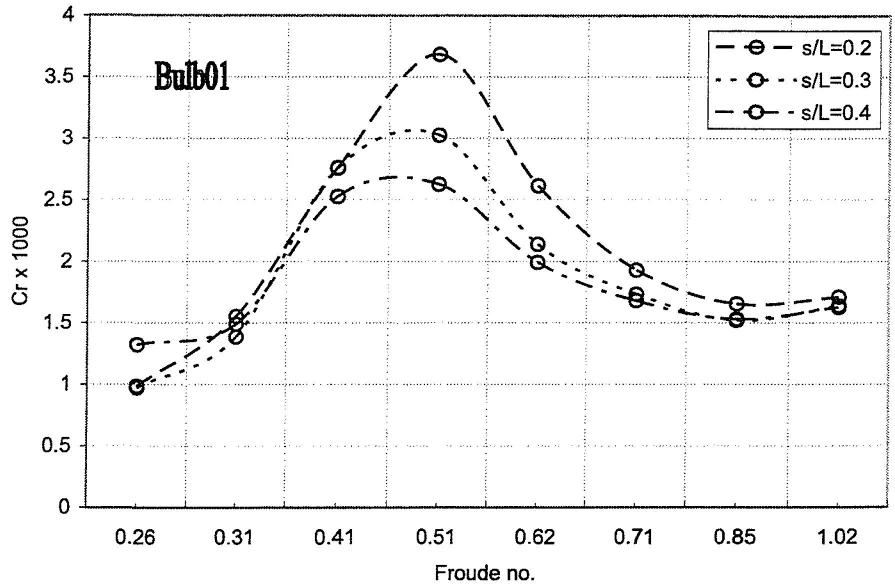

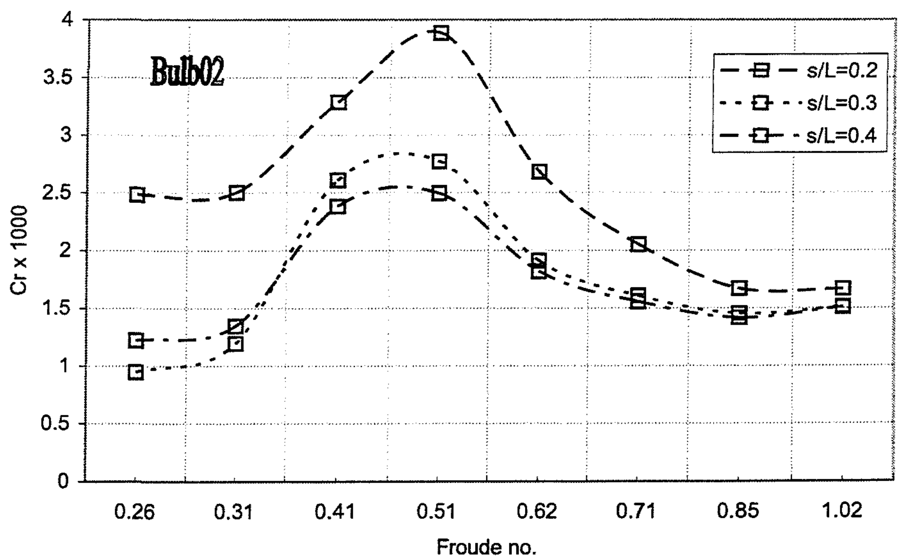

Figure 3.43: Model 5b with bulb01 and bulb02: Effect of s/L

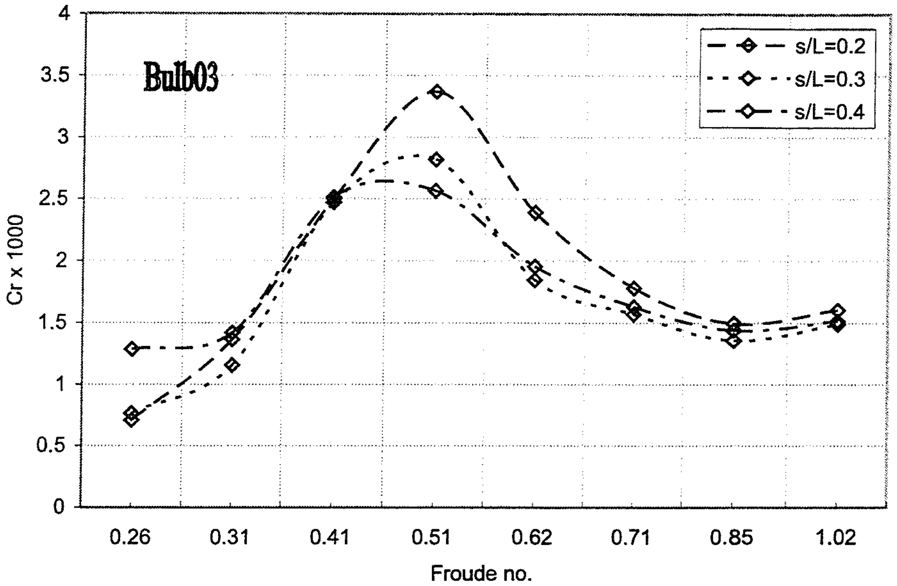

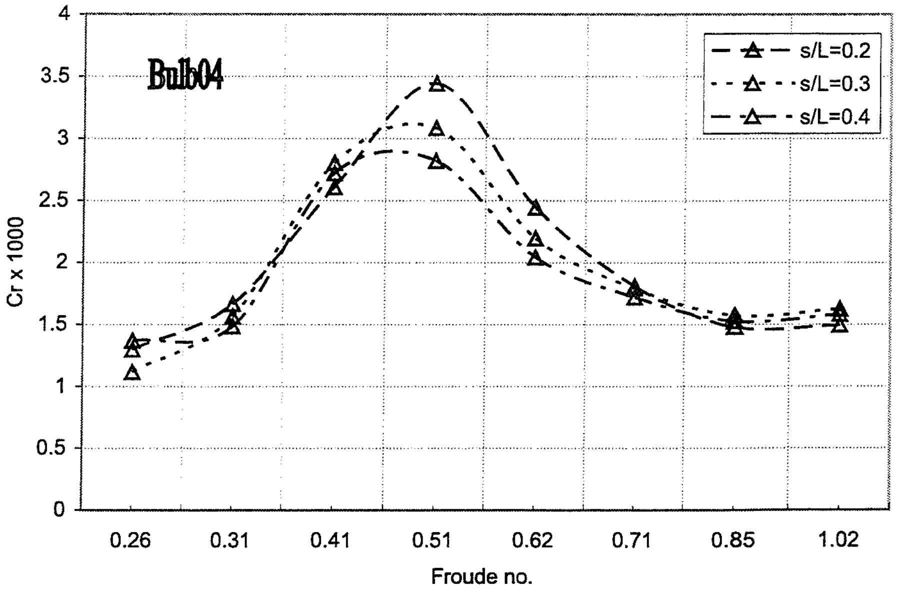

Figure 3.44: Model 5b with bulb03 and bulb04: Effect of s/L

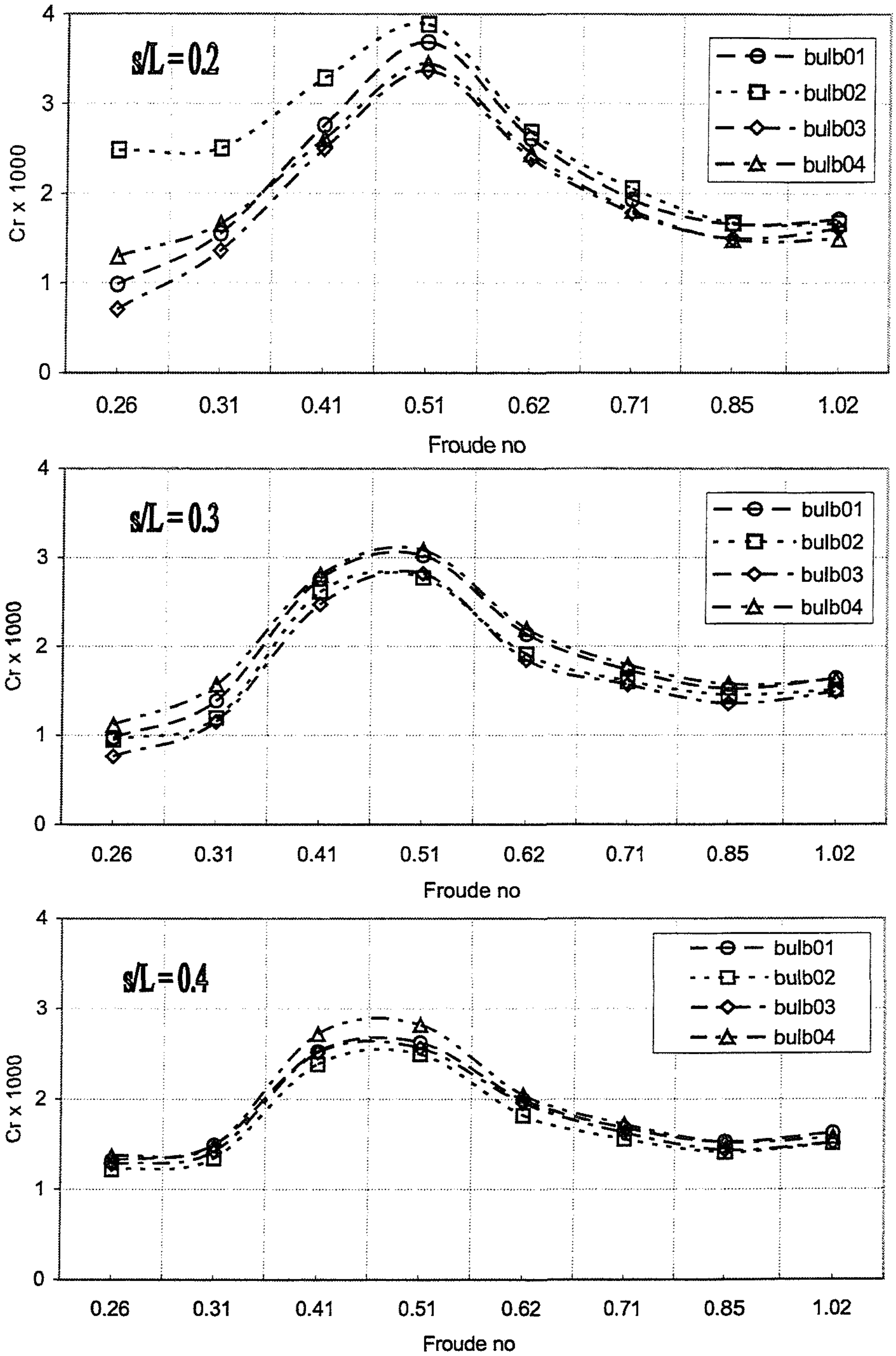

Figure 3.45: The Effect of Bulbous Bow on Residuary Resistance

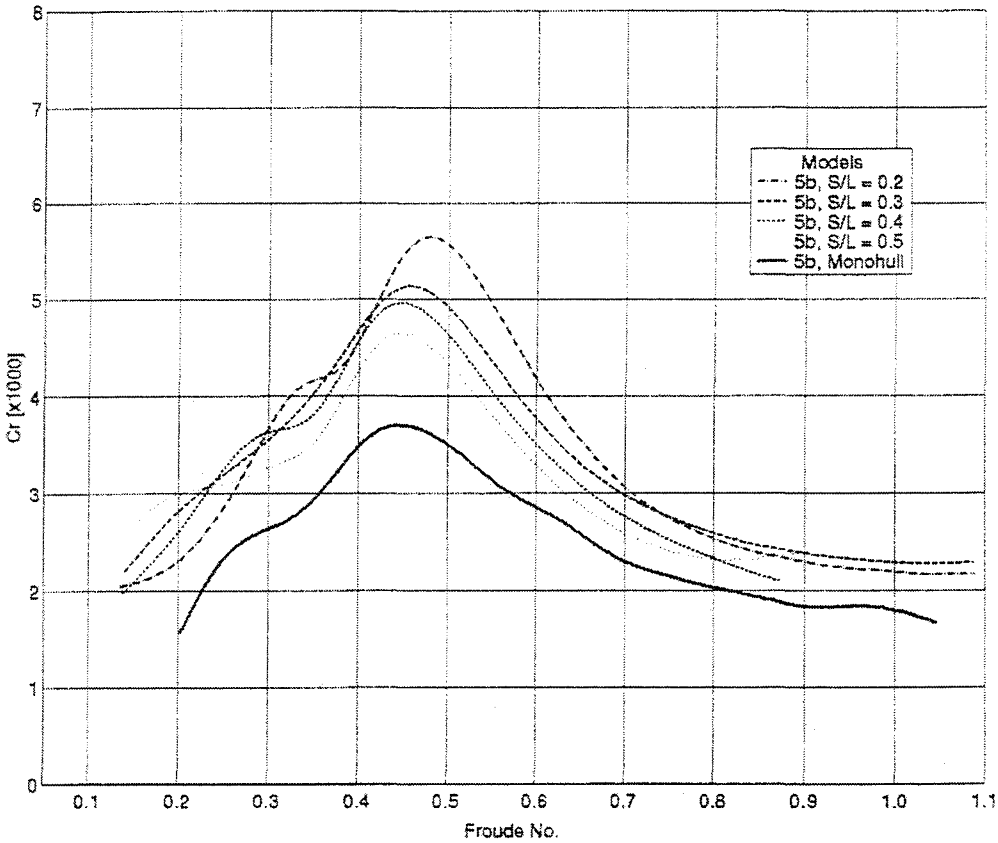

Figure 3.46: Residuary Resistance of Model 5b(Couser,1996)

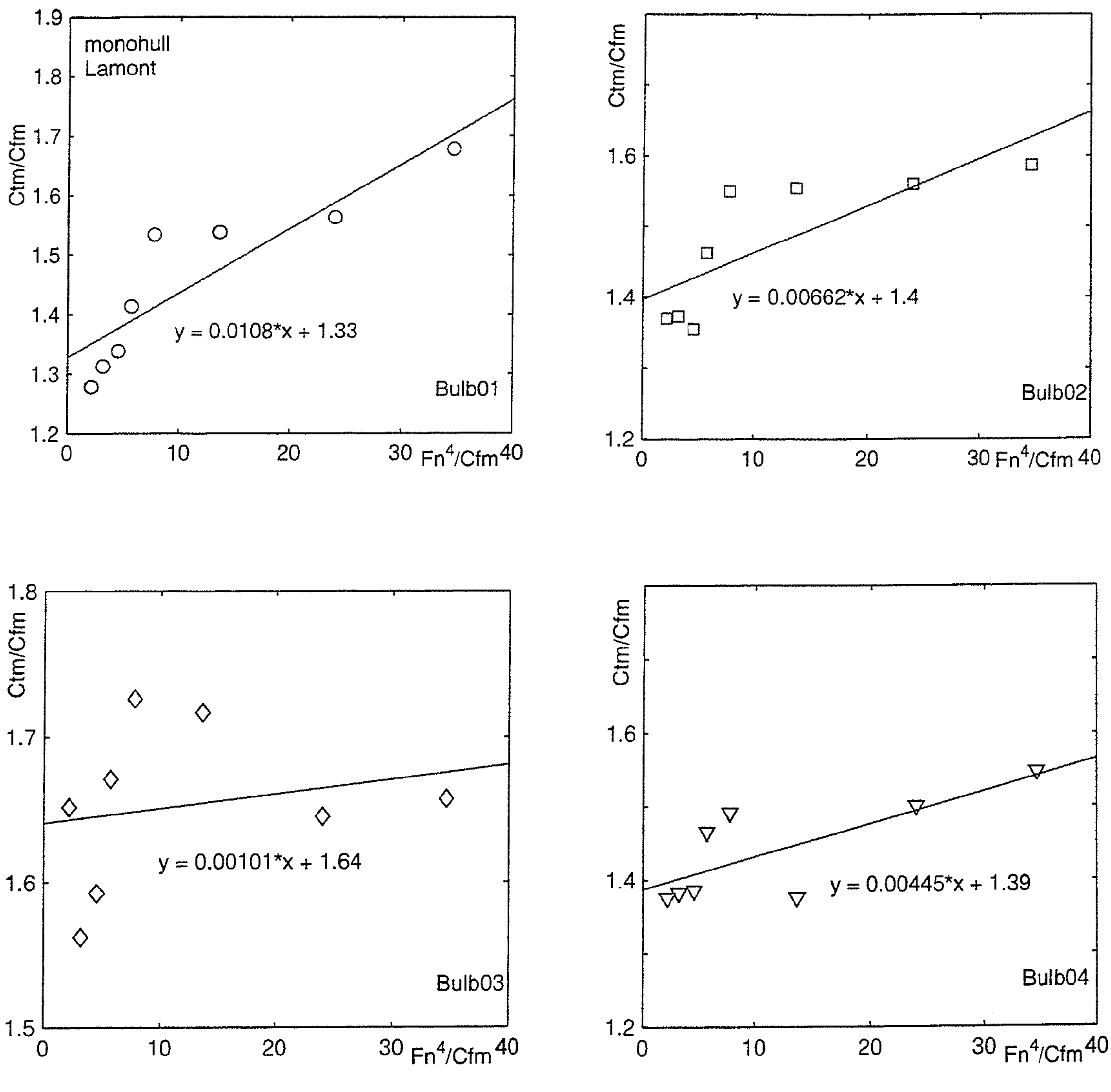

Figure 3.47: Monohull: Prohaska Plot

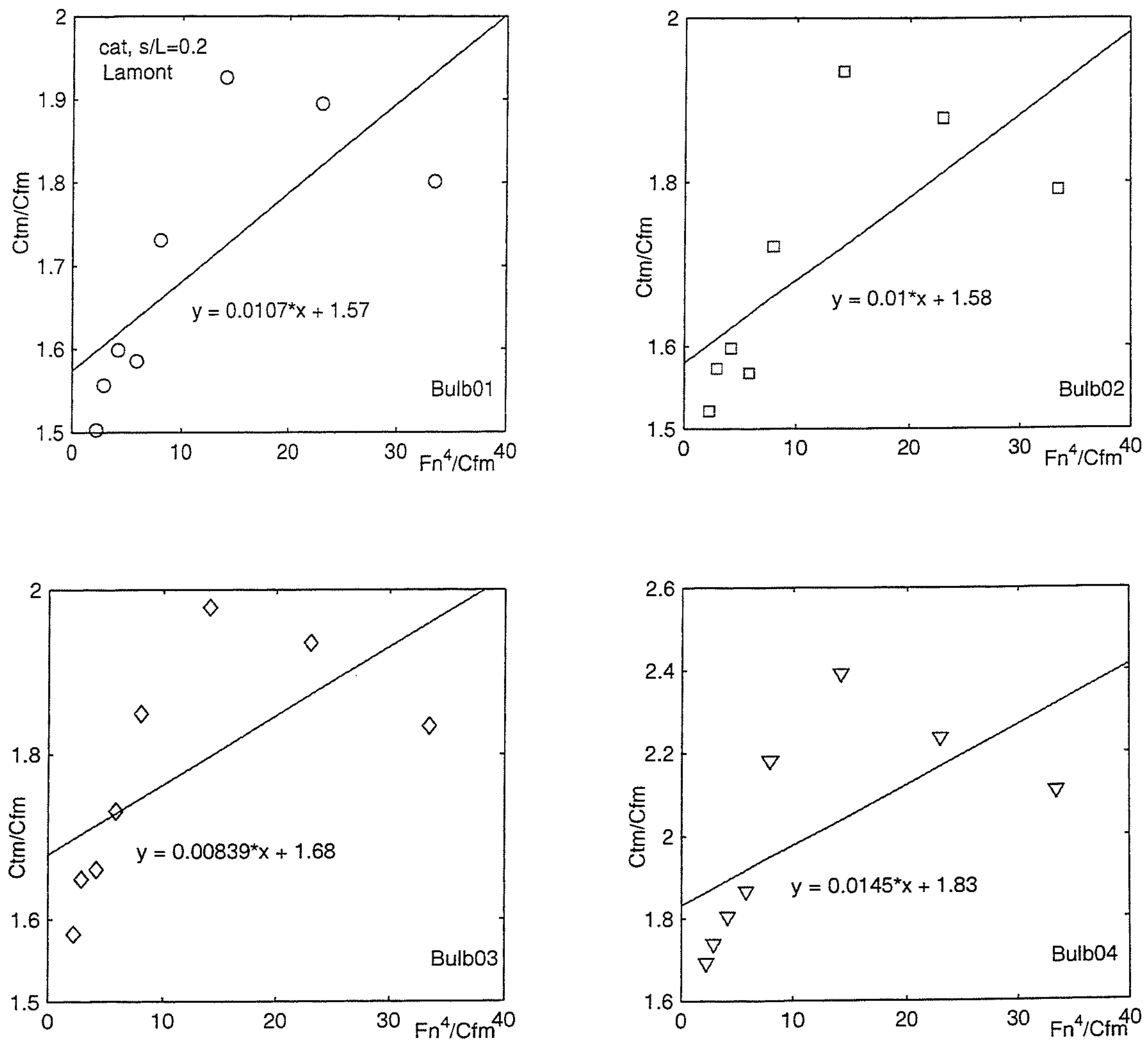

Figure 3.48: Catamaran, s/L=0.2: Prohaska Plot

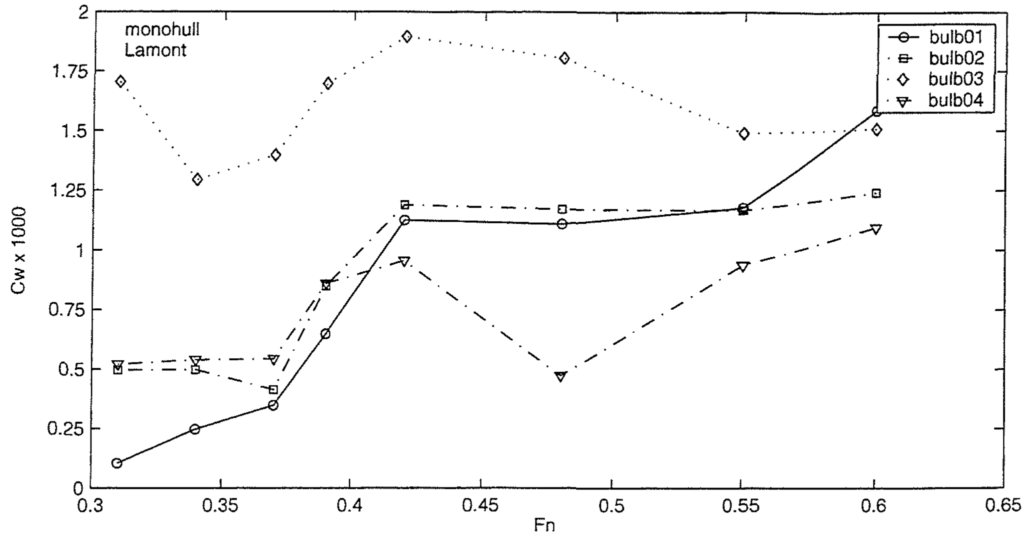

Figure 3.49: Monohull: Wave resistance coefficient C_w against F_n

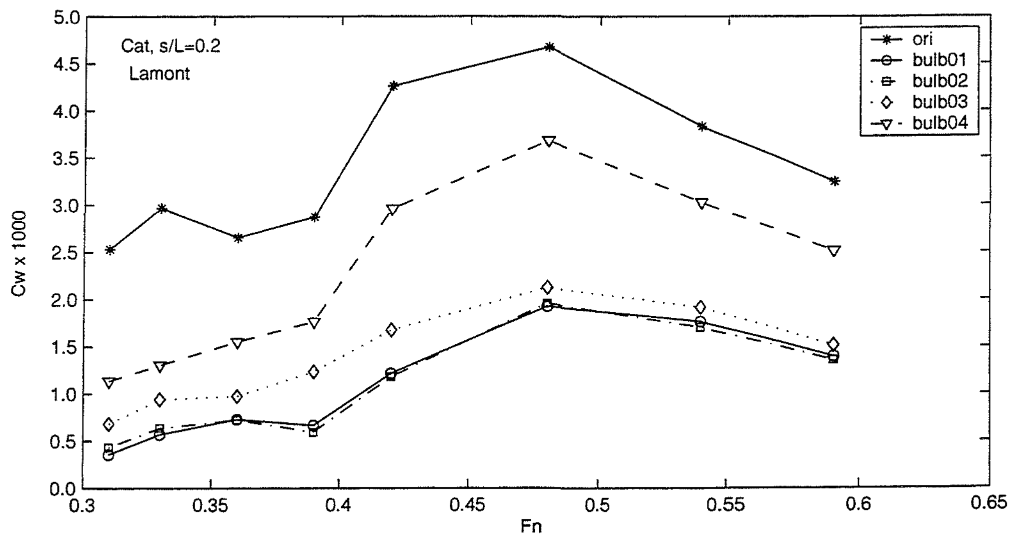

Figure 3.50: Catamaran s/L=0.2: Wave resistance coefficient C_w against F_n

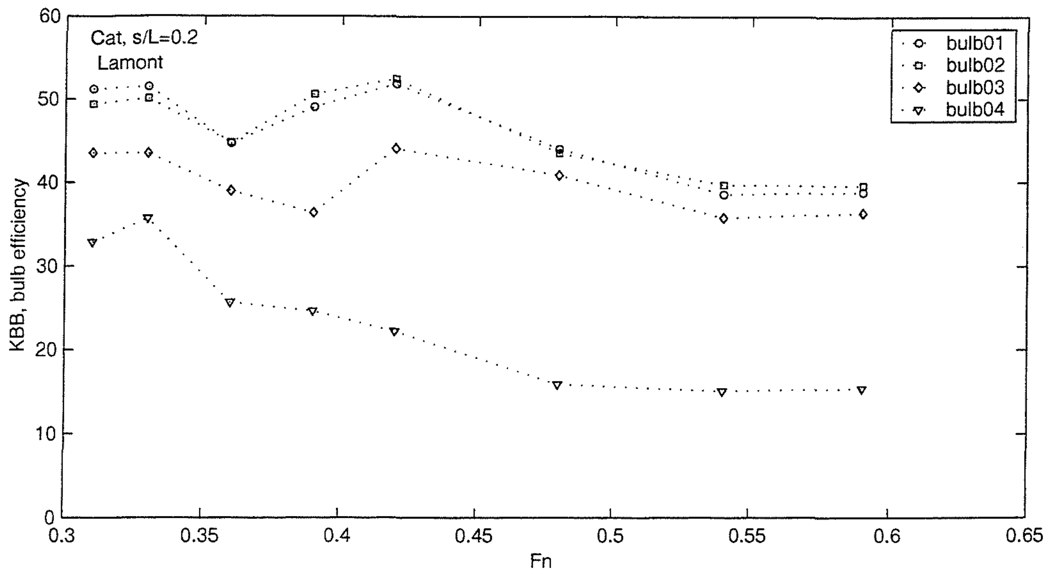

Figure 3.51: Catamaran s/L=0.2: Bulbs Efficiency for four different bulbous bows

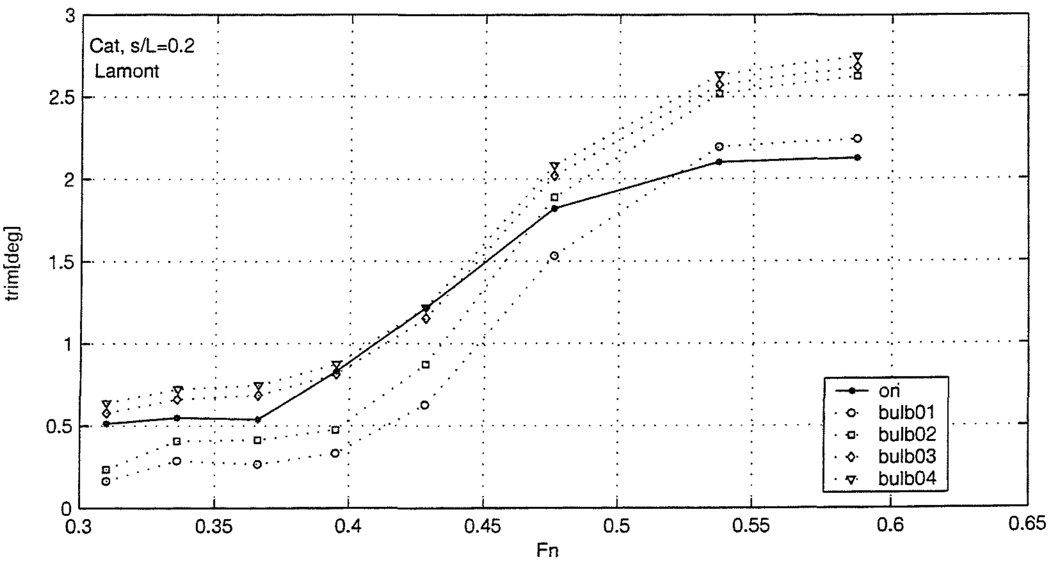

Figure 3.52: Catamaran s/L=0.2: Running trim versus F_n

Chapter 4

Experiment in Regular Waves for high-speed displacement craft

4.1 General

High speed displacement ships are characterized by their high length-beam ratio, sharp bow, and flat stern terminating in a transom. This type of hull is often used for small warships, patrol boats or as fast ferries particularly in a catamaran configuration which combines high-speed capability with good seakeeping characteristics.

Important issues in the design of ships are safety, reliability and economy. To some extent all of these aspects are affected by seakeeping characteristics of the ship. To improve seakeeping or ship seaworthiness is one of the most demanding tasks in the design of high speed craft. Seaworthiness is the performance quality of the ship which allows the accomplishment of her missions under specified sea conditions with acceptable passenger or personnel comfort; minimal deck wetness, motions and hull-wave impact; and also assurance of hull structural integrity.

The resistance or drag of a vessel travelling at constant speed in waves will oscillate at the frequency of the encountered waves. But the average drag in waves will be greater than the drag in calm water. This extra drag which a vessel experiences in a seaway, compared to with in calm water, is known as *added resistance*, R_{AW}.

Seakeeping can be studied in various ways. Hutchison (1991)[52] has enumerated the three most important methods into full-scale measurement, physical scaled model tests and analytical models. Similarly Mark (1963)[70] divided the methods into full scale measurement, laboratory model and theoretical studies.

Regular waves never occur in the real sea but they can be easily produced in towing tanks. The real sea can be represented by a superposition of a large number of regular waves as described by St. Denis and Pierson(1955)[96]. So it is clear that the characteristics of regular waves have a profound influence on the behaviour of ships in rough weather even though they are never encountered at sea, Lloyd(1998)[68].

4.2 Experiments in regular waves

A ship sailing in a seaway experiences the largest added resistance in waves from ahead. For that reason the study has been confined to that important wave heading; head seas. Also due to the limitations of the tank test facility at Southampton Institute of Higher Education (SIHE), only head sea conditions were considered and to simplify the programme the models were towed rather than self-propelled.

Experiments in waves have been carried out on the model fitted with four different bulbs (bulb01, bulb02, bulb03 and bulb04) to compare the pitching and the heaving motions as well as the added resistance.

4.2.1 Tank Facilities

The tank is fitted with flap type wave makers at the one end, capable of generating both regular and irregular waves of various heights and frequencies and also fitted with a beach or wave absorber at the other end. The dimensions of the tank are given in the previous chapter.

This tank has a rectangular section with constant width and depth along its length. In addition to a beach at one end of the tank, there are a number of wooden beaches for wave damping along one side of the tank. These were lifted out of the water during wave wash experiments in order to obtain near perfect wash or ship-generated waves measured by three waves probes fixed at the tank wall.

The tank is equipped with a manned carriage and is rigged with a microcomputer based data acquisition system, two component dynamometer and a heavy model dynamometer. Acceleration distance in the tank is about 20m which was sufficient to achieve the maximum speed used in the experiment, i.e. 4.04 m/s. A section of 15.24m long was used during the measurement.

4.2.2 Instrumentation and measurements

The total model resistance and side force measurements were performed using the Wolfson Unit dynamometer. Total resistance and side force were recorded for all the speeds tested. Side force was monitored at all speeds to ensure that the model yaw degree was acceptable.

The accuracy of the total resistance was found to be in the range of $\pm 0.02N$.

Heave motions were measured with a linear potentiometer attached to the heave post. The accuracy of the linear potentiometer was found to be $\pm 0.1mm$.

Pitch was measured with an angular potentiometer incorporated into the towing fitting. It was measured as angle in degrees and taken positive for bow up. The accuracy of the potentiometers was in the range of $\pm 0.05°$.

The wash or wave cuts during the run were measured by three wave probes; details as mentioned in the previous chapter.

The speed of the model is determined by measuring the time taken by the carriage to cover the constant run length between two switches which are 15m apart. The switches also start and stop the data acquisition process.

V m/s	F_{nl}	Bulb01	Bulb02	Bulb03	Bulb04
1.028	0.26	√	√	√	√
1.226	0.31	√	√	√	√
1.613	0.41	√	√	√	√
2.019	0.51	√	√	√	√
2.448	0.62	√	√	√	√
2.817	0.71	√	√	√	√
3.368	0.85	√	√	√	√
4.042	1.02	√	√	√	√

Table 4.1: The test matrix for experiment in regular waves $\lambda/L = 0.5 - 2.0$

λ/L	$\lambda\ m$	Tsec	$\omega\ rad/s$	$\omega\sqrt{\frac{L}{g}}$
0.50	0.80	0.716	8.778	3.545
0.75	1.20	0.877	7.167	2.894
1.00	1.60	1.012	6.207	2.507
1.25	2.00	1.132	5.551	2.242
1.50	2.40	1.240	5.068	2.047
2.00	3.20	1.432	4.389	1.772

Table 4.2: Regular waves details used in seakeeping experiment

4.2.3 Model details

Since model tests in waves are expensive in terms of tank time, the numbers of parameters in a systematic test series have to be limited to a minimum.

The model used in this work is a catamaran, $s/L = 0.2$ which is fitted with four different bulbous bows. The $s/L = 0.2$ value chosen, corresponding to a demihull separation of 0.32 m, as this is representative of the vast majority of similar high speed catamarans around at the current time as reported by Couser(1996)[15]. The models were accordingly ballasted and trimmed. During testing, the models were free to heave and pitch but restrained in yaw, sway and roll.

4.2.4 Test conditions

The experiments were performed in the Southampton Institute of Higher Education (SIHE) towing tank in head sea conditions. For the present test programmme, regular waves were used covering a wavelength to ship length ratio λ/L, between 0.5 and 2.0 whilst the wave height was maintained at 0.030m. The experiments were carried out for eight ship speeds, corresponding to Froude number between 0.26 and 1.02. The steady speed run length was 15m. The wave frequency were set for each Froude number so that it gave a constant encounter frequency range. The details of regular waves used are shown in Table 4.2.

During regular wave tests the models were allowed to encounter at least 5 to 6 waves before the responses were recorded, so as to allow transients in the response to die out.

The experiments were confined to the design draught only.

4.2.5 Experimental Results

The experimental results are shown in the following figures, where the dimensionless heave and pitch amplitudes and the added resistance are plotted on a base of the ratio waterline and wave length and encounter frequency.

Added Resistance in Regular Wave

The added resistance in regular wave is the difference between the calm water resistance and the resistance in the waves at the same speed. The non-dimensional added resistance is expressed as;

$$\sigma_{AW} = \frac{R_{AW}}{\rho g(\zeta_a)^2(B^2/L)} \tag{4.1}$$

where

R_{AW} added resistance in waves, N

ρ density of water, kg/m^3

g gravity acceleration, m/s^2

B breadth, m

L length, m

ζ_a wave amplitude, m

The added resistance in waves is due mainly to non-viscous effects; thus added resistance experiments can be carried out with small models, since no scale effect has to be considered, Bhattacharyya(1978)[5].

The measured added resistance is not very small as illustrated by the results in the following figures.

Figures 4.1 and 4.2 show dimensionless added resistance as function of non-dimensional encounter frequency for catamaran $s/L = 0.2$ model fitted with bulb01, bulb02, bulb03 and bulb04. These figures show that the added resistance in waves varies with speed.

For model fitted with bulb01, bulb03 and bulb04, the added resistance is found to rise notably when the wavelength decreases especially in the low speed region as illustrated in Figures 4.1 to 4.5.

But the same tendency is not that clear for model fitted with bulb02 as shown in the above figures. It was found that the catamaran fitted with bulb02 produced less resistance in waves in some places compared to the respective calm water resistance. This is not a plausible result, but the reasons at present are not fully understood or explainable.

Added resistance coefficient for original model NPL5b catamaran $s/L = 0.2$ without bulbous bow is shown in Figure 4.3 which is reproduced from Couser(1996) [15].

Figure 4.6 shows a comparison of added resistance coefficient by catamaran $s/L = 0.2$ with and without bulbous bow but not at exactly the same Froude number. The added resistance coefficients for model without bulbous bow are represented by lines(solid, dashed, dotted) whereas for the model with bulbous bow are represented by a combination of dotted lines and symbols(circle, square, triangle). These figures clearly show that the catamarans fitted with bulbous bows produce smaller added resistance coefficient compared to the original hull form without bulbous bow.

In spite of the large scatter of the added resistance coefficient at various Froude numbers, the bulb02 offers the lowest value in all condition as shown in Figure 4.6. This also could be seen in 3D plot as shown in Figures 4.4 and 4.5. These 3D plot have been produced by using *MATLAB* software and its interpolation and smoothing functions.

Pitch and Heave Measurement

For description of ship motion in the vertical plane in waves, the response functions of heave and pitch are sufficient as found out by Blume and Kracht(1985)[7].

Pitch and heave were monitored for all the tests.

The dimensionless motion amplitudes are defined by:

Heave:

$$Z'_a = Z_a/\zeta_a \tag{4.2}$$

Pitch:

$$\theta'_a = \theta_a.L/2\pi\zeta_a \tag{4.3}$$

The experimental frequency response functions of heave and pitch are plotted in Figures 4.7 and 4.8. An alternative presentation of the same results is given in Figures 4.9 and 4.10. Those figures show the results measured for all variants of the model and compared at the same Froude numbers mentioned.

In Figures 4.9 and 4.10 it can be seen that the maximum amplitudes occur for wavelengths between 0.75L to 1.5L. As illustrated by the figures, a bulbous bow has no significant effect on heave and pitch up to $\lambda/L = 0.5$, since there is no significant variation in the maximum amplitudes of heave and pitch produced by bulb01, bulb02, bulb03 and bulb04 below this wavelength.

From Figure 4.8 it shows that an increasing bulb size (i.e bulb03 and bulb04) is accompanied by a reduction of pitch amplitudes in most cases at higher wavelengths, i.e $\lambda/L > 1.0$ for F_n=0.26, $\lambda/L > 0.75$ for F_n=0.51, 0.71 and $\lambda/L > 0.5$ for F_n=0.85. This observation could be connected to the damping coefficients as mentioned by Kracht(1978)[61]. In detail, the bulbous bow mitigates the pitching motion of the ship by its higher damping.

Figures 4.7 and 4.9 showing heaving transfer functions, in some cases it shows that the wavelength and Froude number have a much greater effect than bulbous bow size. A fundamental conclusion in these studies, for wave lengths shorter than 0.5L, there very little model response at any speed as mentioned before.

Figures 4.11 and 4.12 show the heave and pitch transfer function in head seas condition for original hull NPL5b catamaran $s/L = 0.2$ at F_n=0.2, 0.5 and 0.8 respectively. These figures are reproduced from the thesis of Taunton(2001) [99].

The results also have been compared with model fitted with four different bulbous bows as shown in Figures 4.13 and 4.14.

Wash Measurement in Regular Wave

Again wash height measurements were carried out over a speed range of corresponding to F_n=0.26 to 1.02 in regular waves λ/L=0.5, 1.0, 1.5 and 2.0.

Wash was measured by means of three wave probes at three different locations as mentioned in previous chapter. The sample of measured wash at F_n=0.51 in regular waves corresponding to λ/L=0.5, 1.0, 1.5, 2.0 are shown in Figures 4.15, 4.16, 4.17 and 4.18 respectively.

For comparison purposes with wash measured in calm water the following relationship has been introduced.

$$\boxed{\text{Wash in wave} = \text{wash measured in regular wave - input wave}} \quad (4.4)$$

Figures 4.19, 4.20, 4.21 and 4.22 show comparisons of wash measured in calm water and wash in regular waves as obtained from the above relationship. Those figures illustrate that wash measured in calm water has similar trends to wash measured in regular waves, but with small phase shift and oscillations in some places. The reasons behind this have not been investigated, but a possible influencing factor is the relationship between the input wave and the wave generator, which need further investigation. From this preliminary finding, it is demonstrated that wash is independent of sea condition.

4.3 Summary

The work described in this chapter covers the experimental determination of the seakeeping properties of catamaran s/L=0.2 fitted with four different bulbous bows.

Measurements of heave, pitch and wash as well as added resistance due to waves have been made.

For model fitted with bulb01 which is the shortest bulbous bow, the added resistance is found to rise dramatically when the wavelength decreases, and the same thing shown by the model fitted with bulb03 and bulb04. Whereas for model with bulb02, this trend is not very clear but generally it offers the lowest value of added resistance. Based on this, it concludes that the vessel having least resistance in calm water does not necessarily show the lowest added resistance in seaway or rough water. In addition, it was found that the magnitude of added resistance increases as F_n increases.

Pitch motion influenced by the size of the bulbous bow i.e. pitch amplitude decreases as bulbous bow size increases as shown in Figure 4.14. But the effect of bulbous size on heave motion is less pronounced as shown in Figure 4.13. However, in heave motion the wavelength and Froude number have a much greater effect than the size of bulbous bow.

Tables 4.3 to 4.5 show the ranking of the bulbous bows based on the experimental results of model testing in regular waves. These ranking were developed on three criteria namely added resistance in waves, heave and pitch amplitudes. They are arranged from best to worst with best being that bulb which had the lowest added resistance, heave and pitch over the F_n=0.26, 0.51, 0.71 and 0.85.

Fn=0.26	Lambda/L			
Rank	0.5	1	1.5	2
1	bulb04	bulb03	bulb01	bulb04
2	bulb01	bulb02	bulb02	bulb01
3	bulb03/02	bulb04	bulb03/04	bulb02
4	na	bulb01	na	bulb03

Fn=0.51	Lambda/L			
Rank	0.5	1	1.5	2
1	bulb03	bulb04	bulb01	bulb02
2	bulb02/04	bulb01	bulb04	bulb03
3	bulb01	bulb03	bulb03	bulb04
4	na	bulb02	bulb02	bulb01

Fn=0.71	Lambda/L			
Rank	0.5	1	1.5	2
1	bulb03	bulb03	bulb02	bulb02
2	bulb02	bulb04	bulb04	bulb03
3	bulb04	bulb01	bulb01	bulb04
4	bulb01	bulb02	bulb03	bulb01

Fn=0.85	Lambda/L			
Rank	0.5	1	1.5	2
1	bulb03	bulb01	bulb02	bulb02
2	bulb02	bulb02	bulb04	bulb03
3	bulb04	bulb03	bulb03	bulb01/04
4	bulb01	bulb04	bulb01	na

Table 4.3: Catamaran s/L=0.2: Relative Ranking of Bulbous Bows based on Heave Amplitude

Fn=0.26	Lambda/L			
Rank	0.5	1	1.5	2
1	bulb04	bulb04	bulb03	bulb03
2	bulb01	bulb01/03	bulb04	bulb02
3	bulb02	bulb02	bulb01	bulb01/04
4	bulb03	na	bulb02	na

Fn=0.51	Lambda/L			
Rank	0.5	1	1.5	2
1	bulb04	bulb04	bulb03	bulb03
2	bulb01	bulb03	bulb04	bulb02/04
3	bulb02/03	bulb01	bulb01/02	bulb01
4	na	bulb02	na	na

Fn=0.71	Lambda/L			
Rank	0.5	1	1.5	2
1	bulb04	bulb04	bulb04	bulb03
2	bulb01	bulb03	bulb03	bulb04
3	bulb03	bulb01	bulb01	bulb02
4	bulb02	bulb02	bulb02	bulb01

Fn=0.85	Lambda/L			
Rank	0.5	1	1.5	2
1	bulb04	bulb04	bulb04	bulb03
2	bulb03/01	bulb03	bulb03	bulb04
3	bulb02	bulb01	bulb01	bulb01/02
4	na	bulb02	bulb02	na

Table 4.4: Catamaran s/L=0.2: Relative Ranking of Bulbous Bows based on Pitch Amplitude

Table 4.6 shows a cumulative relative ranking of the bulbous bows which is produced from Tables 4.3, 4.4 and 4.5. It is also interesting that the maximum added resistance

Fn=0.26 Rank	Lambda/L 0.5	1	1.5	2
1	bulb02	bulb02	bulb02	bulb02
2	bulb04	bulb01/04	bulb04	bulb04
3	bulb01	bulb03	bulb01	bulb01
4	bulb03	na	bulb03	bulb03

Fn=0.51 Rank	Lambda/L 0.5	1	1.5	2
1	bulb01/02	bulb02	bulb02	bulb02
2	bulb04	bulb04	bulb04	bulb04
3	bulb03	bulb01	bulb01	bulb01
4	na	bulb03	bulb03	bulb03

Fn=0.71 Rank	Lambda/L 0.5	1	1.5	2
1	bulb02	bulb02	bulb02	bulb02
2	bulb01	bulb04	bulb04	bulb01
3	bulb04	bulb01	bulb03	bulb04
4	bulb03	bulb03	bulb01	bulb03

Fn=0.85 Rank	Lambda/L 0.5	1	1.5	2
1	bulb02	bulb02	bulb02	bulb02
2	bulb01	bulb01	bulb04	bulb01/04
3	bulb03/04	bulb04	bulb03	bulb03
4	na	bulb03	bulb01	na

Table 4.5: Catamaran s/L=0.2: Relative Ranking of Bulbous Bows based on Added Resistance

is not accompanied by maximum amplitude of motion. It is believed to be caused by the phase relations between motions and waves which is also play a part in added resistance.

It can be noted that bulb02 is good for resistance whilst bulb03 and bulb04 are good for heave and pitch motions respectively. The weighting of the bulbous bows between the criteria(resistance, heave and pitch) and an ultimate choice will depend on likely weather conditions for a particular route.

Rank	Added Resistance	Heave	Pitch
1	bulb02	bulb03	bulb04
2	bulb04	bulb02	bulb03
3	bulb01	bulb04	bulb01
4	bulb03	bulb01	bulb02

Table 4.6: Catamaran $s/L = 0.2$:Relative Ranking of Bulbous Bows in Regular Waves

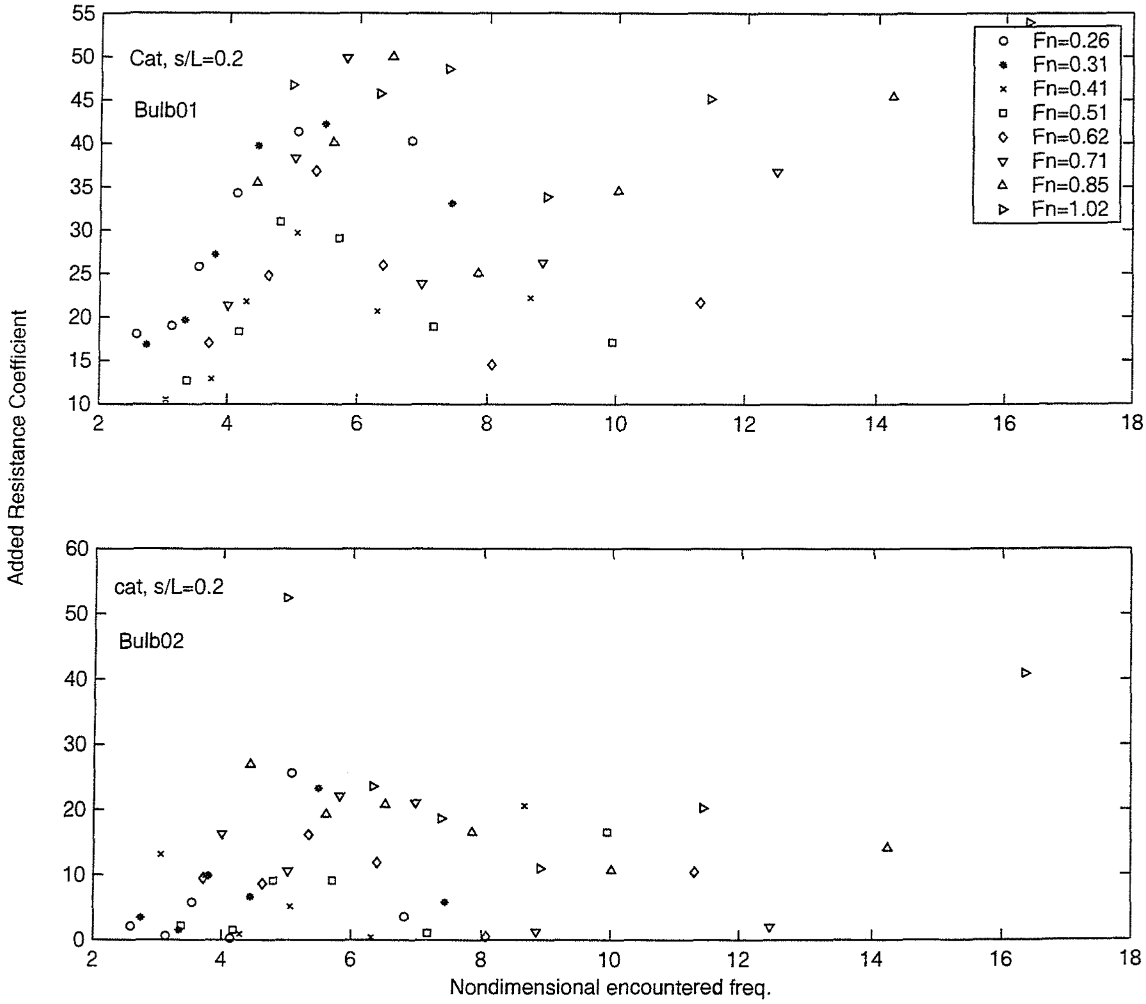

Figure 4.1: Catamaran s/L=0.2 with Bulb01 and Bulb02: Added Resistance Coefficient versus Non-dimensional Frequency of Encounter

Page 90 is missing from volume

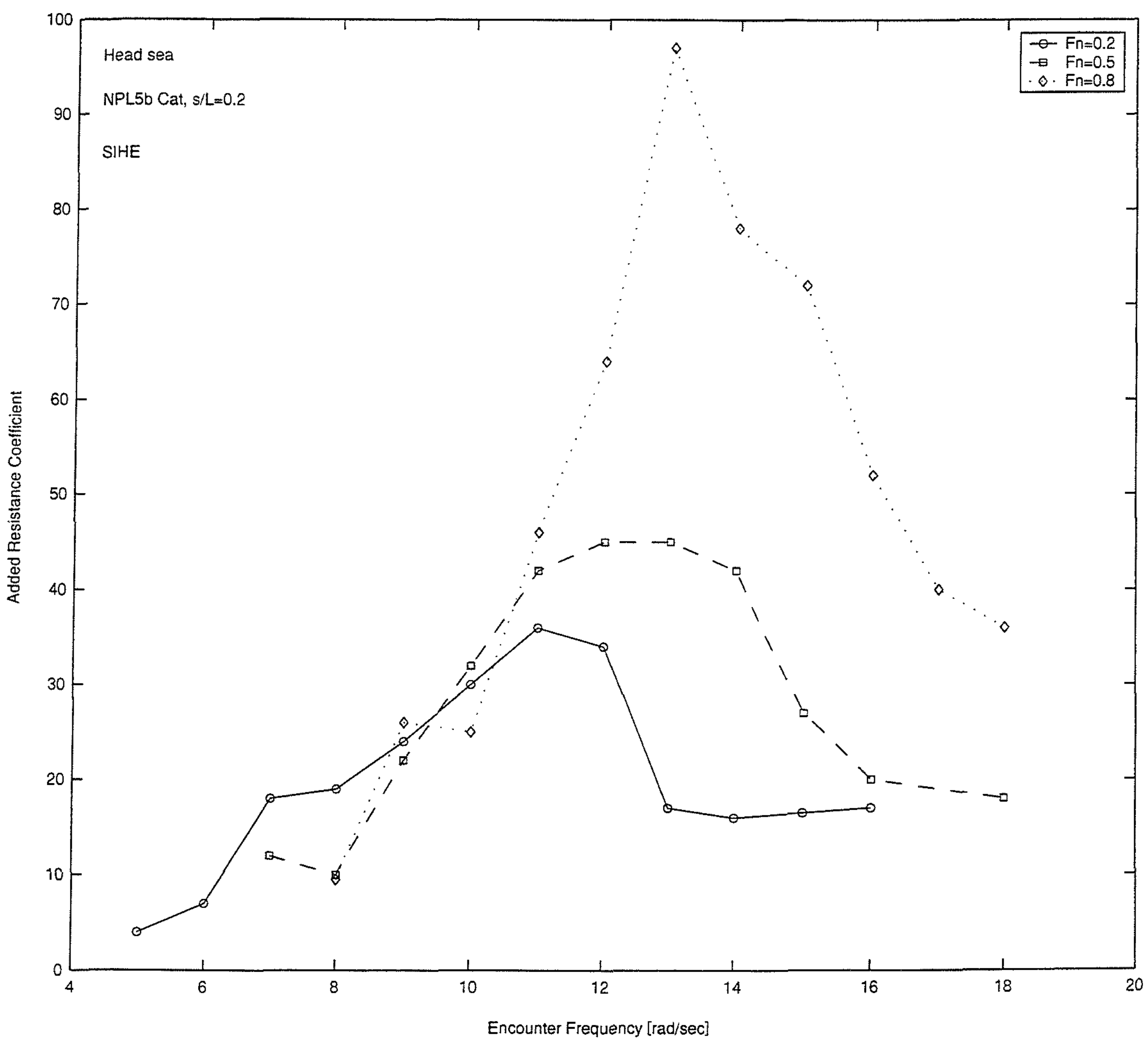

Figure 4.3: Catamaran s/L=0.2 without bulbous bow: Added Resistance Coefficient versus Encounter Frequency[15]

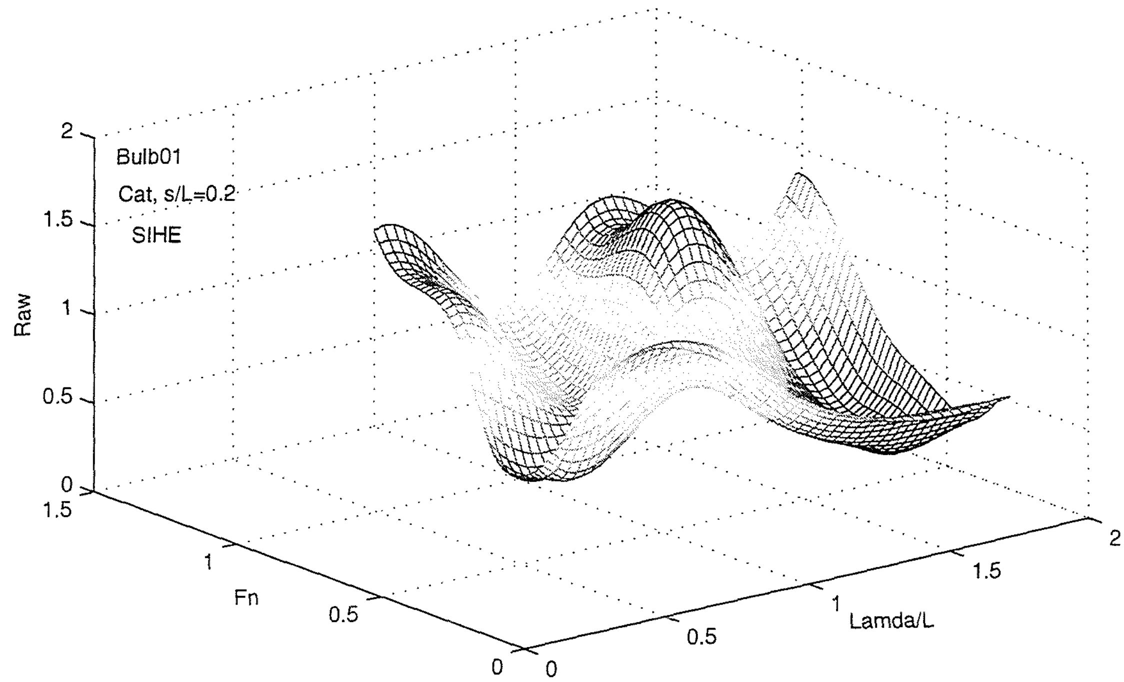

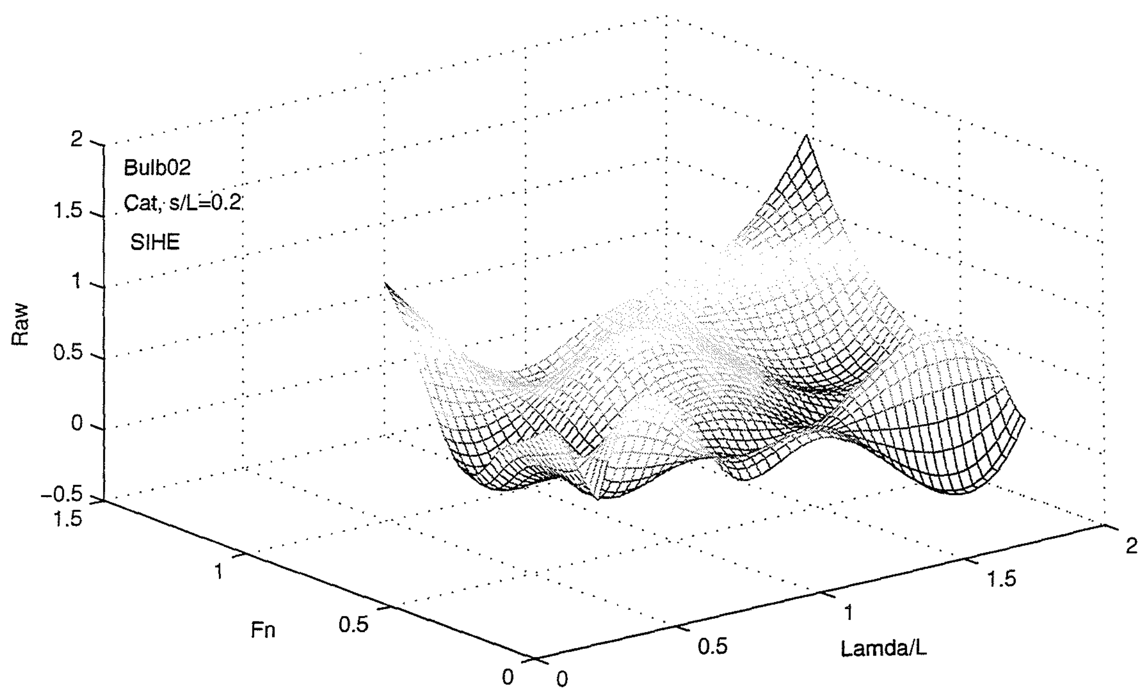

Figure 4.4: Catamaran s/L=0.2 with Bulb01 and Bulb02: Added Resistance in Waves

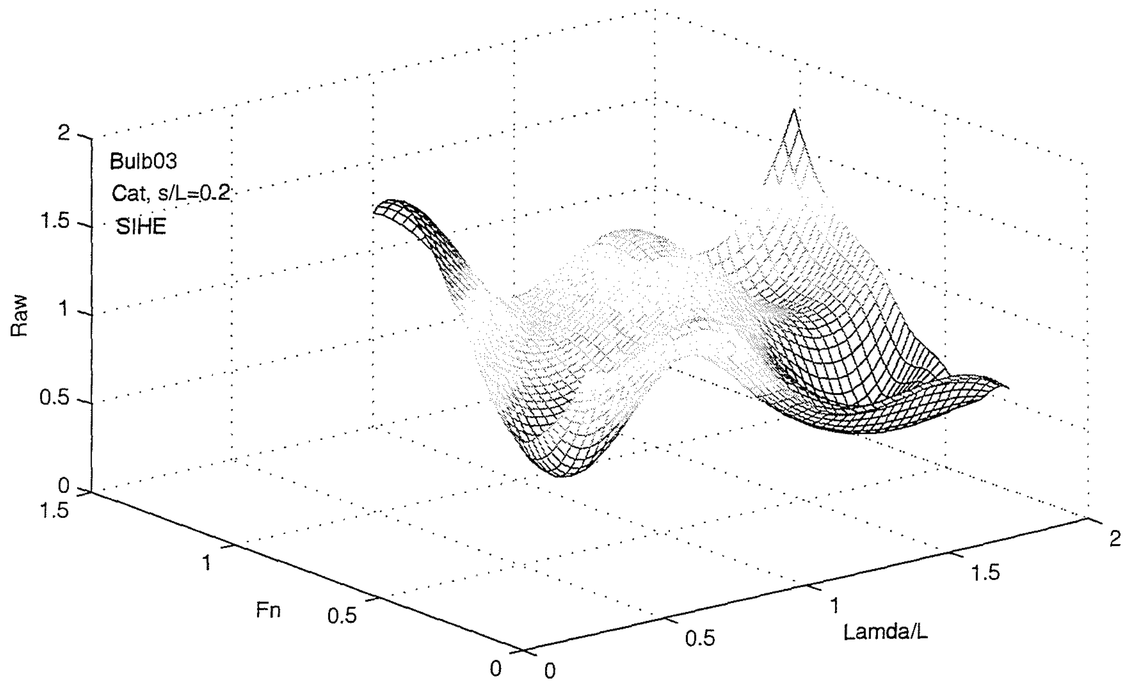

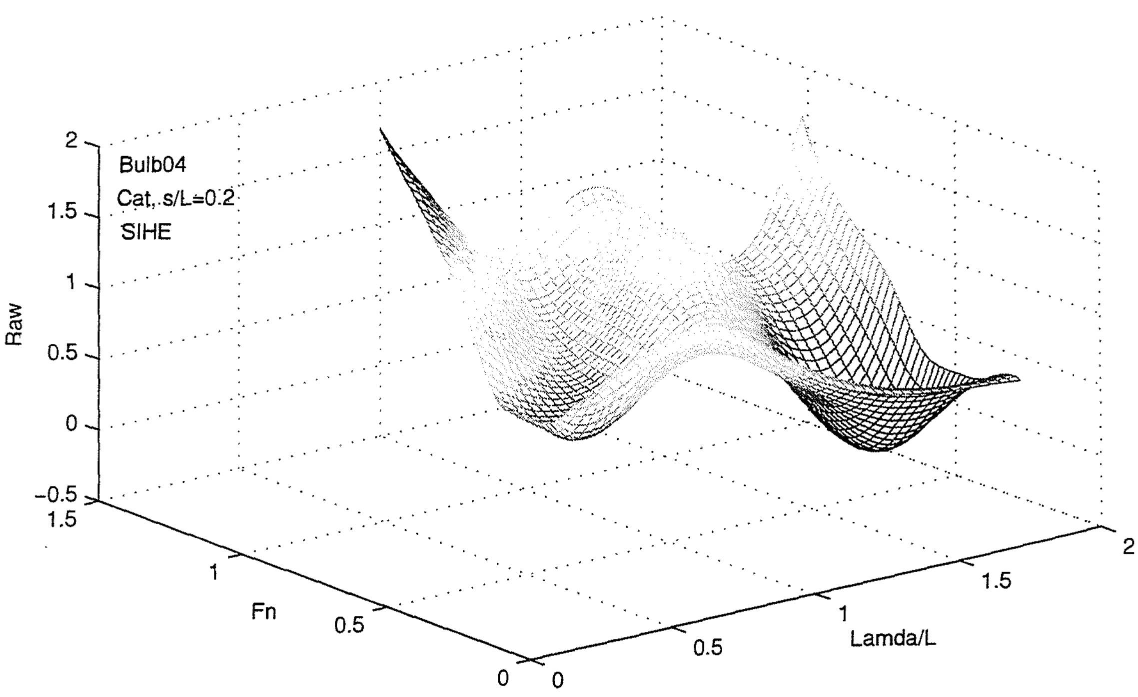

Figure 4.5: Catamaran s/L=0.2 with Bulb03 and Bulb04: Added Resistance in Waves

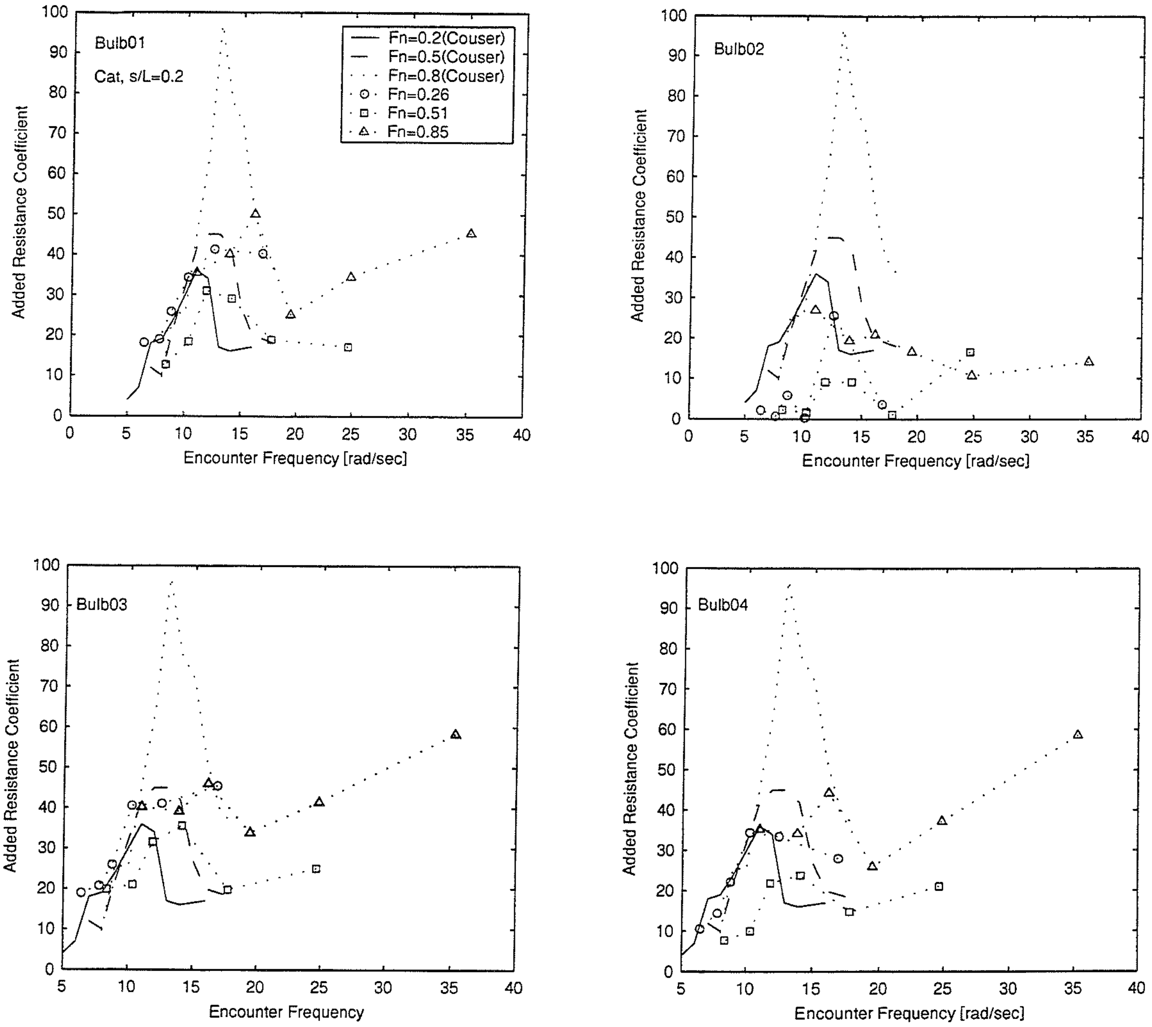

Figure 4.6: Catamaran s/L=0.2 with and without bulbous bow: Added Resistance Coefficient versus Encounter Frequency

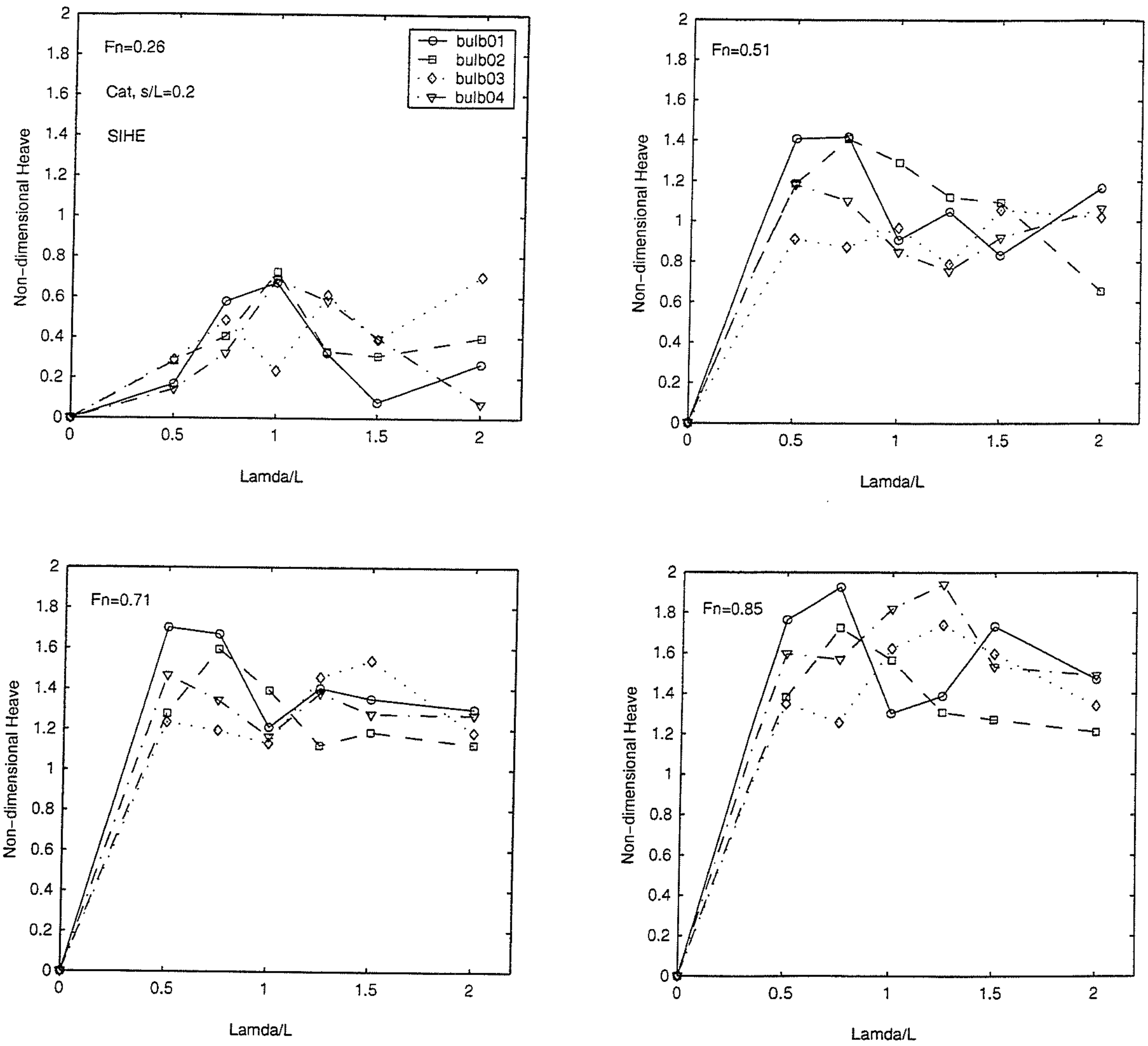

Figure 4.7: Response functions of heave of catamaran s/L=0.2 with different bulbous bows

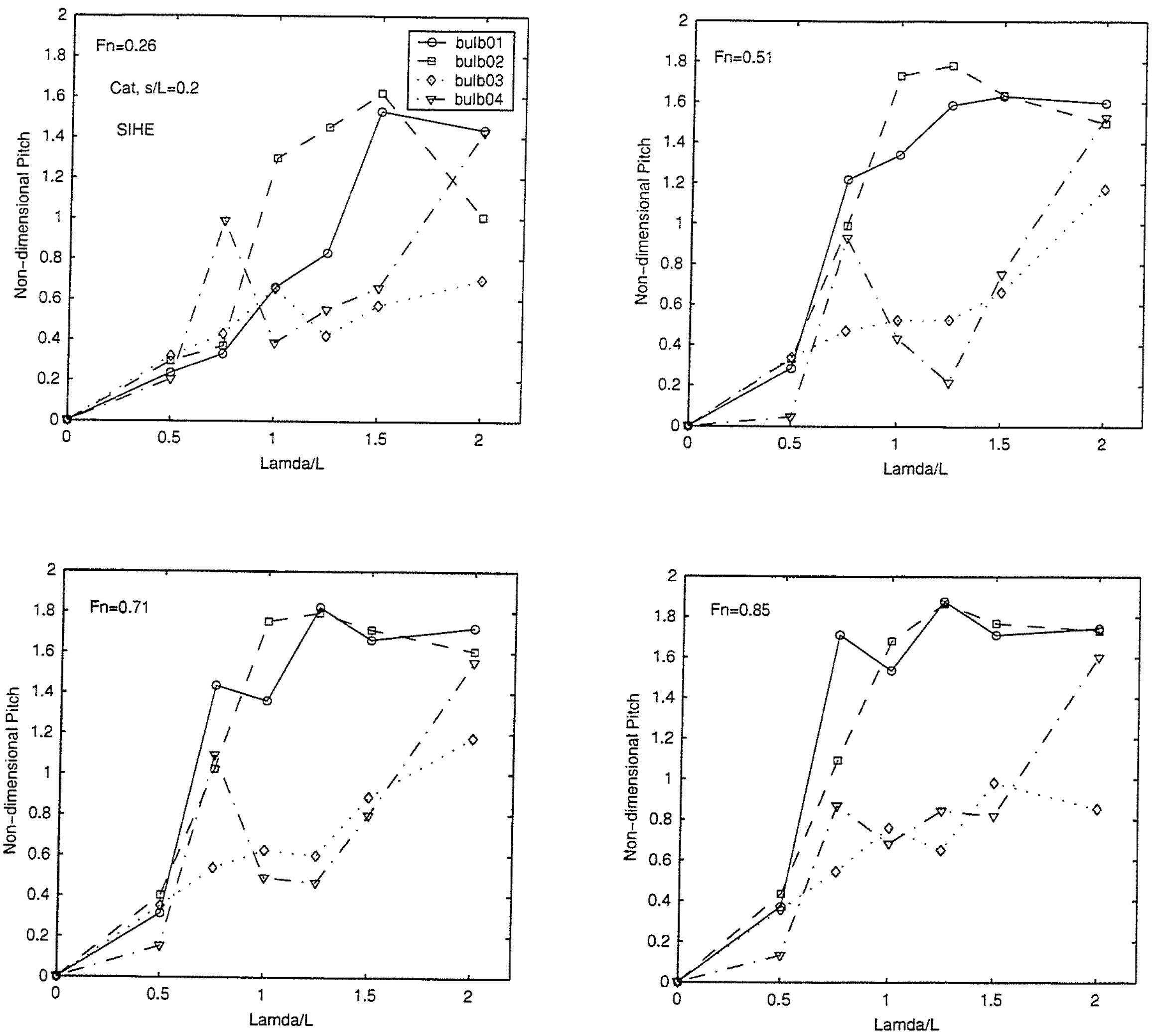

Figure 4.8: Response functions of pitch of catamaran s/L=0.2 with different bulbous bows

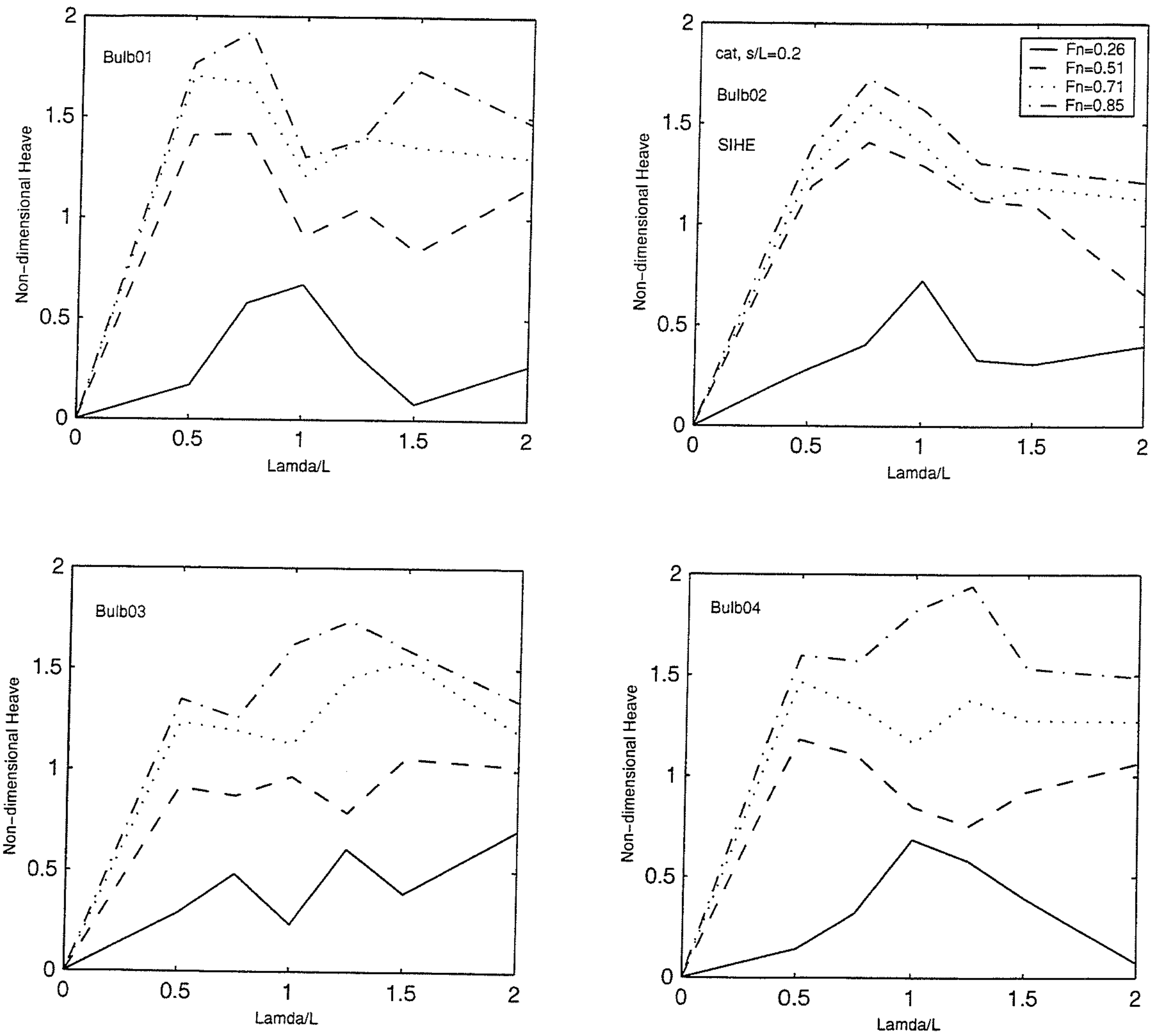

Figure 4.9: Response functions of heave of catamaran s/L=0.2 with different bulbous bows

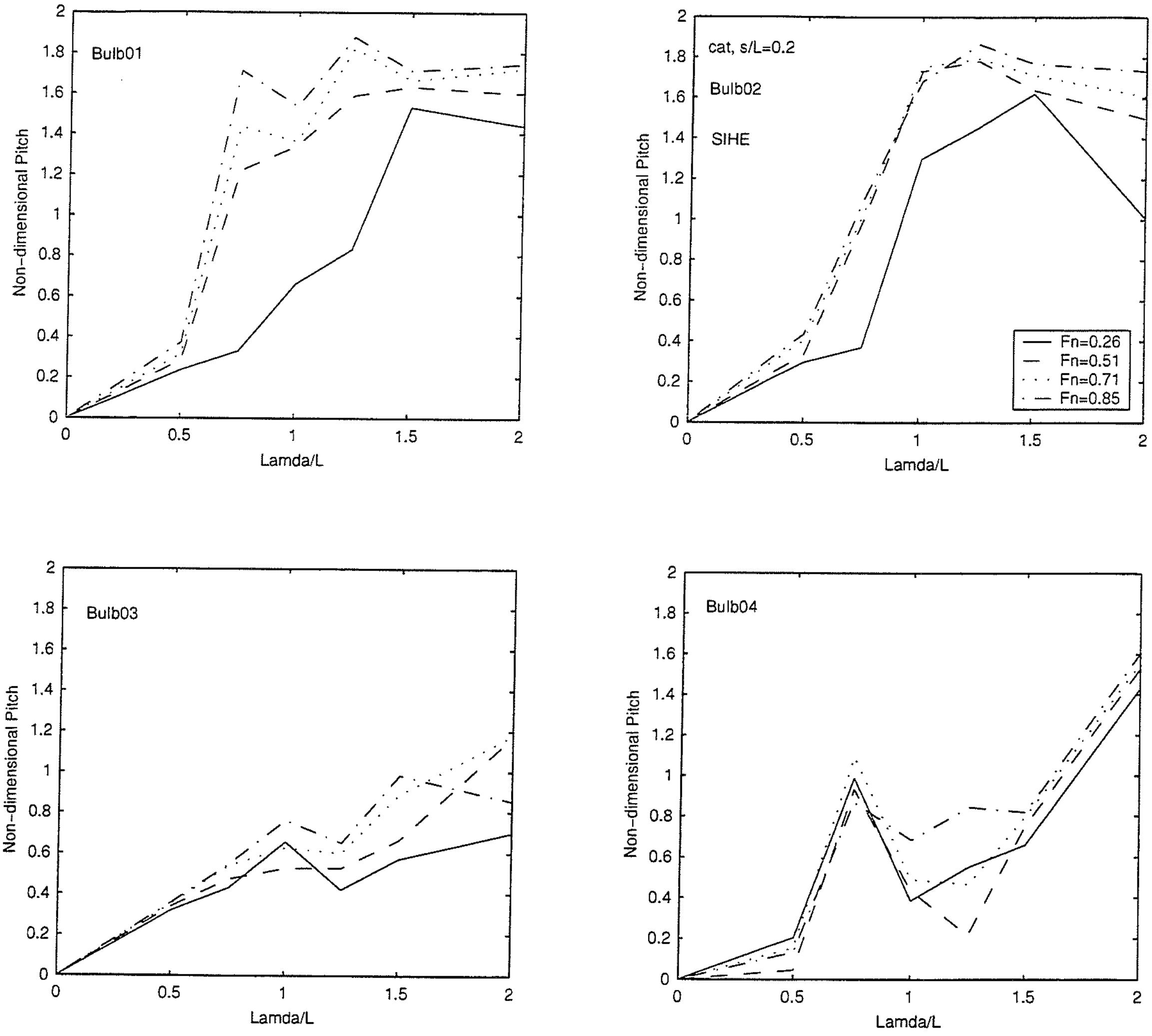

Figure 4.10: Response functions of pitch of catamaran s/L=0.2 with different bulbous bows

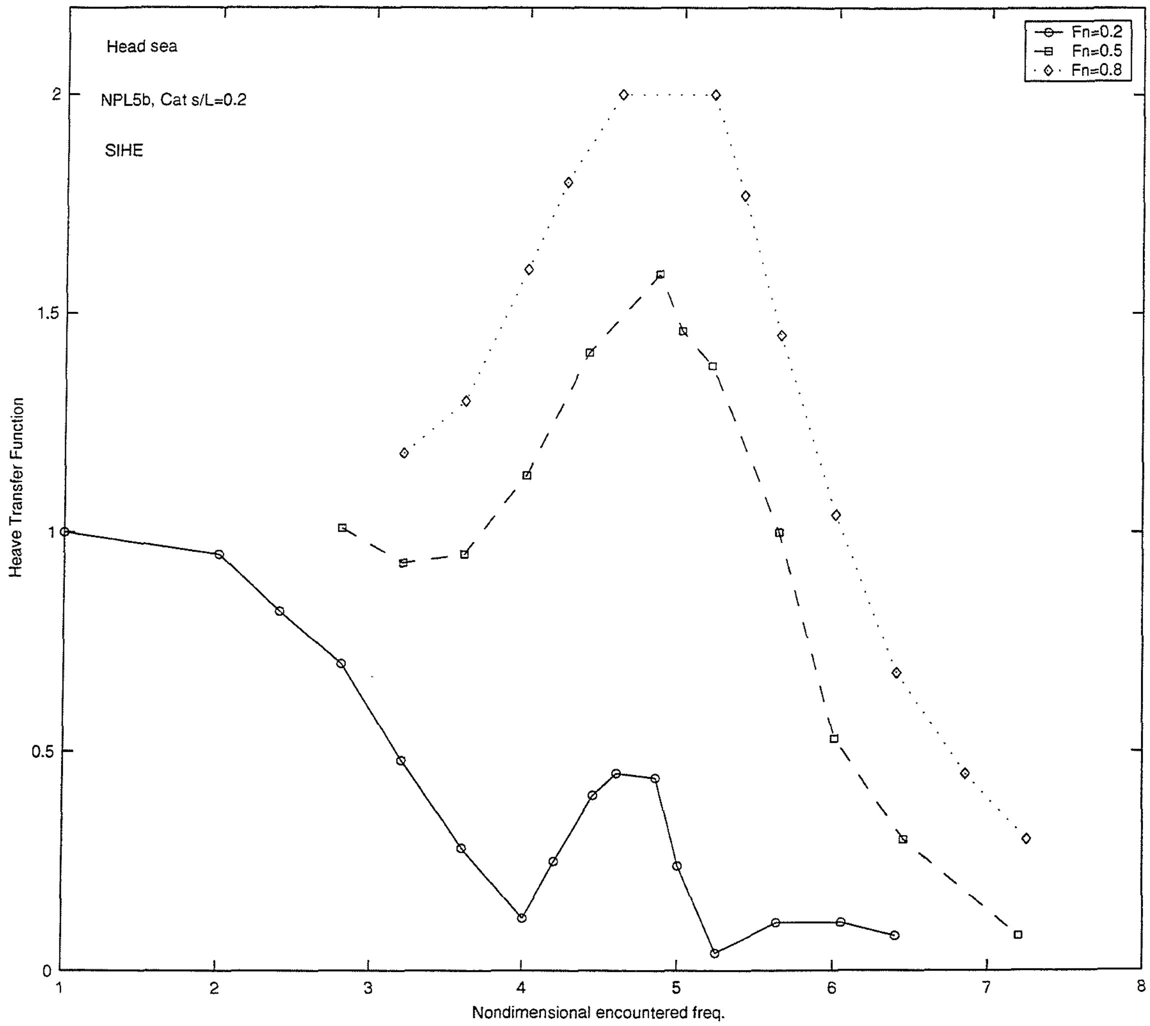

Figure 4.11: Response Functions of Heave for Model NPL5b Catamaran s/L=0.2 in Head Seas[99]

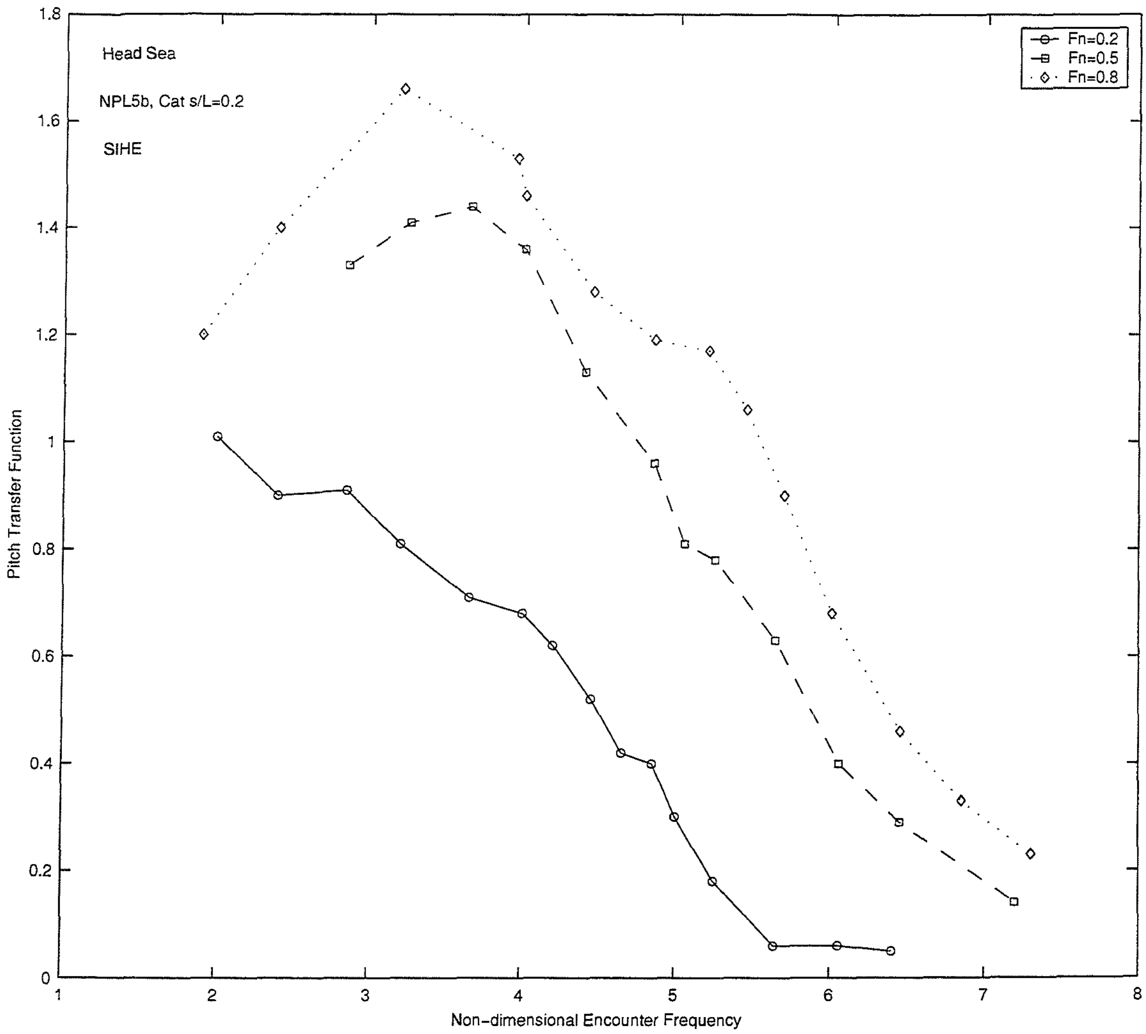

Figure 4.12: Response Functions of Pitch for Model NPL5b Catamaran s/L=0.2 in Head Seas[99]

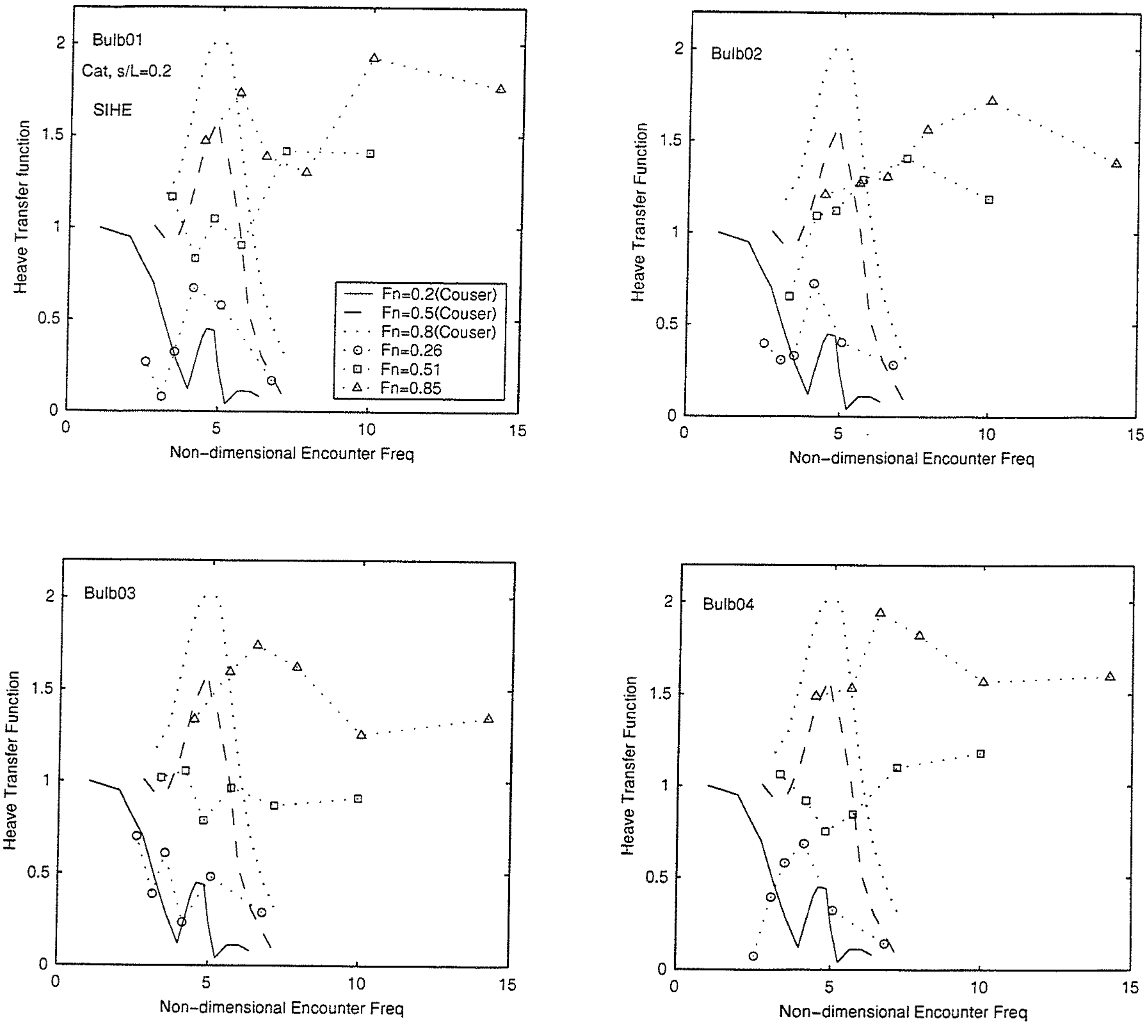

Figure 4.13: Response Functions of Heave for Model NPL5b Catamaran s/L=0.2 with and without bulbous bow

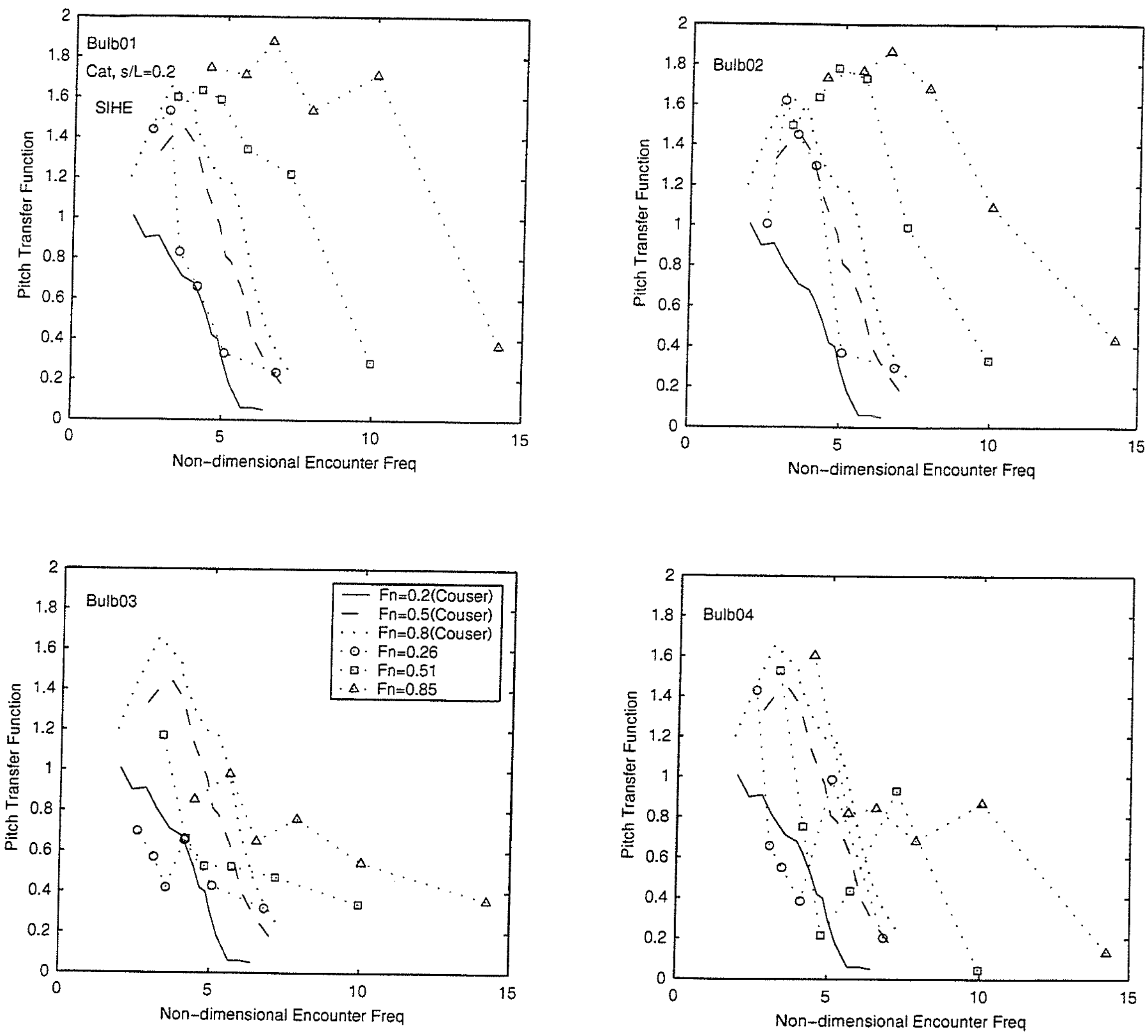

Figure 4.14: Response Functions of Pitch for Model NPL5b Catamaran s/L=0.2 with and without bulbous bow

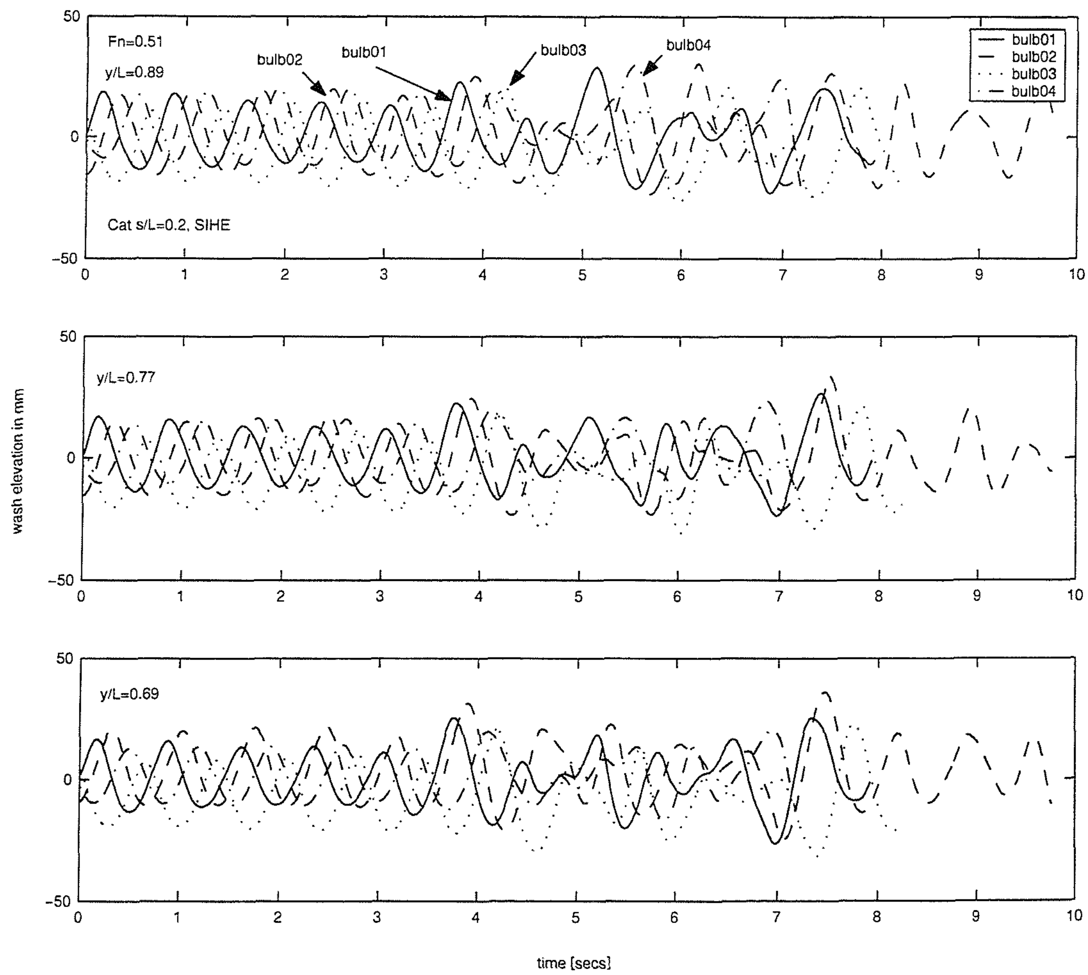

Figure 4.15: Catamaran s/L=0.2: Experimental Wash measured in Regular Wave 0.5L at F_n=0.51

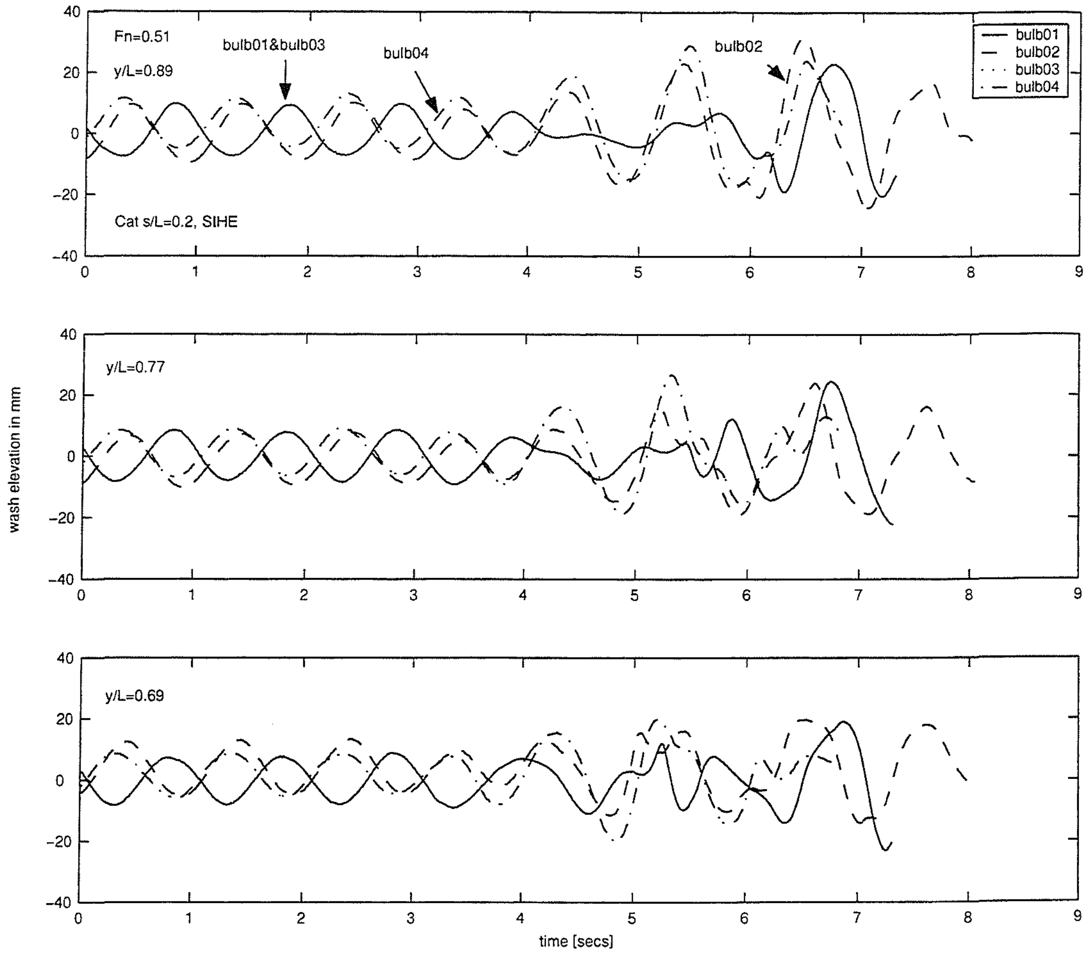

Figure 4.16: Catamaran s/L=0.2: Experimental Wash measured in Regular Wave 1.0L at F_n=0.51

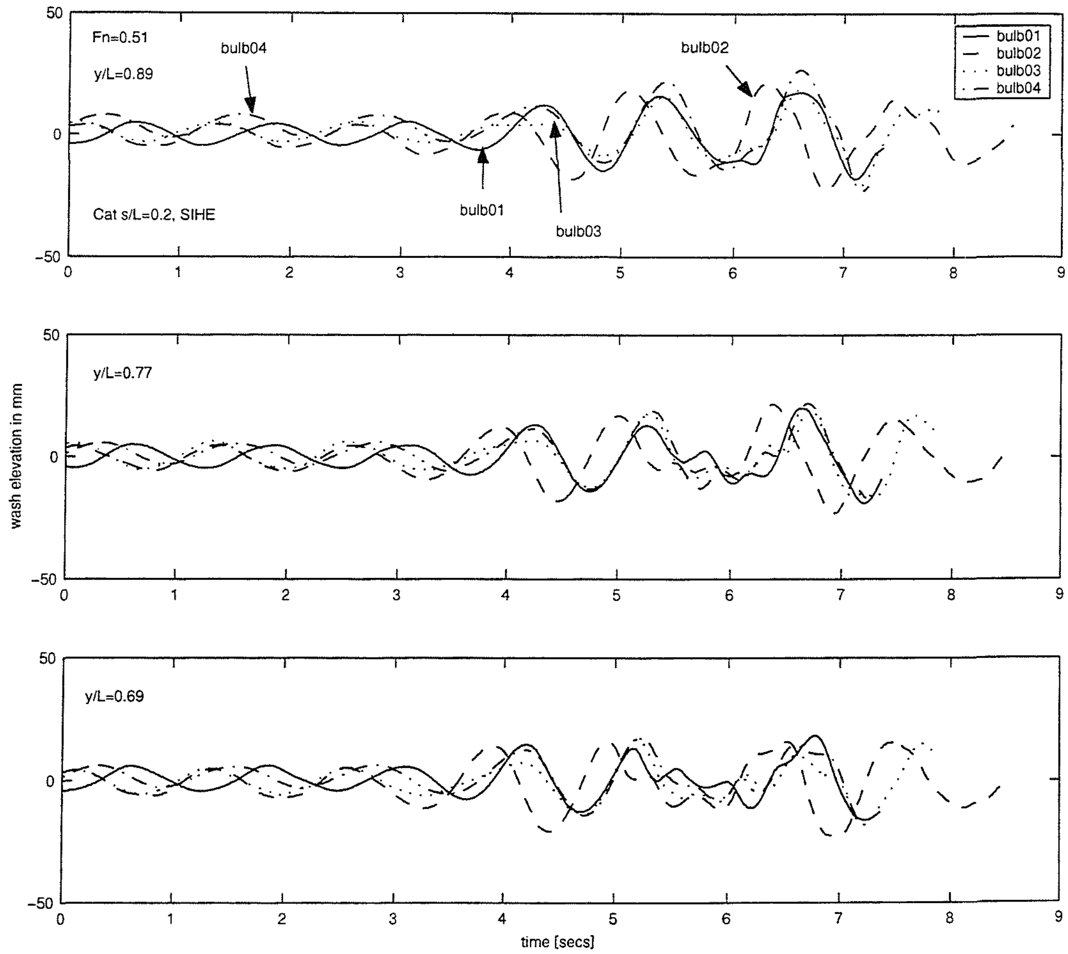

Figure 4.17: Catamaran s/L=0.2: Experimental Wash measured in Regular Wave 1.5L at F_n=0.51

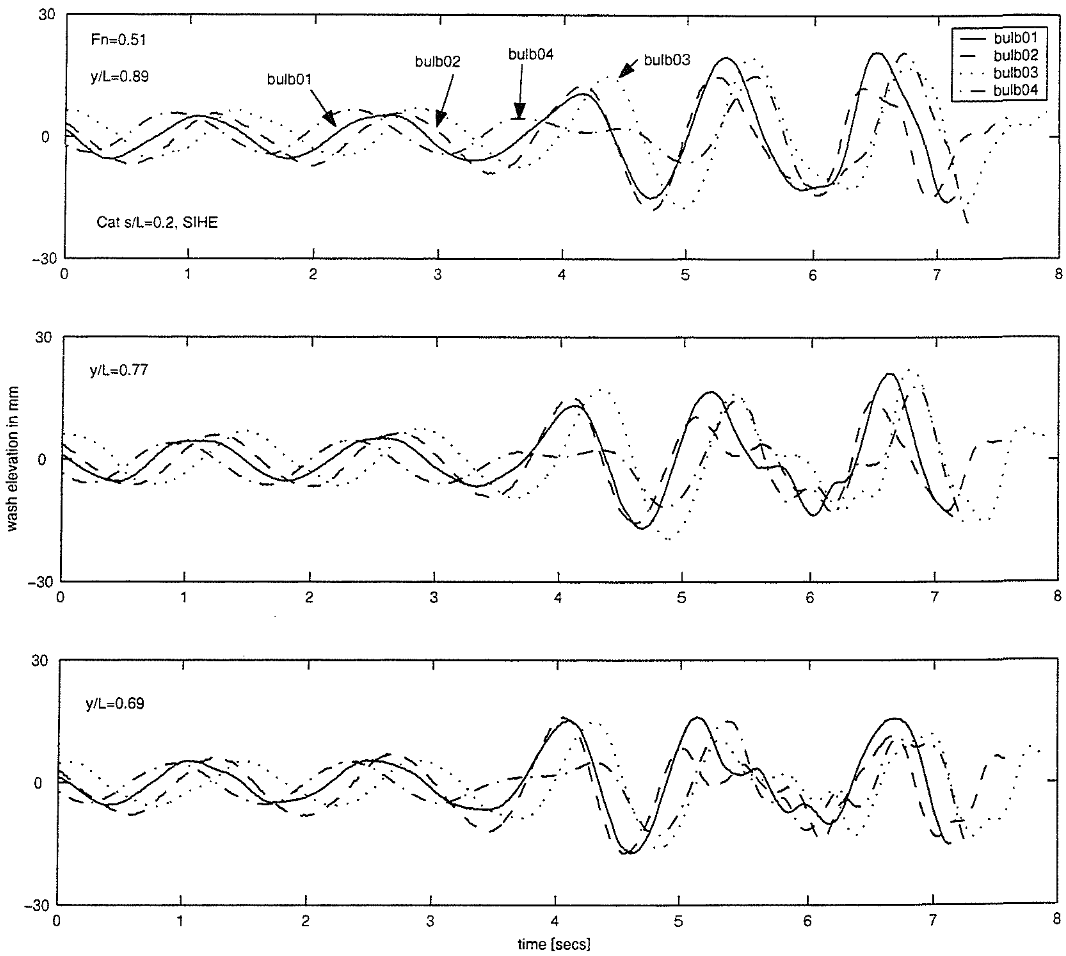

Figure 4.18: Catamaran s/L=0.2: Experimental Wash measured in Regular Wave 2.0L at F_n=0.51

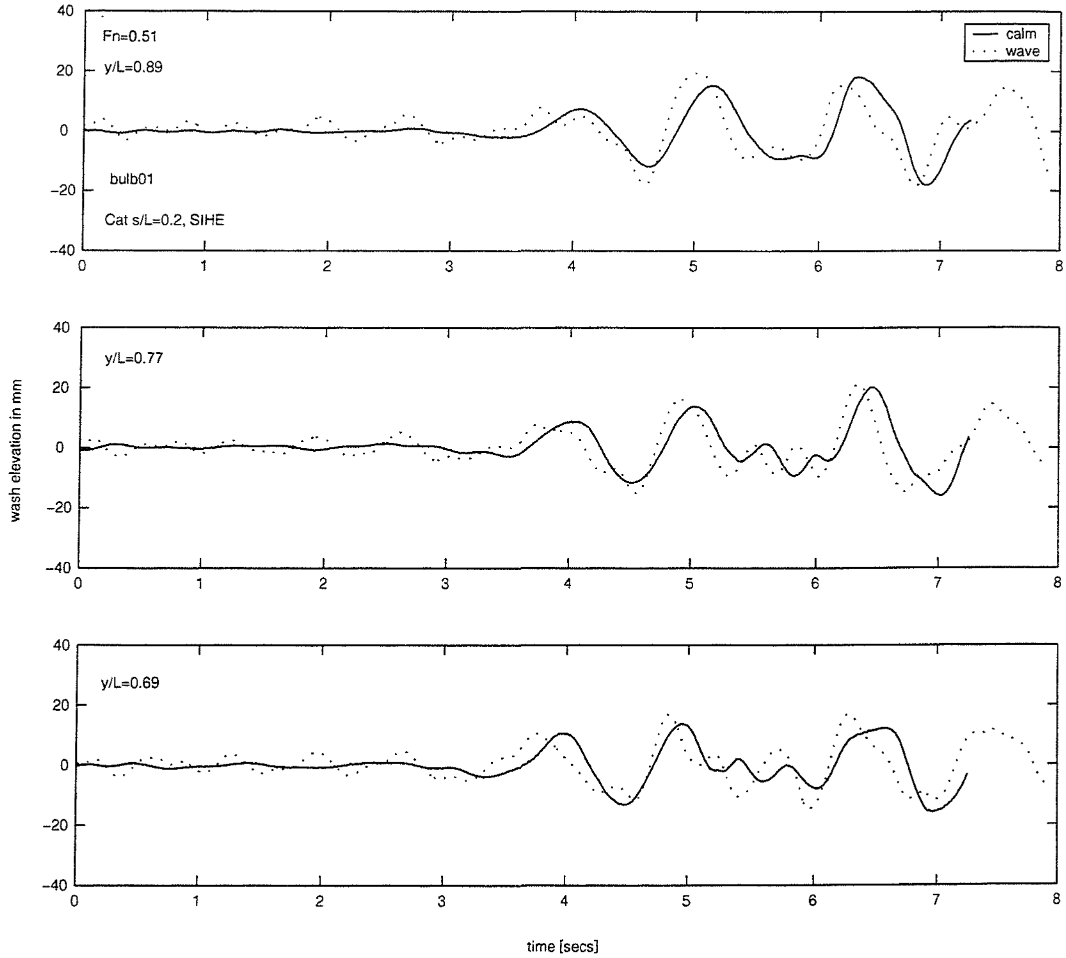

Figure 4.19: Catamaran s/L=0.2 with bulb01: Wash measured in Calm Water and Regular Wave 0.5L at F_n=0.51

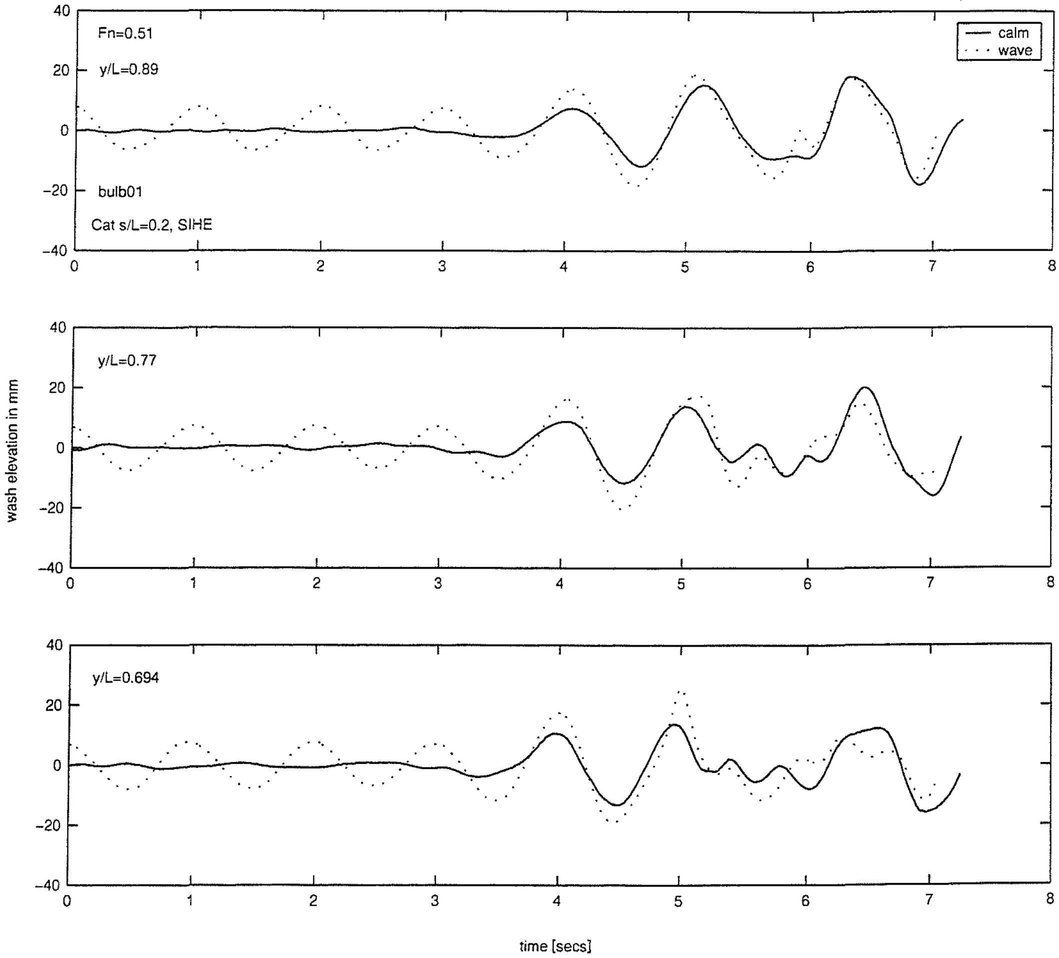

Figure 4.20: Catamaran s/L=0.2 with bulb01: Wash measured in Calm Water and Regular Wave 1.0L at F_n=0.51

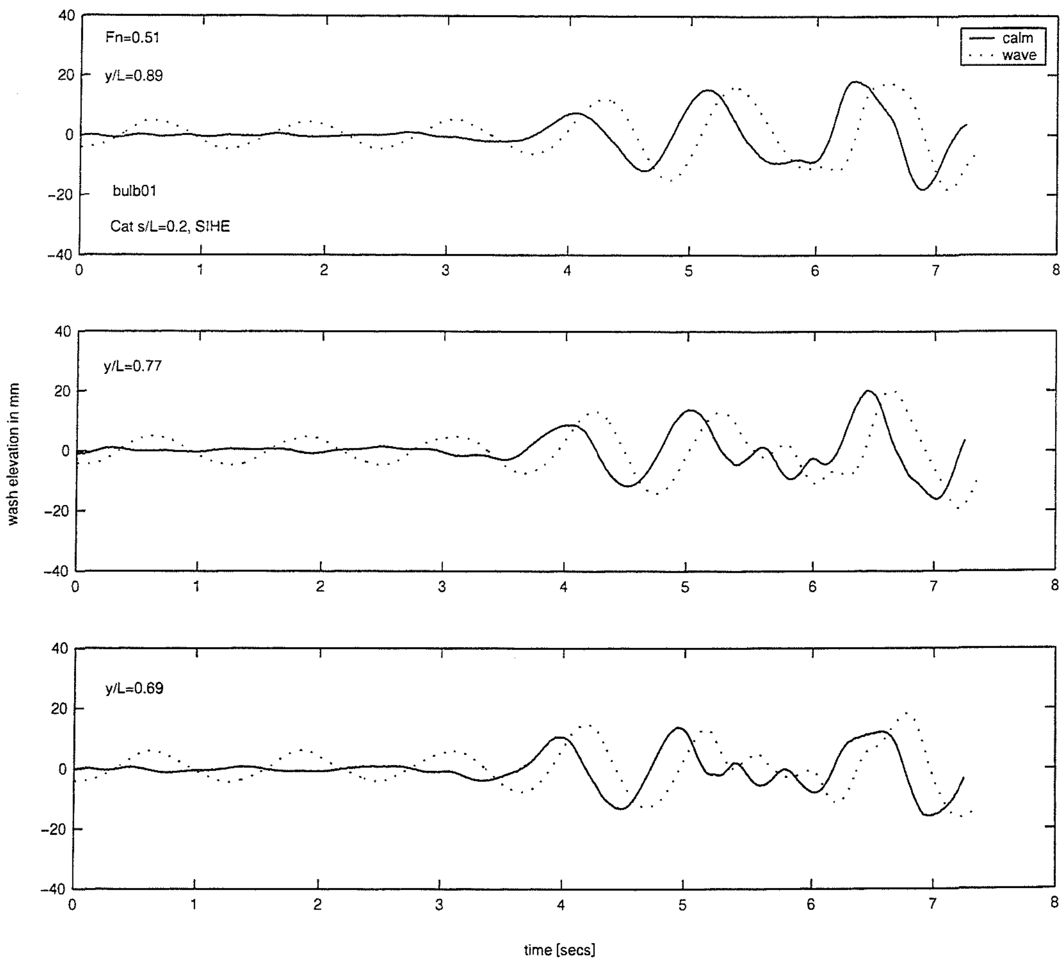

Figure 4.21: Catamaran s/L=0.2 with bulb01: Wash measured in Calm Water and Regular Wave 1.5L at F_n=0.51

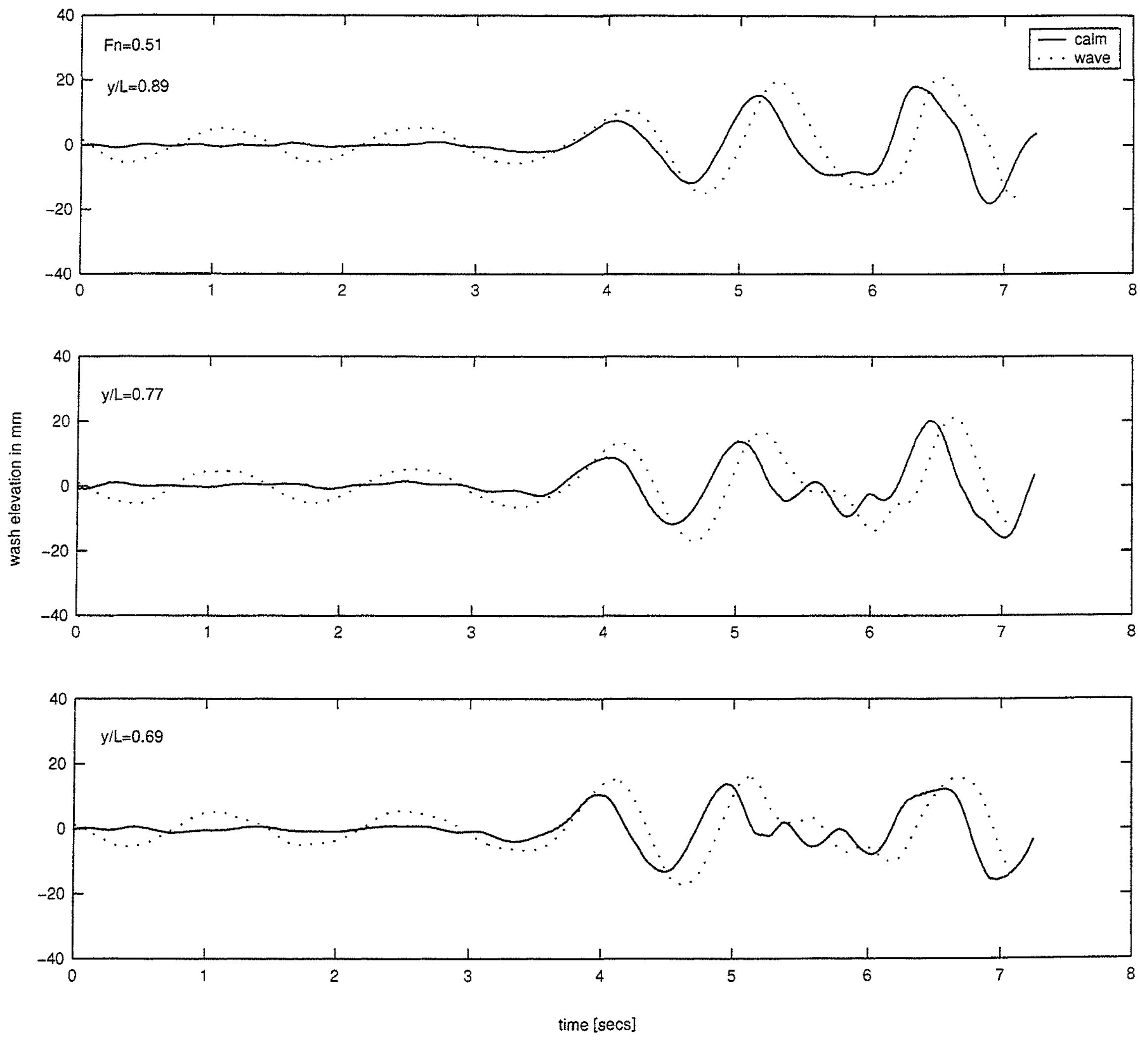

Figure 4.22: Catamaran s/L=0.2 with bulb01: Wash measured in Calm Water and Regular Wave 2.0L at F_n=0.51

Chapter 5

Experiments in shallow water

5.1 General

The effects of shallow water on ship performance although known for over a century and discussed in number of papers, are commonly considered to be of marginal importance in ship design. This is mainly due to the concentration of work in deep water situations where rougher sea condition govern the design principles.

The study of shallow water waves can be easily found in various text books on coastal engineering or oceanographical engineering such as Wiegel[111] and Silvester[88]. In shallow waters, the sea is largely influenced by currents and bottom topography. As a deep water wave approaches shallow waters, the decrease in water depth changes its characteristics. These changes include speed reduction and increase in steepness. Assuming the wave period remains constant, the consequence of speed reduction results in steeper slope (i.e. ratio of crest amplitude to trough amplitude greater than 1) and shorter wave length. The direction of the wave is also altered and depending on the bottom topography the wave rays can diverge or converge. Thus, in shallow waters, extreme sea conditions may result from relatively mild waves originating from deep water. Also, in shallow waters large wash or ship-generated waves may occur for a ship approaching port.

To date, research efforts on ship-generated waves in shallow waters have been rare.

The *raison d'etre* of this study was to investigate the behaviour and performance of the four bulbous bows in shallow waters in a range of speeds covering the *sub-critical, critical* and *super-critical* speeds.

Concerning the critical speed, there are at least three different speeds in shallow water that are close to *critical* as illustrated by Hofman(1998)[46];

- it is the maximum speed of the transverse waves in water depth h, $v = \sqrt{gh}$, *critical.*

- Also, it is the speed corresponding to the peak value of wave-making resistance curve, which may be different.
- Also, the critical speed is sometimes called the speed corresponding to the maximum of shallow water resistance ratio, i.e. the ratio between shallow water resistance and deep water resistance, which may be different.

The adopted methodology is to use a model testing approach to try to understand the performance of ship model fitted with four different types of bulbous bows in shallow waters. Treating such problem theoretically is beyond the scope of this investigation.

5.2 Wash and Ship Resistance in Shallow Water

Wash or ship-generated waves are very small in terms of wave amplitude compared to storm waves but they have a very long wave period. Consequently they build in height rapidly in shallow water at the shoreline causing substantial surges on beach as which can endanger people bathing or walking along the coast; damage to small craft or moored vessels. The main risk to users of coastal is that the waves arrive unexpected and break on the shoreline often after the fast ferry is out of sight, Whittaker(2001)[24].

Shallow water dramatically increases the wash. In shallow waters, the seabed interfere with ship wave-making forcing changes to wave patterns, energy levels and vessel running condition.

Millward et al[71],[72],[73] showed in their work on the fast displacement hull form both theoretically and experimentally that there was an increase in resistance in shallow water at sub-critical speeds, rising to a peak just below the critical speed, but at super-critical speeds a reduction in resistance can be obtained when compared with the value in deep water at the same ship speed. Also see [24] for more explanations.

5.3 Model test in Shallow Water

The shallow water tests were carried out on a 1.6m catamaran model in the towing tank 200m x 4.6m x 0.4m at GKN Westland Aerospace Ltd in Isle of Wight, UK.

The tank has a manned carriage which is equipped with a dynamometer for measuring model total resistance together with computer and instrumentation facilities for automated data acquisition.

The purpose of the model test was to measure the wash generated by the hulls at different speeds in shallow water with different bulbous bow fitted to the hull. Again, the model used in this work is a catamaran, $s/L = 0.2$. Calm water resistance, sinkage, trim and wash measurements were recorded for all the models. All tests were carried out at four speeds ranging from 1 m/s to 4m/s for three different trim conditions namely level trim, stern trim and bow trim as shown in Table 5.1

The accuracy of the total resistance was found to be in the range of $\pm 0.02N$. Sinkage amplitudes were measured with a linear potentiometer attached to the heave post. The accuracy of the linear potentiometer was found to be $\pm 0.1mm$. Trim was measured with an angular potentiometer incorporated into the towing fitting. It was measured as angle in degrees and taken positive for bow up. The accuracy of the potentiometers was in the range of $\pm 0.05°$.

The ship wash was measured by capacitance-type wave probes at three locations by three probe arrays along perpendicular to the sailing line as given in Tables 5.2, 5.3 and 5.4. The arrangement of of those probes in the towing tank are shown in Figure 5.1.

V m/s	F_{nl}	F_{nh}	Bulb01	Bulb02	Bulb03	Bulb04
1	0.25	0.50	√	√	√	√
2	0.50	1.00	√	√	√	√
3	0.75	1.50	√	√	√	√
4	1.00	2.00	√	√	√	√

Table 5.1: Shallow water's test matrix

Probe No.	Distance from Tank's Centreline	y/L
Probe 1	0.688 m	0.43
Probe 2	0.880 m	0.55
Probe 3	1.088 m	0.68
Probe 4	1.280 m	0.80
Probe 5	1.488 m	0.93
Probe 6	1.680 m	1.05
Probe 7	1.888 m	1.18
Probe 8	2.080 m	1.30

Table 5.2: The middle wave probes array position for GKN tank

5.4 Test Results and Observations

The measured data are the resistance, sinkage, trim and the wash generated at the three different locations of probe arrays from the model. The data are plotted against Froude numbers based on water depth and model length. The results are shown in Figures 5.11

Probe No.	Distance from Tank's Centreline	y/L
Probe 1	1.424 m	0.89
Probe 2	1.632 m	1.02
Probe 3	1.824 m	1.14
Probe 4	2.032 m	1.27

Table 5.3: The aft end wave probes array position for GKN tank

Probe No.	Distance from Tank's Centreline	y/L
Probe 1	1.424 m	0.89
Probe 2	1.632 m	1.02
Probe 3	1.824 m	1.14
Probe 4	2.032 m	1.27

Table 5.4: The forward end wave probes array position for GKN tank

to 5.22.

The total resistance measurements were corrected to a standard temperature of 15°. Figure 5.11 and 5.12 show the total model resistance coefficients and resistance components for all four models respectively.

In Figure 5.11 indicates that in the subcritical speed range $F_{nh} < 1.0$ all the four bulbous bows experienced almost the same amount of drag. However, at the critical speed it clearly shows that the bulbous bows i.e. bulb01, bulb02, bulb03 and bulb04 reduced the total resistance coefficient by 16%, 15%, 14% and 13% respectively.

Figure 5.12 shows that the total resistance rising rapidly as the shallow water's critical speed was approached. In this figure also, it can be seen that for depth Froude number 0.75 to 1.25 the residuary resistance is dominant.

For comparing the relative merits of bulbous bows these results are presented in terms of residuary resistance as shown in Figure 5.13. This figure shows the effect of bulbous bows on the residuary resistance varies according to the bulbous bow size. The shortest bulbous bow i.e. bulb01 is superior among the four bulbous bows. At the critical speed in shallow water, bulb01, bulb02, bulb03 and bulb04 reduced the residuary resistance coefficient by 25.3%, 24.3%, 23.0% and 21.2% respectively.

Table 5.7 shows the results as obtained from the model tests in shallow water. It is found that in shallow water, the bulbous bow gives an average increment of about 2.1%, 2.4% and 5.6% of the total model resistance for bulb02, bulb03 and bulb04 respectively.

Figure 5.14 shows the total model resistance plotted against length Froude number in

V m/s	F_{nl}	F_{nh}	Ori	Bulb01	Bulb02	Bulb03	Bulb04
1	0.25	0.50	100	87.8	89.3	87.0	91.6
2	0.50	1.00	100	84.2	84.7	85.7	86.7
3	0.75	1.50	100	85.9	87.3	87.0	92.1
4	1.00	2.00	100	84.4	88.2	87.8	91.0

Table 5.5: Percentage of Total Resistance of Model with and without bulb in Shallow water

V m/s	F_{nl}	F_{nh}	Ori	Bulb01	Bulb02	Bulb03	Bulb04
1	0.25	0.50	100	73.9	77.2	72.3	82.0
2	0.50	1.00	100	74.7	75.4	77.0	78.8
3	0.75	1.50	100	68.6	71.6	71.0	82.4
4	1.00	2.00	100	61.5	70.8	69.9	77.6

Table 5.6: Percentage of Residuary Resistance of Model with and without bulb in Shallow water

deep and shallow waters. It can be seen that the general effect of the shallow water is to cause an increase in resistance at the lower speeds compared with the deep-water value but a reduction in resistance at higher speeds or Froude number. These findings are in agreement with studies undertaken by Millward [71],[72], on high-speed displacement hull form.

At higher speed range, i.e. supercritical speed $F_{nh} > 1.0$ some crossover points occur, but for all four bulbous bows tested it may be concluded that the shortest bulbous bow i.e. bulb01 produces the lowest total resistance in shallow water. In this speed region the longest bulbous bow i.e. bulb04 produce the highest total model resistance whilst bulb02 and bulb03 coincides each other as shown in Figure 5.11.

Figures 5.2, 5.3, 5.4 and 5.5 show wash traces at critical depth Froude number produced by model fitted with bulb01, bulb02, bulb03 and bulb04 respectively. From these figures, it may be concluded that the shortest bulbous bow namely bulb01 produces the lowest wash at critical depth Froude number which was recorded by the middle eight probes array.

Figures 5.6, 5.7, 5.8 and 5.9 show the wash traces recorded by the aft and forward ends probes at critical depth Froude number produced by model fitted with bulb01, bulb02, bulb03 and bulb04 respectively.

As shown in Figures 5.17 to 5.20, the non-dimensional maximum wash for all models increases with Froude number until a critical value. At $F_{nh} \simeq 1.0$ they attain the peak

V m/s	F_{nl}	F_{nh}	Bulb01	Bulb02	Bulb03	Bulb04
1	0.25	0.50	100	101.7	99.1	104.4
2	0.50	1.00	100	100.6	101.8	103.0
3	0.75	1.50	100	101.6	101.3	107.3
4	1.00	2.00	100	104.5	104.1	107.8

Table 5.7: Percentage of Total Model Resistance in Shallow water

values. When $F_{nh} > 1.0$ those peak values decrease with F_{nh}. The non-dimensional maximum wash values were deduced from the wash traces measured at the forward end and aft end wave probes by using Equation 3.4 as discussed earlier in Chapter 3. These plots also revealed that the maximum wash measured at any single fixed point as the ship passes is dependent on its transverse distance from the sailing line of the ship.This is probably due to the interference between the wave trains as well as the general decay away from the ship.

Figures 5.21 and 5.22 show the variation of the maximum wash height with the depth Froude number and the distance from the sailing line. These figures demonstrate that for the critical and super-critical conditions, the maximum wash height increase dramatically at a distance 1.9m or 1.2L from the sailing line. This is probably due to a narrow tank phenomenon.

By comparing the non-dimensional wash from these figures with the one obtained for deep water condition in Chapter 3, it was found that the wash in shallow water increases by 40% to 100% which depends on F_{nh} and bulbous bows (bulbol, bulb02, bulb03 or bulb04).

Figures 5.15 and 5.16 show the sinkage and trim amplitudes in shallow water respectively. It can be seen that both sinkage and trim attain their peak at a Froude depth number of exactly 1.0.

Table 5.9 shows us that the sinkage experienced by the model fitted with bulb02 and bulb04 increased by 46.6% and 27.5% respectively with respect to bulb01 but in contrast bulb03 offered 0.5% reduction.

V m/s	F_{nl}	F_{nh}	Ori	Bulb01	Bulb02	Bulb03	Bulb04
1	0.25	0.50	100	102.1	109.9	107.3	113.8
2	0.50	1.00	100	152.9	131.4	120.5	132.5
3	0.75	1.50	100	41.2	86.3	46.3	41.4
4	1.00	2.00	100	20.5	37.6	20.9	43.3

Table 5.8: Percentage of Sinkage of Model with and without bulb in Shallow water

V m/s	F_{nl}	F_{nh}	Bulb01	Bulb02	Bulb03	Bulb04
1	0.25	0.50	100	107.7	105.1	111.5
2	0.50	1.00	100	85.9	78.8	86.7
3	0.75	1.50	100	209.4	112.2	100.5
4	1.00	2.00	100	183.4	101.9	211.2

Table 5.9: Percentage of Sinkage in Shallow water

V m/s	F_{nl}	F_{nh}	Ori	Bulb01	Bulb02	Bulb03	Bulb04
1	0.25	0.50	100	52.2	75.0	49.9	43.0
2	0.50	1.00	100	103.6	97.9	100.1	97.7
3	0.75	1.50	100	93.3	97.6	92.8	95.8
4	1.00	2.00	100	107.4	93.9	88.7	88.1

Table 5.10: Percentage of Running trim of Model with and without bulb in Shallow water

In Figure 5.16, it shows that the effect of bulbous bows on trim are less significant than on sinkage. For bulb02, bulb03 and bulb04, there are 22.0%, 27.9% and 30.0% reductions in trim with reference to bulb01. These findings agree with the theory since the bulb04 gives more damping than other bulbous bows.

It may be noticed from these result that the bulbous bows do a little to reduce trim.

5.4.1 Observations

Observations of the flow at the transom stern was made during the experiments. The flow at low speed is associated with vortices and the transom stern area is totally wet. At high speeds the flow cleanly separates from the transom stern and the transom stern area is dry. But there is also the condition where the transom was a semi-dry or semi-wet. Similar phenomenon also reported by Insel et al [54] in their work on high-speed craft.

At model speed around 2.0 m/s corresponding to critical speed $F_h = 1.0$, solitons or solitary waves can be observed travelling a bit faster than a ship model as shown in Figure 5.10. The amplitudes of these solitons are much larger than the amplitudes of waves behind the ship. Dand, I. et al,[17] also reported the similar phenomenon observed in their recent work.

In the region of $F_{nh} \geq 1.0$ is known as super-critical region where no waves have greater velocity or speed than the ship speed, because $\sqrt{gh}$ correspond to the maximum wave velocity which can exist in water of depth h. In this region only the diverging waves were observed and no transverse waves were seen.

V m/s	F_{nl}	F_{nh}	Bulb01	Bulb02	Bulb03	Bulb04
1	0.25	0.50	100	14.4	9.6	0.8
2	0.50	1.00	100	94.6	96.7	94.3
3	0.75	1.50	100	104.7	99.5	102.8
4	1.00	2.00	100	87.5	82.5	82.0

Table 5.11: Percentage of Running trim in Shallow water

5.5 Summary

Four different bulbous bows fitted to a catamaran $s/L = 0.2$ were tested in water depth 400mm at speed range 1m/s to 4m/s to measure the total resistance, trim, sinkage and wave elevation or wash. An extensive data base has been established which shows the effects of bulbous bows, length and depth Froude number on resistance, wash, trim and sinkage for high speed displacement catamaran operating in shallow water.

Corrections for water temperature were carried out. The blockage effect due tank walls and floor were found to be small, hence were neglected.

It can be seen the general effect of the shallow water is to cause an increase in resistance compared with the deep-water value.

Figure 5.11 shows the influence of bulbous bows on total resistance coefficient at a range of depth Froude number. It clearly shows that these bulbous bows reduce the total resistance coefficient by 13% to 16%, which the shortest i.e. bulb01 is the best followed by bulb02 and bulb03 which almost coincides each other and bulb04. As expected, the same trends also happen for residuary resistance coefficient where bulb01 offers the lowest coefficient value.

It was found that the non-dimensional maximum wash in shallow water increases by 40% to 100% compared with deep-water value. The increment varies with depth Froude number and bulbous bows.

As shown in Figure 5.16, the effects of bulbous bows on trim are less significant than on sinkage. The longest bulb i.e. bulb04 offers the highest reduction in trim than others. These findings are expected since the bulb04 gives more damping than other bulbous bows.

Hence, for a choice of bulbous bows for operating in shallow water, bulb01 good for resistance and wash, bulb03 for sinkage and bulb04 for trim.

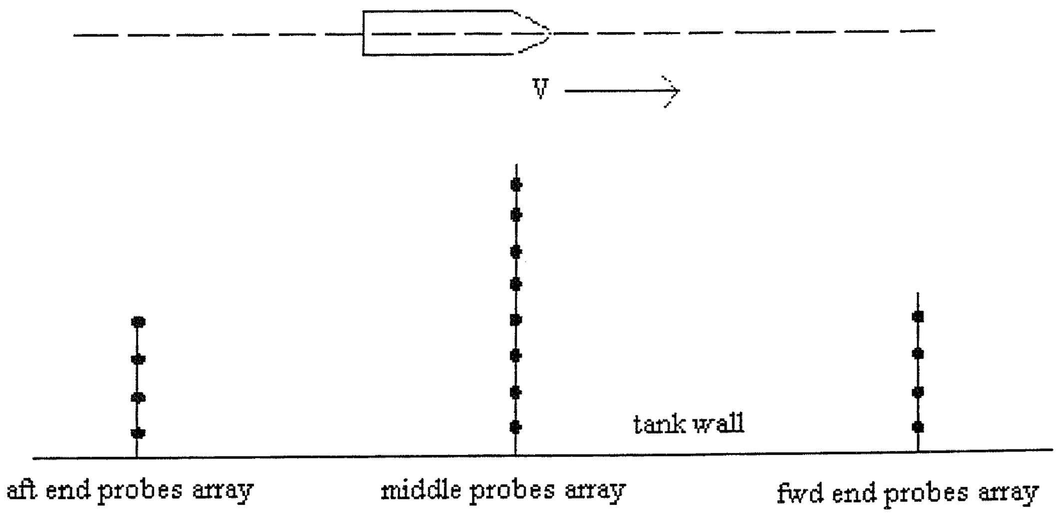

Figure 5.1: Probes Arrangement for Shallow Water Test

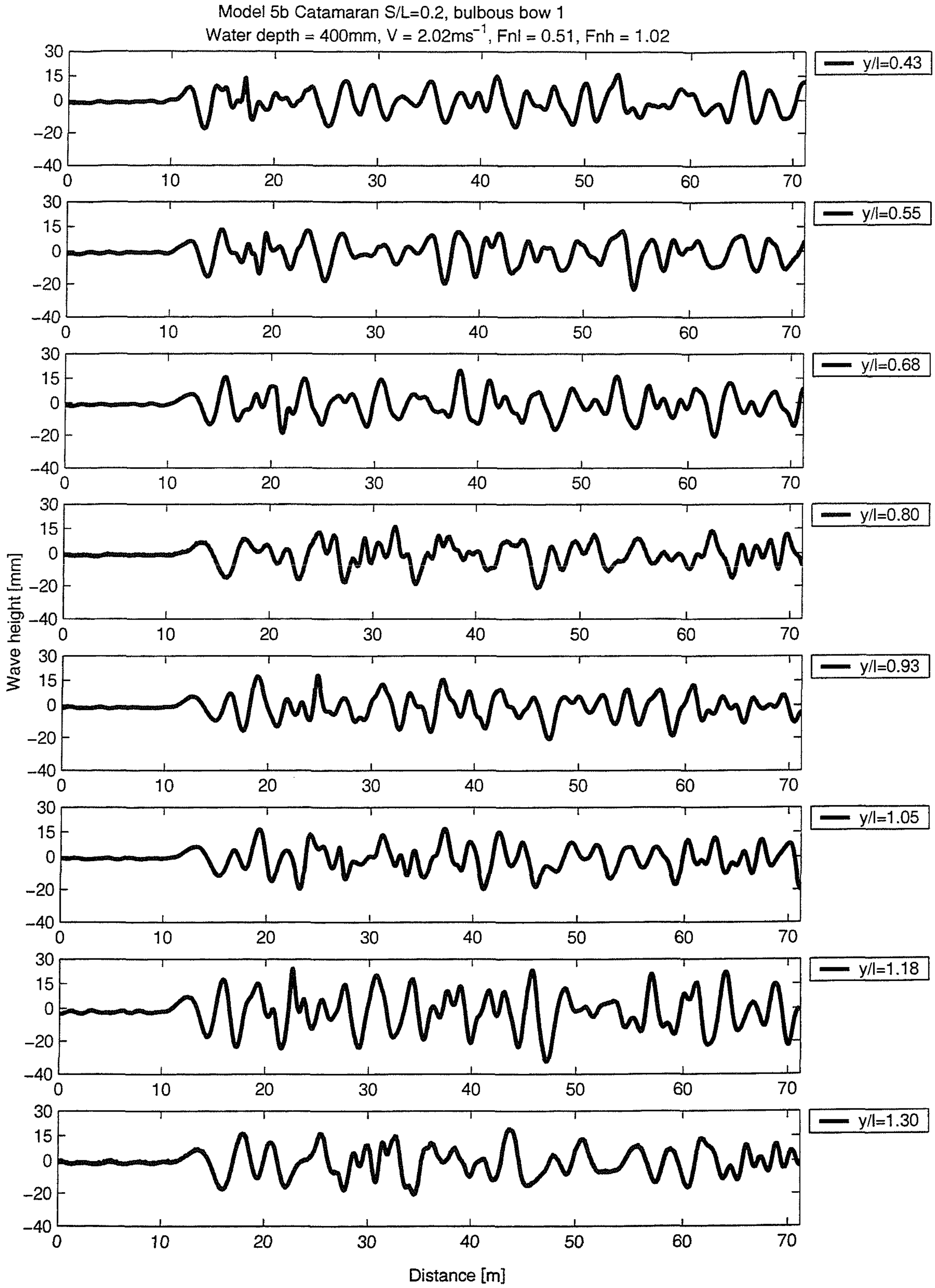

Figure 5.2: Catamaran s/L=0.2 with bulb01: Wash at Critical Depth Froude Number(middle probes)

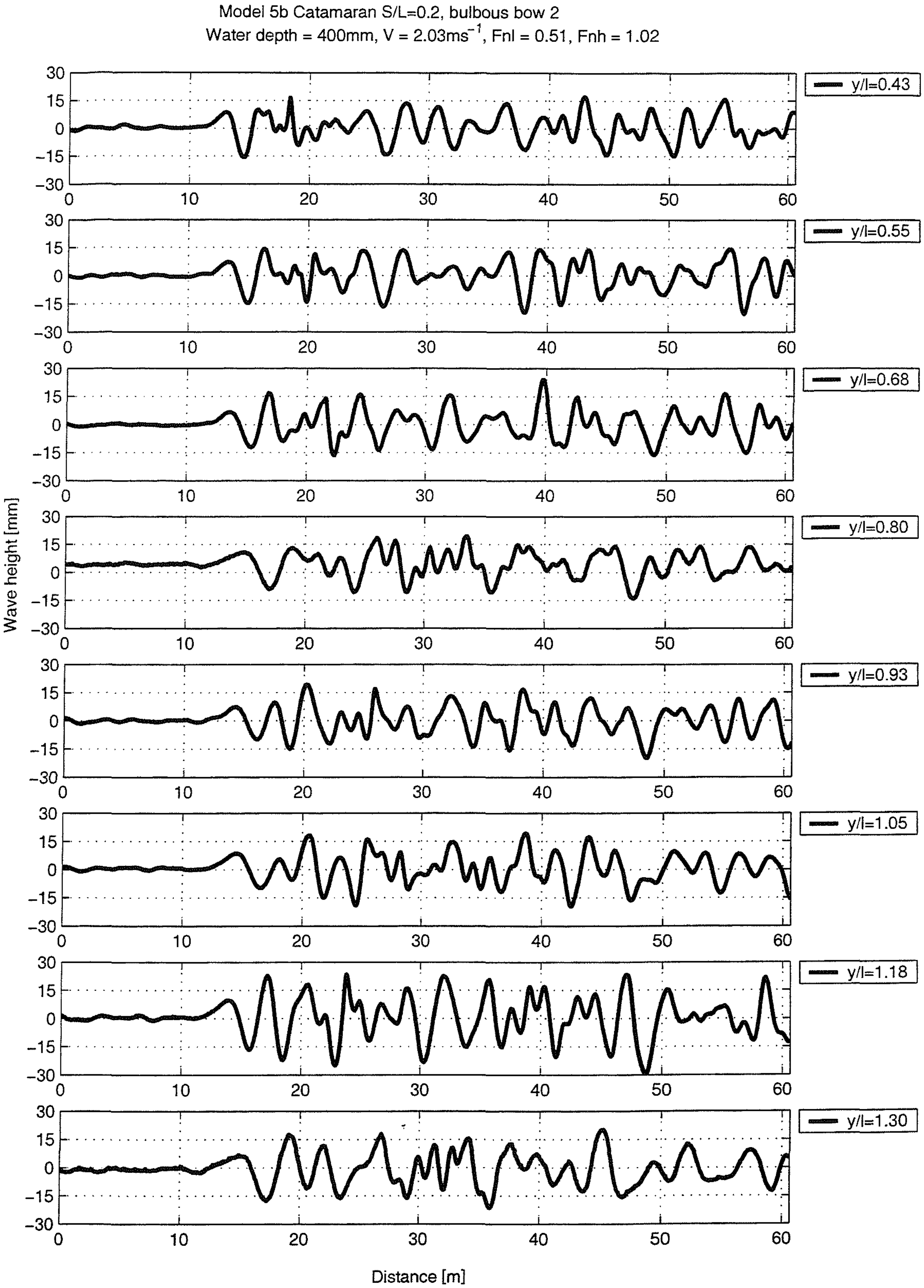

Figure 5.3: Catamaran s/L=0.2 with bulb02: Wash at Critical Depth Froude Number(middle probes)

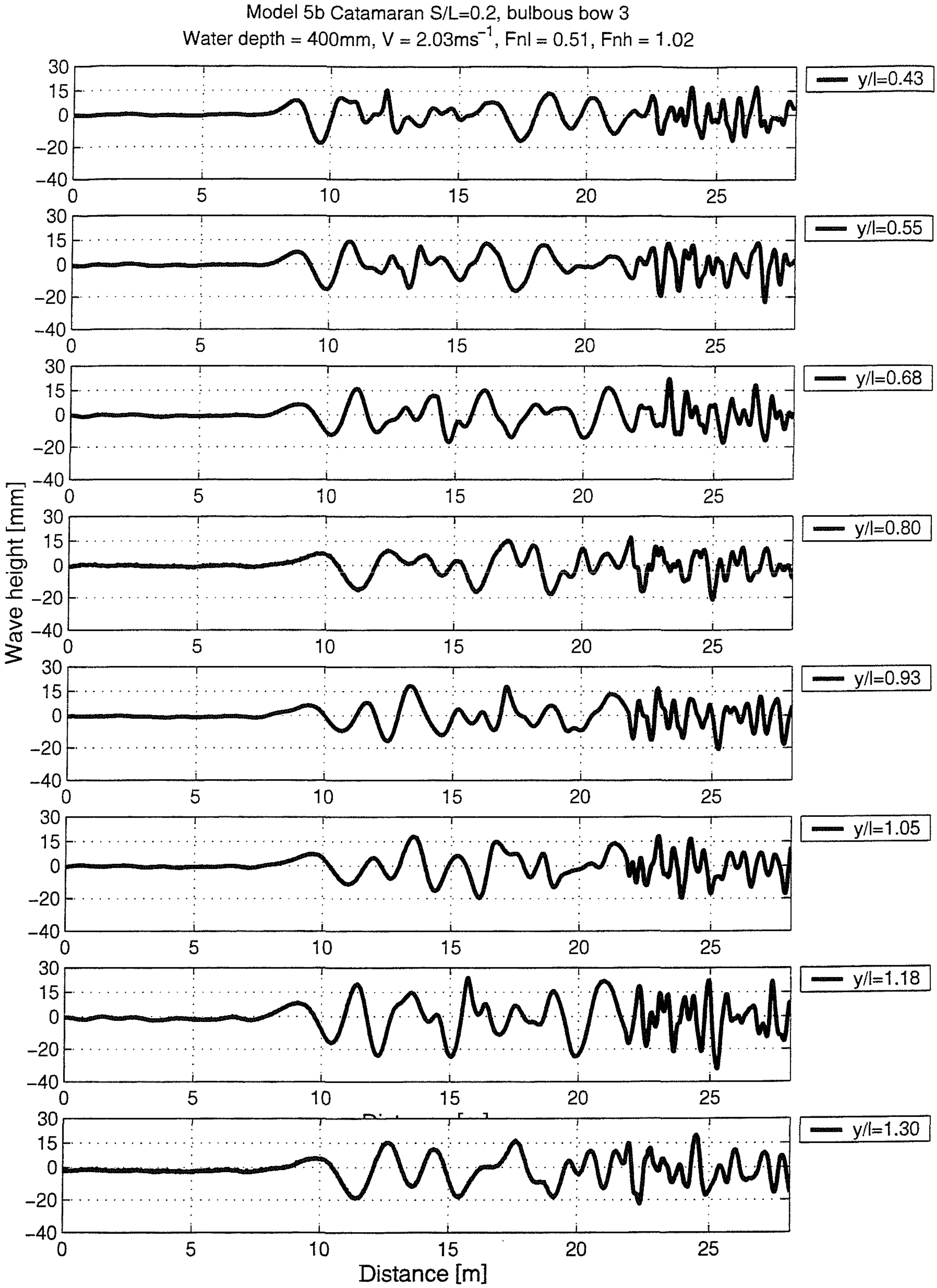

Figure 5.4: Catamaran s/L=0.2 with bulb03: Wash at Critical Depth Froude Number(middle probes)

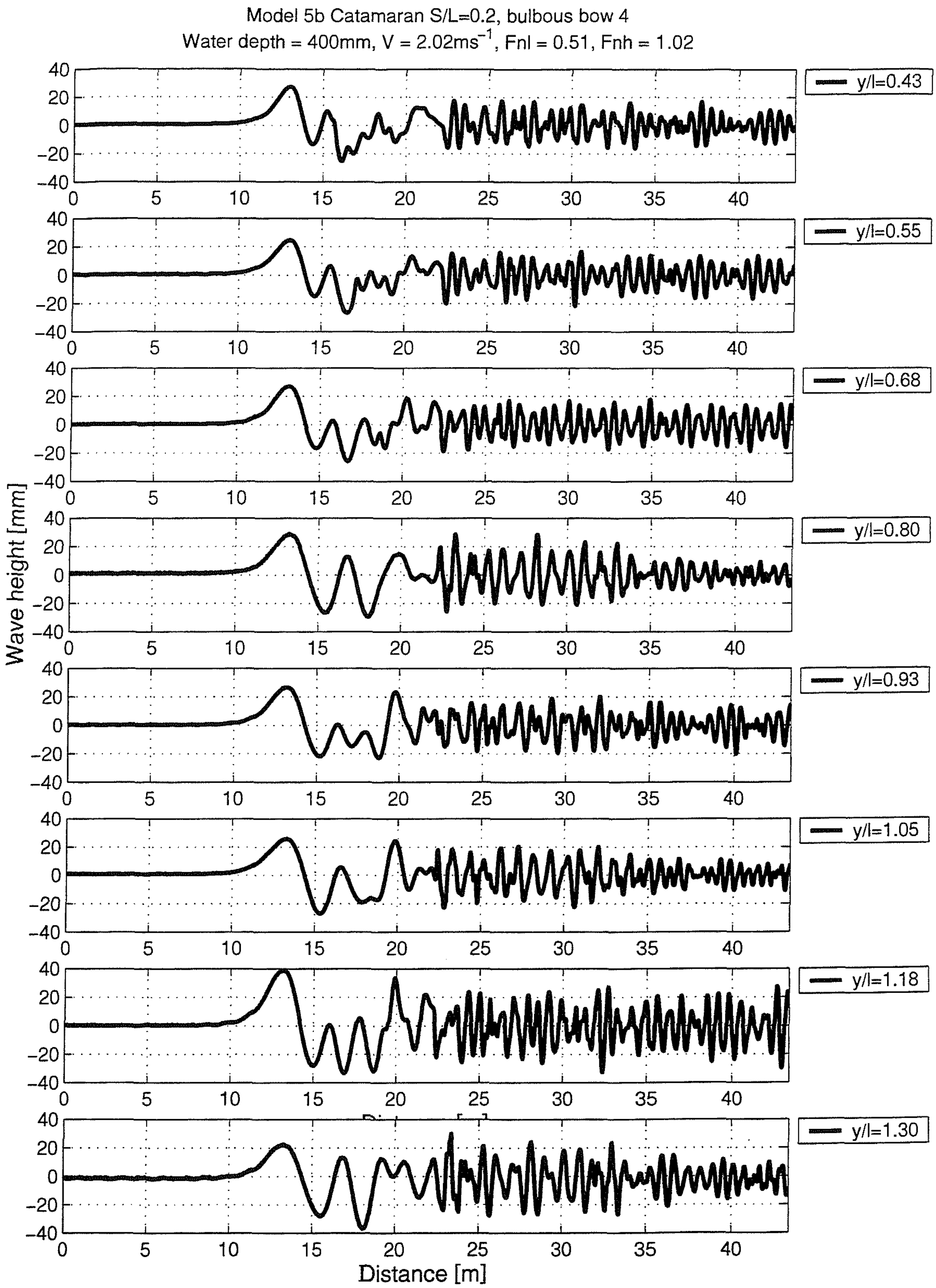

Figure 5.5: Catamaran s/L=0.2 with bulb04: Wash at Critical Depth Froude Number(middle probes)

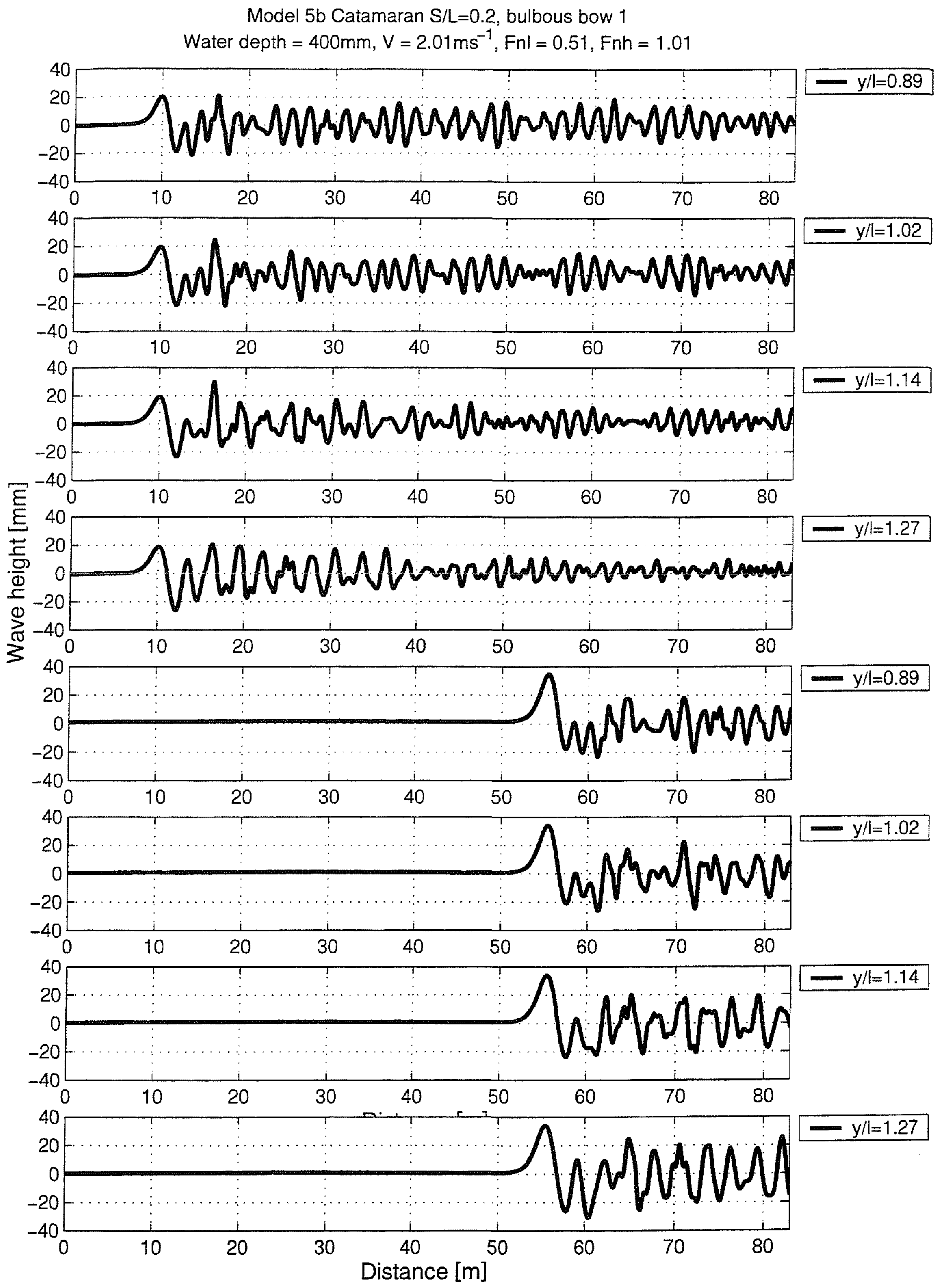

Figure 5.6: Catamaran s/L=0.2 with bulb01: Wash at Critical Depth Froude Number(aft and fwd ends probes

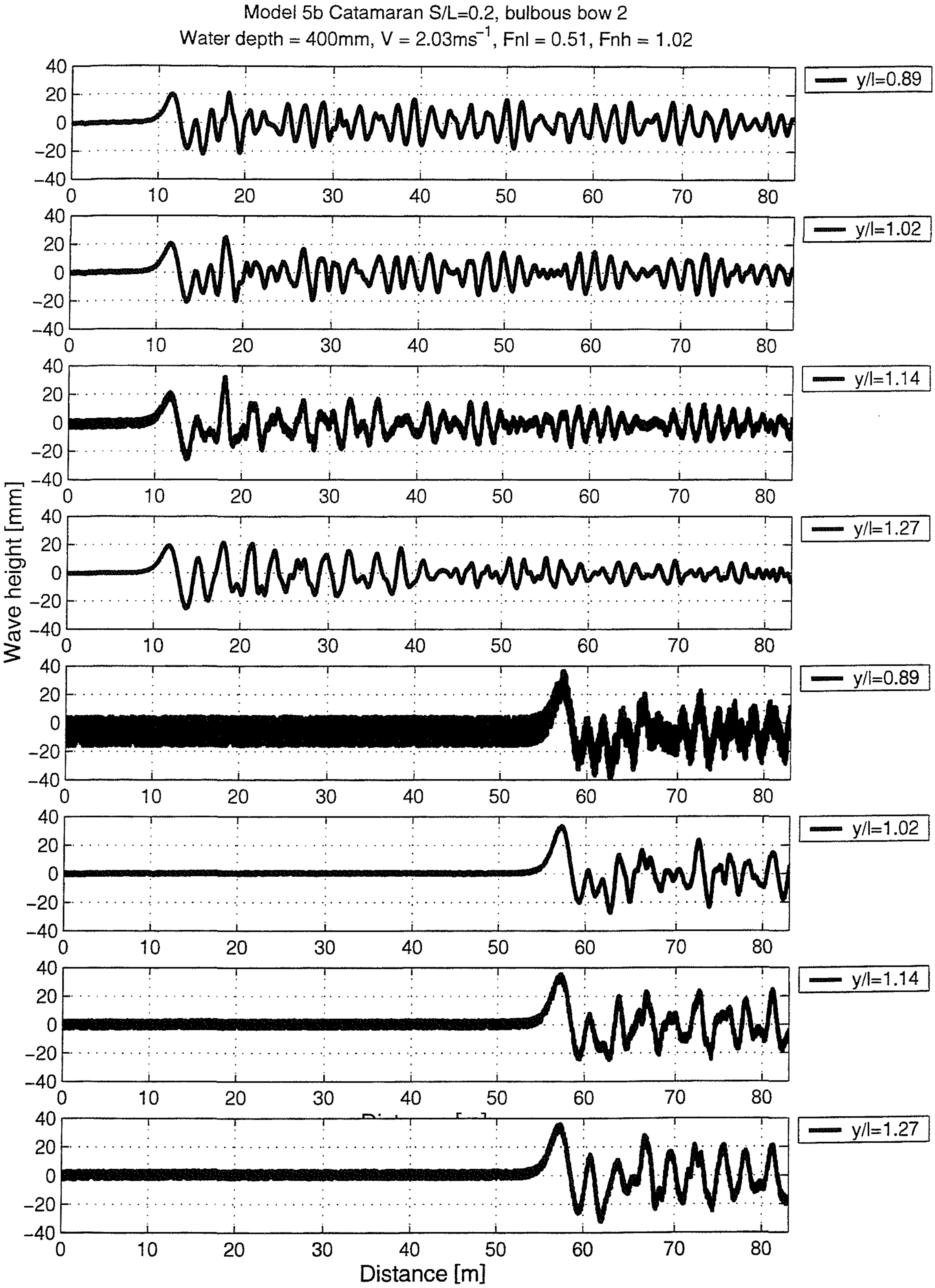

Figure 5.7: Catamaran s/L=0.2 with bulb02: Wash at Critical Depth Froude Number(aft and fwd ends probes

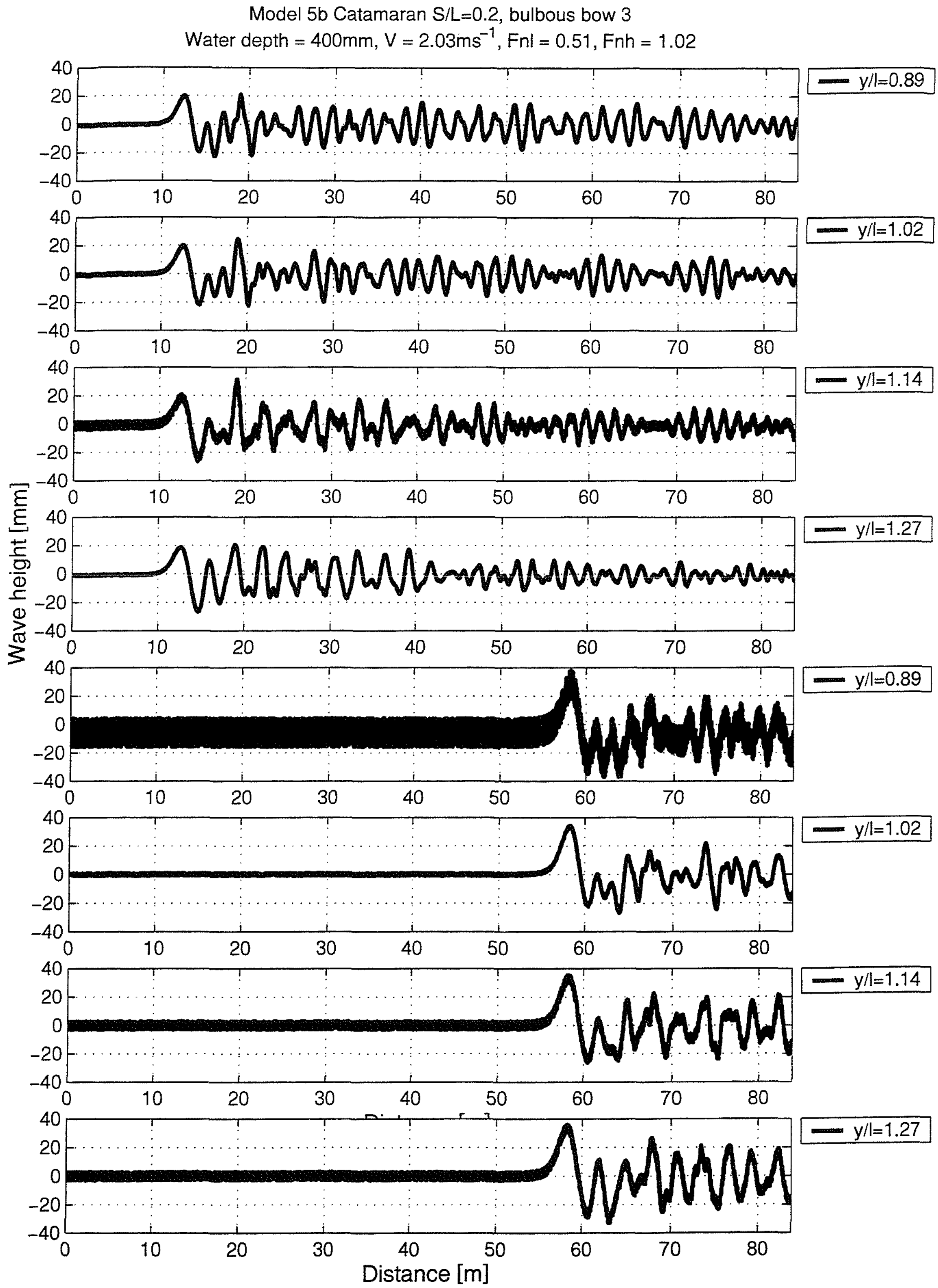

Figure 5.8: Catamaran s/L=0.2 with bulb03: Wash at Critical Depth Froude Number(aft and fwd ends probes

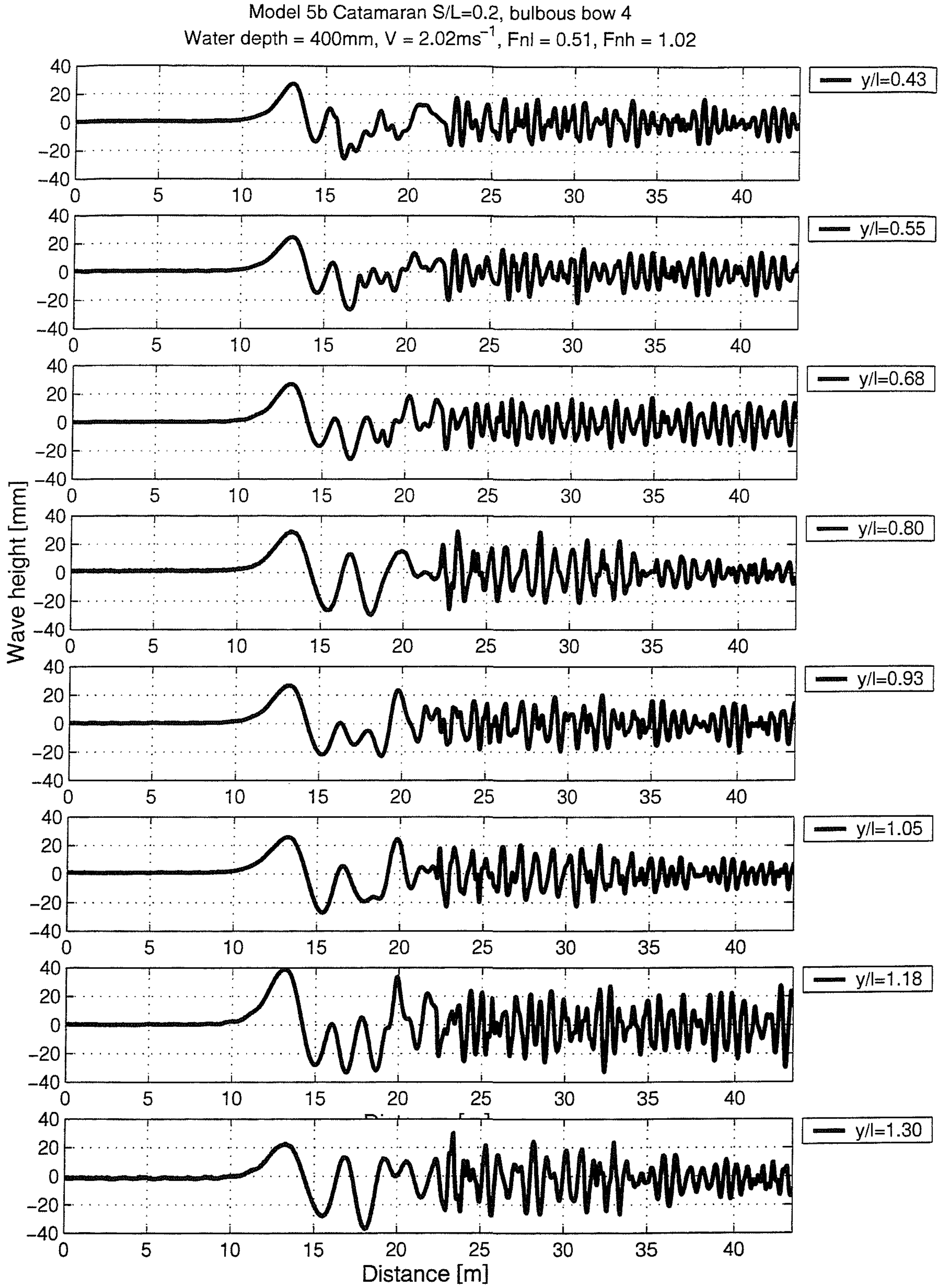

Figure 5.9: Catamaran s/L=0.2 with bulb04: Wash at Critical Depth Froude Number(aft and fwd ends probes

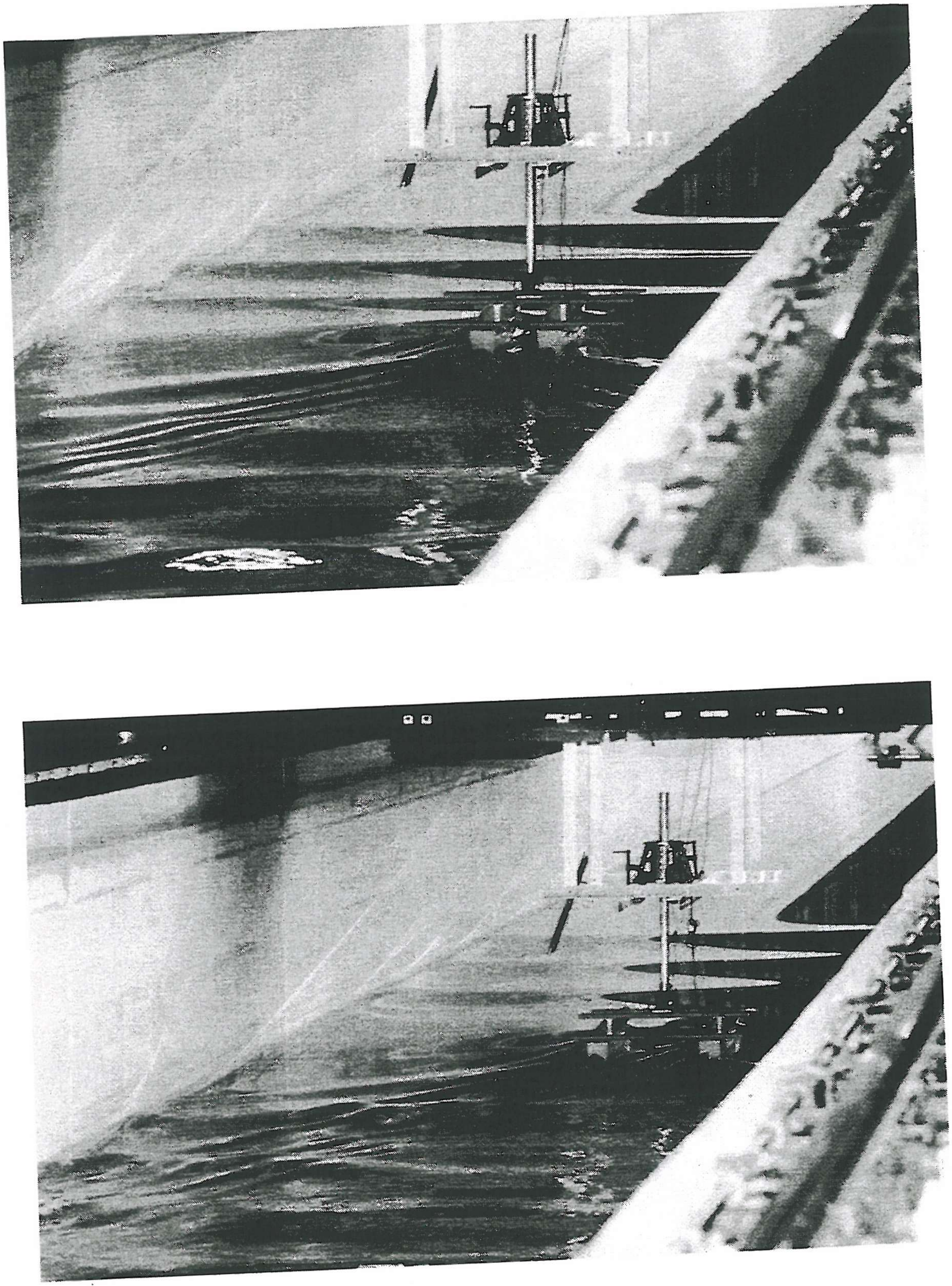

Figure 5.10: Catamaran in Shallow Water Test

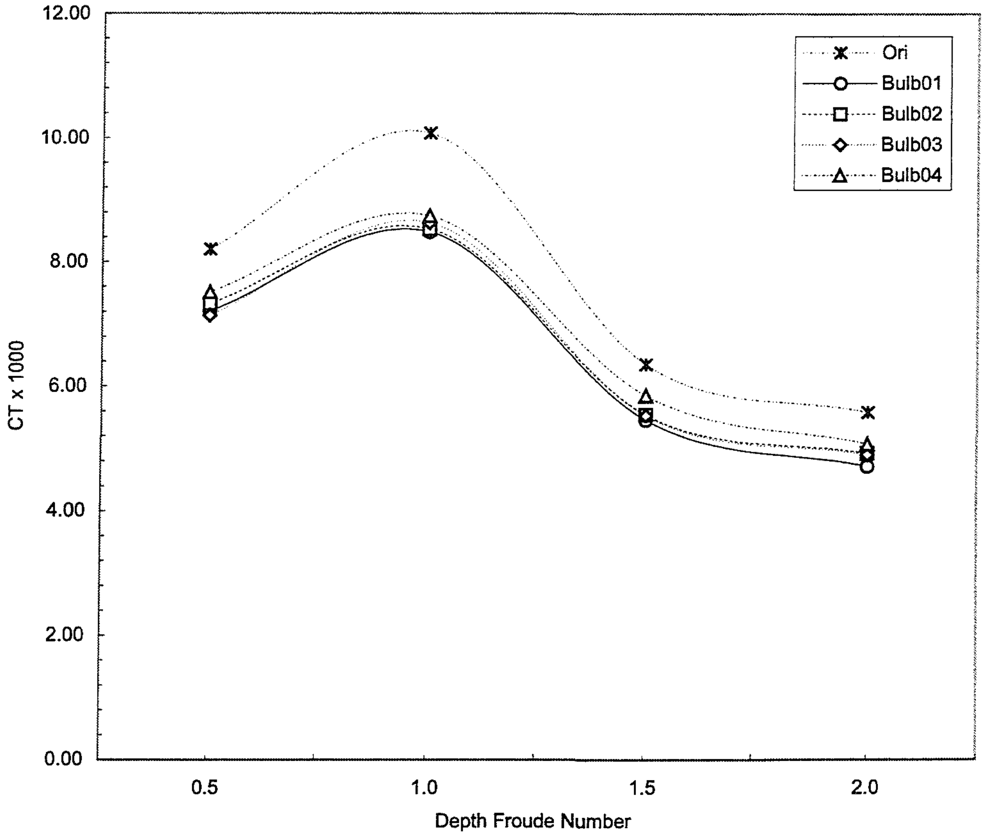

Figure 5.11: Catamaran s/L=0.2: Total Model Resistance Coefficient against Depth Froude number

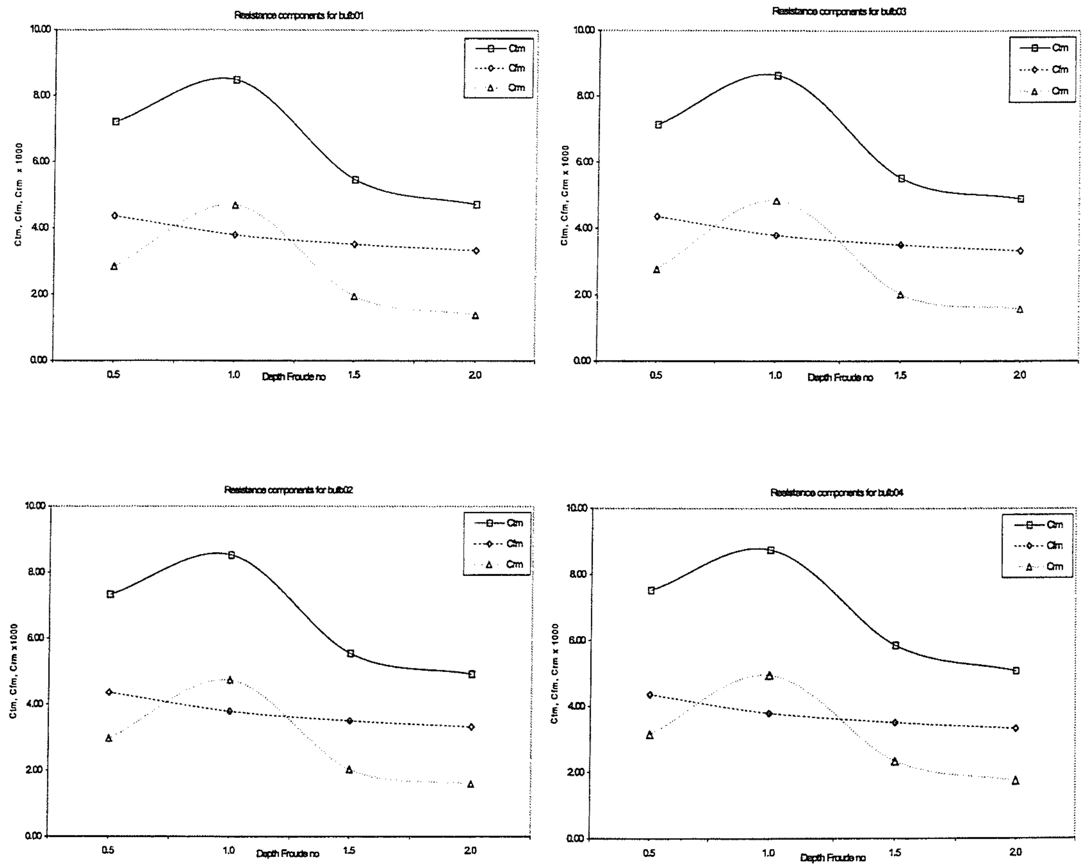

Figure 5.12: Catamaran s/L=0.2 fitted with Bulbous Bows: Resistance Components in Shallow Water

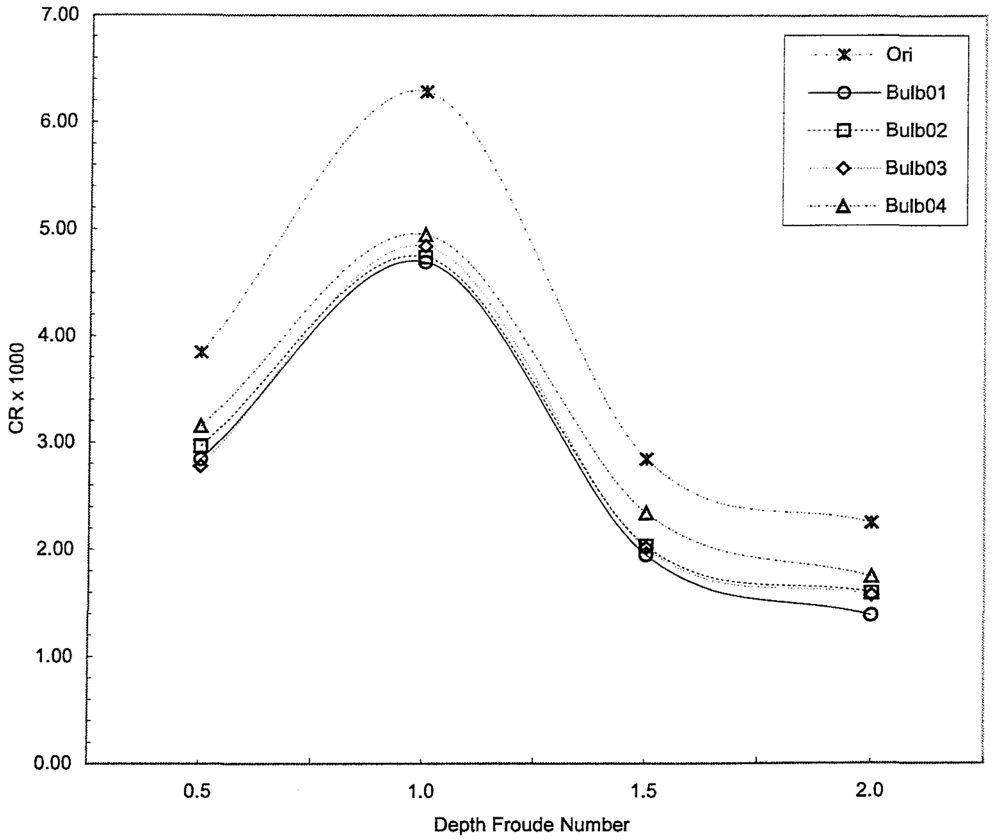

Figure 5.13: Catamaran s/L=0.2: Residuary Resistance Coefficient against Depth Froude Number

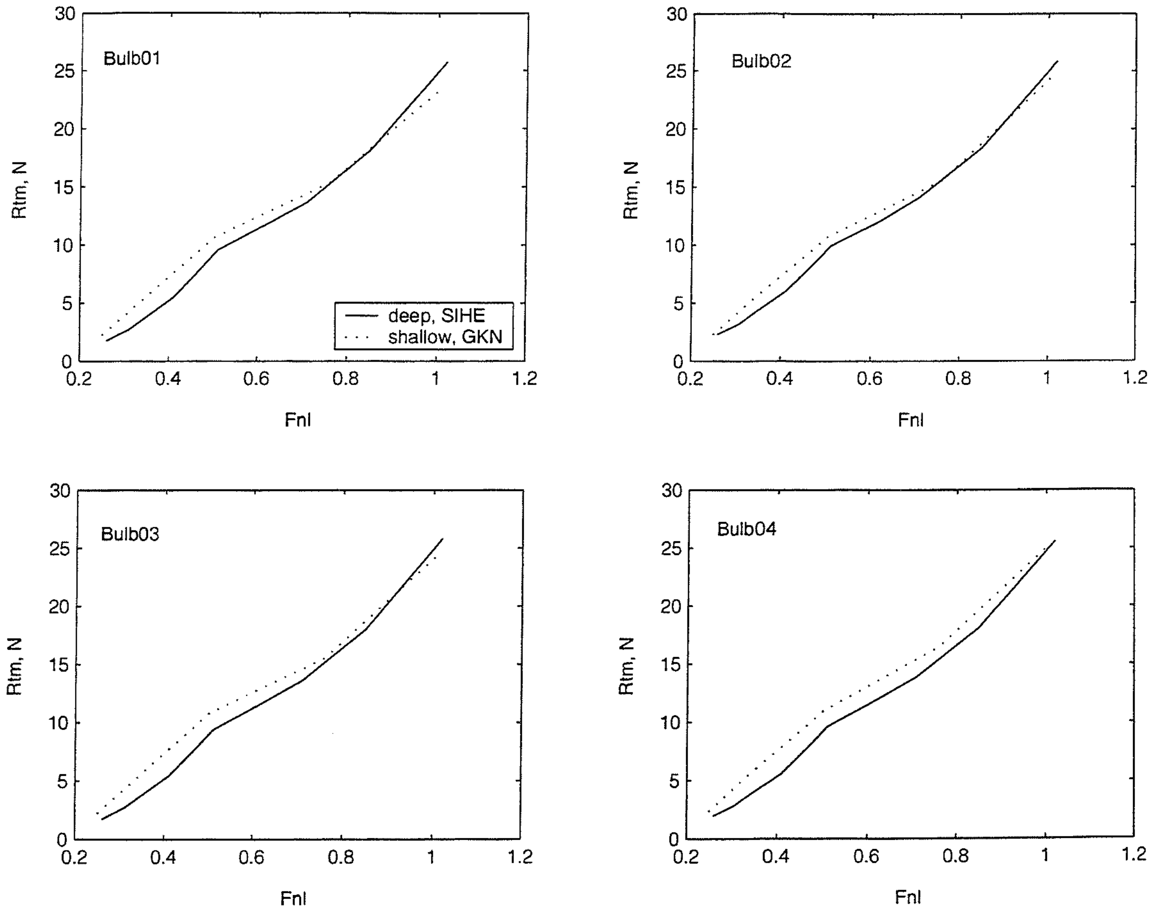

Figure 5.14: Catamaran s/L=0.2 with Bulbous Bows: Total Model Resistance in deep and shallow waters

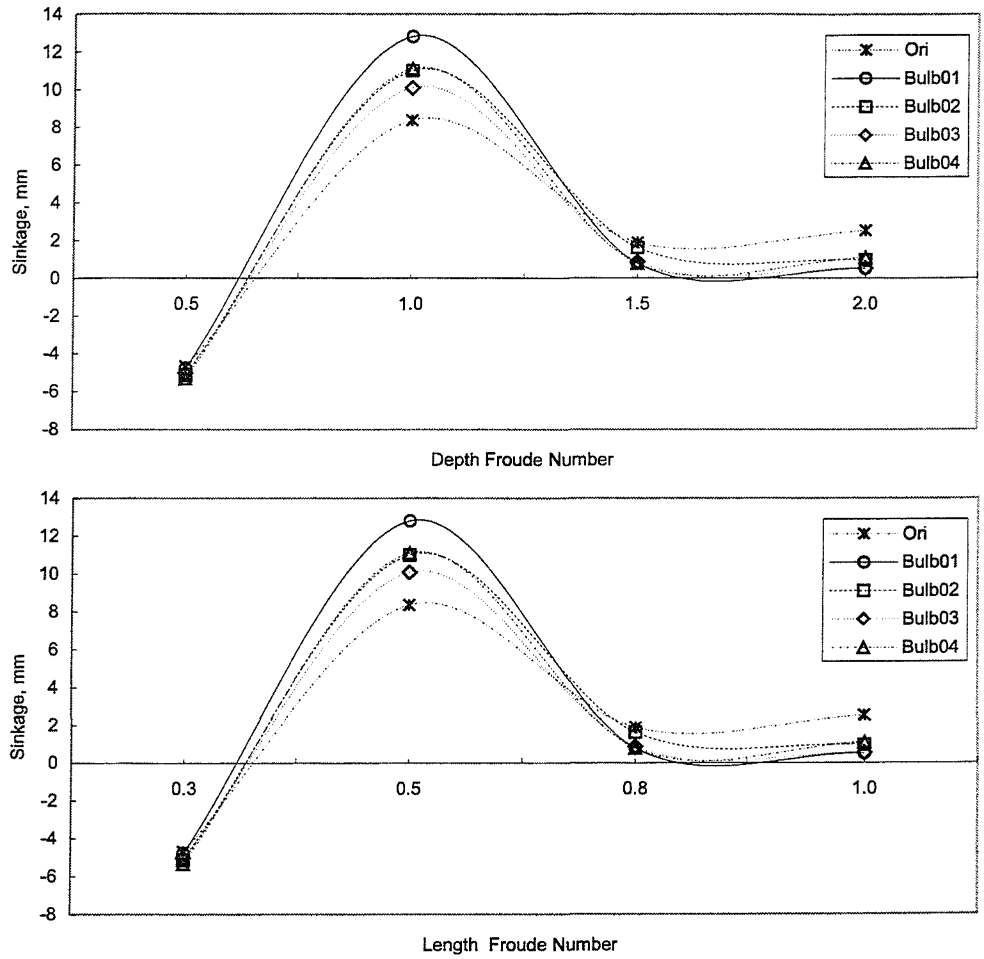

Figure 5.15: Catamaran s/L=0.2 with Bulbous Bows: Sinkage as function of Depth and Length Froude numbers

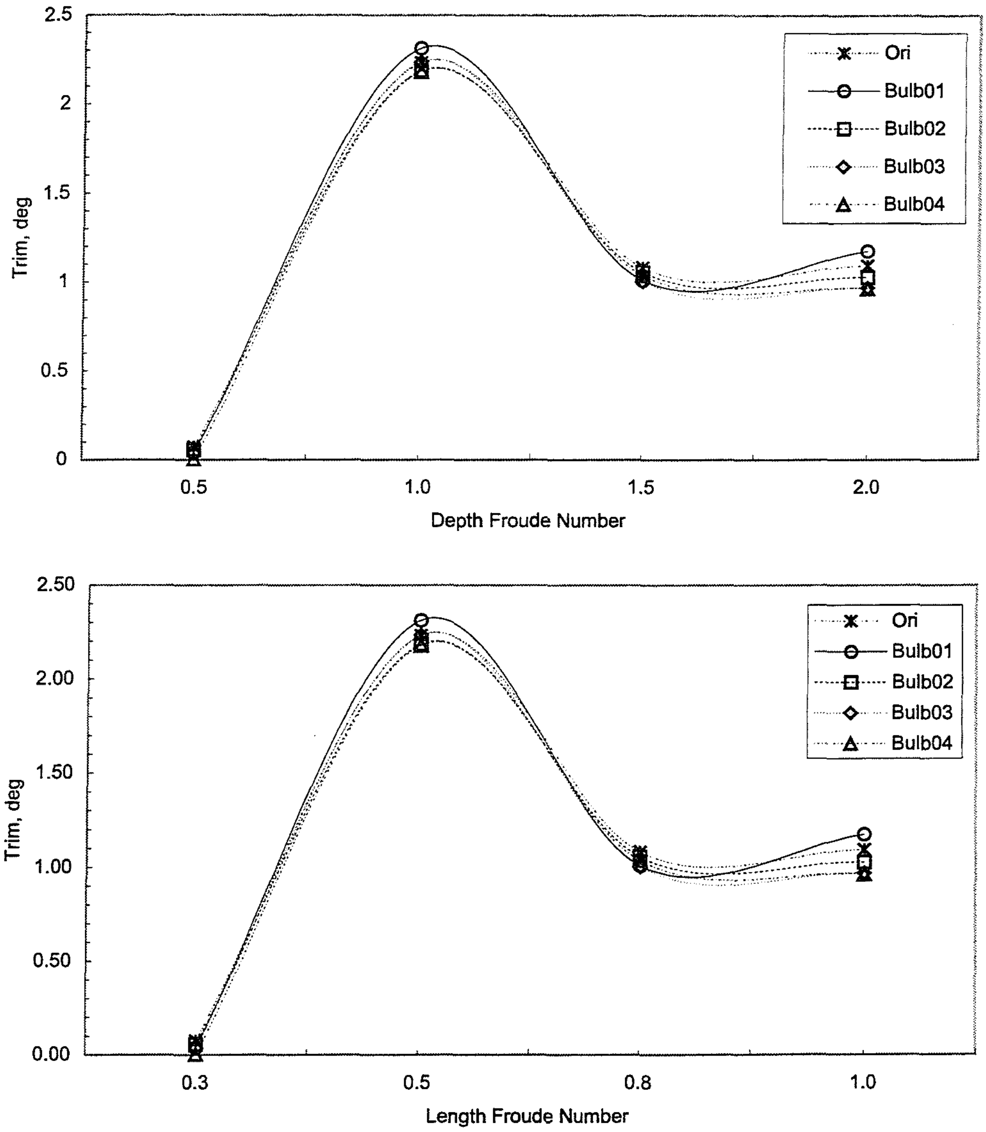

Figure 5.16: Catamaran s/L=0.2 with Bulbous Bows: Running trim versus Fn, Fnh

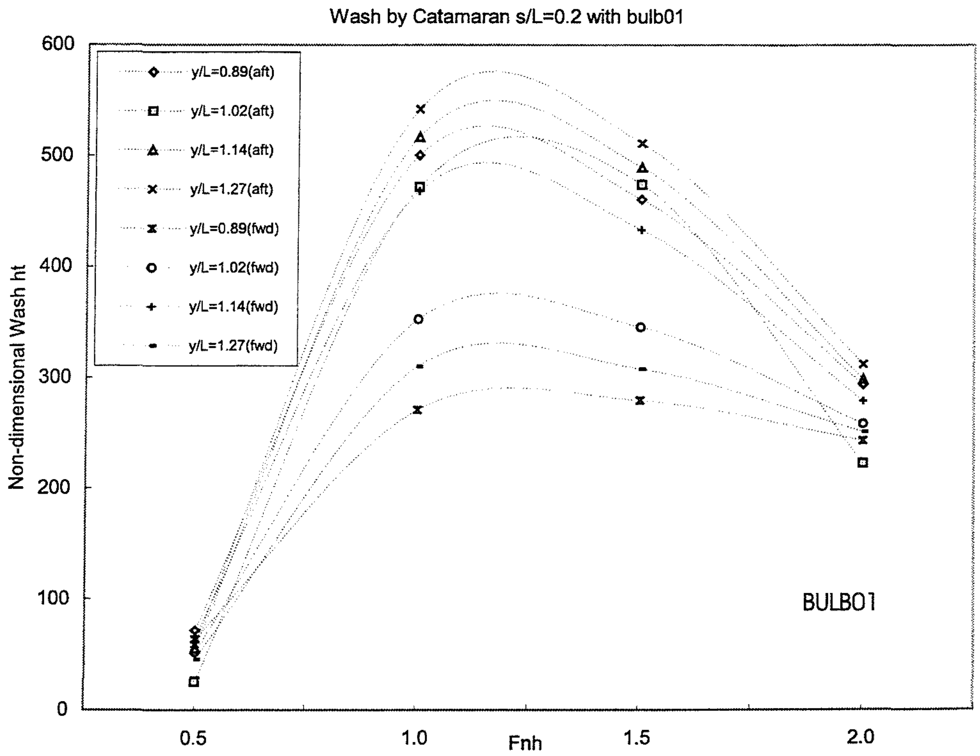

Figure 5.17: Catamaran s/L=0.2 with Bulb01: Non-dimensional Maximum Wash versus Fnh

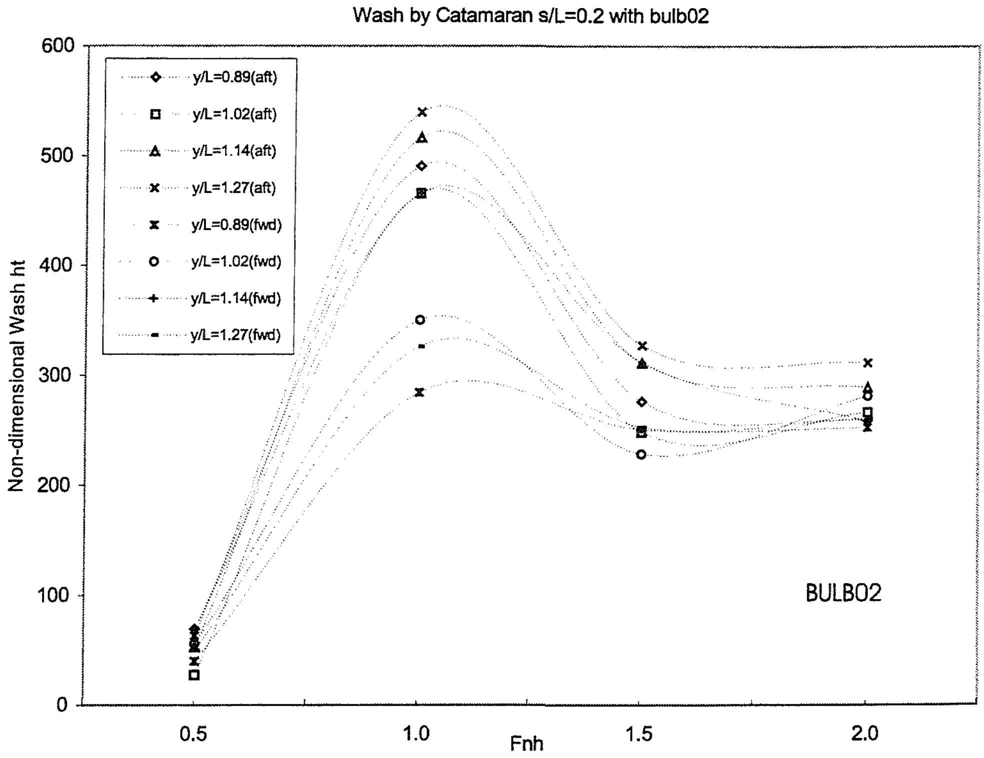

Figure 5.18: Catamaran s/L=0.2 with Bulb02: Non-dimensional Maximum Wash versus Fnh

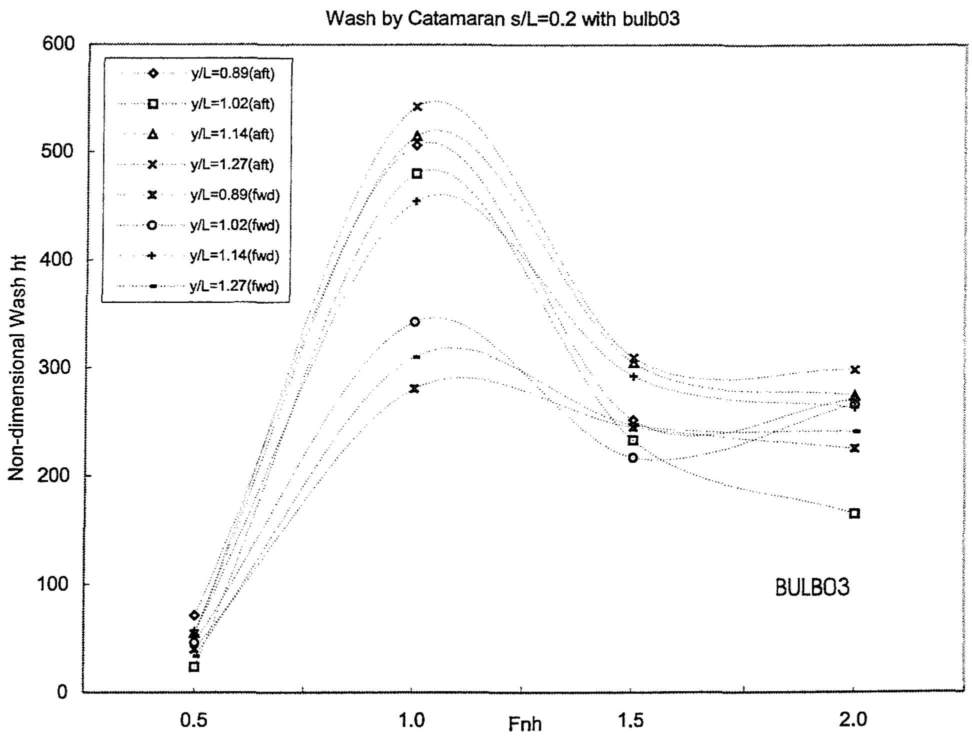

Figure 5.19: Catamaran s/L=0.2 with Bulb03: Non-dimensional Maximum Wash versus Fnh

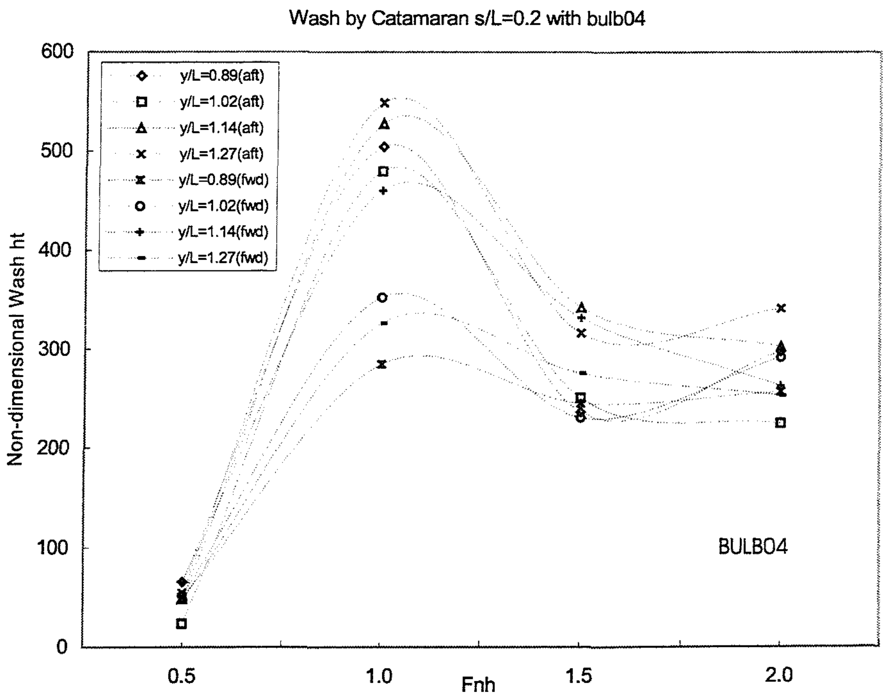

Figure 5.20: Catamaran s/L=0.2 with Bulb04: Non-dimensional Maximum Wash versus Fnh

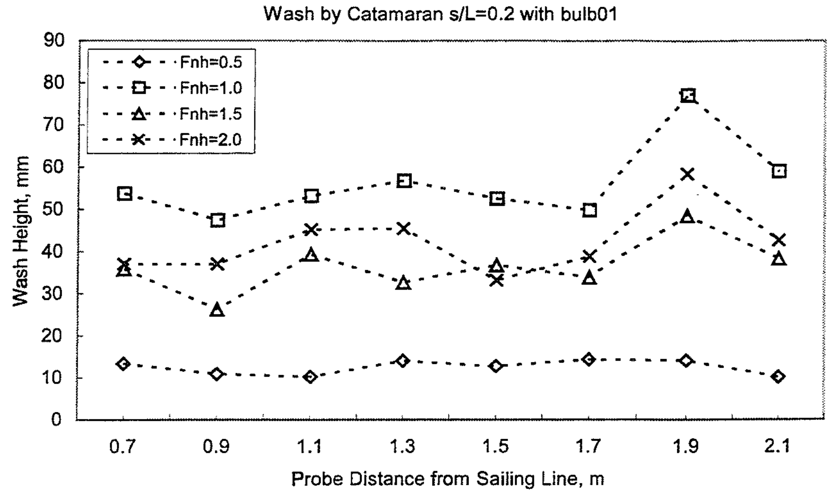

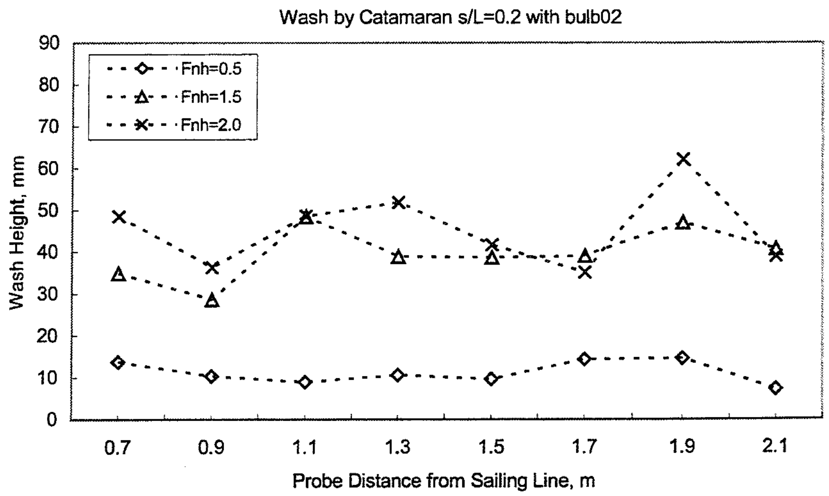

Figure 5.21: Catamaran s/L=0.2 with Bulb01 and Bulb02: Maximum Wash Height

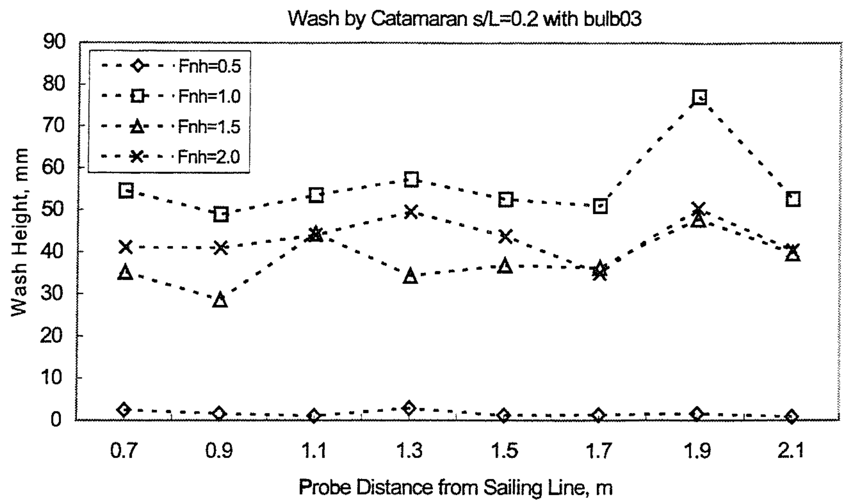

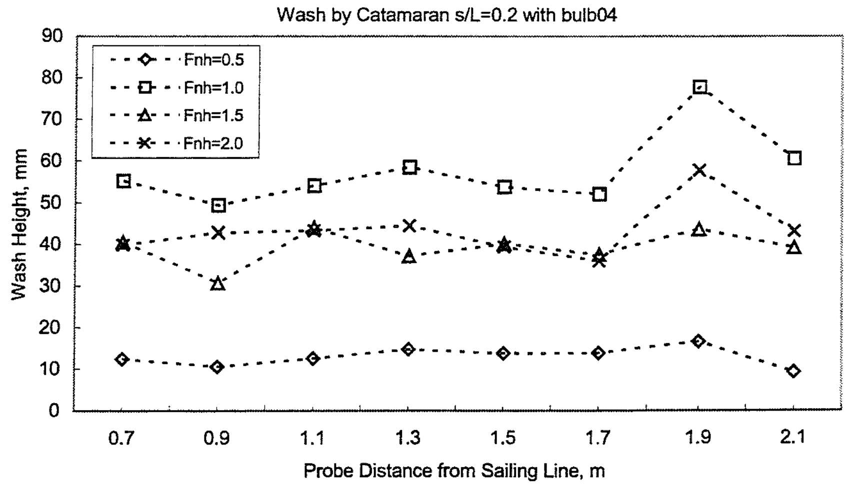

Figure 5.22: Catamaran s/L=0.2 with Bulb03 and Bulb04: Maximum Wash Height

Chapter 6

Comparison with Theoretical Model

6.1 Background

It is well known that the wave resistance of a ship can be determined by integrating the water pressure on the hull surface or by evaluating the energy contained in the wave pattern behind the ship.

Linearised wave resistance theory has been applied to various hull-forms with varying success using the method developed by Mitchell [77]. Although this method does not provide accurate quantitative results, it does provide quite realistic qualitative results for slender forms like the Wigley hull or typical catamarans.

The setback in using thin ship theory occurs for broader hull forms near the limit of the thin ship theory. However, the hullform of interest in this task are generally very thin/slender with L/B in the order of more than 10.

In this current work a computer program developed by Insel [53] and updated by Couser [15] has been used in order to predict wakewash produced by the hull with and without bulbous bow theoretically.

6.2 Thin-Ship Theory

This was introduced by Mitchell in 1898 as a purely analytic approach for predicting the wave resistance of ships. Havelock (1923)[43] extended Michell's work.

There is a method developed at University of Southampton which uses linearised wave resistance theory. In order to approach this theoretically, the following assumptions have been adopted:

a) The fluid is inviscid, incompressible and homogeneous.

b) The fluid motion is steady and irrotational.

c) The surface tension can be neglected.

d) The wave amplitude at free surface is small compared with the wave length.

e) There is no sinkage and trim for the ship while advancing with constant speed.

In such problems the ship is replaced by planar source arrays on the centreline of the ship.

The essential assumption is that the hull is *thin*, that is, the beam is small compared to all other characteristic lengths of the problem.

A computer program has been developed by Insel and modified by Couser in order to produce a theoretical estimate of the far field wave system of the Kelvin sources representing a thin body in a shallow water channel. Insel(1990)[53], divided the hull into a series of rectangular panels defined by uniform grid of stations and waterlines, and the source strengths were calculated from the hull form offsets. Couser(1996)[15] continued the work of Insel, to improve the method by incorporating running trim and sinkage, defining the panels and modelling the transom stern.

6.3 Use of Computer Program

Since the demihulls of catamarans usually are very slender, thin-ship theory would seem ideally suited for predicting the wave making or wash.

To validate the experimental works, the results produced i.e. wash elevation, were compared to those obtained theoretically by mean of thin ship theory program which was developed by previous researchers namely Insel(1990), updated by Couser(1996) and Chandraprabha(2003).

The program calculates the wave profiles and wave pattern resistance of a ship model moving along a rectangular tank, having finite width and depth, with a constant speed. The program allows up three hulls to be calculated. The hull offsets data are generated by a hull fairing program *SHIPSHAPE*, and are then converted into the format required by the thin ship theory program using a program code called *Convert2.for*.

6.3.1 Wash in deep-water

As mentioned and discussed earlier the tests in deep water have been carried out in Lamont and SIHE tanks. The wash or wave cuts measured in these tanks are compared with the theoretical values.

Some of these comparisons are shown in Figures 6.1 to 6.6 for wash or waves cut measured in the Lamont tank. The computer program code used for theoretical wash approximation known as *wavel3d.for* developed by previous researchers. This computer program code is based on thin ship theory where the hull is represented by a series of sources distributed along the centre plane of the body and the details of the theory used are described in Appendix A.

It is seen in Figures 6.1 to 6.6 that the agreement between the theoretical and experimental wash height is not very good, with differences in phase angle and wash height. However, the trend of the curves is very similar especially for higher Froude number. As expected, the theoretical wash height is always higher than the experimental ones.

Recently as reported by Chandraprabha(2003), the program code *wavel3d.for* has been updated by introducing a single source at transom of a hull. The updated version of the computer code known as *wave3d3ss.for*. Also as reported by Molland, et. al [74] a single transom source produced a good approximation to the transom resistance. It can be placed on the centreline of each demihull at the bottom of the transom.

Figures 6.7 to 6.14 show the comparison of experimental wash measured in SIHE tank with the theoretical wash based on *wave3d3ss.for* computer code i.e by putting a single source at the bottom of the transom.

6.3.2 Wash in shallow water

The experimental and theoretical predictions wave cuts at four distances from the model's centreline are plotted and shown in Figures 6.15 to 6.22 i.e for models fitted with bulb01, bulb02, bulb03 and bulb04 respectively. Again, from these figures they show that the *wave3d3ss.for* overestimates the experimental wash height approximately by 36% to 187% with the trends of the curves is very similar.

6.3.3 Comparisons of theories and experiments

The comparison of the experimental results with the theoretical results by using both *wavel3d.for* and *wave3d3ss.for* program codes are shown in Figures 6.23 to 6.34.

The agreement between the theoretical and experimental curves is reasonably good especially for the probe nearer to the sailing line. At $y = 0.54L$ the *wavel3d.for* over predicts the experimental data by approximately 26% to 67% compared to the *wave3d3ss.for* overestimates it by 26% to 100%. For probe position at $y = 0.63L$ the *wavel3d.for* and the *wave3d3ss.for* overestimates it approximately by 46% to 123% and 87% to 223% respectively.

Although some discrepancies exist, primarily with regard to phase angle and wash height, the trend of the curves is very similar at least for higher Froude number.

The discrepancies between the experimental and theoretical wash may be due to inaccuracy in both the experiments and the theoretical method. Overall, it is believed that the phase shift between the theoretical and experimental results is probably caused by the asymmetric flow effect about each demihull which is not taken into account in the theoretical method. Also keeping in mind the simplifications primarily with regard to hull shape, involved in the theoretical procedure.

6.3.4 Wave Pattern Resistance

Figure 6.35 shows the theoretical wave pattern resistances for model with and without bulbous bow in three different towing tanks. From this figure it shows that bulb01 and bulb04 offers the highest and the lowest C_{wp} respectively.

However, it should be noted that the distinction between wave pattern resistance, C_{wp} and wave-making resistance, C_w as mentioned and discussed in previous chapters. Firstly, this wave pattern resistance is the resistance associated with the generation of the far field wave pattern. Secondly, wave-making resistance not only includes the resistance due to creation of the far field wave system but also the resistance associated with wave breaking, spray generation, and other near field and non-linear effects not associated with the viscous resistance, Couser(1996) [15].

6.4 Summary

Various methods are available for calculating the flow around a ship hull, ranging from full Navier-Stokes solutions with turbulence modeling through panel method potential flow solutions using panels distributed over the surface of the ship to thin-ship theory. Both the Navier-Stokes and the full potential flow options require huge amounts of computational time. For the purpose of preliminary design, thin-ship theory is more cost-effective.

The work described in this chapter covers the theoretical prediction of the wash profile and wave pattern resistance of high-speed displacement catamaran $s/L = 0.2$ fitted with four different bulbous bows operating in deep and shallow waters. The thin ship theory program codes used in this work are known as *wavel3d.for* and *wave3d3ss.for*.

It was found that the agreement between the theoretical and experiment wash profile is not very good with differences in phase and wash height, but the trend of the curves is very similar at least for higher Froude number. These discrepancies are likely to be decreased by improving and refining the modelling of the hull shape, especially at the relevant sections to accommodate the bulbous bow, and by systematic manipulation of the source strengths representing the bulbous bow.

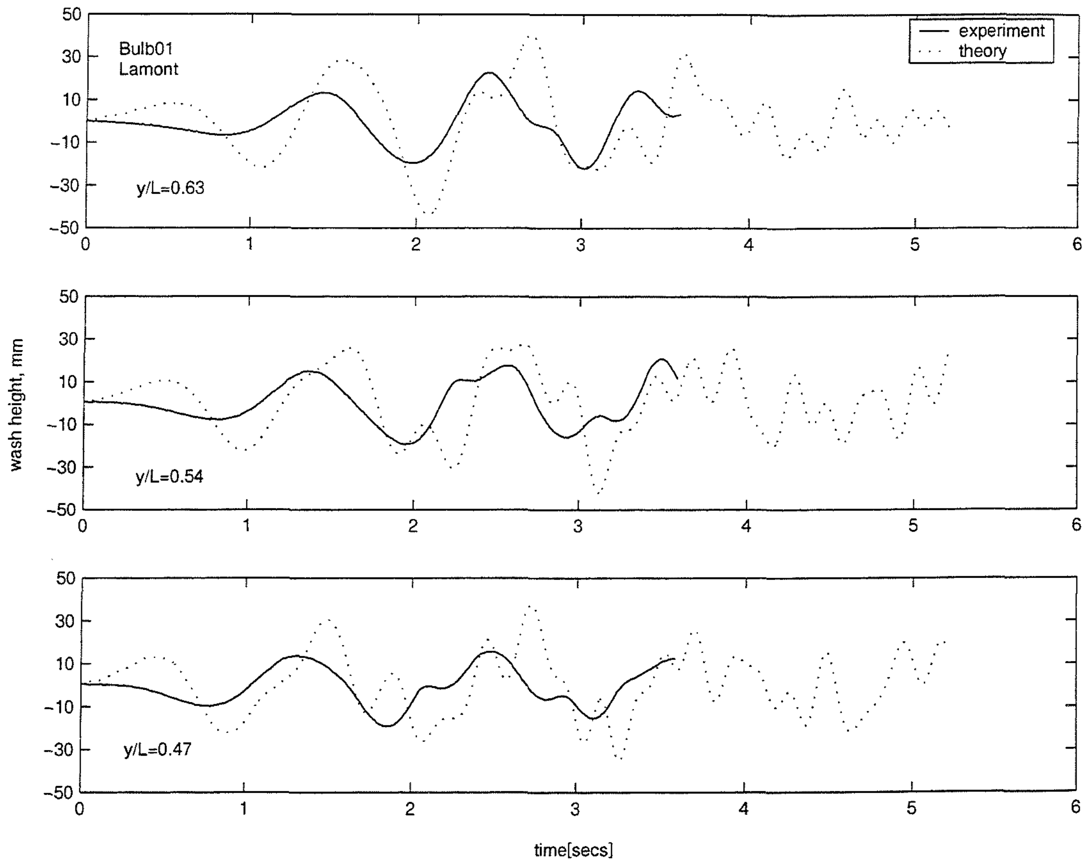

Figure 6.1: Catamaran s/L=0.2 with bulb01:Experimental and theoretical wave cuts at F_n=0.48

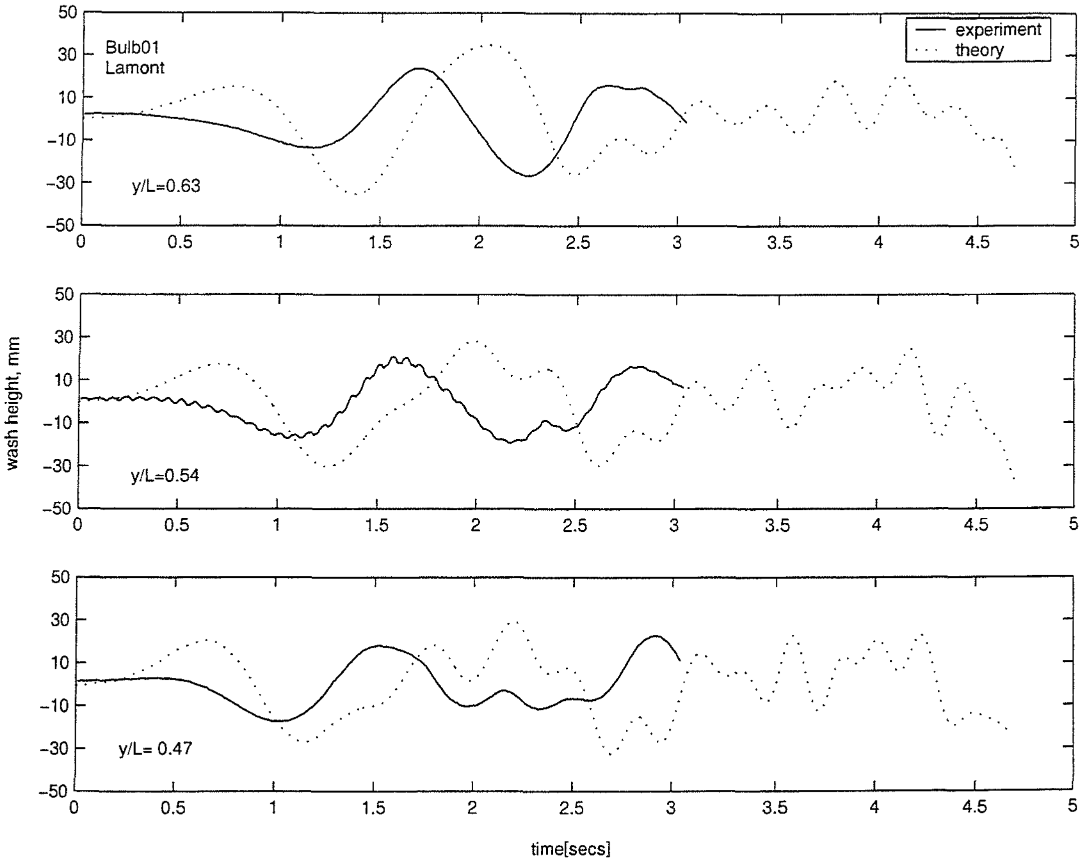

Figure 6.2: Catamaran s/L=0.2 with bulb01:Experimental and theoretical wave cuts at F_n=0.60

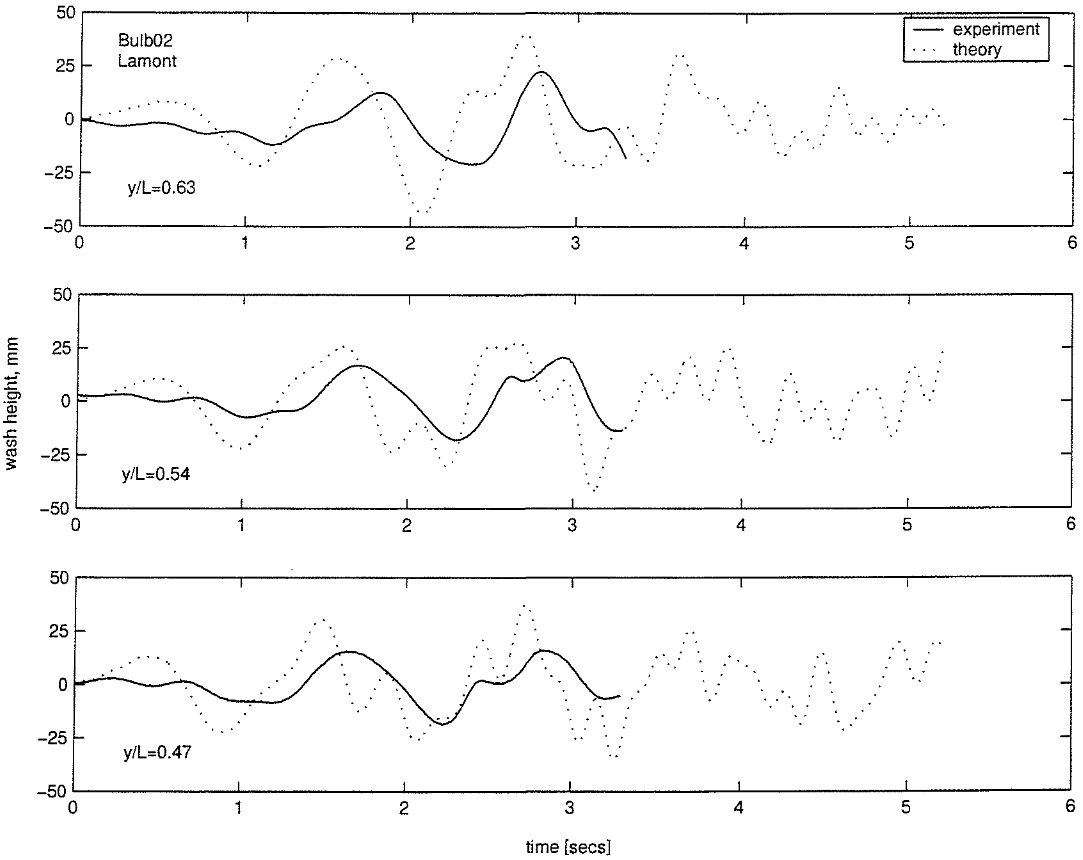

Figure 6.3: Catamaran s/L=0.2 with bulb02:Experimental and theoretical wave cuts at F_n=0.48

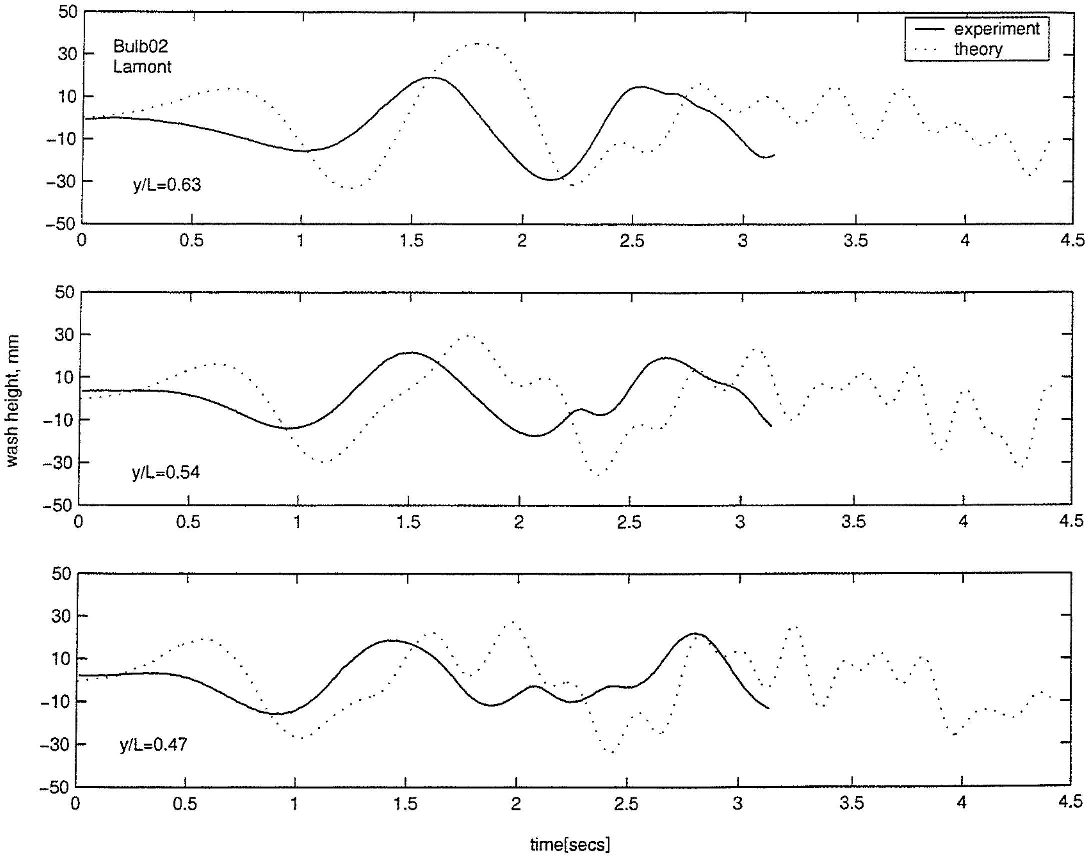

Figure 6.4: Catamaran s/L=0.2 with bulb02:Experimental and theoretical wave cuts at F_n=0.60

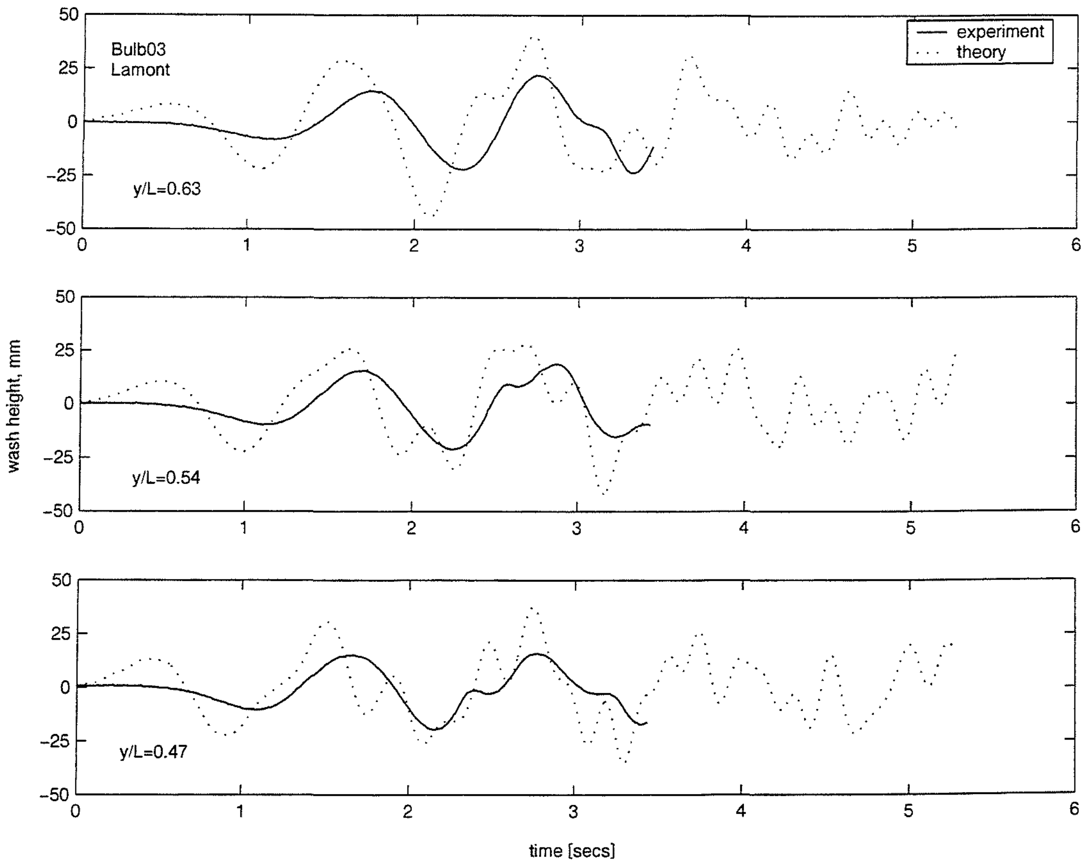

Figure 6.5: Catamaran s/L=0.2 with bulb03:Experimental and theoretical wave cuts at F_n=0.48

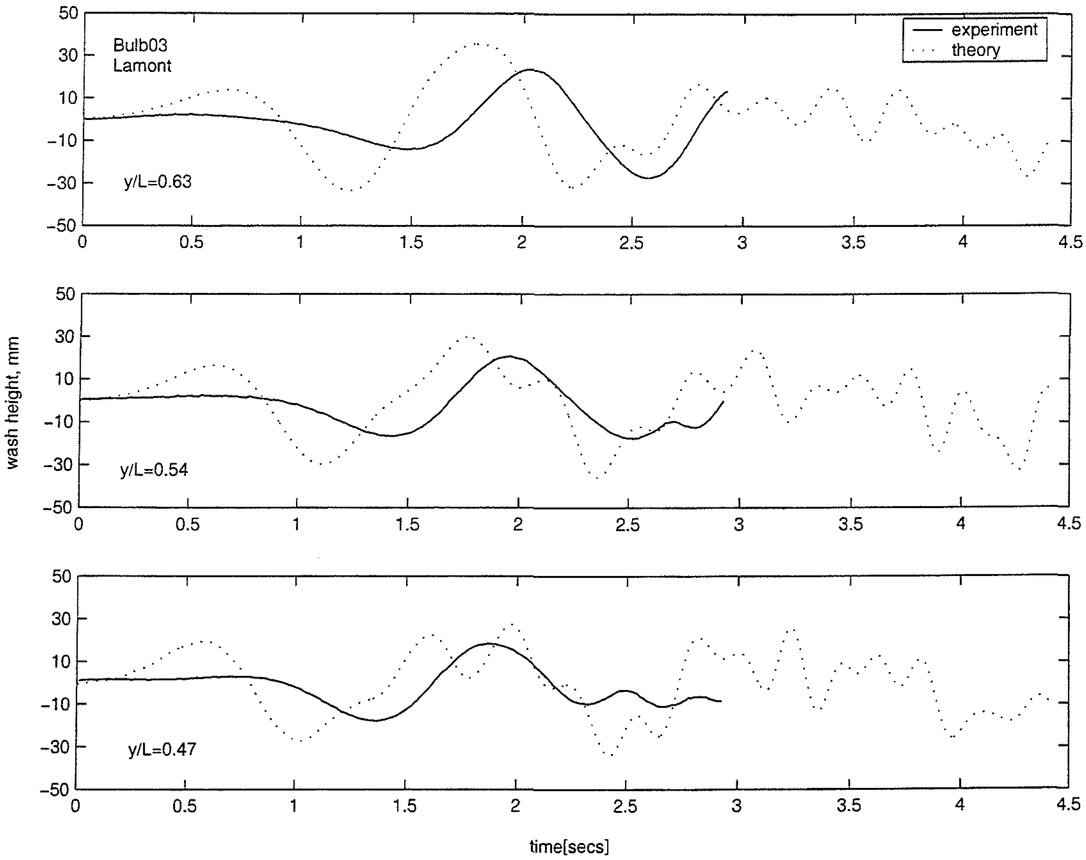

Figure 6.6: Catamaran s/L=0.2 with bulb03:Experimental and theoretical wave cuts at F_n=0.60

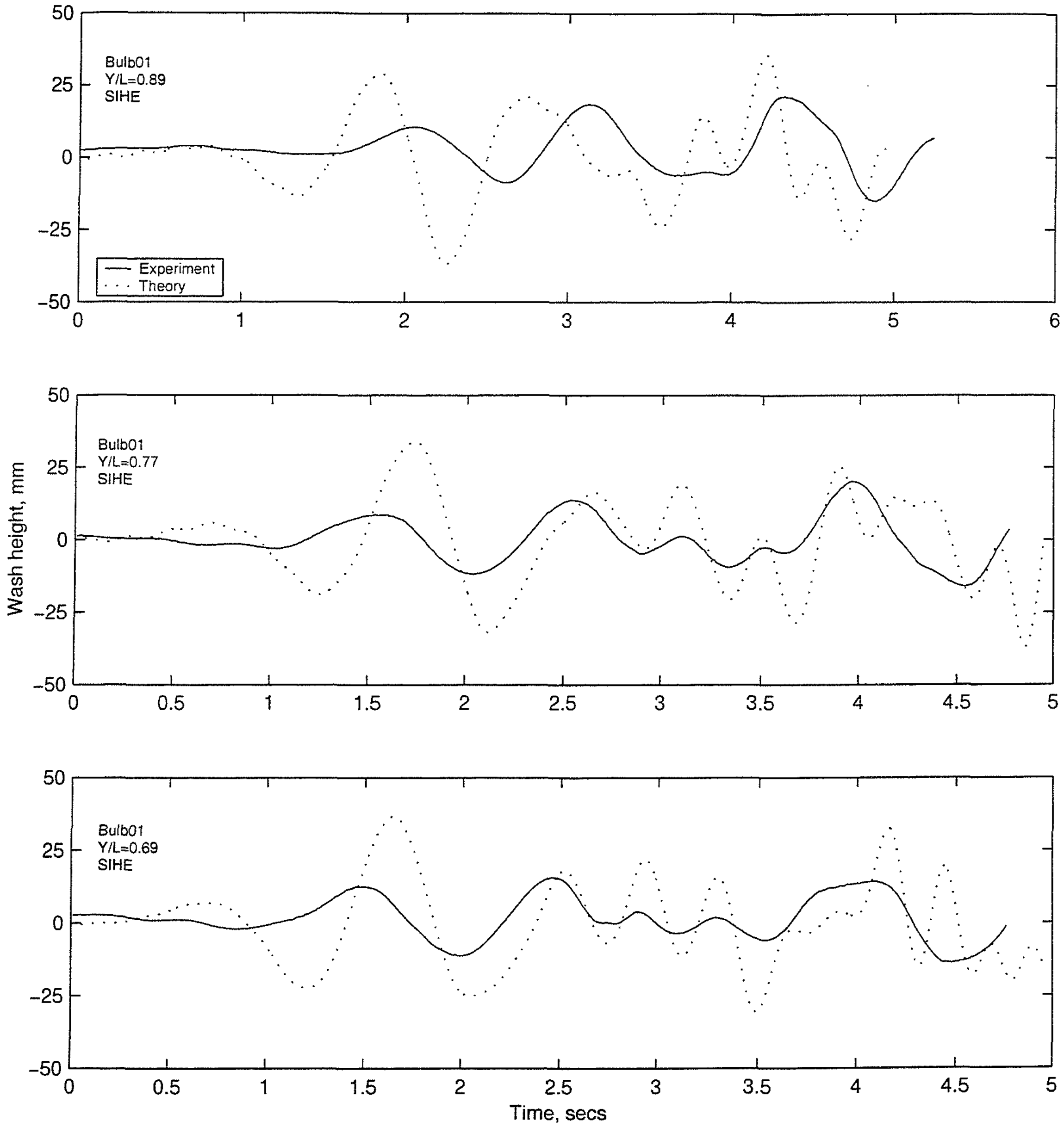

Figure 6.7: Catamaran s/L=0.2 with bulb01:Experimental and theoretical wave cuts at F_n=0.51

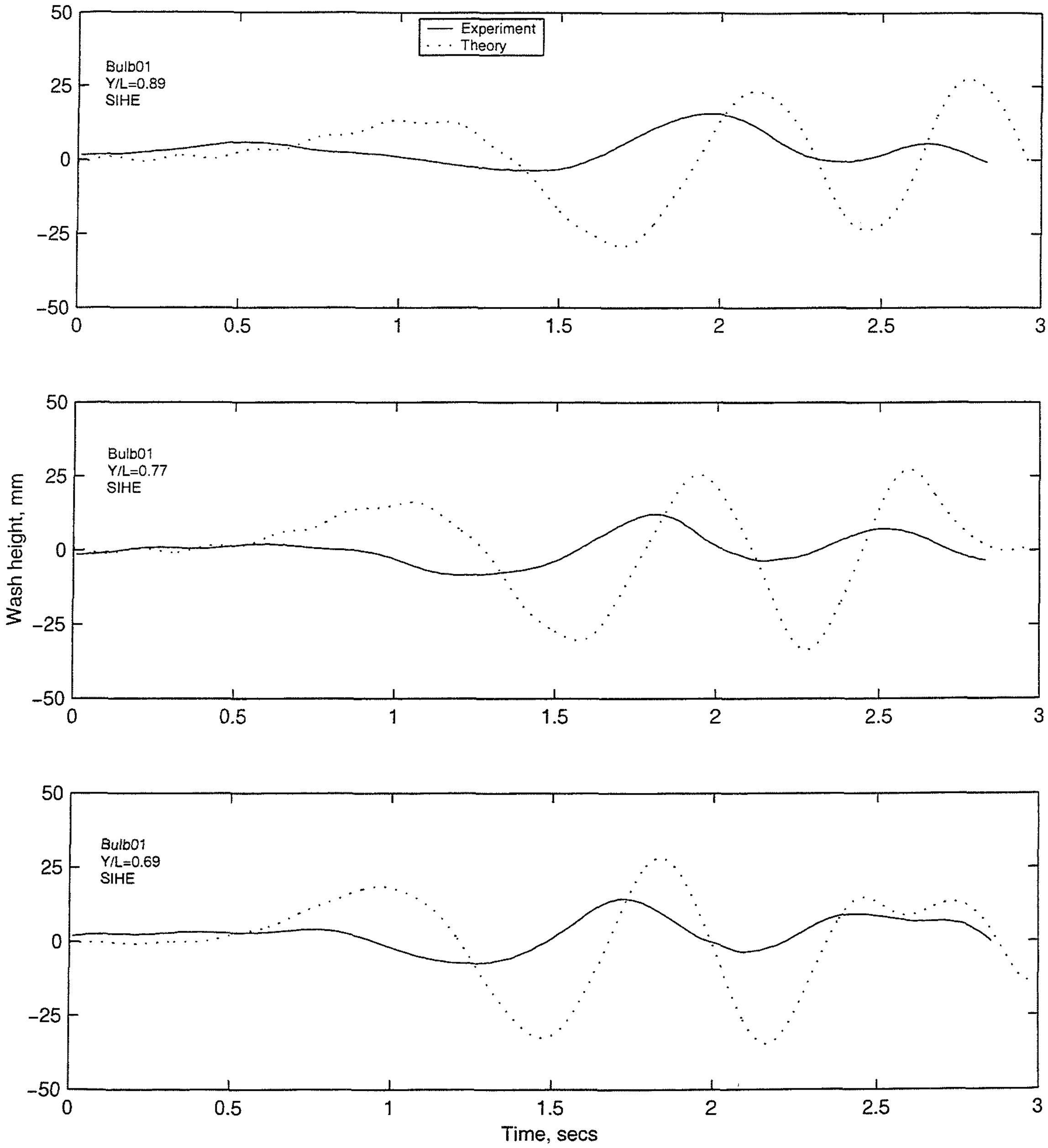

Figure 6.8: Catamaran s/L=0.2 with bulb01:Experimental and theoretical wave cuts at F_n=0.85

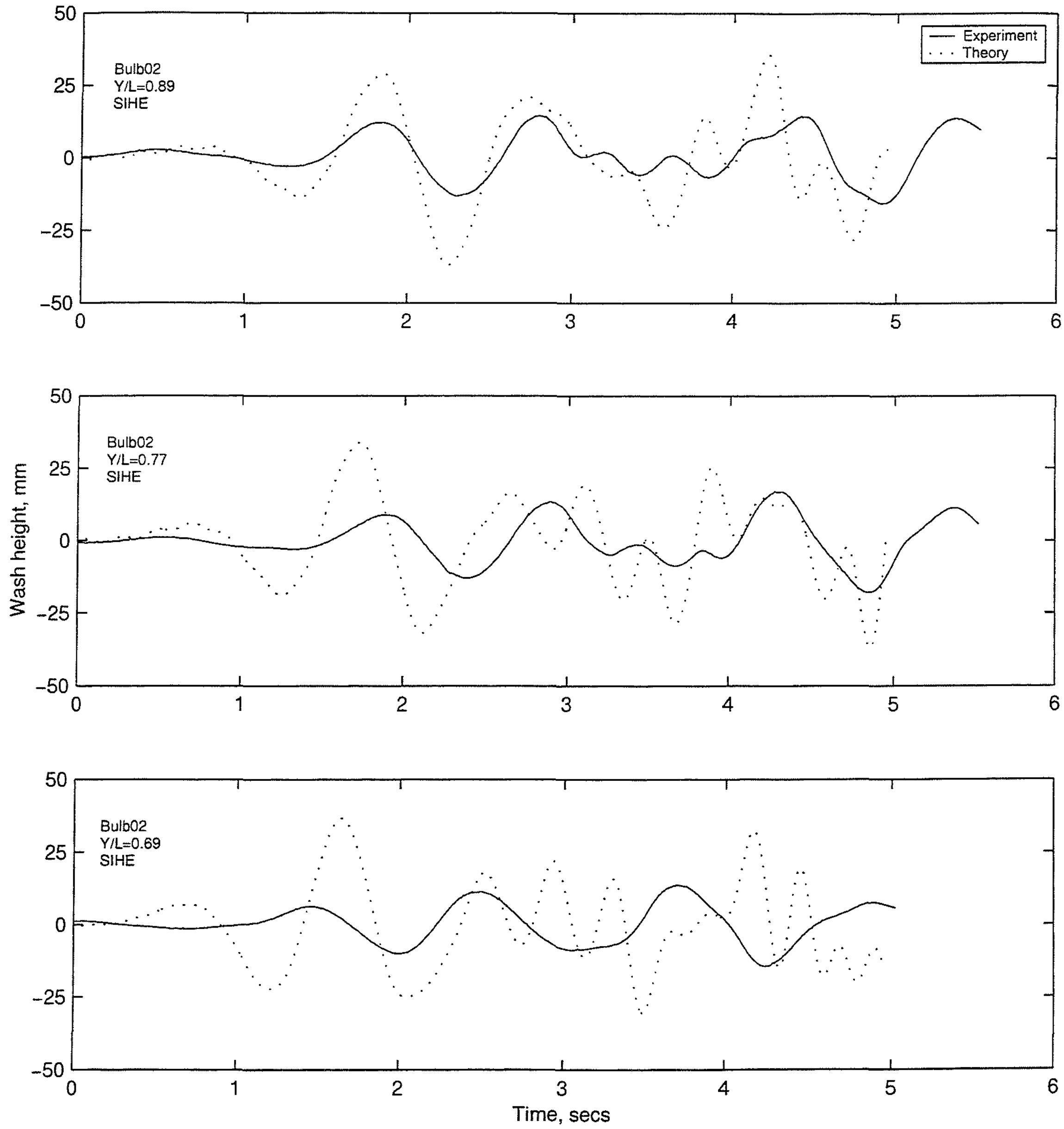

Figure 6.9: Catamaran s/L=0.2 with bulb02:Experimental and theoretical wave cuts at F_n=0.51

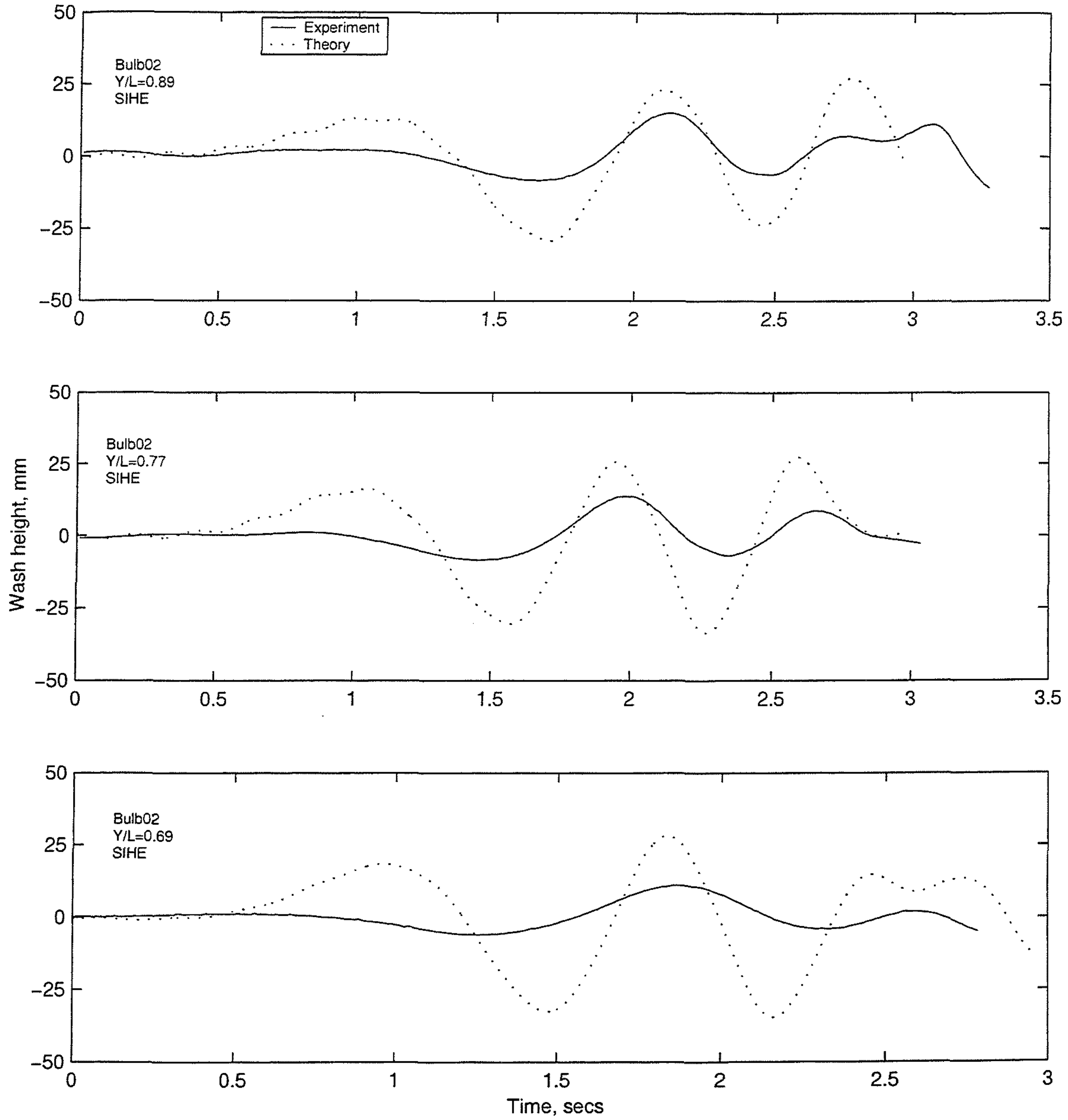

Figure 6.10: Catamaran s/L=0.2 with bulb02:Experimental and theoretical wave cuts at F_n=0.85

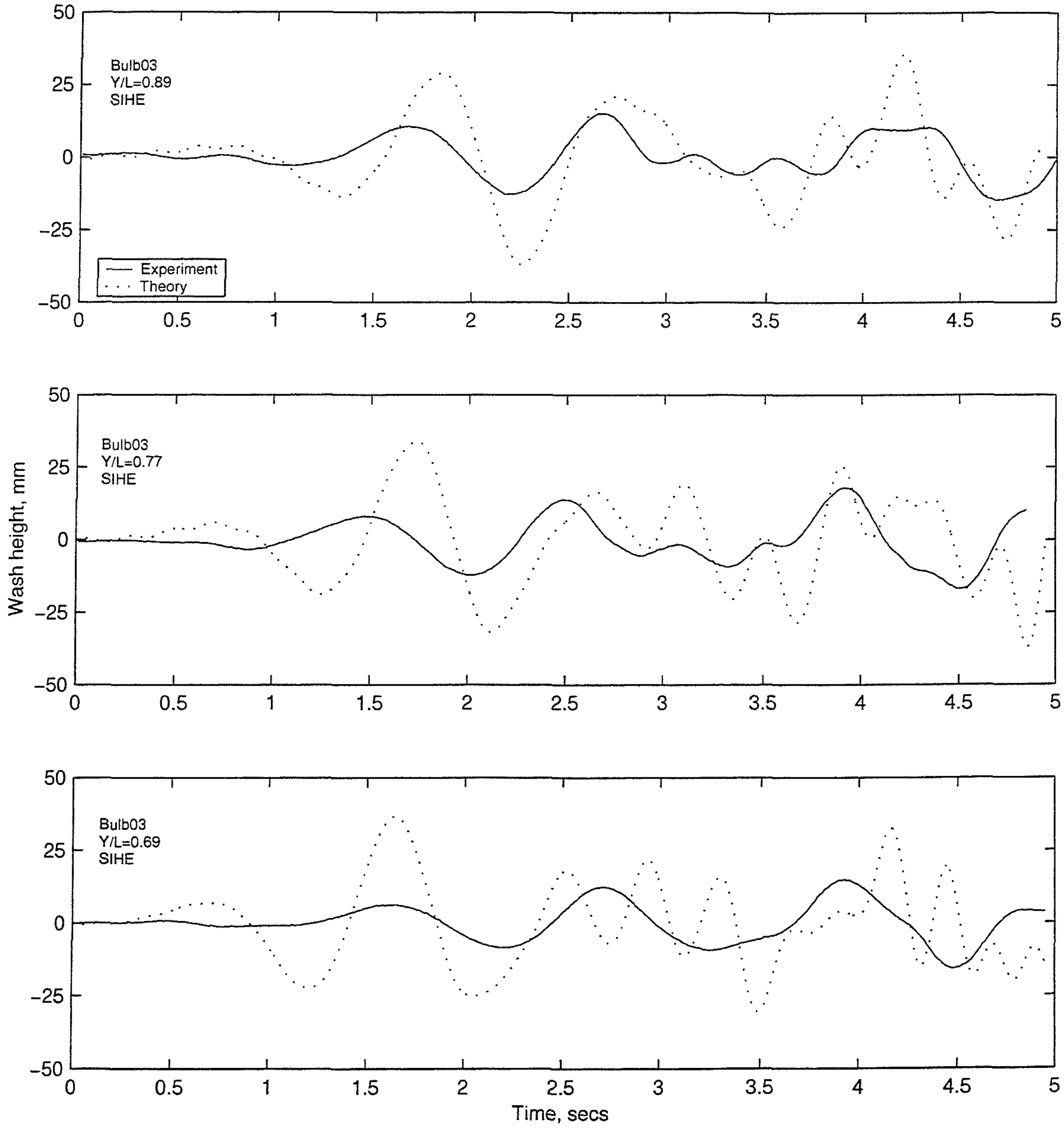

Figure 6.11: Catamaran s/L=0.2 with bulb03:Experimental and theoretical wave cuts at F_n=0.51

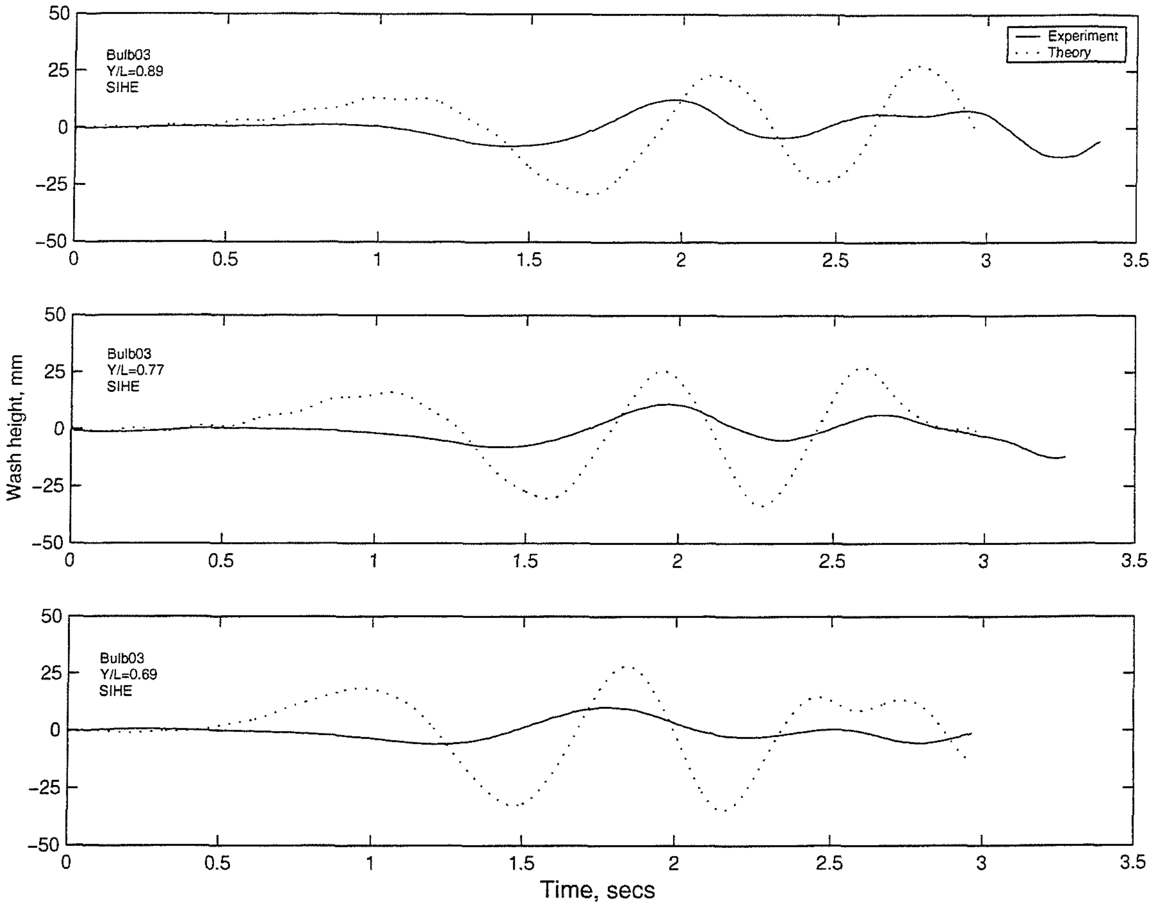

Figure 6.12: Catamaran s/L=0.2 with bulb03:Experimental and theoretical wave cuts at F_n=0.85

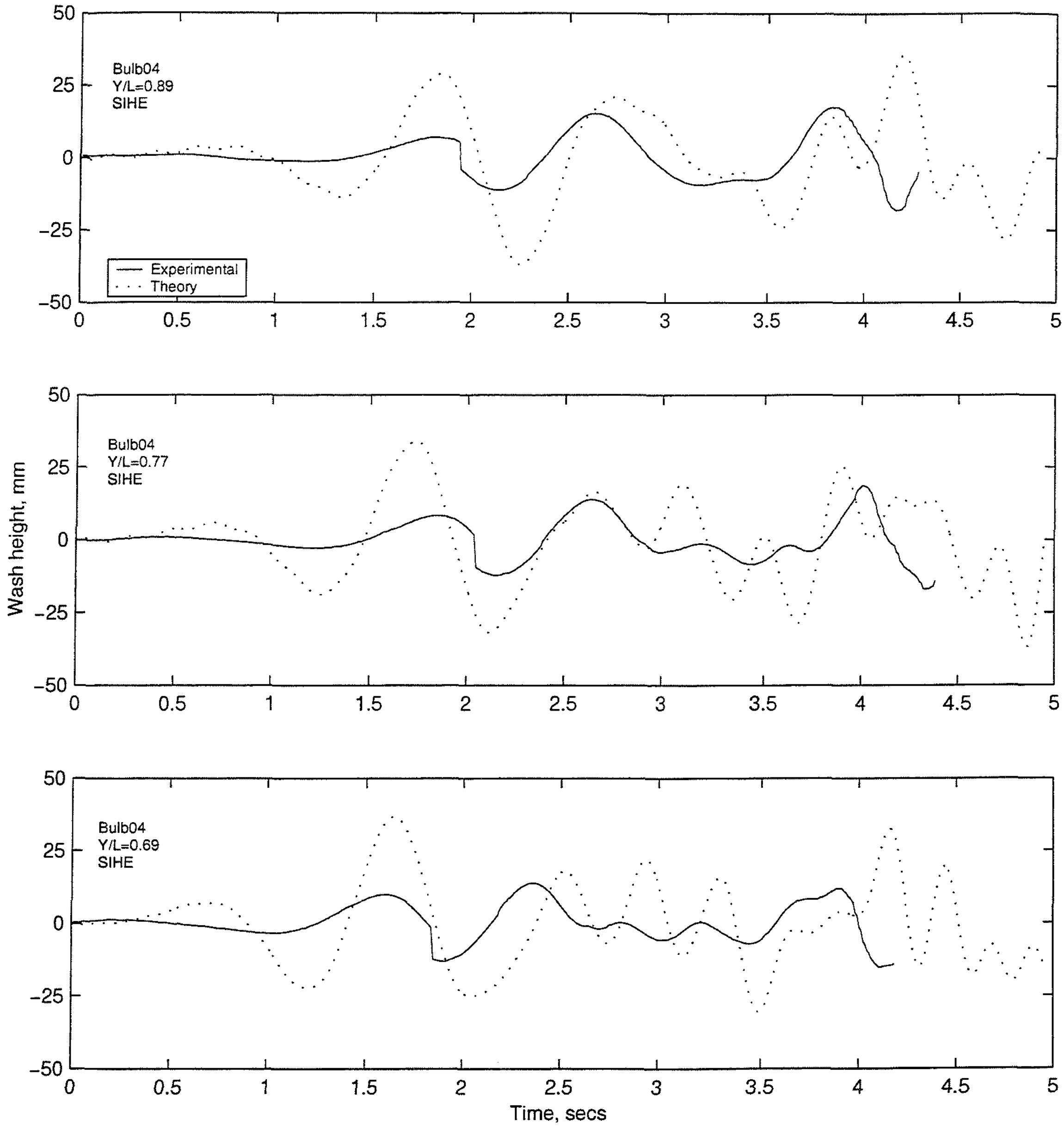

Figure 6.13: Catamaran s/L=0.2 with bulb04:Experimental and theoretical wave cuts at F_n=0.51

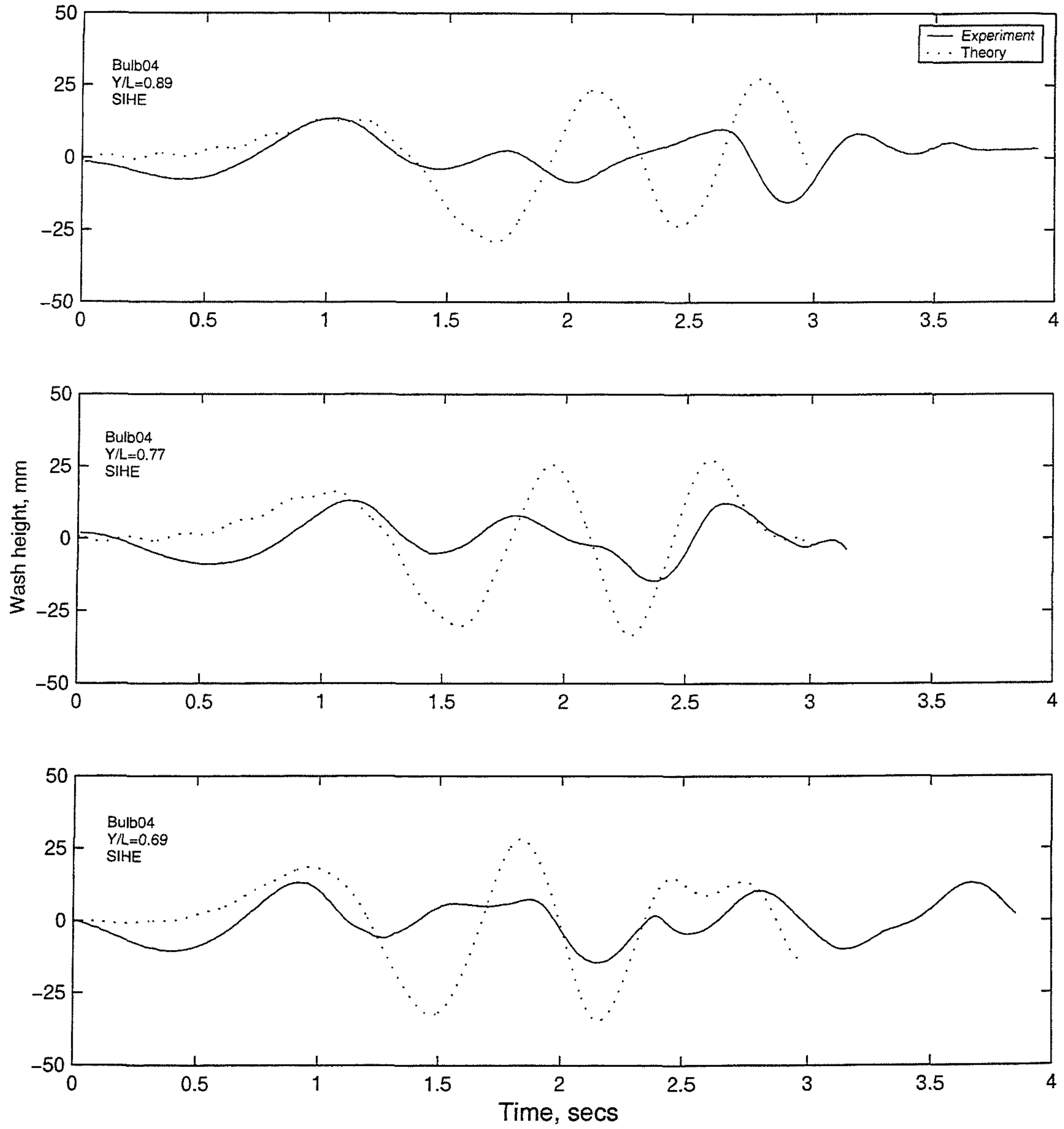

Figure 6.14: Catamaran s/L=0.2 with bulb04:Experimental and theoretical wave cuts at F_n=0.85

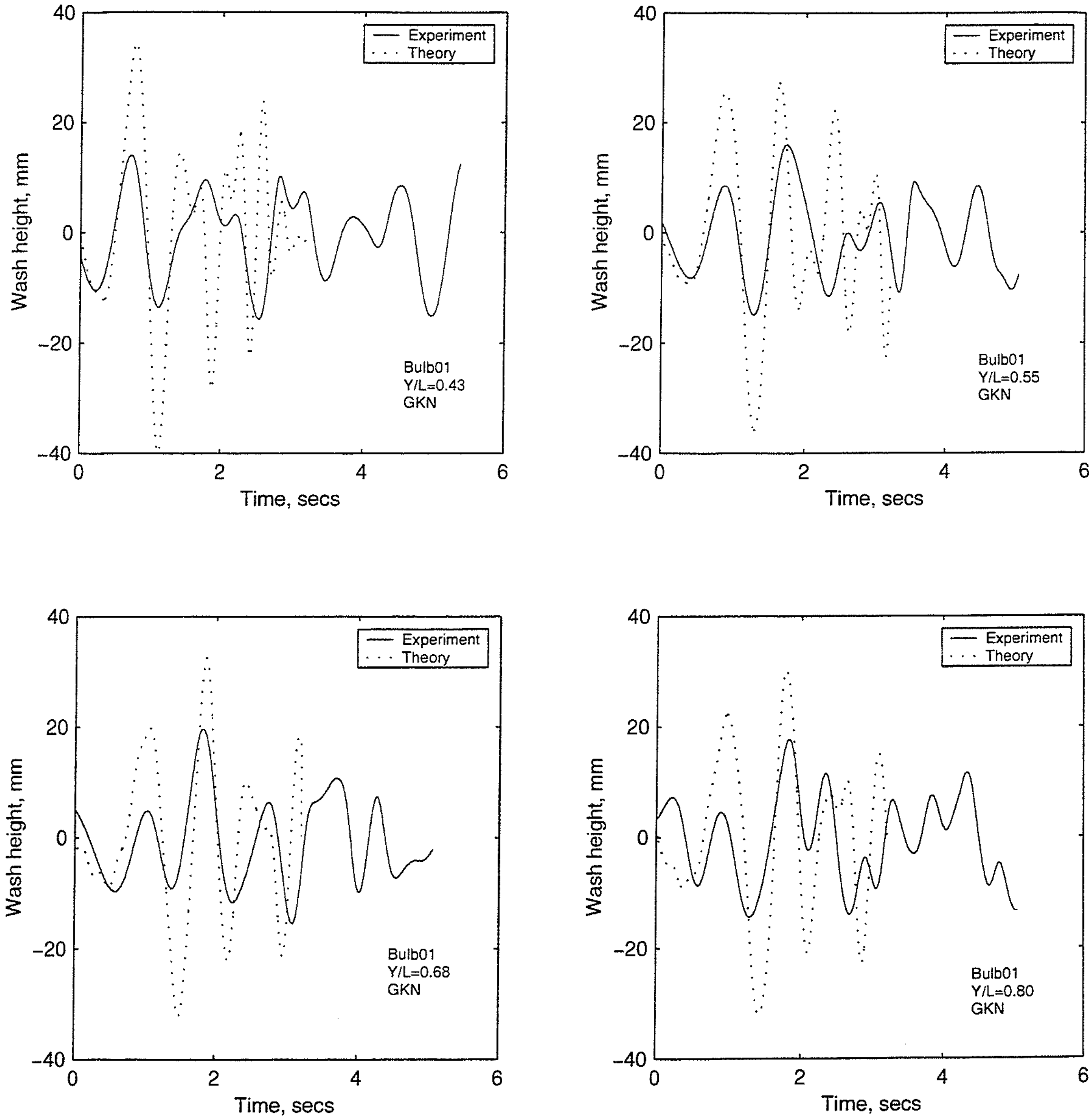

Figure 6.15: Catamaran s/L=0.2 with bulb01: Wave cuts in Shallow Water at F_n=0.8

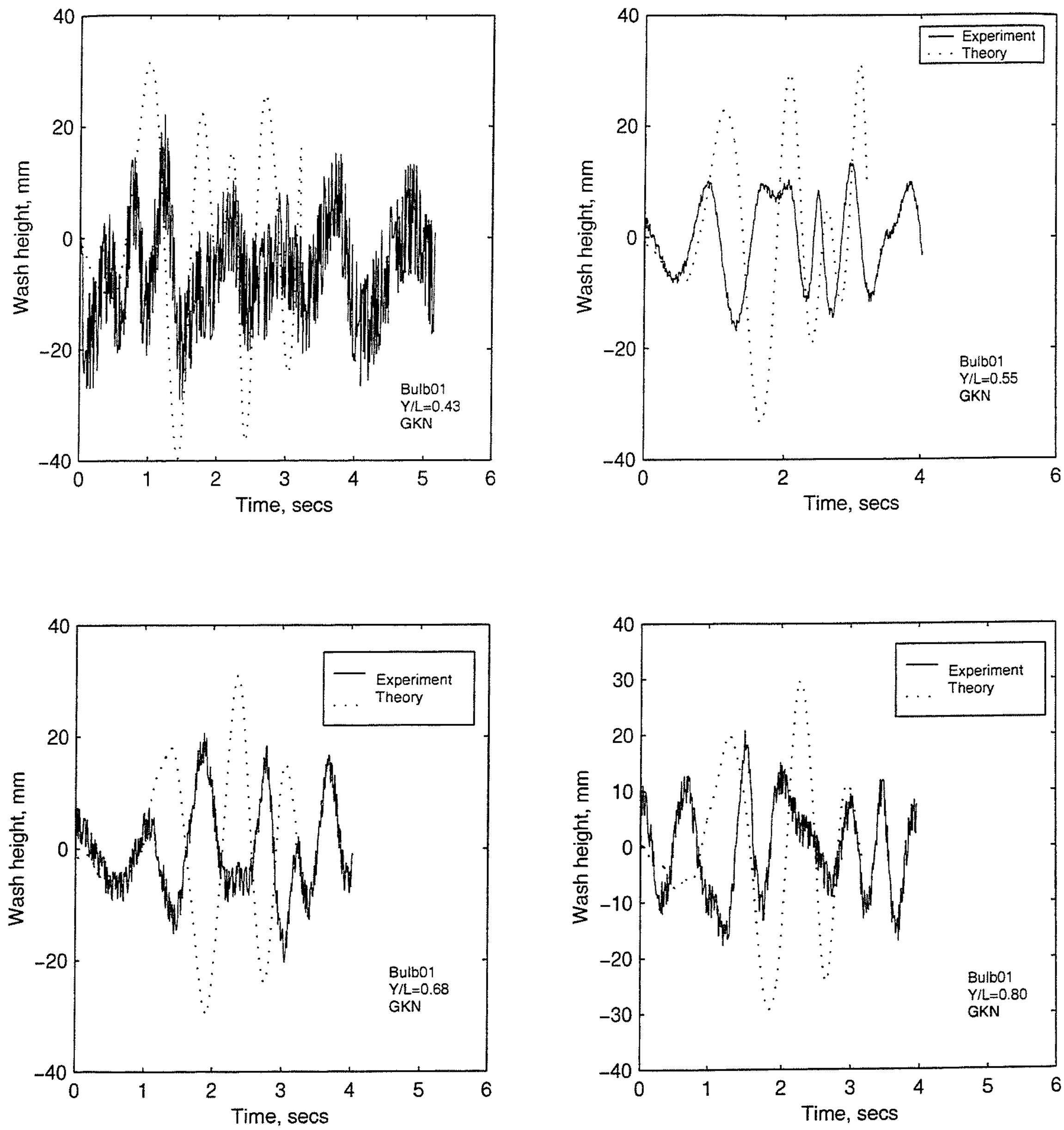

Figure 6.16: Catamaran s/L=0.2 with bulb01: Wave cuts in Shallow Water at F_n=1.0

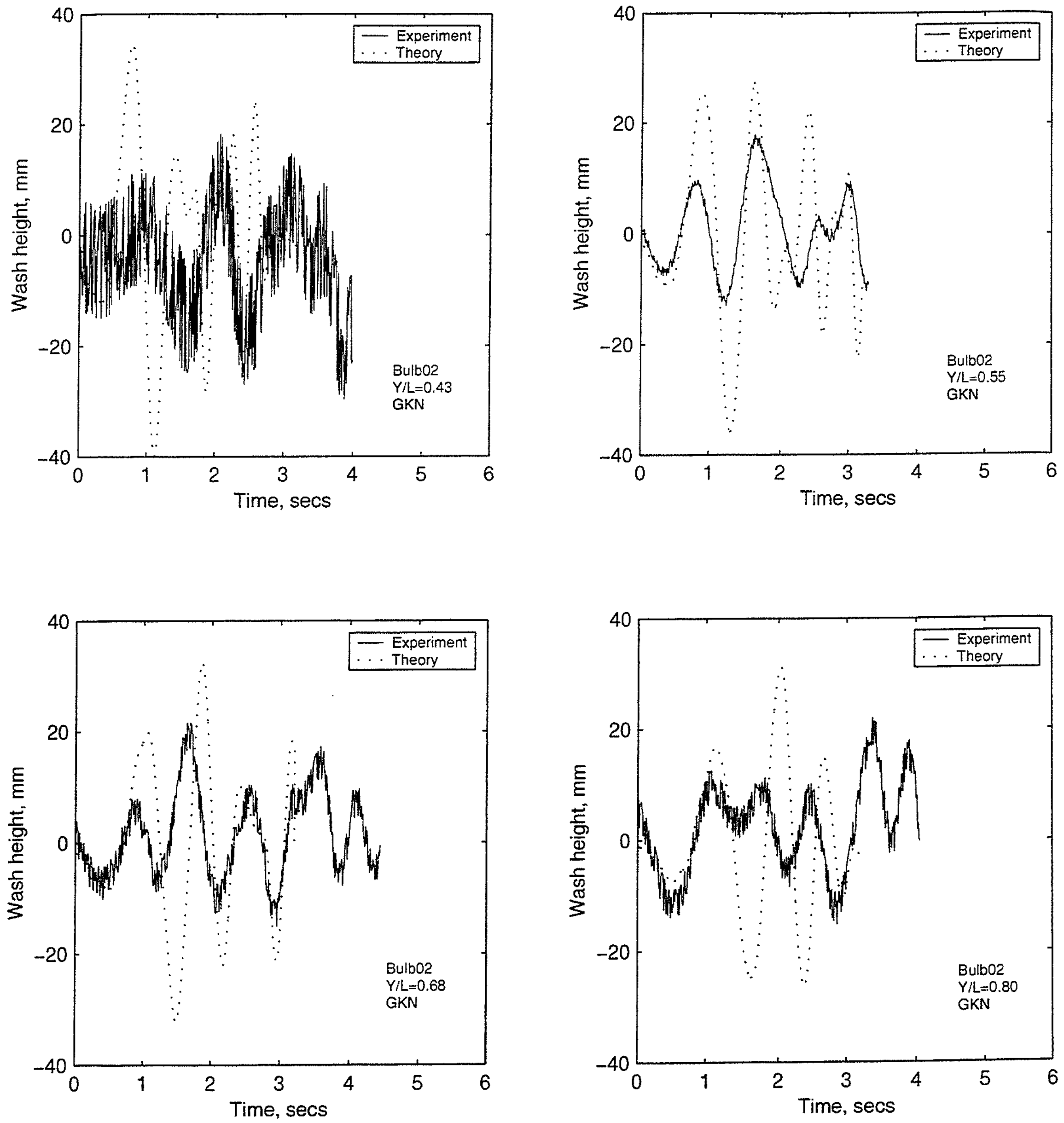

Figure 6.17: Catamaran s/L=0.2 with bulb02: Wave cuts in Shallow Water at F_n=0.8

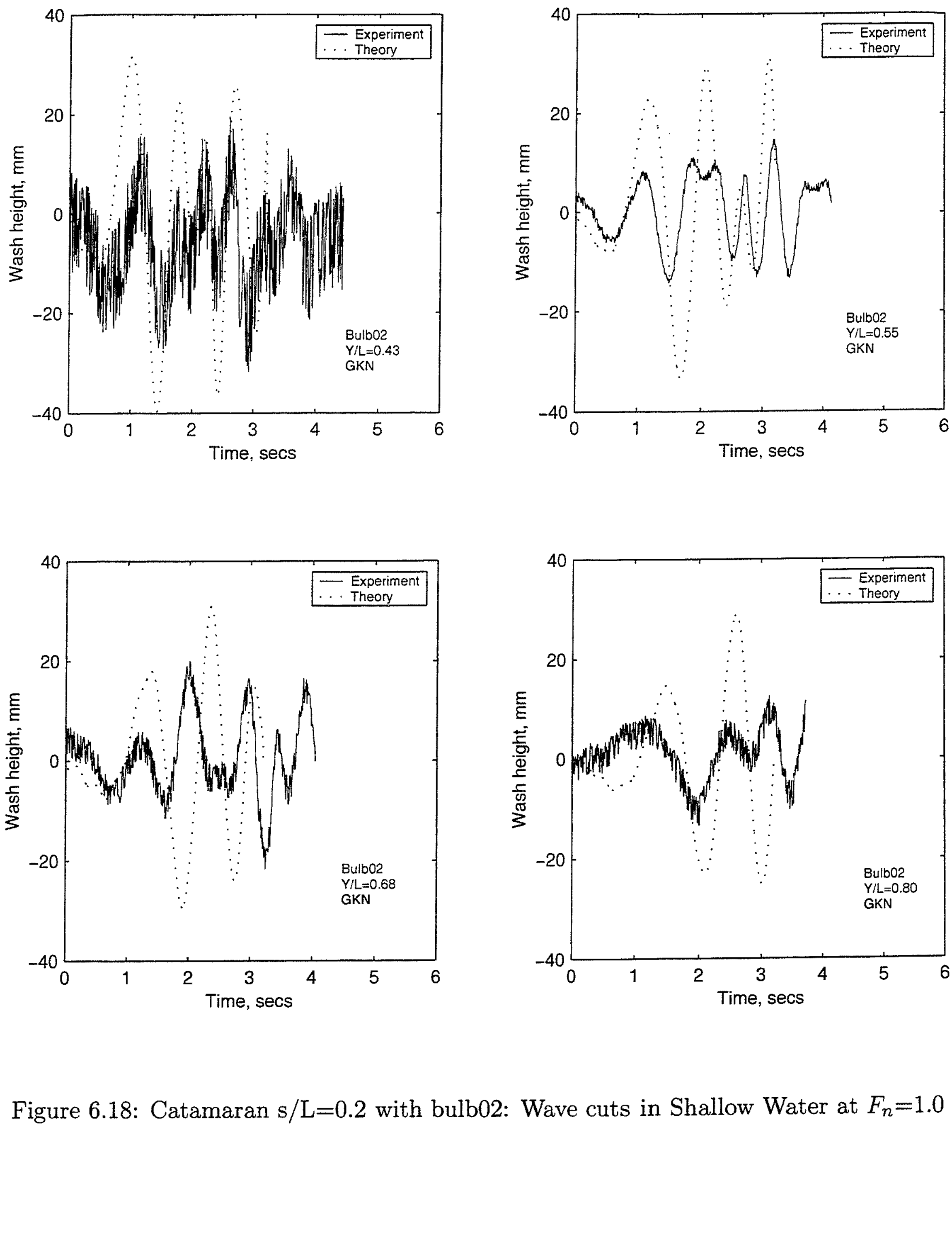

Figure 6.18: Catamaran s/L=0.2 with bulb02: Wave cuts in Shallow Water at F_n=1.0

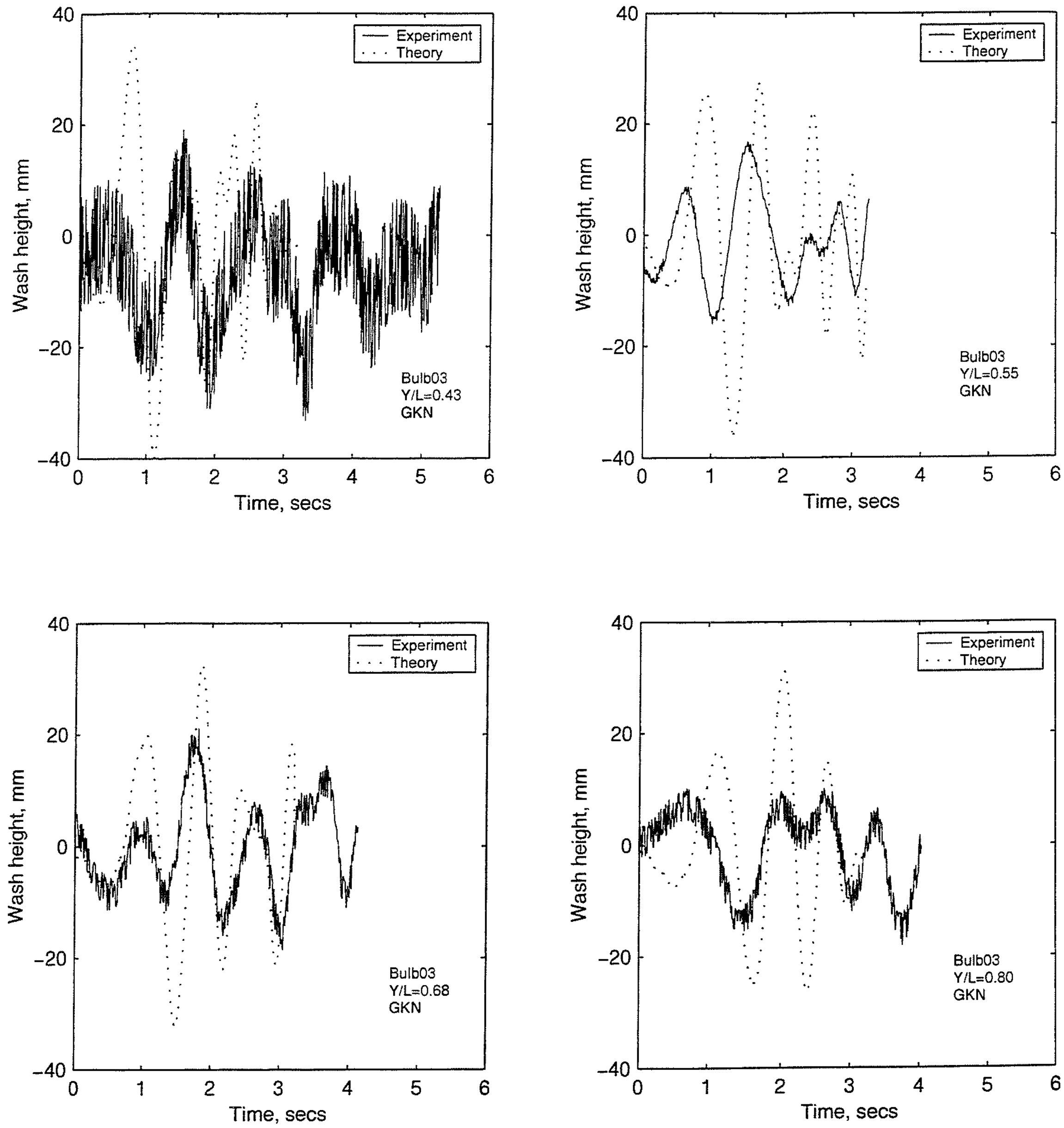

Figure 6.19: Catamaran s/L=0.2 with bulb03: Wave cuts in Shallow Water at F_n=0.8

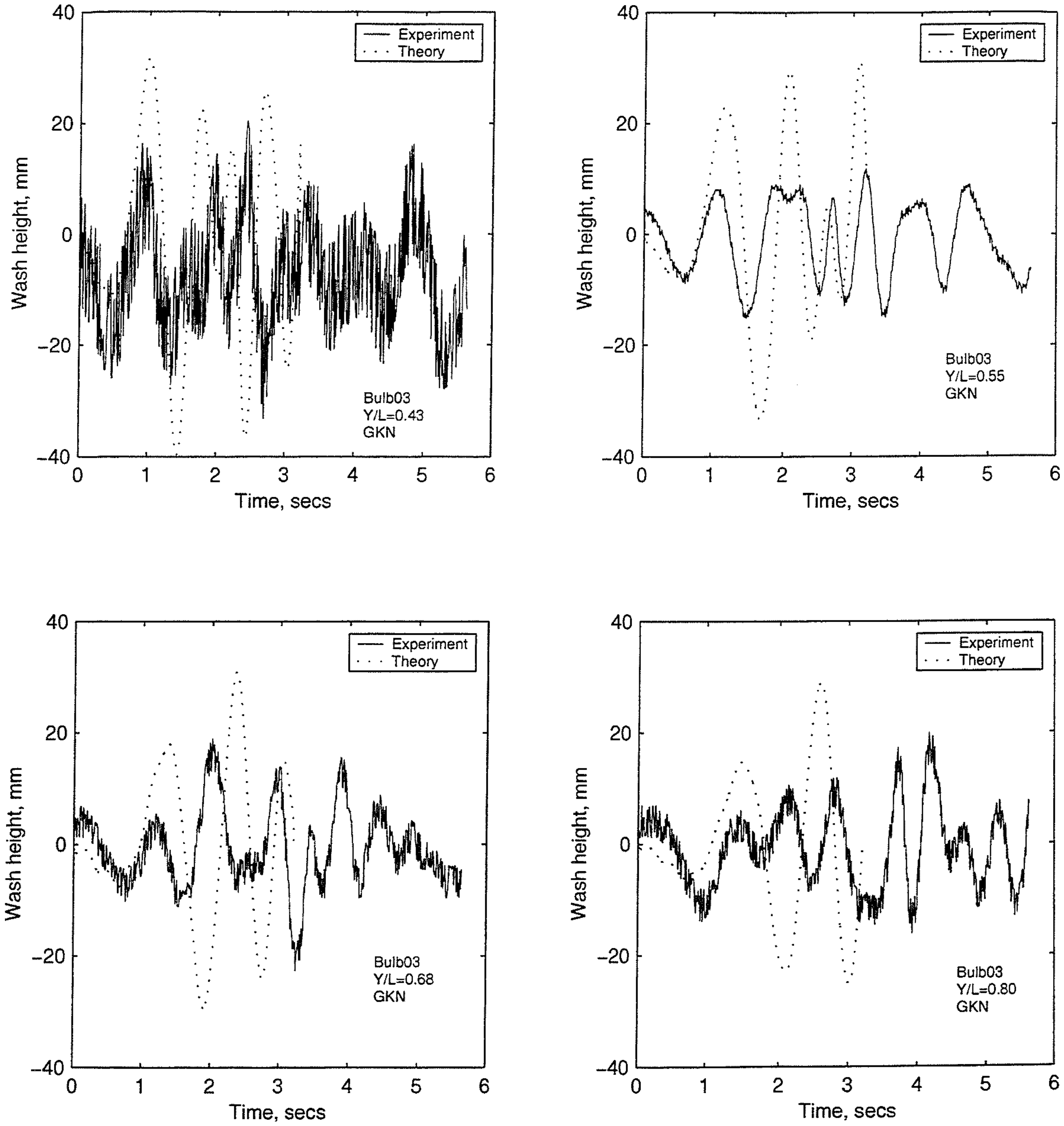

Figure 6.20: Catamaran s/L=0.2 with bulb03: Wave cuts in Shallow Water at F_n=1.0

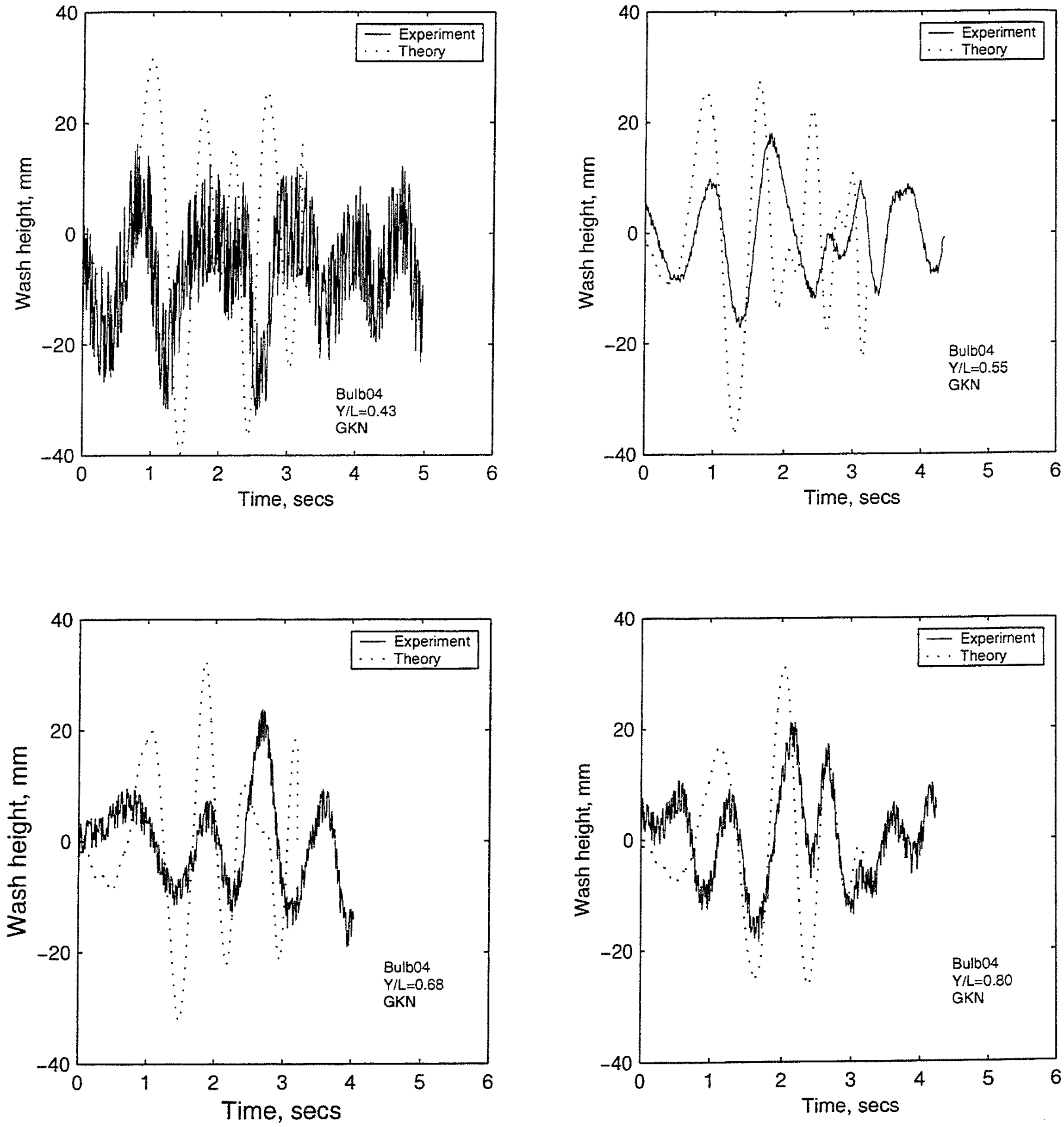

Figure 6.21: Catamaran s/L=0.2 with bulb04: Wave cuts in Shallow Water at F_n=0.8

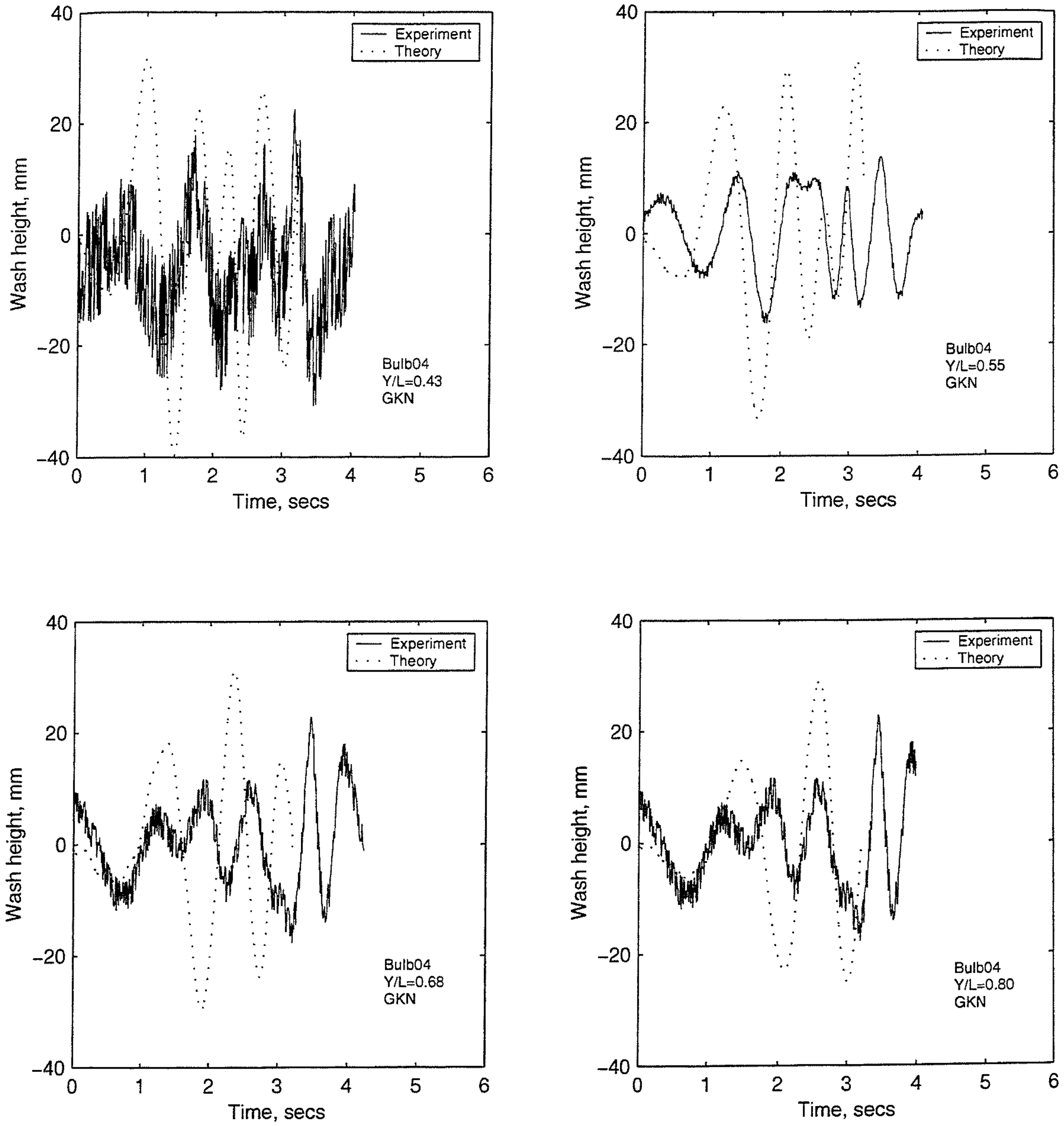

Figure 6.22: Catamaran s/L=0.2 with bulb04: Wave cuts in Shallow Water at F_n=1.0

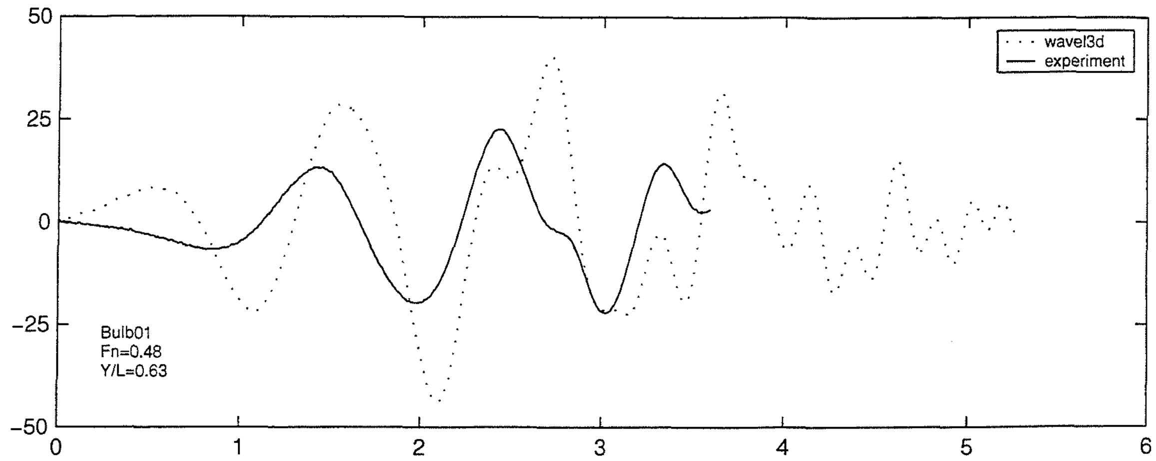

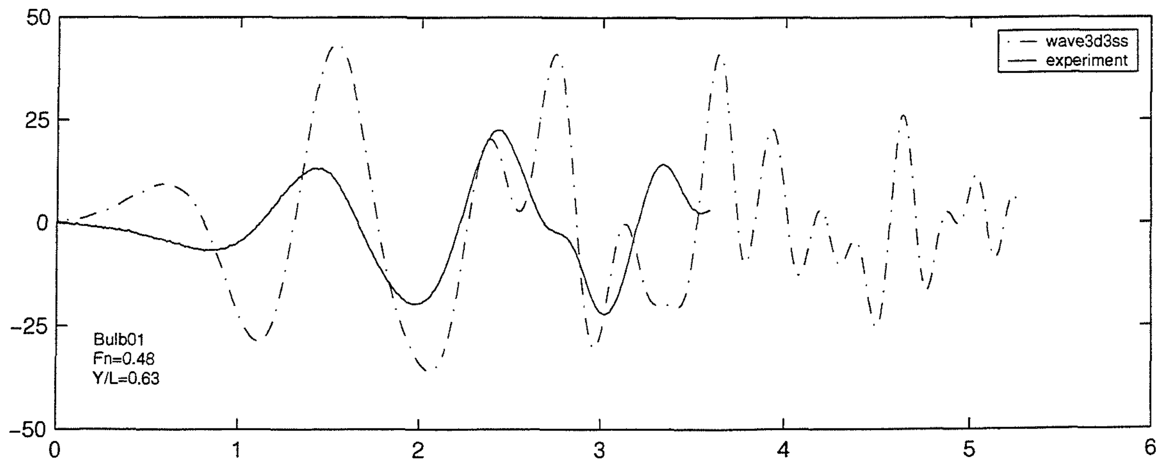

Figure 6.23: Catamaran s/L=0.2 with bulb01:Experimental and theoretical wave cuts at F_n=0.48

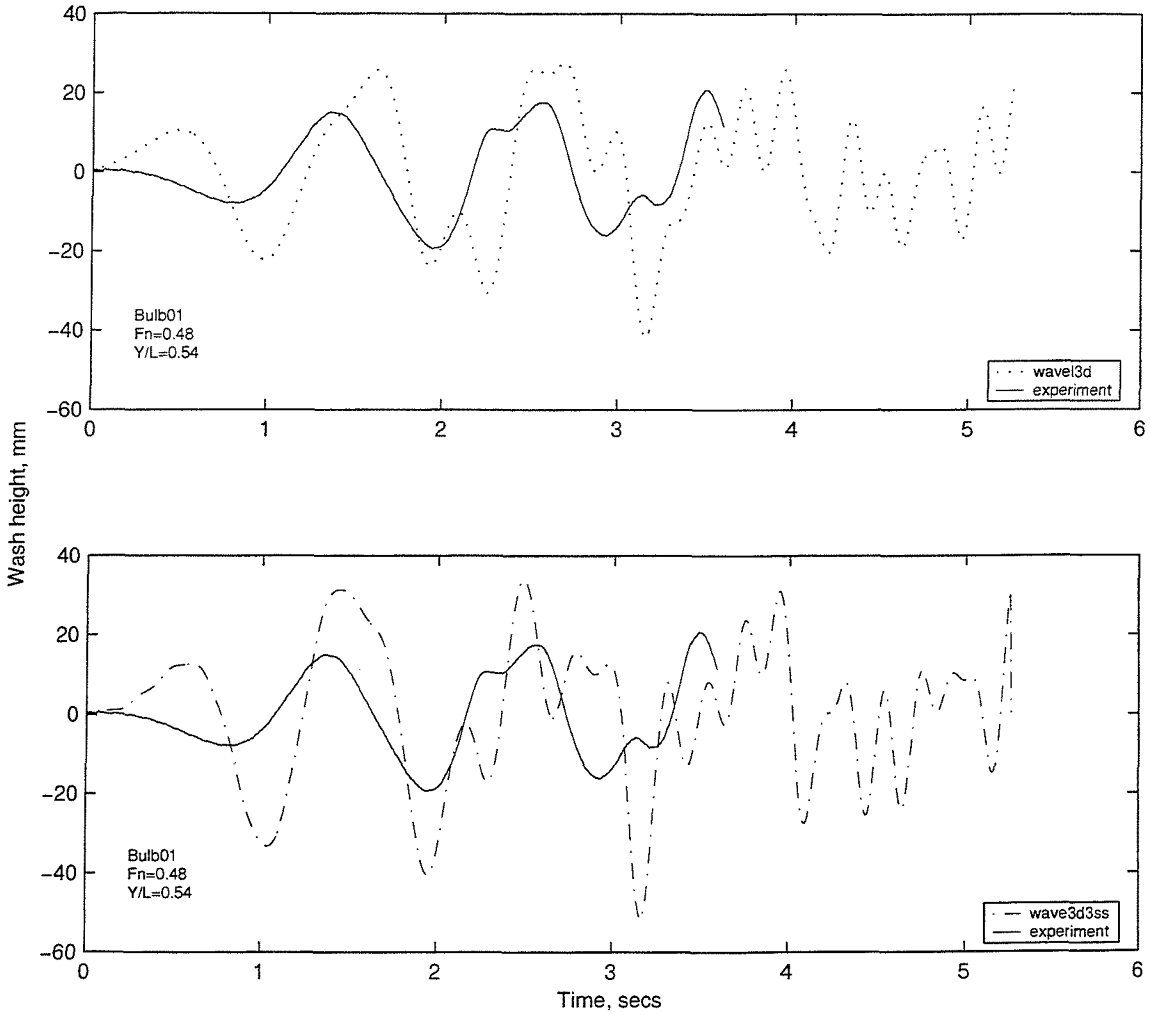

Figure 6.24: Catamaran s/L=0.2 with bulb01:Experimental and theoretical wave cuts at F_n=0.48

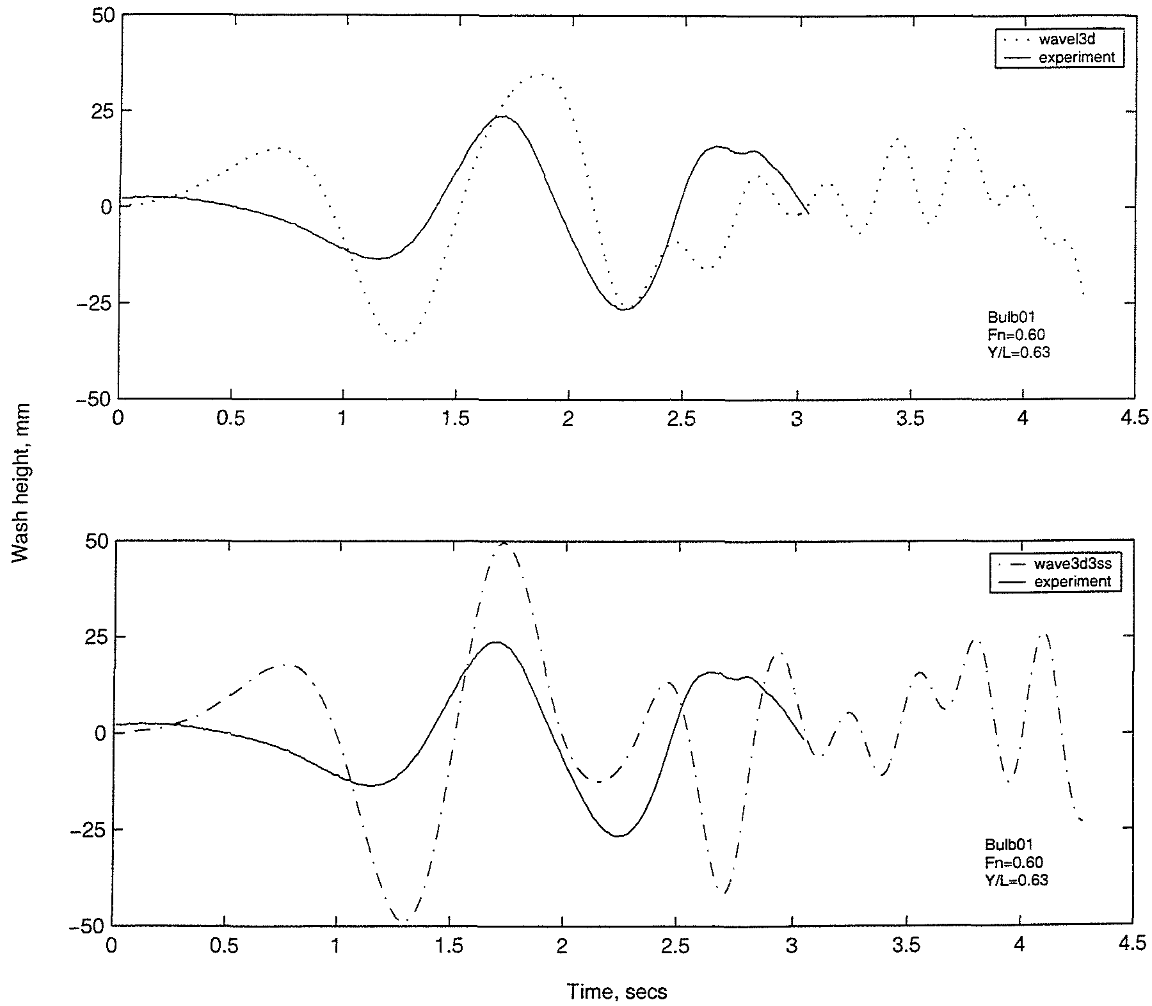

Figure 6.25: Catamaran s/L=0.2 with bulb01:Experimental and theoretical wave cuts at F_n=0.60

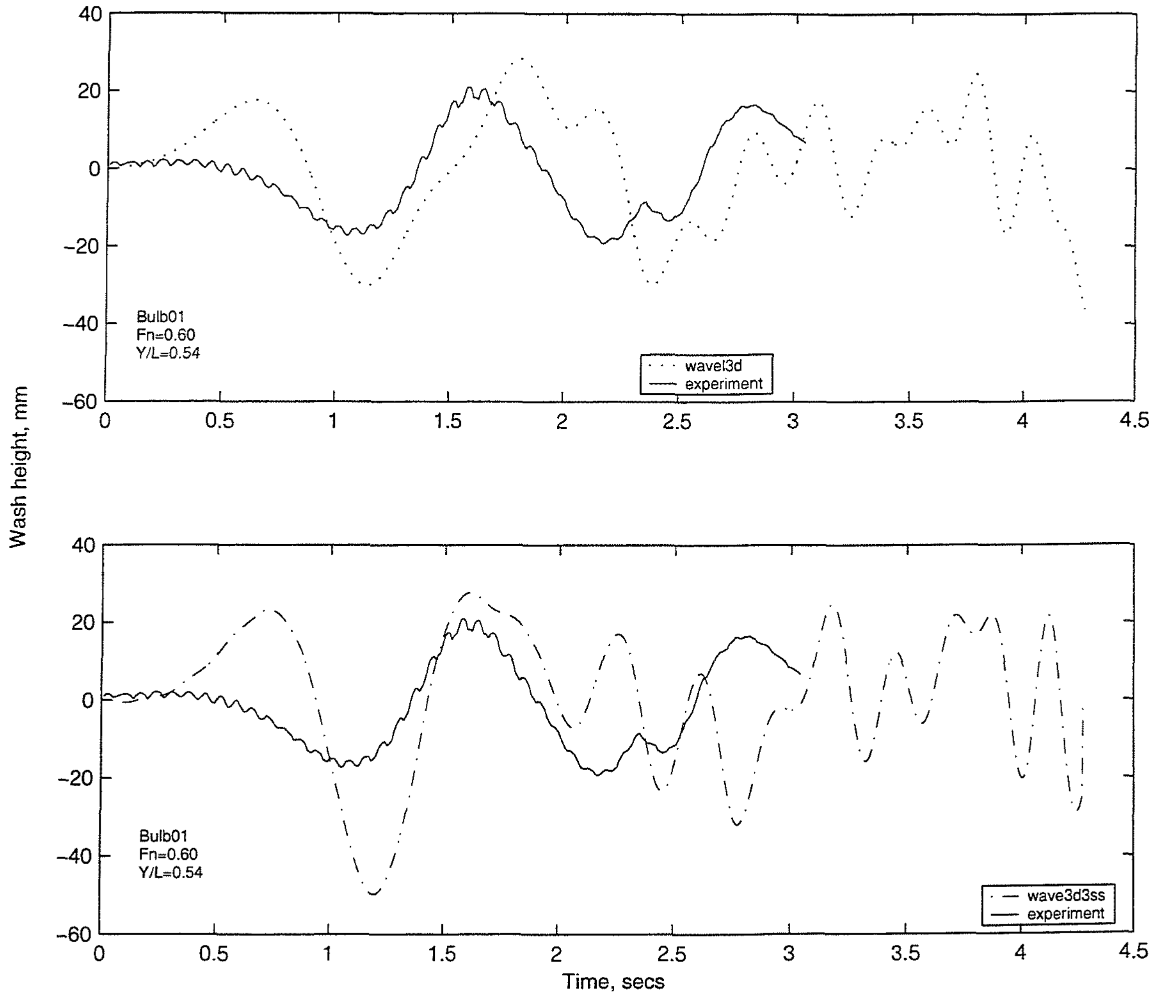

Figure 6.26: Catamaran s/L=0.2 with bulb01:Experimental and theoretical wave cuts at F_n=0.60

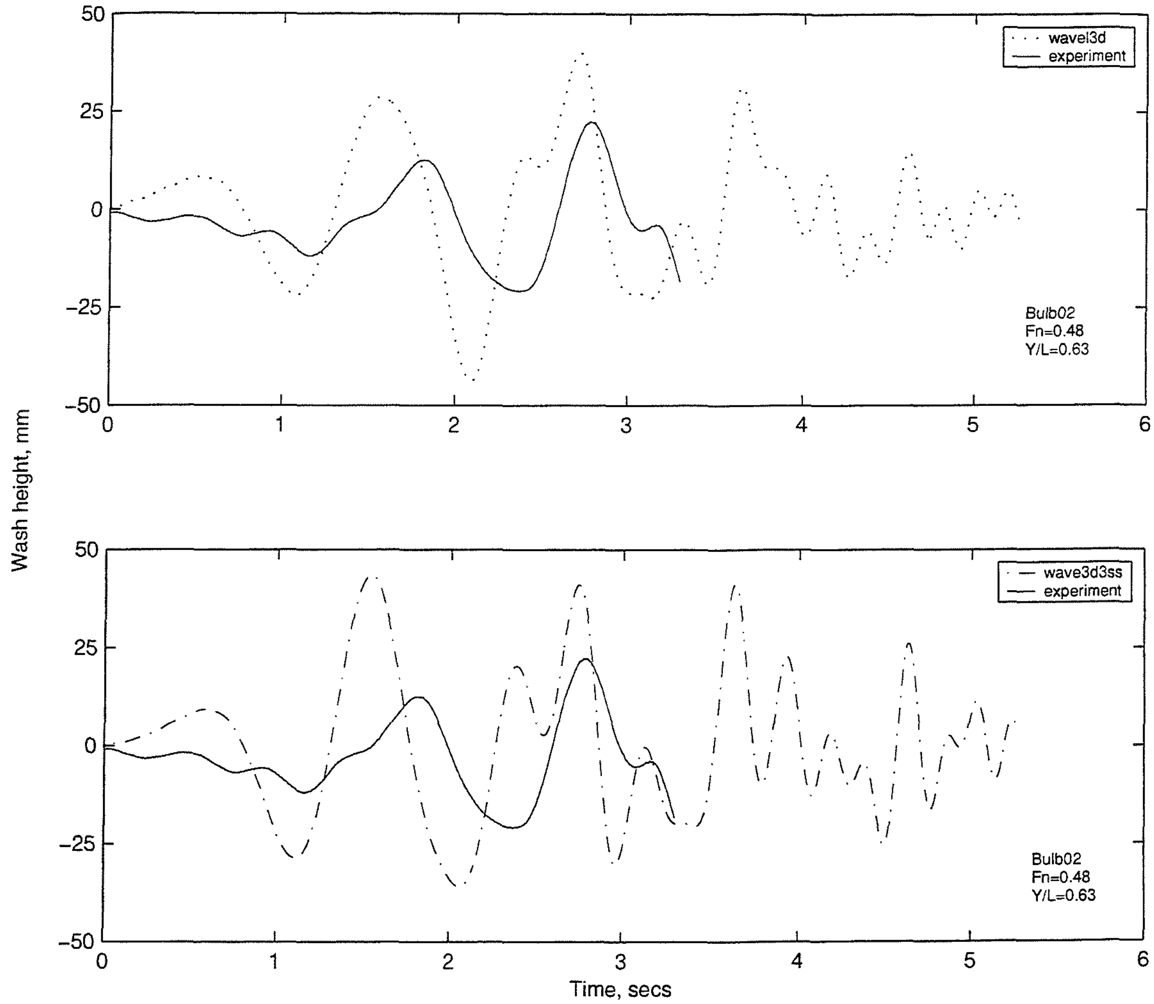

Figure 6.27: Catamaran s/L=0.2 with bulb02:Experimental and theoretical wave cuts at F_n=0.48

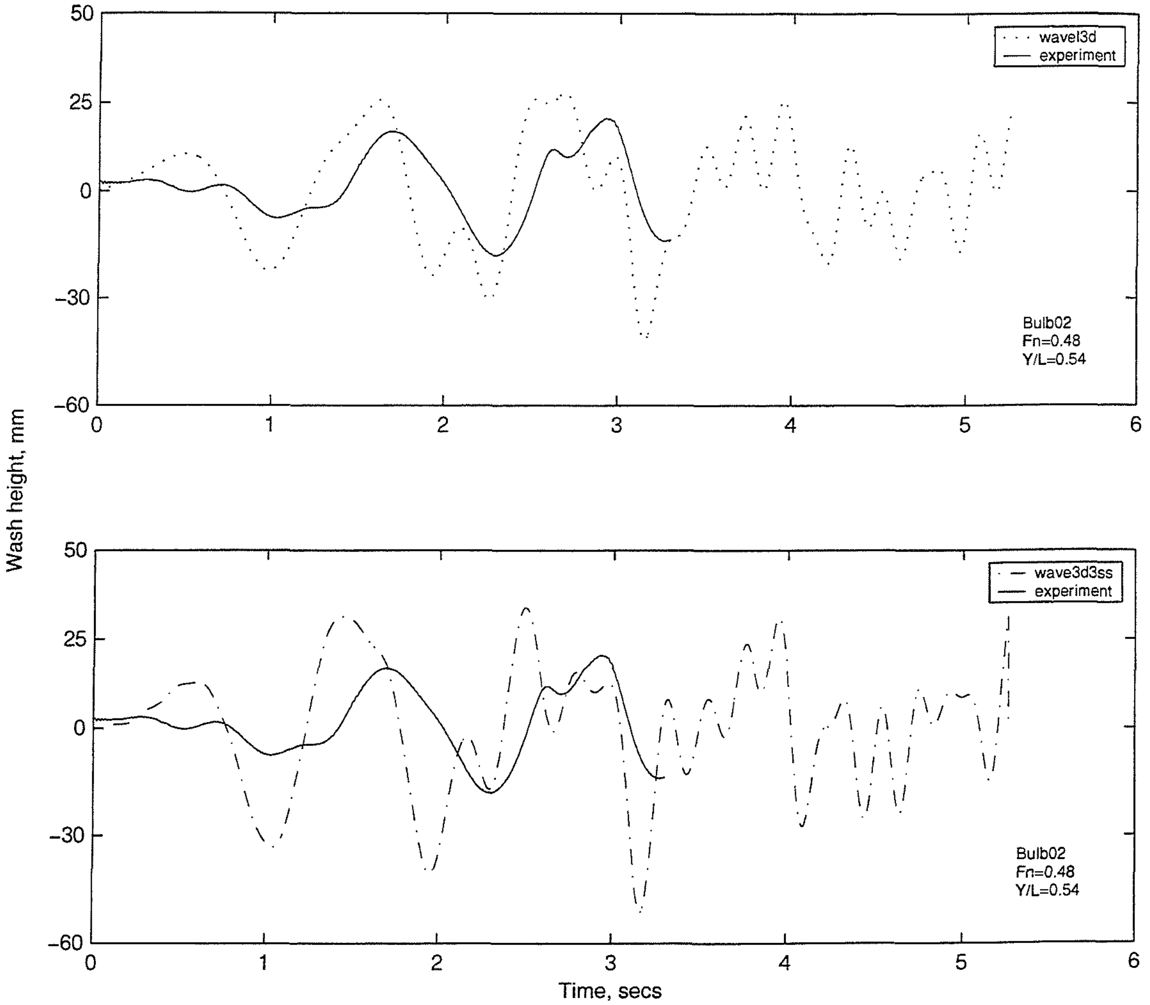

Figure 6.28: Catamaran s/L=0.2 with bulb02:Experimental and theoretical wave cuts at F_n=0.48

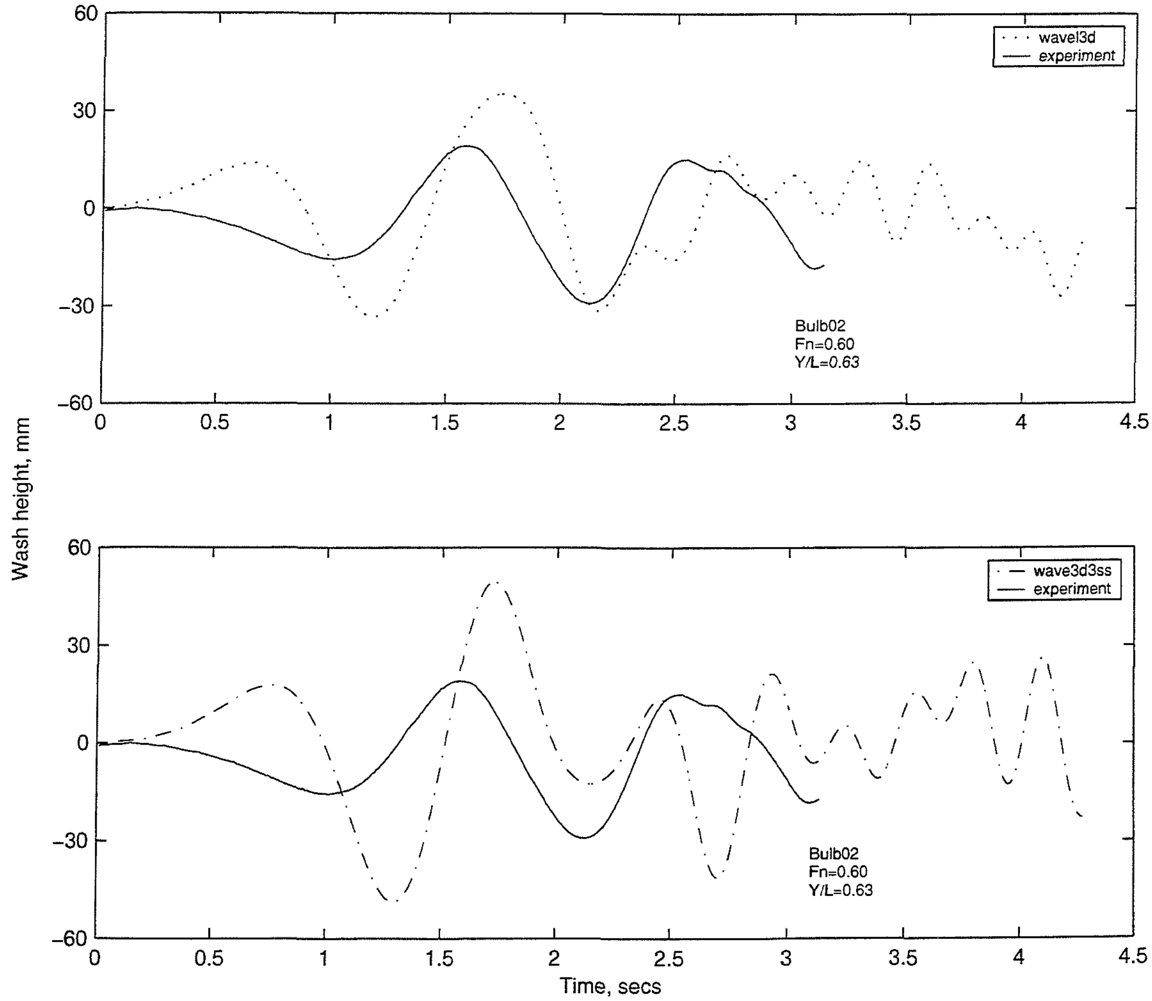

Figure 6.29: Catamaran s/L=0.2 with bulb02:Experimental and theoretical wave cuts at F_n=0.60

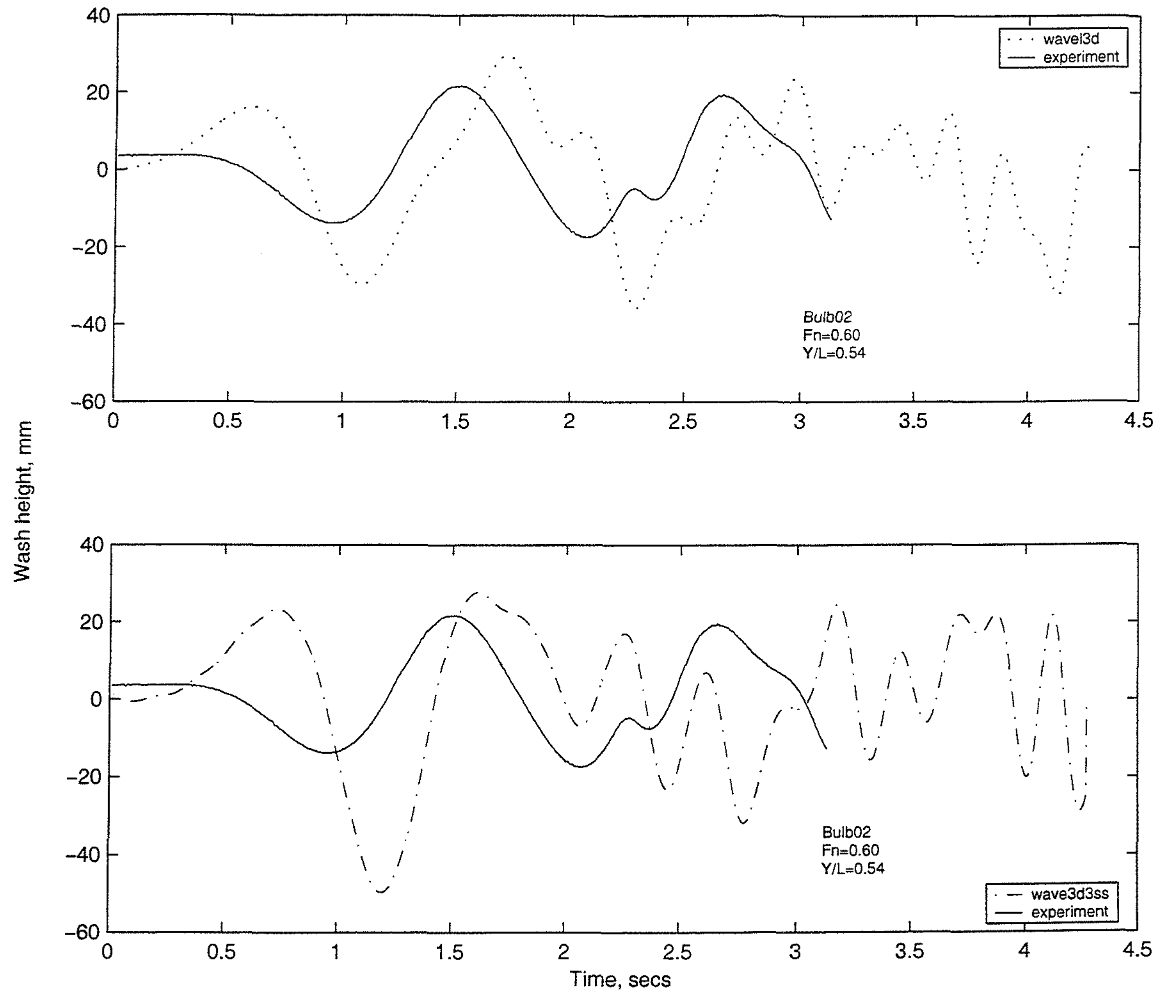

Figure 6.30: Catamaran s/L=0.2 with bulb02:Experimental and theoretical wave cuts at F_n=0.60

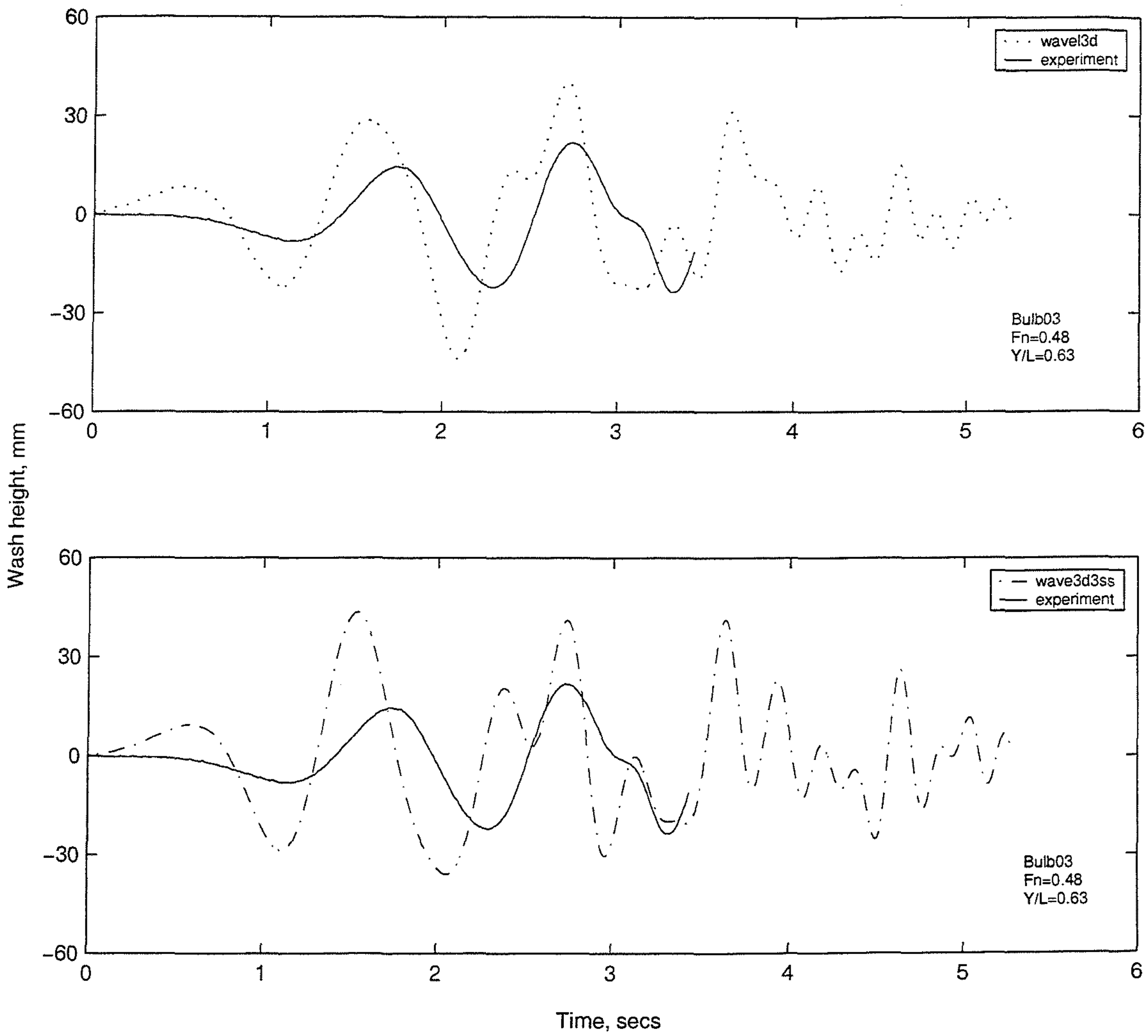

Figure 6.31: Catamaran s/L=0.2 with bulb03:Experimental and theoretical wave cuts at F_n=0.48

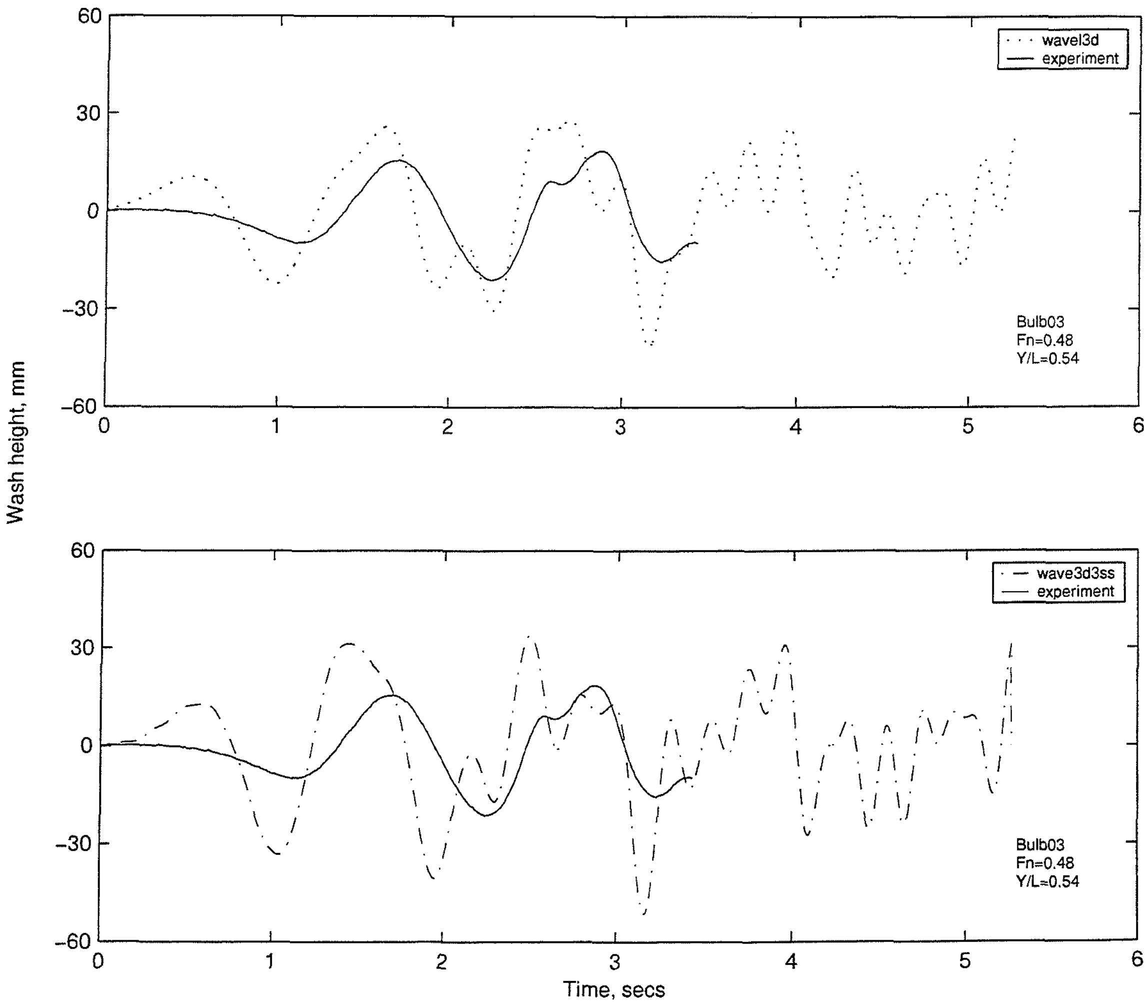

Figure 6.32: Catamaran s/L=0.2 with bulb03:Experimental and theoretical wave cuts at F_n=0.48

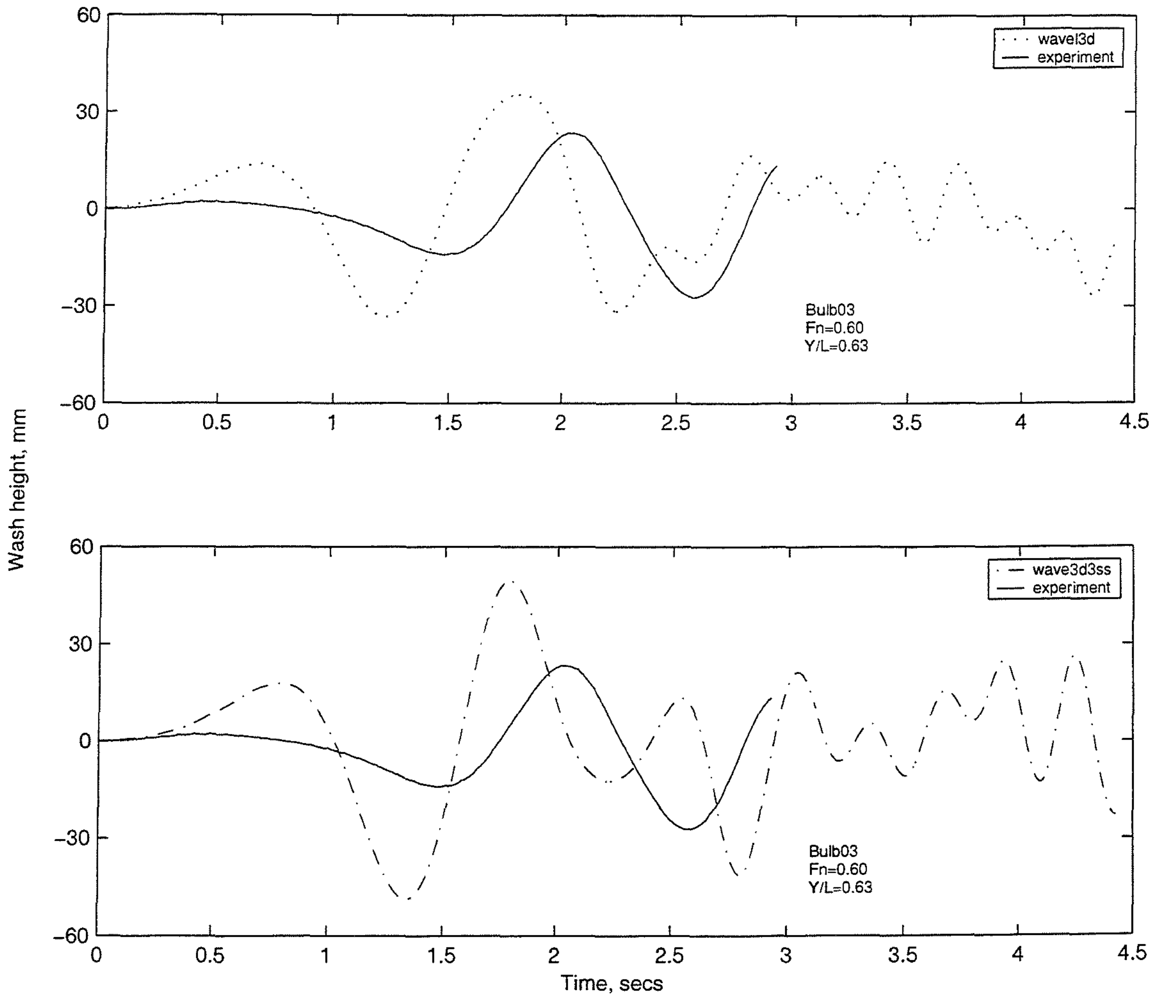

Figure 6.33: Catamaran s/L=0.2 with bulb03:Experimental and theoretical wave cuts at F_n=0.60

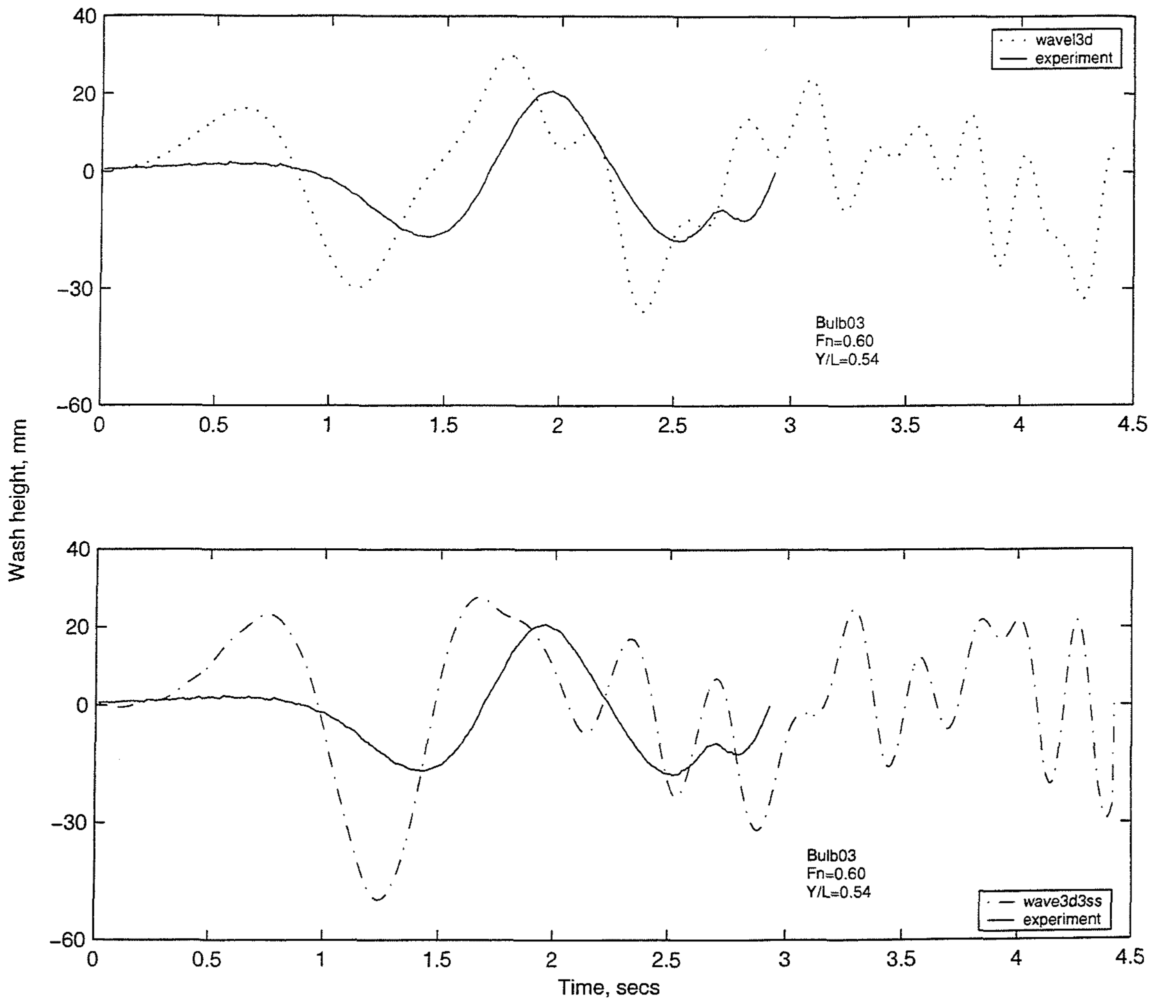

Figure 6.34: Catamaran s/L=0.2 with bulb03:Experimental and theoretical wave cuts at F_n=0.60

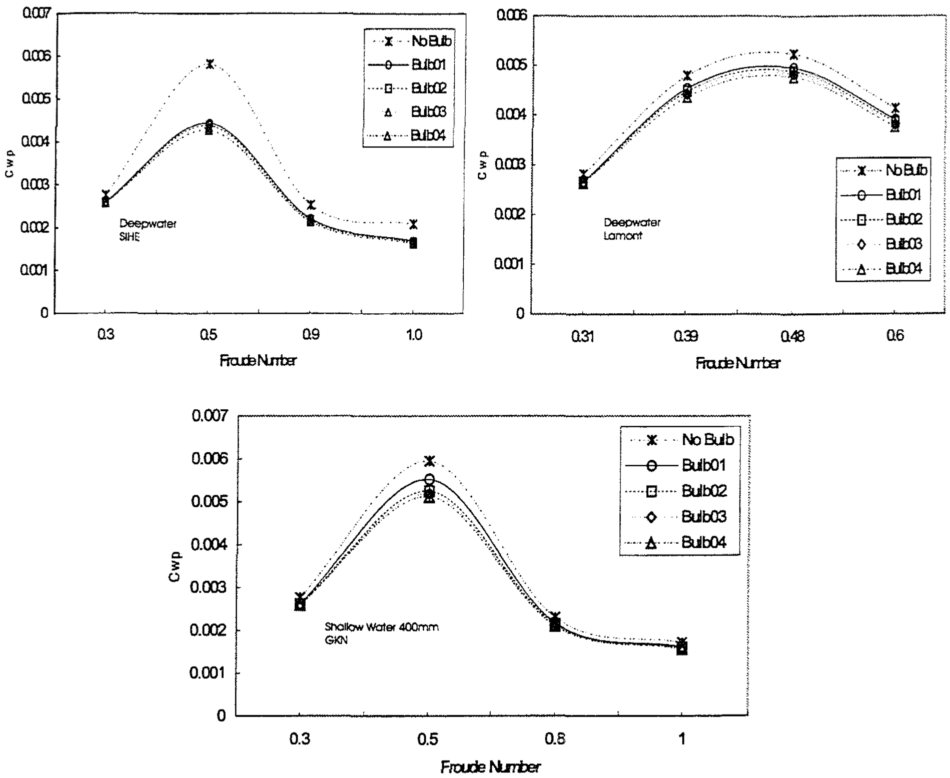

Figure 6.35: Catamaran s/L=0.2: Wave Pattern Resistance(theoretical)

Chapter 7

Conclusions and Future Work

7.1 Deep Water Tests

The results presented in this work clearly show that the high-speed displacement vessel fitted with bulbous bows has some promising characteristics in wash, resistance and seakeeping.

It should be underlined that, all results mentioned in this project are based on the investigation on one of the NPL series of high speed displacement hull form namely Model 5b or known as NPL5b. This model has been tested in monohull and catamaran configurations. In order to investigate the effect of bulbous bow on wash and others ship performance criteria such as resistance and seakeeping, this model underwent slight modification from station 8 up to stem to enable to accommodate the bulbous bow.

From this study, it seems that the bulbous bow has an important effect on the resistance and wash. For catamaran $s/L = 0.2$, it was found that the bulbous bows reduce the residuary resistance coefficient by at least 30%. Hence, bulb03 and bulb04 are preferable since they reduce the maximum residuary resistance coefficient by 40% and 38% respectively. The residuary resistance coefficient of the catamaran configurations ($s/L = 0.2, 0.3, 0.4$) was found tend to a constant value at $F_n > 0.7$, irrespective of the demihull spacing. At moderate Froude numbers i.e. $0.4 < F_n < 0.7$ the residuary resistance was found to increase deliberately with reducing s/L i.e. a smaller separation leads to higher interference.

An important observation can be made about the effects of the bulbous bow geometry on performance. In general, the resistance advantages derived from adding a bulbous bow to the NPL5b hull seemed to increase with increasing bulb volume. Bulb04, (the longest bulb) illustrated this point by having the lowest specific resistance over the considered speed range for monohull configuration and vice-versa for catamaran, $s/L = 0.2$ i.e. bulb01 and bulb02 offer the lowest specific resistance. This is probably due to the effect of wave interference as a result of two demihulls running side by side.

The bulbs efficiency plot for catamaran $s/L = 0.2$, shows that bulb01 and bulb02 are the most efficient compared to bulb03 and bulb04.

The experimental results revealed the tested bulbous bows have positive effect on resistance for all sizes and Froude numbers at full load condition.

In catamaran configurations $s/L = 0.2, 0.3, 0.4$, the wash height decreases with increasing hull separation. For separation ratio, $s/L = 0.2$, bulb04 gives the lowest wash height followed closely by bulb03, bulb02 and bulb01 accordingly. The changes of non-dimensional maximum wash height with F_n appear to produce a similar trend to those of wave-making resistance coefficients as expected.

In monohull configuration, bulb02 produces the lowest wash and almost coincides with the wash produced by bulb04. However, the non-dimensional wash heights produced by bulb01 and bulb03 are approximately four and six times higher than those generated by bulb02 and bulb04 respectively.

The deep water results also found that the running trim varies with speed and bulb size i.e. bulb01 and bulb04 gave the lowest and the highest trim respectively.

7.2 Tests in Waves

Tests on catamaran $s/L = 0.2$ in regular waves have been carried out. It should be noted that the $s/L = 0.2$ value chosen is representative of the vast majority of similar high-speed catamarans around at the current time.

The added resistance in waves varies with speed and the wavelength to ship length ratio λ/L and the model fitted with bulb02 offers the lowest value. It should be noted that the vessel having least resistance in calm water does not necessarily show the lowest added resistance in seaway or rough water.

It was found that the wash measured in calm water is the similar trends as the wash measured in regular waves, but with small phase shift and oscillations in some places. From this preliminary finding, it may be concluded that the wash tends to be independent of sea condition.

From the results of the experiment in regular head waves, it was found that the pitch motion was influenced by the size of the bulbous bows i.e. in this particular case, bulb03 and bulb04 are preferable for a least pitch motion.

The effect of bulbous bow size on heave motion is less pronounced. However, in heave motion the wavelength and Froude number have a much greater effect than the size of bulbous bow.

7.3 Shallow Water Tests

The results of a series of a model experiments for high-speed catamarans in shallow water are discussed. The study concentrated on resistance, wash cuts, sinkage and trim.

It can be seen that the general effect of the shallow water is to cause an increase in resistance especially at the lower speeds compared with the deep-water value.

By referring to the total and residuary resistance coefficients in shallow water, the shortest bulbous bow i.e. bulb01 is superior and preferable among the four bulbous bows.

In comparison with deep water results, it was found that the wash in shallow water increases by 40% to 100% which depends on F_{nh} and bulbous bows (bulbol, bulb02, bulb03 or bulb04). Again, the shortest bulbous bow i.e. bulb01 performs better than others in producing a low wash.

As expected, the trim varies with the size of the bulbous bows.The longest bulbous bow i.e. bulb04 increases trim by 30.0% with reference to bulb01.

The experimental results also show that the sinkage experienced by the model fitted with bulb02 and bulb04 increased by 46.6% and 27.5% respectively with respect to bulb01 but in contrast bulb03 offered a 0.5% reduction.

7.4 Theory

The theoretical prediction of wash generation was carried out using thin-ship theory.

Although discrepancies exist in the theoretical wash profiles compared with the experimental profiles, primarily with regard to phase angle and wash height, the trend of the curves is similar at least for higher Froude number. These discrepancies are likely to be improved and minimised by fine tuning the relevant sections to accommodate the bulbous bow and also by manipulating the source strengths representing the bulbous bow.

The following conclusions also can be drawn from these test:

- It can be seen from the waves traces that the theoretically obtained traces are fairly close to those obtained from measurements taken from model tests.
- It also appears that the trace with the smallest distance from the model centreline is most accurate, and the trace farthest the least accurate in almost all cases.
- Depth of water and distance from sailing line affect the wash height but only to a minor extent compared with speed.

7.5 General Remarks

It is important to note that the bulbous bows with circular cross section offer a significant reduction in wave making resistance coefficients as well as reductions in wash height, together with the practical advantage of a simple construction procedure.

It would be useful for ship designers to have a tool that could predict the wave-making properties of a hull to such an extent that the wash of the vessel could be minimised. As all design is a compromise business in nature, a designer must trade-off the conflicting requirements of minimum wash for minimum resistance and excellent seakeeping.

7.6 Future Work

- Model testing in shallow water for more water depths. Since the current tests were carried out only at one water depth i.e. 400mm, perhaps this can be extended to at least two more water depth, e.g. 200mm and 300mm in order to get more insight of the vessel's performance in shallow water.
- Model testing in oblique seas. This is required since the models were tested in head sea condition only, the coupling of pitch and roll motion in oblique sea would be expected to be much greater and severe for the catamaran.
- Full scale test on prototype. The current investigation has been concerned entirely with model scale. A full scale trial result is important in order to produce a model-ship correlation factor.

For ships with bulbous bow in rough seas, it is believe that slamming is indeed a problem which should be investigated. Slamming occurs mainly on a flat bottom if it impinges on the water surface after complete emergence from the water,[84].

It should be noted that the measurement of slamming impact pressure needs additional high effort and instrumentation.

Appendix A

THEORETICAL APPROACH

A.1 Introduction

The theoretical method can be used to predict wash height and wave pattern resistance of high speed displacement ship using a computer program. The original program is based on thin ship theory and developments of the program included the prediction of wave elevation using the Eggers series. Those program codes known as wavel3d.for and wave3d3ss.for.

A.2 Basic Theory

A.2.1 Calculation of source strengths

The hull is represented by a series of sources distributed along the centre plane of the body. The intersection of waterlines and sections forms a lattice of rectangles on this centre plane, and a source is placed at the centre of each rectangle. The source strength is calculated from the slope of the waterline across the rectangle.

The velocity on the hull surface is zero

$$U\frac{dy}{dx} + \phi_y = 0$$

The flow from a source of strength S is

$$\phi_y = 2\pi.S$$

So the source strength is

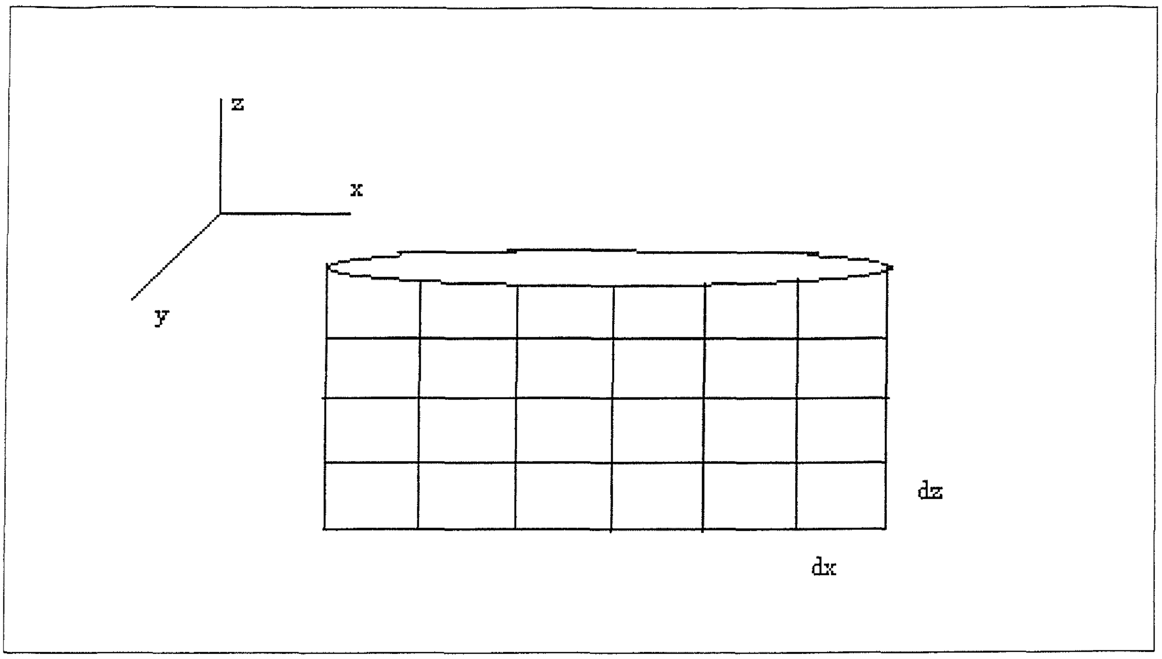

Figure A.1: Slender body Theory

$$S = -\frac{U}{2\pi}\frac{dy}{dx}$$

A.2.2 Calculation of wave elevations

The model travels down in the towing tank i.e rectangular channel at a uniform speed. The wave pattern produced consists of a series of plane gravity waves which travel at various angles θ_n to the direction of travel of the model. The theory is then based on the condition that the wave pattern is symmetrical and stationary.

Wave at angle θ_n has surface elevation ζ_n that is function of $\hat{y}$.

Say

$$\zeta_n = A_n \cos(\gamma_n \hat{y} + \varepsilon_n)$$

now,

$$\hat{y} = y \sin\theta_n - x \cos\theta_n$$

Therefore,

$$\zeta_n = A_n \cos(y\gamma_n \sin\theta_n - x\gamma_n \cos\theta_n + \varepsilon_n)$$

Symmetry means that every component of wave angle θ_n is matched by a component of $-\theta_n$.

Therefore

$$\zeta_n = 2A_n \cos(x\gamma_n \cos\theta_n - \varepsilon_n)\cos(y\gamma_n \sin\theta_n)$$

Or

$$\zeta_n = [\xi_n \cos(x\gamma_n \cos\theta_n + \eta_n \sin(x\gamma_n \cos\theta_n)] \cos(y\gamma_n \sin\theta_n)$$

where ξ_n and η_n are wave amplitude coefficients, calculated from thin ship theory, i.e;

$$\xi_n = 2A_n \cos\varepsilon_n$$

and

$$\eta_n = 2A_n \sin\varepsilon_n$$

The complete wave system is then composed of a sum of a number of waves, known as the Eggers series with total elevation:

$$\zeta = \sum_{n=0}^{\infty} [\xi_n \cos(x\gamma_n \cos\theta_n + \eta_n \sin(x\gamma_n \cos\theta_n)] \cos(y\gamma_n \sin\theta_n) \tag{1}$$

In the program, ζ is summed from zero to the number of harmonics. Longitudinal wave cuts with actual wave elevations can be calculated for a given y position in the tank, with the y position corresponding to the probes position fixed in the tank.

A.2.3 Calculation of wave resistance

Wave speed

The wave pattern moves with the model, so thew wave speed condition is as follows:

$$C_n^2 = \frac{g}{\gamma_n} \tan\gamma_n h$$

If wave at angle θ_n has speed C_n and model has speed C then:

$$C_n = C\cos\theta_n$$

Therefore;

$$\gamma_n \cos^2\theta_n = \frac{g}{C^2} \tanh\gamma_n h \tag{2}$$

Wall reflection

At wall of tank, $y = \frac{b}{2}$, y-component velocities are zero and $\frac{d\zeta}{dy} = 0$

So from the above equation(1);

$$\sin(\frac{b}{2}\gamma_n \sin\theta_n) = 0$$

i.e

$$\frac{b}{2}\gamma_n \sin\theta_n) = 0, \pi, 2\pi, 3\pi....$$

therefore;

$$\gamma_n \sin\theta_n = \frac{2\pi n}{b} \tag{3}$$

where $n = 0, 1, 2, 3...etc.$

Wave resistance

Hence from equations 2 and 3, eliminating θ_n and using $\sin^2\theta + \cos^2\theta = 1$;

$$\gamma_n^2 = \frac{g}{C^2}\gamma_n \tanh\gamma_n h + (\frac{2n\pi}{b})^2 \tag{4}$$

For a channel of finite width there a number of discrete sets of values for γ_n and θ_n. γ_n is found from the roots of equation(4) and θ_n by substituting in equation(3).

Then it can be shown using momentum analysis and Eggers series that; wave resistance can be calculated by the equation below;

$$R_w = 1/4\rho g b\{(\xi_0^2 + \eta_0^2)(1 - \frac{2\gamma_0 h}{\sinh 2\gamma_0 h}) + \sum_{n=1}^{\infty}(\xi_n^2 + \eta_n^2)(1 - 1/2\cos^2\theta_n[1 + \frac{2\gamma_n h}{\sinh 2\gamma_n h}])\} \tag{5}$$

References

[1] Abdul Ghani, M.P and Wilson, P.A. Wake Wash From High Speed Displacement Craft. In *Asia Pacific Maritime Congress - 90th Anniversary KSNAJ*, Kobe, Japan, May 21 - 23 2002.

[2] Bauman, W.D and Keramidas, G.A. A Computer Model for Wave Resistance and far Field Ship Wave Calculations. In *Proc. Second International Conference on Computer Aided Design, Manufacture and Operation in the Marine and Offshore*, Southampton, U.K, September 1988.

[3] Betram, V and Hughes, M. Wash Prediction based on Panel Method. *http://www.ehis.navy.mil/rep499.html*, 1999.

[4] Betram, V and Jensen, G. A Practical Method for Wave Resistance Prediction for SWATH Ships. In *Proc. International High-Performance Vehicle Conference*, Shanghai, November 1988.

[5] Bhattacharyya, R. *Dynamics of Marine Vehicles.* A Wiley-Interscience Publication, USA, 1978.

[6] Birkhoff, G. Theory of the Wave Resistance of Ships. *Transactions of Society of Naval Architects and Marine Engineers*, 15:359–375, 1954.

[7] Blume, P and Kracht, A.M. Prediction of the Behavior and Propulsive Performance of Ships with Bulbous Bow in Waves. *Transactions of The Society of Naval Architects and Marine Engineers*, 93:79–94, 1985.

[8] Brebner, A, Helwig, P.C and Carruthers, J. Waves Produced by Ocean Going Vessels: A Laboratory and Field Study. In *Proceedings of the Tenth Conference on Coastal Engineering, chapter 28*, Tokyo, February 1966.

[9] Brizzolara, S, Bruzzone, D, Cassella, P, Scamardella, A and Zotti, I. Resistance and Wave Patterns for High-Speed Crafts: Validation of Numerical Results by Model Test. In *Proceedings of 22nd Symposium of Naval Hydrodynamics*, Washington D.C, September 1998.

[10] Canestrelli, P and Zotti, I. Experimental Investigation on the Waves Generation of Lagoon Boats in Venice. In *International Conference on Ship and Shipping Research, NAV2000*, Venice, Italy, September 2000.

[11] Chandraprabha, S. *An Investigation into the Wave Wash and Wave Resistance of High Speed Displacement Ships.* PhD thesis, University of Southampton, UK, 2003.

[12] Chen, X. N and Sharma, S.D. Zero Wave Resistance for Ships moving in Shallow Channels at Supercritical Speeds. *Journal of Fluid Mechanic*, 335:305–321, 1997.

[13] Chung, Y.K and Lim, J.S. A Review of the Kelvin Ship Wave Pattern. *Journal of Ship Research*, 35(3):191–197, Sep 1991.

[14] Cooley, J.W and Tukey, J.W. An Algorithm for the Machine Calculation of Complex Fourier Series. *J. Mathematics of Computation*, 19(1), April 1965.

[15] Couser, P.R. *An Investigation into the Performance of High-speed Catamarans in Calm water and Waves.* PhD thesis, University of Southampton, UK, 1996.

[16] Couser, P.R, Wellicome, J.F and Molland, A.F. An Improved Method for the Theoretical Prediction of the Wave Resistance of the Transom-Stern Hulls using Slender Body Approach. *International Shipbuilding Progress*, 45(444):331–349, 1998.

[17] Dand, I.W, Dinham-Peren, T.A and King, L. Hydrodynamics Aspects of Fast Catamaran operating in Shallow Water. In *International Conference Hydrodynamics of High Speed Craft*, London, November 1999.

[18] Das M.M and Johnson J.W. Waves Generated by Large Ships and Small Boats. *Proceedings of the 12th International Conference on Coastal Engineering, chapter 138, ASCE*, 3:2281–2286, 1970.

[19] Day, A.H and Doctors, L.J. Minimal-Resistance Hullforms for High-Speed Craft. *Transactions of The Royal Institution of Naval Architects*, 1996.

[20] Deming, W. and Xiuyan, C. Waves Generated by a Moving Disturbance in a Shallow Water. In *International High-Performance Vehicle Conference*, Shanghai, China, November 1988.

[21] Dillon, E.S and Lewis, E.D. Ships with Bulbous bow in Smooth Water and in Waves. *Transactions The Society of Naval Architects and Marine Engineers*, 63, 1955.

[22] Doctors L.J and Beck R.F. Numerical Aspects of Neumann-Kelvin Problem. *Journal of Ship Research*, 31(1):1–13, Mac 1987.

[23] Doctors, L.J, Renilson, M.R, Parker, G and Hornsby, N. Waves and Wave Resistance of a High-Speed River Catamaran. In *First International Conference on Fast Sea Transportation, FAST'91*, Trondheim, June 1991.

[24] Doyle, R, Whittaker, T and Elsaßer, B. A Study of Fast Ferry Wash in Shallow Water. In *The 6th International Conference on Fast Sea Transportation, FAST2001*, Southampton, Sept 2001.

[25] Editor. In search of Low Wash Hull form. *Ship & Boat International*, March 1991.

[26] Editor. The Quest for Low Wash on the Canals. *Ship & Boat International*, November 1989.

[27] Eggers, K.W.H, Sharma, S.D and Ward, L.W. An Assessment of Some Experimental Methods for Determining the Wavemaking Characteristics of a Ship Form. *Transactions The Society of Naval Architects & Marine Engineers*, 75:112–157, Feb 1967.

[28] Everest, J. T. Some Research on the Hydrodynamics of Catamarans and Multi-Hulled Vessels in Calm Water. *Transactions North East Coast Institution of Engineers and Shipbuilders*, 84, 1968.

[29] Feldtmann, M. Seabed Modifications to Prevent Wake Wash from Fast Ferries. In *International Conference on Coastal Ships and Inland Waterways*, London, February 1999.

[30] Ferguson, A.M and Dand I.W. Hull and Bulbous Bow Interaction. *Transactions the Royal Institution of Naval Architects*, 112, 1970.

[31] Fry, E.D and Graul, T. Design and Application of Modern High-Speed Catamaran. *Marine Technology*, July 1972.

[32] Gadd, G.E. A Method for Calculating the Flow over Ship Hulls. *Transactions of The Royal Institution of Naval Architects*, 112:335–351, 1970.

[33] Gadd, G.E. A Method of Computing the Flow and Surface Wave Pattern Around Full Forms. *Transactions of The Royal Institution of Naval Architects*, 118:207–219, 1976.

[34] Gadd, G.E. The Wash of Boats on Recreational Waterways. *Transactions of The Royal Institution of Naval Architects*, pages 261–280, 1994.

[35] Gadd, G.E. Far Field Waves Made by High Speed Ferries. In *International Conference Hydrodynamics of High Speed Craft*, London, November 1999.

[36] Gebhardt, J.C. A Closed Loop Design Method for Bulbous Bows. In *Proceedings 15th ATTC*, Ottawa, Canada, June 1968.

[37] Goodrich, D. Boat Race. *Engineering*, 240(11), Dec 1999.

[38] Green, A.E, Laws N and Naghdi, P.M. On the Theory of Water Waves. *Proceedings of the Royal Society of London, Series A*, 338:35–43, 1974.

[39] Guilloton, R.S. The Waves Generated by a Moving Body. *Transactions of The Royal Institution of Naval Architects*, 102:77–87, 1960.

[40] Guohua, S, Shaoqiu, D and Dongguang, C. The Research of Wave-Element for a High-Speed Catamaran in the Inland River. In *International High-Performance Vehicle Conference*, Shanghai, China, November 1988.

[41] Hannon, M.A and Varyani K.S. The Wash Effect of High-Speed Ferries in Coastal and Inland Waterways. In *International Conference on Coastal Ships and Inland Waterways*, London, February 1999.

[42] Havelock T.H. The Propagation of Groups Waves in Dispersive Media, with Application to Waves on Water produced by a TravellingDisturbance. *Proceedings of the Royal Society of London, Series A*, (17), December 1908.

[43] Havelock, T.H. The Wave Pattern of a Doublet in a Stream. *Proceeding of the Royal Society of London, Series A*, 141, 1928.

[44] Havelock, T.H. Wave Patterns and Wave Resistance. *Transactions of The Institution of Naval Architects*, 76:430–446, 1934.

[45] Havelock, T.H. Waves Resistance Theory and Its Application to Ship Problems. *Transactions The Society of Naval Architects and Marine Engineers*, 59:13–24, 1951.

[46] Hofman, M. On Optimal Dimensions of Fast Vessel for Shallow Water. In *Proc. of the 7th International Symposium on Practical Design of Ships and Mobile Units, PRAD'98*, The Hague, Sept 1998.

[47] Holthuijsen, L.H, Booij, N and Herbers, T.H.C. A Prediction model for Stationary, Short-Crested Waves in Shallow Water with Ambient Currents. *Coastal Engineering*, 13:23–54, 1989.

[48] Hoyle, J.W. A Bulbous bow Design Methodology for High-Speed Ships. *Transactions of The Society of Naval Architects and Marine Engineers*, 94:31–56, 1986.

[49] Huang, T.T and Wong, K.K. Disturbance Induced by Pressure Distribution Moving Over a Free Surface. *Journal of Ship Research*, 14(3):195–203, September 1970.

[50] Hughes, M. CFD Prediction of Wake Wash in Finite Water Depth. In *International Conference on High-Performance Marine Vehicles HIPER'01*, Hamburg, Germany, May 2001.

[51] Hussaini, M.Y. *Collected Papers of Sir James Lighthill.* Oxford University Press, Oxford, 1997.

[52] Hutchison, B.L. Seakeeping - A Status Report. *Transactions of Society of Naval Architects and Marine Engineers*, 15:359–375, 1991.

[53] Insel, M. *An Investigation into the Resistance Components of High Speed Displacement Catamarans.* PhD thesis, University of Southampton, UK, 1990.

[54] Insel, M and Molland A.F. An Investigation into the Resistance Components of High Speed Displacement Catamaran. *Transactions of the Royal Institution of Naval Architects*, 134, 1992.

[55] Inui, T. Wave-making Resistance of Ships. *Transactions of Society of Naval Architects and Marine Engineers*, 70:283–353, 1962.

[56] Jiang, T. Investigations of Waves Generated by Ships in Shallow Water. In *Proceedings of 22nd Symposium of Naval Hydrodynamics*, Washington D.C, September 1998.

[57] Khattab, O. Design Aspects of Low Wash, High Controllability Hull Forms for Inland Waterways. In *International Conference on Coastal Ships and Inland Waterways*, London, February 1999.

[58] Kirkegaard, J, Kofoed-Hansen, H and Elfrink, B. Wake Wash of High-Speed Craft in Coastal Areas. *Proc. Coastal Engineering Conference*, 1:325–337, 1998.

[59] Kofoed-Hansen, H, Jensen, T, Kirkegaard, J and Fuchs, J. Prediction of Wake Wash from High-Speed Craft in Coastal Areas. In *International Conference Hydrodynamics of High Speed Craft*, London, November 1999.

[60] Kostyukov, A.A. *Theory of Ship Waves and Waves Resistance.* Max Oppenheimer, Jr, Effective Communications Inc., Iowa City, 1959.

[61] Kracht, A.M. Design of Bulbous bow. *Transactions of The Society of Naval Architects and Marine Engineers*, 86, 1978.

[62] Kurata, K and Oda, K. Ship Waves in Shallow Water and Their Effects on Moored Small Vessel. In *Proceedings of the Nineteenth Coastal Engineering Conference*, California, USA, September 1984.

[63] Laitone E.V. Shallow Water Waves in Canals of Variable Section. *Journal of the Waterways and Harbors Division, ASCE*, May 1967.

[64] Larsson, L and Xia, F. Numerical Hydrodynamics - A Useful Complement to Model Testing. In *Proc. Third International Symposium on Practical Design of Ships and Mobile Units, PRAD'87*, Trondheim, June 1987.

[65] Leer-Andersen, M, Clason, P, Ottosson, P, Andreasson, H and Svensson, U. Wash Waves - Problems and Solutions. In *Proceedings SNAME Annual Meeting*, New York, USA, November 2000.

[66] Lewis, E.H. *Principles of Naval Architecture, Vol.II.* SNAME, USA, NJ., 1988.

[67] Lighthill, M.J. River Waves. In *Proceedings Symposium of Naval Hydrodynamics*, Washington D.C, September 1956.

[68] Lloyd, A.R.J.M. *Seakeeping: The Behaviour in Rough Weather.* Ellis Horwood Limited, UK, UK, 1998.

[69] Macfarlane, G.J and Renilson, M.R. Wave Wake: A Rational Method for Assessment. In *International Conference on Coastal Ships and Inland Waterways*, London, February 1999.

[70] Mark, W. The Application of Spectral Analysis and statistics to seakeeping. *T & R Bulletin, SNAME*, 1963.

[71] Millward, A. Fast Ships in Shallow Water. *Occasional Publication No.4, RINA*, 1982.

[72] Millward, A and Bevan, M. G. Effect of Shallow Water on a Mathematical Hull at High Subcritical and Supercritical Speeds. *Journal of Ship Research*, 30(2):85–93, June 1986.

[73] Millward, A and Sproston, J.L. The Prediction of the Resistance of a Fast Displacement Hull in Shallow Water. *Occasional Publication No.9, RINA*, 1988.

[74] Molland, A.F and Lee, A.R. The Theoretical Investigation of a Series of High Speed Displacement Catamaran Forms. *Ship Science Report 87, University of Southampton, UK*, 1995.

[75] Nakos, D.E and Sclavounos, P. D. On Steady and Unsteady Ship Wave Patterns. *Journal of Fluid Mechanics*, 215:263–288, 1990.

[76] Nakos, D.E and Sclavounos, P. D. Kelvin Wakes and Waves Resistance of Cruiser and Transom-Stern Ships. *Journal of Ship Research*, 38(1):288–294, Mac 1994.

[77] Newman, J.H. *Marine Hydrodynamics.* MIT Press, Cambridge, Mass., 1977.

[78] Noblesse, F. A Slender-Ship Theory of Wave Resistance. *Journal of Ship Research*, 27(1):13–23, Mac 1983.

[79] Noblesse, F, Hendrix, D.M and Kahn, L. Nonlinear Local Analysis of Steady Flow About a Ship. *Journal of Ship Research*, 35(4):288–294, Dec 1991.

[80] Racliffe, A.T, Fisher, P.J. and Mitchell, G.H.G. An Experimental Study of the Parameters affecting the Drag of Ships in Current and Waves. In *Proceedings of the 13th Annual Offshore Technology Conference*, Houston, Texas, May 1981.

[81] Raven, H.C. Numerical Wash Prediction using a Free Surface Panel Code. In *International Conference Hydrodynamics of High Speed Craft*, London, November 2000.

[82] Roddan, G. Bulbous bows for Trawler Yachts and the Long Range Cruiser. In *Fifth Annual West Marine Trawler Fest*, Poulsbo, Washington, USA, November 1999.

[83] Saunders, H. *Hydrodynamics in Ship Design.* SNAME, USA, NJ., 1957.

[84] Schneekluth, H. *Ship Design for Efficiency and Economy.* Butterworths, London, UK., 1987.

[85] Sendagorta, M and Grassse, J. A Method for Calculating the Michell and Havelock Integrals. *Journal of Ship Research*, 32(1):19–28, Mac 1988.

[86] Shinozuka, M and Jan, C.M. Digital Simulation of Random Processes and Its Applications. *Journal of Sound and Vibration*, 25(1):111–128, 1972.

[87] Shinozuka, M and Wai, P. Digital Simulation of Short-Crested Sea Surface Elevation. *Journal of Ship Research*, 23(1):76–84, Mac 1979.

[88] Silvester, R. *Coastal Engineering, 1-Generation, Propagation and Influence of Waves.* Elsevier Scientific Publishing Co., UK, 1974.

[89] Sireli, E.M, Goren, O and Insel, M. The Effects of Transom Stern on the Resistance of High Speed Craft. In *IMAM 2000 Congress*, Naples, Italy, April 2000.

[90] Sorensen, R.M. Investigation of Ship-Generated Waves. *Journal of the Waterways and Harbors Division, ASCE*, pages 85–99, Feb 1967.

[91] Sorensen, R.M. Waves Generated by Model Ship Hull. *Journal of the Waterways, Harbours Division, ASCE*, 95(4):513–538, 1969.

[92] Sorensen, R.M. Ship-generated Waves. *Advances in Hydroscience, Academic Press, New York*, 9:49–83, 1973.

[93] Sorensen, R.M. Water Waves Produced by Ships. *Journal of the Waterways, Harbours Division, ASCE*, 99(2):245–256, 1973.

[94] Sorensen, R.M and Weggel, J.R. Development of Ship Wave design Information. In *Proceedings of the Nineteenth Coastal Engineering Conference*, California, USA, September 1984.

[95] Stan Stumbo, Ken Fox, Larry Elliot. Hull Form Considerations in the Design of Low Wake Wash Catamarans. In *Fifth International Conference on Fast Sea Transportation, FAST'99*, Seattle, USA, Aug 31 - Sept 2 1999.

[96] St.Denis, M and Pierson, W.J. On the Motion of Ships in Confused Seas. *Transactions of the Society of Naval Architects and Marine Engineers*, 63:386–435, 1955.

[97] Stumbo, S, Fox, K, Dvorak, F and Elliott, L. The Prediction, Measurement, and Analysis of Wake Wash from Marine Vessels. *Marine Technology*, 36(4):248–260, 1999.

[98] Taato, S.H, Aage, C and Arnskov, M.M. Waves from Propulsion Systems of Fast Ferries. In *Proceedings of the 14th Fast Ferry International Conference*, Copenhagen, Feb. 1998.

[99] Taunton, D.J. *Methods for assessing the Seakeeping Performance of High-Speed Displacement Monohulls and Catamarans.* PhD thesis, University of Southampton, UK, 2001.

[100] Thiart, G.D and Damant, P.D. Simplified thin-ship theory with application to the design of bulbous bows. *R and D Journal of the South African Mechanical Engineering Institution*, 12:22–27, 1996.

[101] Trillo, R.L. High Speed Over Water, Ideas from the Past, the Present and for the Future. In *First International Conference on Fast Sea Transportation, FAST'91*, Trondheim, June 1991.

[102] Tuah, H, and Hudspeth, R.T. Comparisons of Numerical Random Sea Simulations. *Journal of the Waterway, Port, Coastal & Ocean Division, ASCE*, 108, 1982.

[103] Tuck, E.O. Ship-Hydrodynamic Free-Surface Problems Without Waves. *Journal of Ship Research*, 35(4):277–287, Dec 1991.

[104] Ursell, F. On Kelvin's Ship-Wave Pattern. *Journal of Fluid Mechanics*, 8:418–431, 1960.

[105] Van Wyk A.C and Zwamborn J.A. The Effect of Wave Direction on Ship Motions in a Harbour Entrance Channel Model Study Approach. In *Proceedings of the Nineteenth Coastal Engineering Conference*, California, USA, September 1984.

[106] Warren, N. Wash From Fast Ferries. *Ship & Boat International*, April 1991.

[107] Wehausen, J.V. The Wave Resistance of Ships. *Advances in Applied Mechanics*, 13:93–245, 1973.

[108] Wehausen, J.V and Laitone, E.V. *Encyclopedia of Physics, Section 21, Surface Waves*. Springer-Verlag, Berlin, 1960.

[109] Whittaker, T, Bell, A, Shaw, M, and Patterson, K. A Investigation of Fast Ferry Wash in Confined Waters. In *International Conference Hydrodynamics of High Speed Craft*, London, November 1999.

[110] Whittaker, T Doyle, R. and Elsaßer, B. An Experimental Investigation of the Physical Characteristics of Fast Ferry Wash. In *International Conference on High-Performance Marine Vehicles HIPER'01*, Hamburg, Germany, May 2001.

[111] Wiegel, R.L. *Oceanographical Engineering*. Prentice-Hall, NJ, 1964.

[112] Wigley, W.C.S. The Theory of Bulbous Bow and its Practical Application. *Transactions of NECIES*, 52:65–88, 1936.

[113] Yim, B. A Simple Design Theory and Method for Bulbous Bows of Ship. *Journal of Ship Research*, 18(3):359–375, sept 1974.